Ollscoil na hÉireann, Corcaigh

National University of Ireland, Cork



UCC

University College Cork, Ireland

Coláiste na hOllscoile Corcaigh

New technologies in the study of Alzheimer's disease aetiology

Thesis presented by

Michael B Vaughan BSc(Hons)

for the degree of

Doctor of Philosophy

University College Cork

Department of Physiology, School of Medicine

Supervisors: Dr Mark G. Rae & Dr Dervla O'Malley

Head of Department: Professor Ken D. O'Halloran

2025

DECLARATION

This is to certify that the work I am submitting is my own and has not been submitted for another degree, either at University College Cork or elsewhere. All external references and sources are clearly acknowledged and identified within the contents. I have read and understood the regulations of University College Cork concerning plagiarism and intellectual property. The generative AI model, ChatGPT was used in the preparation of this thesis, as a conversation partner, spellchecker, and for assessing the consistency of writing style and flow, but not for the generation of core content. No AI tool was used to fabricate or falsify data, generate results, or replace core academic tasks such as critical thinking, argumentation, or hypothesis formulation.

Michael B Vaughan

Date

ACKNOWLEDGEMENTS

The road has been long and no words will ever be sufficient to convey gratitude to all those who have helped me along the way. But I will try.

Firstly, a sincere thank you to my supervisors Dr Mark Rae & Dr Dervla O'Malley. Mark I was allocated to you by alphabetical lottery for an assignment during my third year of undergrad. From the very beginning you were willing to facilitate me in whatever avenue of learning I wanted to pursue, while also letting me train at your elbow to build the foundation of my benchtop problem solving skill-set. Dervla you were willing to come and help guide me, adding a structure and focus I sorely lacked. I have caused you both countless hours of stress and frustration over the years. Please know I will be forever grateful for everything.

The list of colleagues and friends, past and present, I have to thank is endless:

In UCC Physiology, Ken, Greg, Marcella, Miriam, Jackie, Nora, Jack, Eric and everyone of the department, Physiology was always so welcoming to me. You all, through your time, patience and generosity made that so. To the UCC community at large, those I met through the School of Medicine, the College of Medicine & Health, the Ignite Program, the Blackstone Launchpad, the PostGrad Council, thank you for teaching me about your worlds, and supporting me in my ideas.

In London, the LTC, ye welcomed in a stray, and just kept letting him back in. The fun and excitement of discovery and scheming has never faded. I miss Ben terribly, but even with that grief, knowing that we share it together, and get to continue to 'choose to work like this' is a beautiful solace.

In Ghent, for everyone of the FunGen and TE labs, thank you all for adopting me. Thank you for making me feel welcome upon my arrival in a new country, with very little knowledge of how anything was supposed to work. The true celebration of this work for me, will be getting the opportunity to continue to work and solve problems with ye into the future. Sarah, your patience and generosity will never be forgotten. Eva, your support, enabling, and friendship were, and still are, excellent. First to Nore, and then to all of the students in both labs: ye never stopped cheering me on. I will never stop cheering ye on. I am so proud of all of you.

To the Physiology Department Junior Surf Team; Tony, Misha, Joana, Lucia, Sebastião. People literally thought we were a cult. In the post COVID world, we fell together, and I haven't stopped smiling since. From surfing to movie nights, the times when we were all together are some of the greatest of my life.

To my friends that I may only see once every three or four business months, but who always had time, encouragement, and a smile for me. Frances, Richard, Niamh, Evan, Sinéad, Nú, Abby. Ye never have to ask me how the writing is going ever again.

To the three people that let me hide away from the world to write, kicked me up the arse when I needed it, and are the only people that can actually get me to do anything.

Bríd, you said from the start this would take longer than expected, you are always right. Thank you.

V, you always find a way to inspire me to do and be better, tre fiammiferi in ogni buio. Thank you.

Keith, you're simply the best. I can't say much better than that.
Thank you for everything.

Finally, my family. Mam, Dad, Davie, Grace, Nan, and everyone further afield, still with us and no. I love you all, so much. Thank you for loving me, and putting up with me, for forever pushing me forward, and believing in me. Thank you.

ABSTRACT

Alzheimer's disease (AD) is the most prevalent form of dementia, projected to affect over 150 million people worldwide by 2050. Clinically, AD manifests as progressive memory loss and cognitive decline. Neuropathologically, it is characterised by extracellular amyloid-β plaque deposition and intracellular neurofibrillary tau tangle formation, followed by synaptic loss and neural cell death. To date, candidate therapies and interventions have been developed almost exclusively in transgenic animal models, yet little success has been achieved in clinical trials. This translational failing has driven a growing departure from the classical amyloid-cascade hypothesis, upon which these animal models were developed, towards several alternative hypotheses of AD aetiology. Ethical and practical limitations on accessing living human brain tissue for research have, until recently, left the field without an appropriate experimental system to evaluate these alternative hypotheses.

This thesis is primarily concerned with the utility of human induced pluripotent stem cell (iPSC)-based two- and three-dimensional neural culture technologies to investigate these alternative hypotheses of AD in a species-relevant model. Initially, we worked on developing neural progenitor cells (NPCs), mature dentate gyrus (DG) like neurons using a novel differentiation protocol, and cerebral organoids from iPSCs derived from healthy control donors and from a patient carrying the $PSEN1_{M139V}$ mutation. Building on these iPSC-derived materials, we examined two major mechanisms central to alternative hypotheses of AD in NPCs; calcium dysregulation and altered metabolic function. Using live-cell calcium imaging and Seahorse metabolic flux analysis, we characterized how $PSEN1_{M139V}$ NPCs differ from controls in intracellular Ca^{2+} handling and bioenergetic profiles. Finally, we reviewed current evidence derived from human studies and human cellular or tissue models for herpes simplex virus (HSV)-induced disruption of the neuronal intracellular trafficking system in AD development. Although primary data in human cells are limited, alterations in lysosomal load, endoplasmic reticulum and Golgi architecture, and upregulation of activity-regulated cytoskeleton-associated protein (ARC) mRNA, emerge as promising metrics of disruption for future HSV studies in human iPSC-derived systems.

In summary, this work (1) validates presenilin-mutant neural phenotypes previously observed only in animal models, (2) generated an efficient differentiation method for DG like mature neurons, and (3) synthesised the human-specific evidence linking HSV-infection to intraneuronal trafficking disruption.

CONTENTS

Declaration i

Acknowledgements ii

Abstract iv

Contents v

List of Figures ix

List of Tables xi

Abbreviations xii

1 General Introduction 1

1.1 Alzheimer's disease . . . 1

1.1.1 Amyloid β . . . 3

1.1.2 Tau . . . 6

1.2 Presenilin . . . 8

1.2.1 Presenilins in Mitochondrial Function . . . 10

1.2.2 Presenilins in Cellular Timing . . . 11

1.3 Alternative Aetiological Hypotheses . . . 13

1.3.1 The Calcium Hypothesis . . . 15

1.3.2 The Endo-Lysosomal Hypothesis . . . 18

1.3.3 Mitochondrial Cascade Hypothesis . . . 20

1.3.4 Inflammation Hypothesis . . . 21

1.3.5 Viral Activation Hypothesis . . . 23

1.4 Traditional Models of AD . . . 25

1.4.1 Transgenic Rodents . . . 25

1.4.2 Non-human Primates . . . 28

1.4.3 Other Mammals . . . 29

1.4.4 Invertebrates . . . 29

1.5 Human Stem Cell Technology . . . 31

1.5.1 Disease Modelling . . . 31

1.6 Thesis Hypothesis &Aims . . . 34

2 Materials &Methods 35

2.1 Cell & Tissue Culture . . . 35

2.1.1 Cell Lines . . . 35

2.1.2 Culture System Design 36
2.2 Core Laboratory Materials 38
2.2.1 Core Equipment 38
2.2.2 Core Materials 39
2.2.3 Core Reagents 39
2.3 Induced Pluripotent Stem Cell Culture 40
2.3.1 Source Manual & Materials 40
2.3.2 Maintenance 41
2.3.3 Cryopreservation 44
2.3.4 Vial Thaw 44
2.4 Neural Progenitor Cell Culture 45
2.4.1 Source Manual & Materials 45
2.4.2 Induction 46
2.4.3 Maintenance 47
2.4.4 Cryopreservation 47
2.4.5 Vial Thaw 47
2.4.6 Coverslip Culture 48
2.5 Mature Human-derived Neuronal Culture 49
2.5.1 Source Manual & Materials 49
2.5.2 Dentate Gyrus Mature Neuron Induction 50
2.6 iPSC-derived Cerebroid Culture 51
2.6.1 Source Manual & Materials 51
2.6.2 Generation 54
2.7 Air-Liquid Interface Cerebral Organoid Culture 55
2.8 Calcium Imaging 57
2.8.1 Core Imaging Design 57
2.8.2 Experimental Design 59
2.8.3 Data Analysis 59
2.9 Metabolic Analysis 60
2.9.1 Seahorse Analysis 60
2.9.2 BCA Protein Assay Data Normalisation 64
2.9.3 OCR Statistical Analysis 65
2.9.4 Resipher Live Tracking of Neural Progenitor Cell Respiration 66
2.10 Immunofluorescent labelling 68
2.10.1 Immunocytochemistry 68
2.10.2 Confocal Microscopy 70
2.10.3 3D Sample Fixation & Labelling 70
2.10.4 Multiscale 3D Cerebroid Phenotyping 73

3 Development of Human Neural Tissue for Exploration of Cellular Changes Associated with Alzheimer's Disease 76
3.1 Introduction . . . 76
3.1.1 iPSC-derived human neuronal tissue (2D and 3D) . . . 76
3.1.2 Stem cell-derived models investigating AD-related neuronal pathophysiology . . . 77
3.1.3 Chapter Hypothesis and Aims . . . 78
3.2 Results . . . 79
3.2.1 Generation of human NPC cultures . . . 79
3.2.2 NPCs express maturing neuronal cytoskeletal proteins . . . 81
3.2.3 Neural progenitor culture products exhibit physiological functionality . . . 85
3.2.4 Generation of human-derived mature dentate gyrus-like neuronal cultures . . . 87
3.2.5 Generation and maturation of cerebroid cultures . . . 96
3.3 Discussion . . . 108
3.4 Conclusion . . . 112

4 Coupled Dysregulation of Calcium handling and Bioenergetics in a Human Neural Presenilin Model 113
4.1 Introduction . . . 113
4.1.1 Chapter Aims . . . 115
4.2 Results . . . 116
4.2.1 PSEN1 mutant NPCs show increased basal cytosolic calcium . 116
4.2.2 Voltage-gated calcium entry is increased in PSEN1 mutant NPCs 118
4.2.3 Calcium store release is increased in PSEN1 mutant NPCs . . 121
4.2.4 Bioenergetics are suppressed in PSEN1 mutant NPCs . . . 124
4.2.5 Real-time OCR measurements corroborate suppressed metabolic state in presenilin 1 (PSN1) neural progenitor cells (NPCs) . . 128
4.2.6 Dantrolene pretreatment differentially alters NPC respiration and glycolysis . . . 130
4.2.7 Acute NMDA treatment shows weak effect on baseline NPC metabolic readings . . . 138
4.2.8 NMDA treatment shows no effect on NPC metabolic measures 141
4.3 Discussion . . . 147
4.4 Conclusion . . . 149

5 HSV in Human Neuronal Trafficking 150
5.1 Introduction . . . 151
5.1.1 Rationale . . . 151

5.1.2 Objectives . . . 152
5.1.3 Research Question . . . 153
5.2 Methods . . . 153
5.2.1 Search Strategy . . . 154
5.2.2 Eligibility Criteria . . . 155
5.3 Results and Discussion . . . 156
5.3.1 HINT Alteration . . . 160
5.3.2 Lysosome . . . 160
5.3.3 ER and Golgi . . . 161
5.3.4 ARC Protein . . . 162
5.4 Conclusion . . . 165
5.4.1 Limitations . . . 166

6 Conclusions **167**
6.1 Overview of Research Findings . . . 167

Bibliography **170**

Appendices **204**
Publications and Abstracts . . . 205

LIST OF FIGURES

1.1 Amyloid precursor protein processing. 5
1.2 Tau hyperphosphorylation. 7
1.3 γ-secretase. 9
1.4 AD clinical trials and hypothesis overview. 14
1.5 The Calcium Toolkit 16

2.1 Culture System Relatedness. 37
2.2 Morphological changes of iPSCs during differentiations 42
2.3 Brightfield images of induced pluripotent stem cells (iPSC) culture confluency 43
2.4 Brightfield images of iPSCs and NPCs. 46
2.5 Cerebroid Generation Timeline 51
2.6 ALI-CO Culture Schematic 56
2.7 Seahorse XF96 Mito Stress Test Experimental Profile 61
2.8 Resipher probe design. 66
2.9 Resipher components and experimental outputs 67
2.10 mesoSPIM v5.1 75

3.1 Simplified schematic of neural progenitor cell induction protocol 79
3.2 Morphological changes observed during NPC induction 80
3.3 Immunofluorescence Characterisation of Neural Progenitor Cells I 82
3.4 Immunofluorescence Characterisation of Neural Progenitor Cells II 84
3.5 NPC culture calcium responses 86
3.6 Simplified schematic of dentate gyrus like neuronal culture protocol . . . 87
3.7 Morphological changes of mature dentate gyrus like neuron differentiation. 89
3.8 Immunofluorescent PROX1 labelling of dentate gyrus-like neuronss (DGNs) 91
3.9 DGN culture calcium responses 93
3.10 Real-time recording of change in OCR in response to DGN media 95
3.11 Simplified schematic of cerebral organoid culture protocol 96
3.12 Cerebral organoid morphology develops over time 98
3.13 Immuno Characterisation of Cerebroids I 99
3.14 Immuno Characterisation of Cerebroids II 101
3.15 Immuno Characterisation of Cerebroids III 102
3.16 Live FLIM Characterisation of Cerebroids 103
3.17 ALI-CO culture calcium responses 105
3.18 Images of SHIELD Fixed Organoid Embedding 106
3.19 MesoSPIM Images of Cerebroids 107

4.1 Basal cytosolic calcium fluorescence is increased in NPCs containing a presenilin 1 (PSEN1) mutation . . . 117
4.2 Calcium fluorescence trace in response to 50 mM K^+ in NPCs . . . 119
4.3 Calcium signalling in response to 50 mM K^+ increased PSEN1 mutant NPCs. 120
4.4 Altered calcium release dynamics in PSN1 mutant NPCs. . . . 122
4.5 Accelerated calcium release in PSN1 mutant NPCs. . . . 123
4.6 Mitochondrial respiration impaired in PSN1-mutant NPCs . . . 126
4.7 Glycolytic capacity reduced in PSN1 mutant NPCs . . . 127
4.8 Real-time measures of OCR in NPCs . . . 129
4.9 Dantrolene pretreatment increases basal respiration in NPCs . . . 132
4.10 Dantrolene pretreatment increases ATP-linked and maximal respiration in NPCs . . . 133
4.11 Dantrolene pretreatment increases non-mitochondrial respiration and spare respiratory capacity in NPCs . . . 134
4.12 Dantrolene pretreatment does not affect NPC proton leak or coupling efficiency . . . 135
4.13 Dantrolene pretreatment increases basal ECAR in NPCs . . . 136
4.14 Dantrolene pretreatment does not affect maximal ECAR or glycolytic reserve in NPCs . . . 137
4.15 Acute NMDA exposure and time decreases basal NPC respiration . . . 139
4.16 Neither time nor acute NMDA exposure affect basal NPC ECAR . . . 140
4.17 Acute NMDA exposure has no effect on NPC Basal nor ATP-Linked Respiration in unpaired analysis . . . 142
4.18 Acute NMDA exposure has no effect on maximal or non-mitochondrial respiration in NPCs . . . 143
4.19 Acute NMDA exposure has no effect on proton leak or coupling efficiency in NPCs . . . 144
4.20 Acute NMDA exposure has no effect on spare respiratory capacity or basal ECAR in NPCs . . . 145
4.21 Acute NMDA exposure has no effect on maximal ECAR or glycolytic reserve in NPCs . . . 146

5.1 HINT &Herpes . . . 153
5.2 Systematic Review Flowchart . . . 156

LIST OF TABLES

2.1 **Characterisation of Cell Lines** 35
2.2 **Culture System products and corresponding cell developmental stages** 36
2.3 **iPSC Materials** 40
2.4 **NPC Materials** 45
2.5 **DGNeuron Media Composition** 49
2.6 **DGNeuron Media Materials** 50
2.7 **Cerebroid Materials** 52
2.8 **STEMdiff™ Cerebral Organoid Media Preparation** 53
2.9 **Cutting Solution Preparations** 56
2.10 **HBSS Solution Preparations** 58
2.11 **aCSF Solution Preparations** 58
2.12 **Mito Stress Test Experimental Run Protocol** 63
2.13 **OCR-Stats Definitions** 65
2.14 **4% Paraformaldehyde Fixative Preparation** 69
2.15 **Immunocytochemical reagents and their targets** 69
2.16 **Modified SHIELD OFF Solution Preparation** 71
2.17 **eFlash Compatible Antibodies/Stains** 72
2.18 **SmartLabel Settings** 72
2.19 **Fixation &Labelling Materials** 73

5.1 **Search Eligibility Criteria.** 155
5.3 **Summary of Studies Meeting Eligibility Criteria.** 157
5.5 **Direct Evidence of HSV alteration of HINT System.** 164

ABBREVIATIONS

$[Ca^{2+}]_i$	intracellular calcium concentration
3xTG	triple-transgenic
Aβ	amyloid β
A.F.U.	arbitrary fluorescence units
ACH	Amyloid Cascade Hypothesis
aCSF	artificial cerebrospinal fluid
AD	Alzheimer's disease
ADAM	a disintegrin and metalloprotease
AICD	APP intracellular domain
ALI-CO	air-liquid interface cerebral organoid
AMPA	α-amino-3-hydroxy-5-methyl-4-isoxazolepropionic acid
AMPAR	α-amino-3-hydroxy-5-methyl-4-isoxazolepropionic acid receptor
ApoE	apolipoprotein E
APP	amyloid precursor protein
ARC	activity-regulated cytoskeleton-associated protein
ARHGEF5	rho guanine nucleotide exchange factor 5
ATP	adenosine triphosphate
ATP6AP1	ATPase H^+ transporting accessory protein 1
BACE1	beta-site APP cleaving enzyme 1
BCA	bicinchoninic acid
bFGF	basic fibroblast growth factor
BSA	bovine serum albumin
CADRO	Common Alzheimer's Disease Research Ontology
CICR	Ca^{2+}-induced calcium release
CNS	central nervous system
CSF	cerebrospinal fluid
CTF	C-terminal fragment
CTF-β	C-terminal fragment β
CTSF	cathepsin F
CTX	cholera toxin subunit B conjugated to Rhodamine Red™-X
DG	dentate gyrus
DGN	dentate gyrus-like neurons
DHPG	dihydroxyphenylglycine
EB	embryoid body
ECAR	extracellular acidification rate
EGF	epidermal growth factor
EGFR	epidermal growth factor receptor
EOFAD	early onset familial AD

ER	endoplasmic reticulum
ESC	embryonic stem cell
FAD	familial disease
FCCP	carbonyl cyanide-4 (trifluoromethoxy) phenylhydrazone
GCDR	Gentle Cell Dissociation Reagent
HBSS	HEPES buffered saline solution
Hg	herpetic glycoprotein
HHV	human herpes virus
HINT	human intraneuronal trafficking
HR	hazard ratio
HSV	herpes simplex virus
HSV-1	herpes simplex virus 1
HSV-2	herpes simplex virus 2
IL-1β	interleukin-1β
IL-6	interleukin-6
IP_3R	inositol trisphosphate receptor
iPSC	induced pluripotent stem cells
KI	knock-in
KO	knock-out
LAMP2	lysosomal-associated membrane protein 2
LAT	latency-associated transcript
LC3	microtubule-associated protein 1 light chain 3
LIPA	lipase A
LOAD	sporadic/late onset AD
MAM	mitochondria-associated endoplasmic reticulum membrane
MAP2	microtubule associated protein 2
MAPT	microtubule-associated protein tau
mGluR	metabotropic glutamate receptor
Miro2	mitochondrial Rho GTPase 2
NCX	sodium-calcium exchanger
NFT	neurofibrillary tangle
NHP	non-human primate
NIH	National Institutes of Health
NMDA	N-Methyl-D-aspartic acid
NMDAR	N-Methyl-D-aspartic acid receptor
NPC	neural progenitor cell
NPC1	Niemann-Pick disease, type C1
NPCC	neural progenitor coverslip cultures
NSAID	non-steroidal anti-inflammatory

OCR	oxygen consumption rate
PBS	phosphate-buffered saline
PD	Parkinson's disease
PERK	protein kinase R-like ER kinase
PFA	paraformaldehyde
PICO	population, intervention, comparison and outcome
PLO	Poly-L-ornithine
PRISMA	Preferred Reporting Items for Systematic Reviews and Meta-Analyses
PSEN1	presenilin 1
PSEN2	presenilin 2
PSN1	presenilin 1
PSN2	presenilin 2
rcf	relative centrifugal force
RIPA	radioimmunoprecipitation assay buffer
ROCK	Rho-associated, coiled-coil containing protein kinase
ROI	region of interest
ROS	reactive oxygen species
RyR	ryanodine receptor
sAPPα	soluble APP alpha
SCOUT	Single-cell and Cytoarchitecture analysis of Organoids using Unbiased Techniques
SGL	subgranular layer
SHIELD	stabilization to harsh conditions via intramolecular epoxide linkages to prevent degradation
SVZ	subventricular zone
TG	transgenic
TNF-α	tumour necrosis factor α
TRPC	transient receptor potential cation channel
UPR	unfolded protein response
VGCC	voltage-gated calcium channel
VZV	varicellar zoster virus
Wnt	wingless-related integration site

1.1 Alzheimer's disease

In 1906, German psychiatrist and neuroanatomist Alois Alzheimer was the first to describe the eponymous condition as, this "peculiar severe disease process of the cerebral cortex", which he initially observed in a middle-aged patient, Auguste Deter (Alzheimer 1907). Suffering from paranoia, severe memory deficits, mood/behavioural changes and a loss of independence, Auguste's story ended in her death five years after entering his care. Upon autopsy, Alzheimer, a proponent of cutting-edge histological analysis, described mass brain atrophy, atherosclerotic damage, dense neurofibril impregnation of cells and miliary foci (plaques) made up of a "special substance". Several years later, after studying another patient, Josef F., Alzheimer believed that Josef's cortical disease was a plaque-only variant of Auguste's affliction. Due to the lucky re-discovery of brain-slice preparations from both patients decades later, we now understand that Alzheimer was observing two separate time points in the progression of the same pathology. Alzheimer's disease (AD) had its first comprehensive description in 1911 in Alois's "Über eigenartige Krankheitsfälle des späteren Alter" - "On certain peculiar diseases of old age" (Alzheimer 1911).

Alzheimer's disease (AD) is the most common form of dementia, accounting for two-thirds of all diagnosed cases. While predisposition to AD varies due to gender (Fisher, Bennett, and Dong 2018), ethnicity (Kulminski *et al.* 2020), and geography (Fox *et al.* 2013), it is consistently a disease of the elderly, affecting approximately 10.9% of people aged 65 years and approximately 33.4% of those over 85 years in the United States (Rajan *et al.* 2021). It exists as a gross acceleration and amplification of the "normal" cognitive decline seen in ageing. AD is a progressive neurodegenerative disorder that is characterized behaviourally by the gradual development of memory and identity impairments (Huntley *et al.* 2021; Norberg 2019). Histopathologically, it is defined by the deposition of extracellular amyloid β (Aβ) protein plaques (Alois' miliary foci) and the intracellular neurofibrillary tangles (NFTs). These NFTs consist of aggregated tau proteins that are hyperphosphorylated and resistant to proteolysis (Buée *et al.* 2000; Gendron and Petrucelli 2009). The disease also involves chronic neuroinflammation and significant neuronal loss, especially in the hippocampus and neocortical regions of the brain (Heneka *et al.* 2024; Scheff *et al.* 2006; West *et al.* 1994). This pairing of behavioural and histopathological symptomology has long formed medicine's understanding of the disease.

With the advent of molecular screening, AD can now be further sub-categorized under

the titles of sporadic/late onset AD (LOAD) and early onset familial AD (EOFAD). The majority of cases (95%) occur sporadically after the age of 65 with no known specific cause (Bertram and Tanzi 2004; Durmaz *et al.* 2019). The remaining 5% occur before age 65 (early onset), with 20% (1% of all cases) being linked to autosomal-dominantly inherited mutations that cause EOFAD. These familial disease (FAD) cases are caused by a mutation of at least one of three genes, coding for presenilin 1, presenilin 2, and amyloid precursor protein (APP) (Tanzi 1999). In the 1980s and 1990s, the identification of these FAD genes and their capacity to alter Aβ production provided a foundation for the development of mechanistic disease hypotheses. While this thesis will focus on ancillary hypotheses of AD aetiology, it is important to highlight the central knowledge of the field.

The most popular and longest-reigning hypothesis of AD causation for the past 32 years (at time of writing) has been the Amyloid Cascade Hypothesis (ACH).

Successive proteolytic cleavage of the membrane-bound APP leads to the production of Aβ (see Fig. 1.1). Presenilin 1 and 2 proteins form the catalytic core of γ-secretase, responsible for the final cleavage step in the amyloidogenic process. These genetic findings led to the development of the ACH, first described in 1992 (Hardy and Higgins 1992), which postulates that the initial pathological event in AD is the build-up and deposition of insoluble Aβ within the neuropil. Within this framework, Aβ nucleation is proposed to promote plaque formation, which is thought to subsequently drive tau pathology. These NFTs then are thought to cause synapse disruption, leading to cognitive decline and eventual death. The recognition of the presence of Aβ in both the senile plaques of AD patients, in cases of adult Down syndrome, coupled with the discovery of the causative role of amyloid-relevant gene mutations, formed the basis of the ACH (Armstrong 2014; Behl 2024).

Years of scrutiny and contradictory data however have, for some scientists, caused a shift away from considering ACH to be the 'conclusive model' of AD. Pioneers of the ACH, such as Professor John Hardy himself, have talked at length about the errors made by early researchers, and the lack of scepticism by journal editors at the time (Hardy 2017). The inability of the ACH to encompass and/or reconcile several observations about Aβ pathology that have been made subsequent to its initial publication lends credence to its ineffectiveness to describe AD pathology. The most notable of these discrepancies is the lack of a direct correlation between Aβ plaque density and cognitive decline (Arriagada *et al.* 1992), as substantial plaque deposition has been observed in cognitively unimpaired elderly individuals (Nelson, Braak, and Markesbery 2009; Zolochevska and Taglialatela 2016). Transgenic AD models with only mutations of

amyloidogenesis-promoting genes only display minor NFTs localized to senile plaques, not total brain tau pathology (Sturchler-Pierrat *et al.* 1997).

AD treatments based upon the ACH, such as anti-Aβ antibodies and metal-complexing agents have also shown little success in stopping disease progression even when clearly evidenced to reduce plaque build-up and presence in clinical trials (Doody *et al.* 2014; Ostrowitzki *et al.* 2022; Salloway *et al.* 2014; Vandenberghe *et al.* 2016). In July 2022, an extensively publicized investigation revealed fraudulent data supporting the pathogenic role of the specific amyloid beta 56 oligomer species (Lesné *et al.* 2006; Piller 2022). While amyloid accumulation may cause large swathes of AD symptoms, there is a belief that the initiation of AD progression occurs much earlier than clinical symptom presentation, a consideration which has led to the development of multiple alternate hypotheses (Hampel *et al.* 2021; Palmqvist *et al.* 2017).

The various alternative aetiological hypotheses discussed in this general introduction all attempt to explain the onset and progression of AD in the context of either Aβ proteins, Ca^{2+} dysregulation, tau pathology, mitochondrial impairment, oxidative stress and/or neuroinflammation. In practice, while determining the sequence of events in disease pathology is crucial for the development of treatments, it is essential to recognize that focusing solely on any one hypothesis fails to consider the complete range of factors involved in disease progression. The growing recognition of multiple potential factors calls into question AD's status as a single disease entity. It is likely a feed-forward collection of pathological mechanisms, each described by a separate hypothesis, which culminate in the AD spectrum recognised in patients.

1.1.1 Amyloid β

Amyloid β is a 4 kDa peptide derived from the larger APP, and is what we now recognise as Alzheimer's "special substance" (Divry 1927). APP is synthesised within the rough endoplasmic reticulum and trafficked to the cell surface, acting as an integral membrane protein. APP contains multiple enzyme cleavage sites, whose products can enter either the so-called amyloidogenic, or non-amyloidogenic, processing pathways (see Fig. 1.1).

To be amyloidogenic means to be predisposed to the production of amyloid deposits. A major amyloidogenic processing pathway is recognised as being due to β-secretase activity (see Fig. 1.1). Beta-site APP cleaving enzyme 1 (BACE1) mediates this β-secretase activity in neuronal cells and cleaves APP at the N terminus of the Aβ peptide

sequence, leaving C-terminal fragment β (CTF-β) for further processing. In the brain, the subsequent γ-site cleavage is mediated by a protein complex composed of four components: anterior pharynx defective 1, nicastrin, presenilins 1/2, and presenilin enhancer 2 (see Fig. 1.3) (Zhang *et al.* 2014). This γ-secretase cleaves the C terminus of the peptide sequence producing Aβ. Aβ1-40 is 40 amino acids in length, is the predominant form of Aβ produced, and is linked to the neurotoxic effects of amyloid. However, longer forms of amyloid, which can also be produced via this process (e.g. Aβ1-42 and Aβ1-43), are more amyloidogenic than Aβ1-40 (Braun *et al.* 2022; Chen *et al.* 2017).

BACE1 cleavage of APP is the rate-limiting step for the production of Aβ (Cai *et al.* 2001; Kwak *et al.* 2011). As both are membrane-bound proteins this would dictate the importance of APP and BACE1 co-localization for pathway progression. Following this logic, Das et al. (2013), deduced the existence of separate neuronal trafficking pathways, spatially segregating the enzyme and the substrate during non-amyloidogenic processing (Das *et al.* 2013). They found that upon exit from the trans-Golgi network, separate organelles carry these proteins to the cell membrane. Retrograde transport and subsequent co-localization of both proteins occurs following endocytosis. BACE1 endocytosis can operate under clathrin-independent and/or clathrin-mediated mechanisms, while APP is endocytosed in a clathrin-dependent manner (Das *et al.* 2013). Subsequent APP/BACE1 convergence is dependent on APP endocytosis (Koo and Squazzo 1994) and largely takes place in the recycling endosome within dendrites (Rajendran *et al.* 2006; Wei *et al.* 2010). Mobile BACE1 vesicles mostly co-localize with recycling endosome markers (Tfr and syntaxin13), while stationary vesicles are also positive for Rab5 (a marker for early endosomes) (Das *et al.* 2016). These immobile BACE1 vesicles are more commonly observed in axonal transport (Buggia-Prévot *et al.* 2014) and add to the work describing differential Aβ production between presynaptic and postsynaptic compartments (DeBoer *et al.* 2014; Wang *et al.* 2009b).

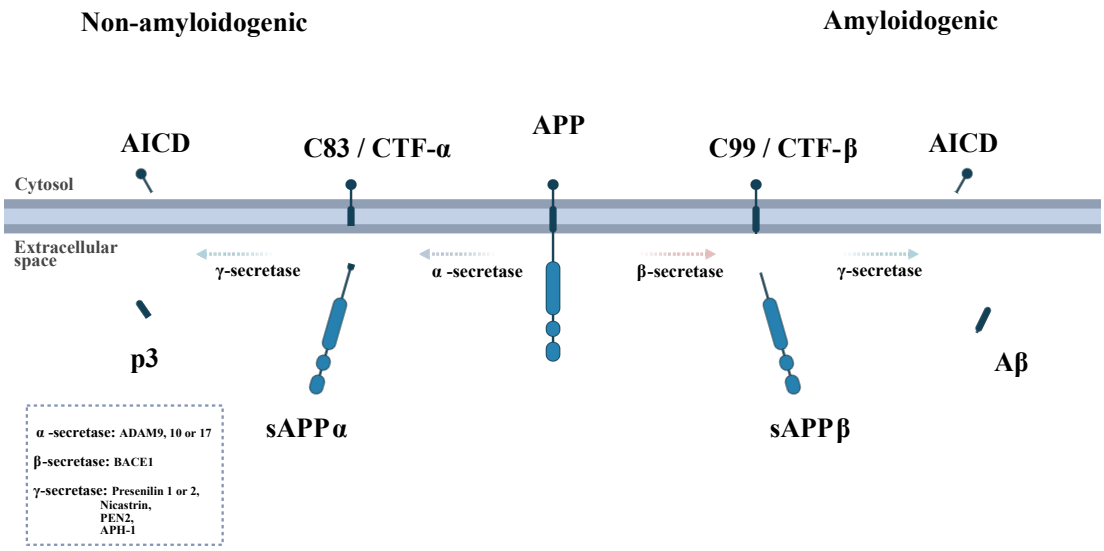

Figure 1.1: **Pathways involved in amyloid precursor protein (APP) processing.** Amyloid precursor protein (APP) is a single transmembrane protein. In the non-amyloidogenic pathway (left), it is cleaved by a disintegrin and metalloprotease (ADAM) proteases, producing the membrane-bound C83 fragment and extracellular soluble APP alpha (sAPPα). In the amyloidogenic pathway (right), beta-site APP cleaving enzyme 1 (BACE1) cleavage generates CTF-β, which is further processed by γ-secretase (Presenilin 1/2, Nicastrin, PEN2 and APH-1), releasing extracellular amyloid β (Aβ) and intracellular APP intracellular domain (AICD). Created with BioRender.com.

1.1.2 Tau

Tau is the name given to a series of proteins, derived from alternate splicing of the microtubule-associated protein tau (MAPT) gene, that are involved in microtubule stabilisation (Murphy, Johnson, and Borisy 1977; Trinczek *et al.* 1995). Although previously believed to be 'axon-specific', this is incorrect as tau proteins aid tubulin integration within the microtubule and provide structure and flexibility in neuronal somata, dendrites, axons and synapses, as well as in glial cells (Kanaan 2024). Tau protein isoforms are differentiated by their number of binding domains, and all act as phosphoproteins, with phosphorylation negatively regulating their capacity to stimulate microtubule construction (Buée *et al.* 2000; Mandelkow *et al.* 1995).

The intracellular accumulation of aggregated tau fibrils, referred to as "tauopathy", typically occurs following hyperphosphorylation of tau proteins by abnormal kinase activity (see Fig. 1.2) (Alonso *et al.* 2001; Noble *et al.* 2013). The hyperphosphorylated proteins remove themselves from the microtubule scaffold, adding to the pool of "free" tau within cells. Subsequent phosphorylation of this soluble tau leads to enhanced fibrinogenation and the self-assembly of the AD hallmark NFTs within neurites (Hanger, Anderton, and Noble 2009; Hanger *et al.* 2007; Johnson and Stoothoff 2004). It should be noted however that NFT formation is not unique to AD, and is also found in other neurodegenerative disorders, such as frontotemporal dementia (Bigio *et al.* 2001; Jiang *et al.* 2000; Rizzu *et al.* 1999), Parkinsonism-dementia complex of Guam (Arif *et al.* 2014; Qi *et al.* 2023; Steele 2005), Huntington's disease (St-Amour *et al.* 2018; Fernández-Nogales *et al.* 2014; Vuono *et al.* 2015), among others (Cummings *et al.* 2023b; Langerscheidt *et al.* 2024; Momota *et al.* 2022). Tauopathic cell disruption has two primary theorised mechanisms of pathology, which are not mutually exclusive; breakdown of the microtubule fast axonal transport starves cell extremities of nutrients, leading to the degradation of neural projections (Mandelkow *et al.* 2003; Reddy 2011; Roy *et al.* 2005), and physical impedance of intracellular functions by NFTs, stimulating attempted autophagic clearance of the excess tau, resulting in neurite damage (Gendron and Petrucelli 2009; Keck *et al.* 2003; Rodríguez-Martín *et al.* 2013).

Despite their presence being required for a definitive clinical diagnosis of AD (Braak and Braak 1991; Braak *et al.* 2006), the role of NFTs in AD pathogenisis remains unclear. While strongly associated with synaptic dysfunction, no causal relationship has been established, and NFT formation may reflect a protective or compensatory response to underlying disease processes (Arendt, Stieler, and Holzer 2016; Langerscheidt *et al.* 2024; Sexton *et al.* 2022). To support this, NFTs have been detected in healthy individuals, with pregnant neurons observed to survive for decades (Morsch, Simon,

and Coleman 1999). Tau, rich in lysine-serine-proline domains, can act as an oxidative sponge, taking the majority of oxidative damage within the neuronal process upon itself (Wataya *et al.* 2002). Finally, the aggregatory function of individual tau filaments may allow tangles to protect the cells in which they accumulate, like other intracellular inclusions (Chen *et al.* 2011; Taylor *et al.* 2003). For example, inclusion-body formations, consisting of Huntington aggregates, promote resistance to neurodegeneration in Huntington's disease cell cultures (Arrasate *et al.* 2004).

Pathogenic or otherwise, NFTs are an integral part of AD symptomology, with the AD brain containing approximately four times more hyperphosphorylated tau than a "healthy" aged adult brain.

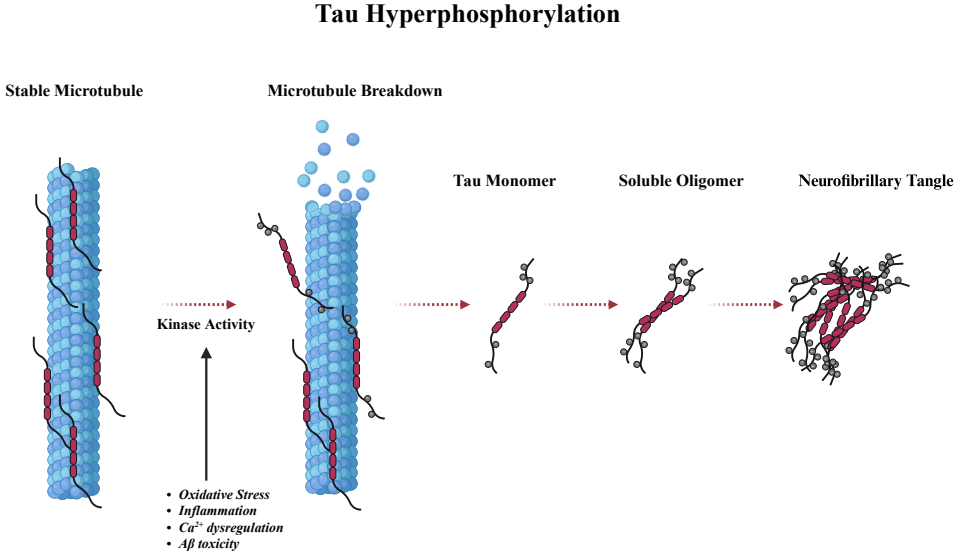

Figure 1.2: **Tau hyperphosphorylation and tangle formation.** Tau is a microtubule-associated protein that stabilizes axonal microtubules. Under pathological conditions, Tau becomes hyperphosphorylated by kinases such as GSK-3β and CDK5, reducing its affinity for microtubules. This leads to microtubule destabilization and Tau mislocalization. Further unchecked phosphorylation leads to the formation of toxic aggregates including neurofibrillary tangles (NFTs) in the cytoplasm. Created with BioRender.com.

1.2 Presenilin

First identified in genetic screens for mutations in EOFAD patients (Sherrington *et al.* 1995), the presenilins are a family of proteins with six to nine transmembrane domains (Levy-Lahad *et al.* 1995). Existing in two main forms, PSEN1 and presenilin 2 (PSEN2) are highly homologous (Rogaev *et al.* 1995) but differ in their subcellular locations. PSEN1 is broadly distributed across multiple compartments of the secretory and endocytic pathways, including the endoplasmic reticulum, Golgi apparatus, and plasma membrane, whereas PSEN2 localises predominantly to late endosomes and lysosomes (Annaert *et al.* 1999; Sannerud *et al.* 2016; Wolfe and Yankner 2016). It is difficult to discuss the physiological role of the presenilins without mentioning their association with AD. Since their discovery was due to AD research, almost all subsequent studies on presenilins have focused on their involvement in neurodegenerative pathogenesis. A 2013 study reported Alzheimer's initial patient Auguste Deter had a c.526T->C point mutation within the *PSEN1* gene following targetted exon sequencing of paraffin embedded tissue samples (Müller, Winter, and Graeber 2013). This finding was, however, quickly disputed by a subsequent study that attempted to validate the reported mutation but found no evidence of nonsynonymous hetero- or homozygous mutations in the exons of APP, *PSEN1*, or *PSEN2*, concluding that further investigation was required (Rupp *et al.* 2014).

As mentioned previously, the presenilins form the catalytic core of the γ-secretase protease complex (see Fig. 1.3). In addition to APP, in excess of 140 γ-secretase substrates have been identified to date, including Notch, CD44 and E-cadherin (Güner and Lichtenthaler 2020; Hou *et al.* 2023). γ-secretase-dependent involvement of presenilin mutations in AD pathogenesis was believed to be due to the impedence of the cleavage of longer Aβ peptides, increasing the ratio of Aβ42/Aβ40 length protein fragments. However, a complete analysis of 138 presenilin 1 pathogenic mutations however, illustrated that 55 of the mutations that had been examined decreased Aβ42/Aβ40 ratio, while 42 of the mutations completely abolished Aβ42 and Aβ40 production altogether (Sun *et al.* 2017).

Aside from their γ-secretase role, also referred to as their carboxypeptidase function, presenilins have highly conserved γ-secretase-independent regulatory/trafficking functions, including autophagy, lysosomal functioning and wingless-related integration site (Wnt) signalling (Coen *et al.* 2012; Saura 2010). Another pertinent γ-secretase-independent role of presenilin is related to endoplasmic reticulum (ER) calcium homeostasis. Specifically, Tu et al., (2006) proposed that healthy holoprotein presenilins act as passive Ca^{2+} "leak" channels across the ER membrane (Tu *et al.* 2006). Significantly, however, some

mutated presenilins do not maintain this ability, disrupting Ca^{2+} homeostasis within AD cells (Tu *et al.* 2006).

PSEN1 and 2 can also modulate intracellular ryanodine receptor (RyR) behaviour, with a reduction in the PSEN1/2 ratio increasing intracellular Ca^{2+} release by RyRs (Payne *et al.* 2013). These receptors are key intracellular calcium channels that mediate calcium-induced calcium release from the endoplasmic reticulum, playing a crucial role as an amplifier in cellular signalling, synaptic transmission, and calcium homeostasis.

Presenilins exert their influence on both "healthy" ageing brains, and AD brains, with *PSEN* mutations observed in brains of individuals with EOFAD mimicking non-functioning presenilins that occur during "normal" ageing (Sama and Norris 2013). The role of calcium homeostasis in ageing and AD will be addressed in a later segment (section 1.3.1), but increasing evidence suggests a link between mutant presenilins and disruption of Ca^{2+} homeostasis in neurodegenerative pathologies (Makarov *et al.* 2023; Ryan *et al.* 2021).

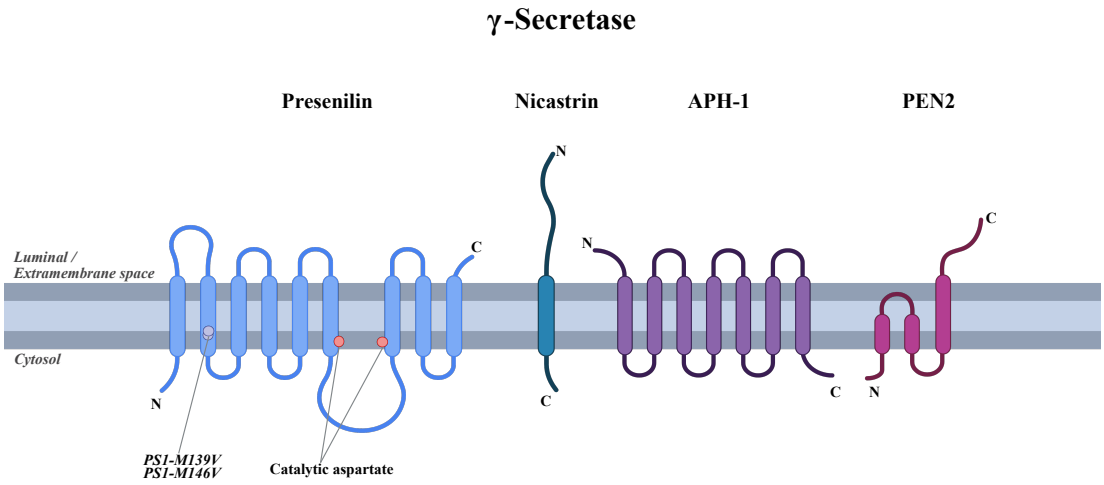

Figure 1.3: **γ-secretase complex.** γ-secretase is a multi-subunit intramembrane protease complex composed of Presenilin 1 or 2 (catalytic core), Nicastrin (substrate recognition), APH-1 (structural support and complex stability) and PEN2 (complex maturation). The complex resides in the lipid bilayer of several organelles and mediates the final cleavage of APP, releasing Aβ into the extracellular space. Created with BioRender.com.

1.2.1 Presenilins in Mitochondrial Function

In 2009, it was reported that PSN1 is highly enriched in mitochondria-associated endoplasmic reticulum membranes (MAMs) (Area-Gomez *et al.* 2009). While presenilin mutants had previously been considered to affect mitochondria via the amyloid cascade (see section 1.3.3), their enrichment in MAMs suggests a potential for direct effects on the critical functions of these domains, including phospholipid biosynthesis, cholesterol esterification, calcium transport, and the maintenance of mitochondrial and ER homeostasis (Area-Gomez 2014; Area-Gomez *et al.* 2009; Hayashi *et al.* 2009). A study by Han *et al.* investigated how five PSN1 mutations (A431E, E280A, H163R, M146V, and Δexon9) affected mitochondrial function in H4 glioblastoma cells (Han *et al.* 2021). While all mutants showed decreased γ-secretase activity, indicated by the accumulation of APP-CTFs, they each exhibited distinct profiles of mitochondrial dysfunction. The Δexon9 mutant induced mitochondrial fragmentation, whereas A431E, E280A, H163R, and M146V mutants increased MAMs formation. A431E, E280A, M146V, and Δexon9 mutants also promoted mitochondrial reactive oxygen species (ROS) production. The A431E mutant impaired both complex I and peroxidase activity, while the M146V mutant impaired only peroxidase activity. All PSN1 mutants compromised mitochondrial membrane potential, and cellular adenosine triphosphate (ATP) levels were reduced in cells expressing the A431E, M146V, and Δexon9 mutations.

Mitochondrial morphology and intracellular distribution are frequently disrupted in AD neurons (Baloyannis 2006; Tyumentsev *et al.* 2018; Zhang *et al.* 2016), with shortened mitochondria indicative of enhanced fission, and reduced localisation outside the soma suggesting impaired organelle trafficking (Wang *et al.* 2009a, 2008). In SH-SY5Y cells, the presenilin 2 (PSN2) D439A mutation significantly decreased expression of the GTPase regulator rho guanine nucleotide exchange factor 5 (ARHGEF5), and reduced the GTPase activity of mitochondrial Rho GTPase 2 (Miro2), a key mediator of mitochondrial transport (Gao *et al.* 2024). PSN2 was also found to bind directly to Miro2, and the D439A mutation diminished this interaction, leading to decreased Miro2 expression. However, experiments in PSN1 knockdown and PSN2 knockout neurons and astrocytes, derived from Cre/flox mice models, did not recapitulate the mitochondrial phenotypes observed in the immortalized cell lines (Contino *et al.* 2021). As with many aspects of AD pathomechanistic mapping, findings remain inconsistent across species and model systems. Further investigation is required to clarify the amyloid-independent roles of presenilins in mitochondrial homeostasis.

1.2.2 Presenilins in Cellular Timing

PSEN1 plays a crucial role in stem cell differentiation, particularly in the context of neurogenesis and neural cell fate specification (Feng *et al.* 2001; Handler, Yang, and Shen 2000). Neural progenitor cells (NPCs) are a type of stem cell found in the adult brain, specifically within the subventricular zone (SVZ) and the subgranular layer (SGL) of the dentate gyrus. These neurogenic niches support the self-renewal, proliferation, and differentiation of NPCs into neurons and glia throughout life (Fuentealba, Obernier, and Alvarez-Buylla 2012). Previous studies using genetic mouse models have demonstrated that PSN1 is essential for neuronal differentiation during neural development such that PSEN1 knockout mice showed a severe reduction in the number of NPCs and impaired interkinetic nuclear migration, a process critical for NPC proliferation (Kim and Shen 2008). Further research using lentiviral vectors to knock down PSEN1 expression in adult mouse brain NPCs revealed a dramatic enhancement of cell differentiation, with PSN1-deficient cells differentiating into neurons, astrocytes, and oligodendrocytes. This function of PSEN1 is γ-secretase-dependent, as neurosphere cultures treated with γ-secretase inhibitors similarly exhibited enhanced cell differentiation. Although these findings suggest an inhibitory regulatory role for PSN1 in differentiation, PSN1 actively promotes self-renewal and maintains NPC multipotency by ensuring adequate Notch-dependent self-renewal signalling (Hernández-Sapiéns *et al.* 2021; Veeraraghavalu *et al.* 2010; Zhou *et al.* 2022).

Furthermore, PSEN1 regulates NPCs by modulating the signalling pathways of proliferation factors such as epidermal growth factor (EGF) and basic fibroblast growth factor (bFGF) (Gadadhar, Marr, and Lazarov 2011; Tang, Yu, and Cheng 2017). Reduced expression of PSEN1 in NPCs leads to decreased levels of the EGF receptor and β-catenin, indirectly contributing to impaired progenitor maintenance (He and Shen 2009). Through its γ-secretase-mediated carboxypeptidase activity, PSN1 is responsible for the intramembrane cleavage of Notch receptors, releasing the Notch intracellular domain, which translocates to the nucleus to act as a transcriptional activator. Mutations in presenilin genes disrupt the γ-secretase cleavage of Notch, impairing the Notch signalling pathway and altering cellular timing (Fortini 2001; Hernández-Sapiéns *et al.* 2021). Notch signalling is critical for cell fate decisions, particularly through lateral inhibition, a process that ensures neighbouring cells adopt distinct identities, thereby generating cellular diversity (Sancho, Cremona, and Behrens 2015). Proper timing of Notch receptor activation and subsequent cleavage is essential for the accurate execution of these decisions, as premature Notch activation can lead to inappropriate differentiation, ultimately affecting the overall cellular composition and timing of neurogenesis (Ehebauer, Hayward, and Arias 2006; Trylinski, Mazouni, and Schweisguth 2017).

In addition to Notch signalling, recent research has implicated APP itself in the regulation of neurogenic timing. In a study of human cortical development, APP knockout selectively impaired the slower-tempo cortical neurogenesis, without affecting the faster motor neurogenesis (Shabani *et al.* 2023). Quantitative analysis revealed that, after seven days of differentiation, control NPCs produced on average eight progenitors and 3.6 neurons per cell, whereas APP-deficient NPCs produced only 1.25 progenitors but 22.9 neurons. This shift from a self-renewing to a neurogenic state suggests that APP is critical for the absolute temporal scale of cortical neurogenesis, although it does not alter the relative birth order of cortical neurons. To date, no equivalent temporal mapping has been conducted for PSEN1 or PSN2 knockouts during human cortical neurogenesis. While both *in vivo* and *in vitro* studies of mouse NPCs lacking APP have shown inconsistent effects on neurogenesis (Cappello *et al.* 2016; Hu *et al.* 2013; Ma *et al.* 2008), the findings from human systems highlight the need for further investigation into how presenilin mutations influence neurogenic timing. As we now know from the work of Shabani *et al.*, premature differentiation does not inherently imply accelerated maturation and/or ageing of post-mitotic neurons(Shabani *et al.* 2023), currently assumed in presenilin defects.

Taken together, it is worth considering that key 'Alzheimer's disease-associated proteins' are not only involved in classical pathogenic cascades but also play pivotal roles in regulating the timing of neurogenic maturation. This convergence of AD-linked genes on developmental temporal control mechanisms raises the possibility that alterations in the pace and regulation of neurogenesis may constitute a uniquely human vulnerability. The protracted, neotenous trajectory of human cortical development, characterised by extended periods of neural progenitor self-renewal, delayed differentiation, and protracted synaptogenesis (Libé-Philippot *et al.* 2024; Linker *et al.* 2022), may amplify the pathological consequences of dysregulated temporal signalling. In this light, the human-specific elongation of neurogenic programs may help explain why AD manifests so prominently and distinctively in humans, and not in other species with faster and less plastic neurodevelopmental timelines.

1.3 Alternative Aetiological Hypotheses

As previously noted, while the ACH has been the dominant hypothesis describing AD pathogenesis for many years (Behl 2024; Selkoe and Hardy 2016), an ever-growing body of research highlights the possible involvement of numerous other factors that may contribute to AD onset and progression. These alternative hypotheses span a diverse range of mechanisms, including altered calcium signalling (Berridge 2010; Mattson *et al.* 1992), chronic inflammation (Kinney *et al.* 2018; McGeer *et al.* 1988), infectious agents (Itzhaki *et al.* 1997; Seaks and Wilcock 2020), metabolic disturbances (Hoyer 1998; Morgen and Frölich 2015), intracellular trafficking and endo-lysosomal dysfunction (Nixon 2000; Perdigão *et al.* 2020), and vascular impairment (de la Torre 2004; Scheffer *et al.* 2021), each of which has been proposed to contribute to the multifactorial pathobiology of AD.

The diversity of aetiological hypotheses, and their relative weight within the research community, can be illustrated by the number of clinical trials conducted under each framework. Liu *et al.*'s (2019) review provides a comprehensive summary of the AD clinical trial landscape at the time and remains a highly cited source (see Fig. 1.4 A) (Liu *et al.* 2019). Since 2016, Prof. Jeffrey Cummings, an eminent scientist and clinician based at the University of Nevada Las Vegas, has annually published the "Alzheimer's Disease Drug Development Pipeline" report in collaboration with the Alzheimer's Association. Although the report is based solely on the ClinicalTrials.gov registry maintained by the US National Library of Medicine under the National Institutes of Health (NIH), it captures all trials conducted in the United States, which remains the leading region globally for AD clinical research activity (Cummings *et al.* 2025a). Moreover, many trials conducted outside the US are also registered there, despite not being legally required to do so. Analysis of the proportion of trials associated with each Common Alzheimer's Disease Research Ontology (CADRO) mechanism of action offers insights into both the expanding range of AD hypotheses and the distribution of clinical research focus among them (see Fig. 1.4 B).

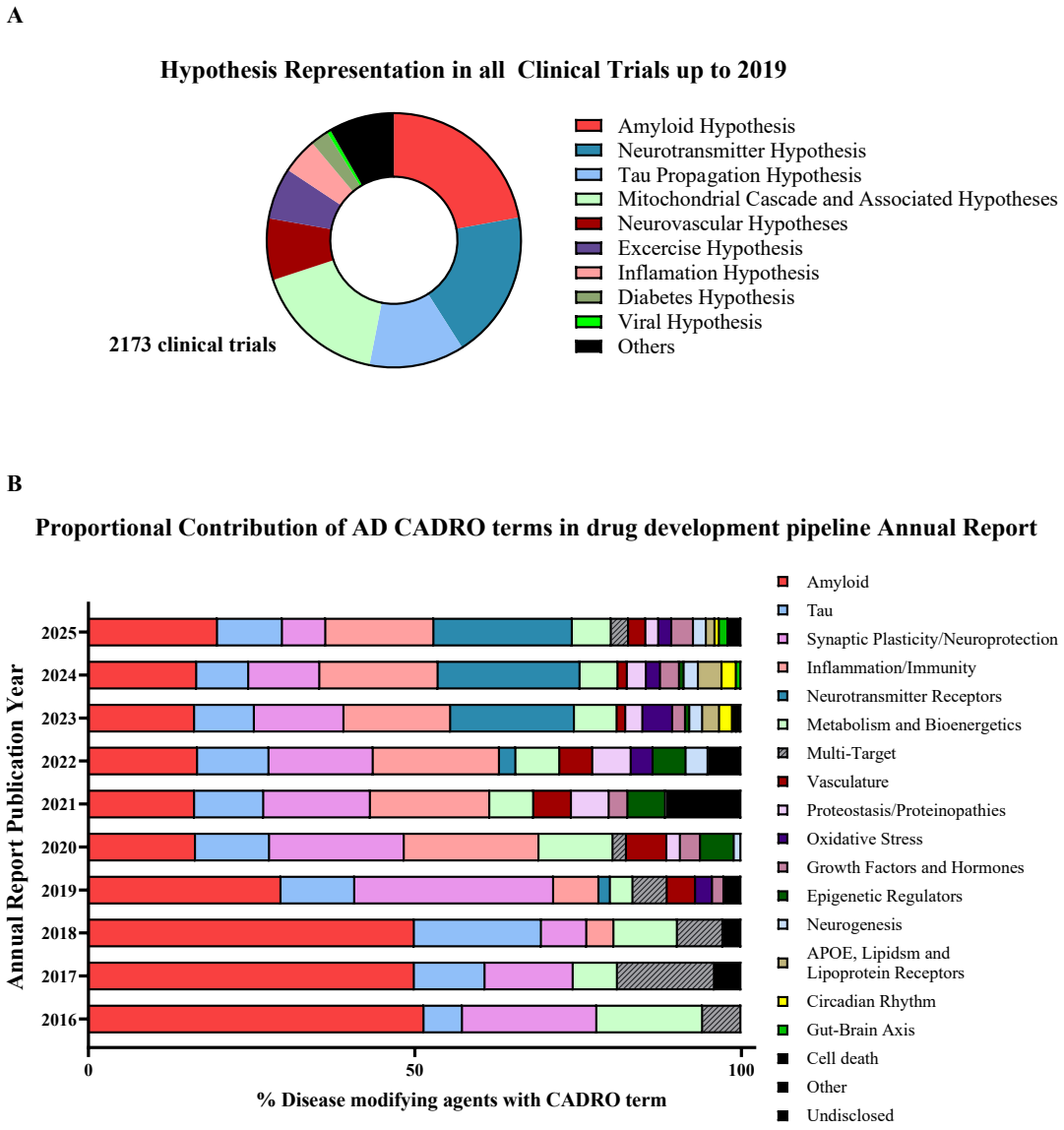

Figure 1.4: **Overview of AD hypothesis variation and clinical trial focus. A**: Pie chart illustrating the proportion of AD specific clinical trials up until 2019 focused on each hypothesis of AD pathology. Adapted from Liu *et al.* (2019) (Liu *et al.* 2019). **B**: Original stacked bar chart representing the proportion of disease-modifying agents under clinical trial possessing a given CADRO mechanism of action classification, reported in a given year. Data were extracted, aggregated, and reclassified by the author from the Alzheimer's disease drug development pipeline annual reports published by Prof Cummings and colleagues (Cummings *et al.* 2017, 2022, 2019, 2020, 2018, 2021; Cummings, Morstorf, and Lee 2016; Cummings *et al.* 2023a, 2024; Cummings *et al.* 2025b). Figure created in GraphPad Prim v10.4.

1.3.1 The Calcium Hypothesis

The calcium hypothesis of AD (Alzheimer's Association Calcium Hypothesis Workgroup *et al.* 2017) posits that altered intracellular calcium handling links amyloid metabolism to both cognitive dysfunction and neurodegeneration in AD.

1.3.1.1 Calcium Signalling

Calcium is often considered to be the 'king' of intracellular signalling, with regulatory control over an array of cellular processes, including cell proliferation, neurotransmitter secretion, inter-organelle communication, gene transcription, metabolic regulation, and the induction of programmed cell death pathways such as apoptosis (Berridge 1995; Berridge, Lipp, and Bootman 2000; Gill, Ghosh, and Mullaney 1989). To facilitate this multitude of functions, a versatile Ca^{2+} signalling 'toolkit' is required, made up of second messengers, channels, pumps and sensors (see Fig. 1.5)(Berridge, Bootman, and Roderick 2003). For example, neuronal excitation produces an intracellular Ca^{2+} signal; this signal can be differentiated from others, and thus only activate its target pathway, due to its possession of unique characteristics, such as its amplitude, duration, frequency, and intracellular location (Balaji *et al.* 2017). Calcium spikes, defined as transient increases in cytosolic Ca^{2+} concentration, can arise through the activation of influx pathways or due to release from intracellular stores can be utilised in local nanodomains, and in the whole cell body. Additionally, inhibited efflux or buffering mechanisms can result in sustained elevations or delayed decay of cytosolic Ca^{2+} signals. Calcium's utility is due to these varying cytosolic concentrations, which are the result of tightly regulated channels connecting extra- and intra-cellular molecular pools (Berridge, Lipp, and Bootman 2000). A constant equilibrium between calcium influx and efflux across the plasmalemma exists in healthy cells, with cytosolic buffering proteins maintaining the 20,000-fold gradient between high extracellular Ca^{2+} and low intracellular free Ca^{2+}, that accommodates the high signalling speed of the cation (Bootman *et al.* 2001). Given this breadth of regulatory influence, even subtle disturbances in calcium homeostasis can have profound consequences for neuronal viability and function.

1.3.1.2 Intracellular Calcium Release

Ca^{2+} release from the ER occurs primarily via activation of IP_3Rs and/or ryanodine receptors (RyRs) in a highly regulated manner that is controlled by Ca^{2+}, ATP, kinases and phosphatases (Ivanova *et al.* 2014). RyRs and IP_3Rs, of which there are three subtypes each, differ significantly from one another in terms of their expression, localisation, activation mechanisms and physiological roles. Numerous tissues express multiple IP_3R isoforms, although IP_3R1 is enriched in neurons, IP_3R2 in the heart and liver, and IP_3R3 in lymphocytes and multiple cell lines. Neurons express all three

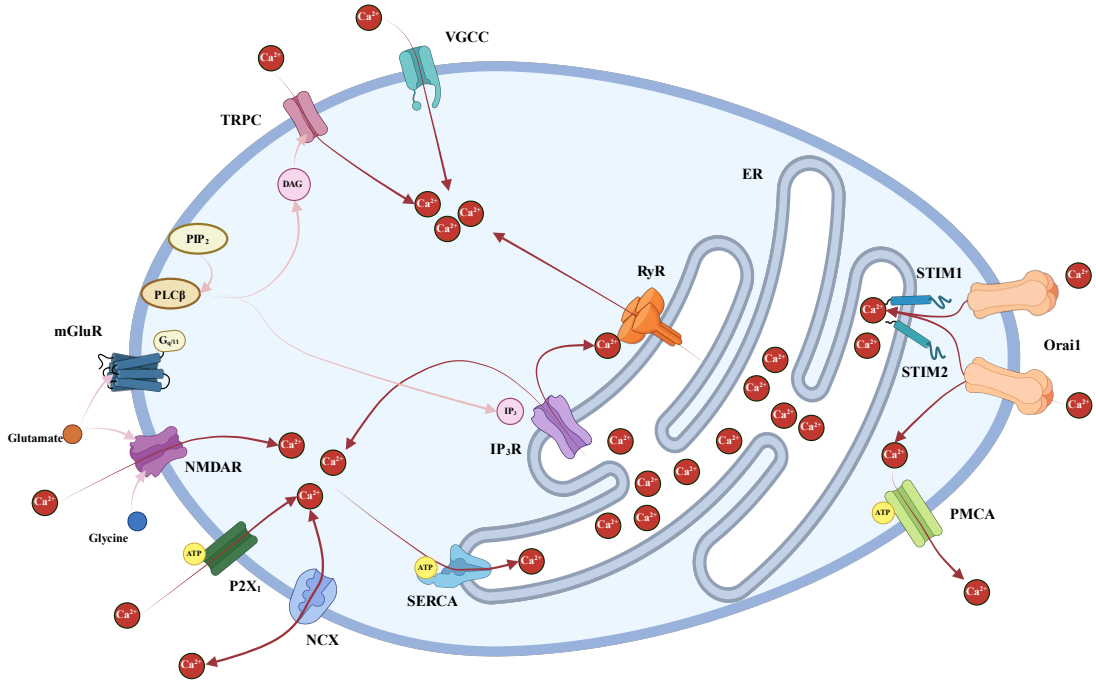

Figure 1.5: **Examples of the calcium toolkit within the cell.** Cartoon illustrating the movement of free Ca^{2+} between the intracellular, extracellular and organellar spaces, by means of pumps (SERCA, PMCA, $P2X_1$), ligand gated channels (inositol trisphosphate receptor (IP_3R), N-Methyl-D-aspartic acid receptor (NMDAR), transient receptor potential cation channel (TRPC), metabotropic glutamate receptor (mGluR)), voltage-gated calcium channels (VGCCs), calcium-induced calcium release channels (RyR) and unidirectional-exchangers (sodium-calcium exchanger (NCX)). Second messengers (IP_3, DAG), and store operated calcium entry facilitatory proteins (STIM, Orai1) are also highlighted. Inspired by Lichtman et al., 2017 (Lichtman *et al.* 2017), created with BioRender.com.

subtypes of both RyRs and IP_3Rs, although IP_3R1 and RyR2 expression predominate (Berridge, Bootman, and Lipp 1998; Franzini-Armstrong and Protasi 1997; Furuichi *et al.* 1994). RyR2 is distributed widely in the brain, RyR3 expression is predominant in the CA1 hippocampal region and RyR1 is almost exclusively expressed in cerebellar Purkinje cells (Furuichi *et al.* 1994). Generally, IP_3R and RyRs colocalise on subsurface cisternae originating from the ER and are distributed throughout the compartments of the neuron (Fagni *et al.* 2000) including axonal endings and dendritic spines (Berridge, Bootman, and Lipp 1998; Sharp *et al.* 1993). Aside from this general pattern of co-localisation, RyRs are also distinctly localised to the soma of neurons. Furthermore, in the CA3 and hilar hippocampal regions, as well as in the cerebral cortex, RyRs are more prominently expressed at dendritic spines than IP_3Rs (Finch and Augustine 1998; Sharp *et al.* 1993). N-Methyl-D-aspartic acid receptor (NMDAR), a glutamate receptor and

key Ca^{2+} channel in neurons (Jewett and Thapa 2025), is essential for synaptic plasticity. In addition to facilitating influx of Ca^{2+} and Na^{+}, NMDAR-mediated signalling can trigger intracellular Ca^{2+} through IP_3R and RyR via activation of phospholipase C and Ca^{2+}-induced calcium release (CICR) mechanisms (Goussakov, Miller, and Stutzmann 2010).

1.3.1.3 Calcium Dysregulation

Calcium handling within cells of the brain changes with ageing and is thought to be a prime factor in age-dependent cognitive decline (Datta *et al.* 2021; Moore *et al.* 2023; Uryash *et al.* 2020). Alterations in voltage-gated calcium channel (VGCC) mediated Ca2+ influx and rapid Ca2+ buffering compensation have been observed in ageing rat models (Murchison and Griffith 2007). As previously mentioned (see section 1.1), "age-typical" cognitive deterioration, including calcium handling, is intensified in AD, possibly due to mismanagement of amyloid processing. Further, a feed-forward relationship exists between calcium dysregulation and Aβ/NFT pathology (Kuchibhotla *et al.* 2008; Wang *et al.* 2005; Yamamoto *et al.* 2005), with disruption of neuronal calcium homeostasis further exacerbating amyloidogenic Aβ metabolism *via* ROS production (D'Alessandro *et al.* 2025; Liu *et al.* 2018; Quintana *et al.* 2020), whilst accumulation of Aβ oligomers and tau proteins provoke further calcium dysregulation by the breakdown of intracellular proteins and lipid transport (Mahoney *et al.* 2020; Malchiodi-Albedi *et al.* 2011; Small *et al.* 2009). The basis of the 'Calcium Hypothesis of AD' is the induction of pathology by the sporadic breakdown of the calcium regulatory machinery, long before clinically detectable "hallmark" symptoms arise.

In 2002, the non-competitive N-Methyl-D-aspartic acid (NMDA) receptor antagonist memantine, was approved for sale and clinical use in Europe for the treatment of AD (Reisberg *et al.* 2003). Its proposed mechanism of action involves low-affinity, uncompetitive antagonism of the NMDA receptor, producing a voltage-dependent blockade of excessive Ca^{2+} influx during pathological glutamatergic signally, thereby reducing the potential for glutamate-induced excitotoxicity in the brain (Johnson and Kotermanski 2006; Kuns *et al.* 2025). Memantine was considered one of the rare exceptions to the general failure of drug treatments in neurodegenerative disease, consistently demonstrating restorative and prophylactic properties in AD animal models (Karimi Tari *et al.* 2024). However, its efficacy has been called into question over time. Meta-analyses have yielded mixed results, and in 2012, the French Pharmacoeconomic Committee downgraded its rating of medical benefit in AD from "major" to "low" (Blanco-Silvente *et al.* 2018; "Drugs for Alzheimer's Disease" 2012). An interesting cellular agent in the context of the calcium hypothesis of AD is caffeine. Caffeine promotes Ca^{2+} efflux

from the ER *via* activation of RyRs (Arias-Cavieres *et al.* 2018; Kong *et al.* 2008), potentially mitigating the calcium store overload often observed in neurodegenerative conditions (Kolahdouzan and Hamadeh 2017; Smith *et al.* 2005). Interestingly, cohort studies are demonstrating coffee and/or tea consumption is associated with slower cognitive decline (Gardener *et al.* 2021; Wang *et al.* 2024a).

1.3.2 The Endo-Lysosomal Hypothesis

Disruptions of the endocytic trafficking pathway are the earliest detectable AD pathologies currently recognized but are often not even a footnote in the general study of AD (Nixon 2017). The so-called Endo-Lysosomal theory of AD proposes that AD progression may be due to disruptions of neuronal intracellular trafficking that lead to the retention of toxic substrates, starvation of cell regions of essential components/proteins, and/or impaired intracellular signalling (Chung, Lee, and Lee 2018; Correia, Perry, and Moreira 2016; Tang 2009; Wang *et al.* 2013). This Endo-Lysosomal theory is supported by a collection of genetic, anatomical and biochemical evidence summarised below.

1.3.2.1 Intraneuronal Cell Trafficking

Neuronal function is intimately linked to the geometric morphology of the cell (Chklovskii 2004). The soma integrates inputs from multiple dendrites and transmits signals through axonal processes (Ramón y Cajal 1904). To sustain this complex structure-function relationship, neurons depend on an intricate intracellular trafficking system to maintain cellular health and function (Wang *et al.* 2013). This system, which can be likened to a city, includes highways, loading docks, transport vehicles, and regulatory mechanisms that ensure smooth intracellular logistics.

Intracellular directionality is largely governed by polarised microtubules, which dynamically assemble to provide structural support and serve as tracks for cargo transport (Desai and Mitchison 1997; Stephens and Edds 1976). Composed of tubulin, microtubules have a fast-growing ‘positive’ end and a more stable ‘negative’ end (Howard and Hyman 2003). Axonal microtubules are uniformly oriented with their positive end distal to the soma and predominantly bind tau. In contrast, dendritic microtubules exhibit mixed polarity and primarily associate with microtubule associated protein 2 (MAP2) (Baas *et al.* 1988; Conde and Cáceres 2009; Cooper 2000). Interwoven with the microtubule network is the actin cytoskeleton, which forms shorter filaments with polarised ends, with ATP-dependent polymerisation occurs preferentially at the positive

end (Letourneau 2009). Actin filaments interface with the plasma membrane and act as peripheral sites for docking and cargo capture, supporting transport and local organisation (Hasaka, Myers, and Baas 2004). Motor proteins utilise these cytoskeletal tracks to transport organelles and macromolecules. The primary motor families include kinesins, dyneins, and myosins (Cheney and Baker 1999; Hirokawa 1998; Karki and Holzbaur 1999). Kinesins mediate anterograde transport toward the microtubule positive end (Pfister *et al.* 1989), while dyneins facilitate retrograde transport toward the negative end (Paschal, Shpetner, and Vallee 1987). Myosins, although more commonly associated with muscle contraction, move along actin filaments and support short-range transport and tethering of organelles (Hammer and Wagner 2013).

Critical to this system is the cargo itself, organelles such as mitochondria and endosomal vesicles must be accurately positioned to perform localised functions (Yap and Winckler 2012). Given that most organelles and proteins are synthesised in the soma, while endocytic uptake occurs at distal neuronal processes, efficient and regulated cargo transport is essential. Endocytic vesicles formed at the membrane follow actin filaments to converge and generate early endosomes (Doherty and McMahon 2009; Kirchhausen, Owen, and Harrison 2014; Mayor and Pagano 2007). These endosomes serve as sorting hubs, directing cargo for recycling, lysosomal degradation, or incorporation into multivesicular bodies destined for long-range transport (Hurley *et al.* 2010).

1.3.2.2 Endo-lysosomal Disruption

Meta-analysis of large cohort genome-wide association studies have brought to light over 20 susceptibility loci for LOAD (Jansen *et al.* 2019; Lambert *et al.* 2013) including, but not limited to, BIN1, CD2-AP, PICALM, and SORL1, all of which are associated with cell trafficking and endocytosis (Gauthier *et al.* 2007; Klinger *et al.* 2016; Kobayashi *et al.* 2004; Sahlender *et al.* 2013; Wigge *et al.* 1997).

The strongest genetic risk factor for LOAD, Apolipoprotein E (ApoE)-ε4, is also involved in lipid endocytosis (Faraji, Kühn, and Ahmadian 2024; Haney *et al.* 2024). Although its exact role in AD progression has still to be fully elucidated, ApoE-ε4 expression is known to impair Aβ clearance (Wildsmith *et al.* 2013), promote intracellular retention of AMPA and NMDA receptors (Chen *et al.* 2010). This hampers synaptic plasticity, and alters lipid metabolism which, in turn, affects membrane trafficking (Rapp, Gmeiner, and Hüttinger 2006). Therefore, the often-cited "genetic complexity" of AD (Andrews *et al.* 2023; Rogaeva, Kawarai, and George-Hyslop 2006), which may explain the failings of most hypotheses reliant on a single-mechanism or single-target, a

so-called ‘silver bullet’, supports the Endo-Lysosomal theory.

Enlargement of Rab5-positive early endosomes, and upregulated Rab5 and related protein gene expression are signature “endosomopathies” of AD neurons, with early endosomal enlargement not occurring in regular brain-aging or other neurodegenerative diseases (Cataldo *et al.* 2000; Urwin *et al.* 2009). Endocytic disruption does occur in sporadic AD patient brain regions prior to Aβ or tau ingress (Jaye, Sandau, and Saugstad 2024), this is supported by Down syndrome model mouse foetal tissues showing signs of pathway disruption (Cataldo *et al.* 2003, 2004; Hibaoui *et al.* 2014). The transition from Rab5 presence to another GTPase, Rab7, on the endosomal membrane demarks the change in endosomal function and classification (*i.e.* early to late) in a process called the Rab cascade (Borchers *et al.* 2023; Borchers, Langemeyer, and Ungermann 2021). Faults during factor-recruitment, or step completion can lead to disruptions of the entire endocytic pathway. In this regard, Xu et al,. (2016) have investigated the pathogenic mechanism of early endosomal growth within AD and Down syndrome (Xu *et al.* 2016). They found that both full-length APP and its β-secretase-cleaved form, CTF-β, increase Rab5 activation. This, in turn, causes early endosomal enlargement and a subsequent decline in neuronal growth factor transport and signalling within cultured mouse basal forebrain cholinergic neurons. CTF-β recruits APPL1, which stabilizes Rab5 in its active GTP-bound state, prolonging Rab5 activity (Kim *et al.* 2016). Completing the destructive positive feedback loop, isolated Rab5-overexpression increases CTF-β concentration, and ensuing Aβ production (Grbovic *et al.* 2003). Expression levels of genes mapping Rab5 and Rab7 are selectively upregulated in CA1 neurons of patients with LOAD and mild cognitive impairment (Ginsberg *et al.* 2010).

The role of specific presenilin dysfunction within the Endo-Lysosomal theory is complex and requires further research. As described above, CTF-β is proposed to play a toxic role within AD pathogenesis. As such, loss-of-function presenilin mutations and age-related presenilin protein failure will reduce γ-secretase cleavage of CTF-β, possibly facilitating its stimulation of Rab5. The presenilins may also have an amyloid-independent effect on cellular trafficking as PSEN1 can interact directly with Rab6, Rab11 and Rab GDP dissociation inhibitors, which are all integral trafficking components (Dumanchin *et al.* 1999; Scheper *et al.* 2000; Scheper, Zwart, and Baas 2004).

1.3.3 Mitochondrial Cascade Hypothesis

Swerdlow & Kahn’s mitochondrial cascade hypothesis posits that neuronal APP expression and processing is altered by mitochondrial function (Swerdlow and Khan

2004). They were particularly interested in the 'random' occurrence of LOAD and sought to determine the differences within each individual that could lead to AD development. Within their model, individuals' basal mitochondrial function is genetically inherited. From this, their basal rate of reactive oxygen species (ROS) production, and therefore the pace at which acquired mitochondrial damage accumulates, is determined. This damage accumulation rate is further altered by environmental factors. The decline of mitochondrial function due to this accumulation propels ageing phenotypes (Kujoth *et al.* 2005; Ross *et al.* 2013; Trifunovic *et al.* 2004). The cell's response to this altered mitochondrial function induces AD pathology. APP has been repeatedly observed to localise within the mitochondria of post-mortem brain tissue in both AD and non-demented individuals (Devi *et al.* 2006; Vaillant-Beuchot *et al.* 2021; Walls *et al.* 2012). In animal and cell models major amyloidogenic processing components, mainly γ-secretase subunits, have also been repeatedly found within mitochondria (Behbahani *et al.* 2010; Hansson *et al.* 2004; Pavlov *et al.* 2011). Bio-energetic modulation by direct inhibition of glycolysis and/or mitochondrial respiration has been shown to alter APP glycosylation (Henriques *et al.* 2005), decrease sAPPα levels (Gasparini *et al.* 1999, 1997), and increase Aβ accumulation (Arias *et al.* 2002; Fu *et al.* 2015; Leuner *et al.* 2012), in many cell types.

However, APP processing may not be the only mechanism through which mitochondrial disruption could lead to AD. For example, neurons in AD display significantly elevated ROS-mediated damage and a marked reduction in mitochondrial number (Hirai *et al.* 2001). Excessive ROS production or inadequate antioxidant defence leads to oxidative stress upstream of the clinical onset of AD and the appearance of Aβ pathology (Uttara *et al.* 2009). Multiple *in vitro* and *in vivo* studies indicate a direct link between oxidative stress and neuronal dysfunction in AD (Kamat *et al.* 2016; Manczak *et al.* 2006). Notably, Aβ-mediated endocytosis lowers the surface expression of NMDA receptors in neuronal cultures and AD mouse models (Snyder *et al.* 2005), while excessive Aβ may also promote excitotoxicity and stress-related pathways by increasing intracellular Ca^{2+} influx (as discussed in section 1.3.1), exacerbating oxidative stress, and impairing energy metabolism (Bezprozvanny and Mattson 2008).

1.3.4 Inflammation Hypothesis

Chronic brain inflammation, or a heightened predisposition to entering an inflammatory state has become a central component in nearly all proposed mechanisms of AD development (Bagyinszky *et al.* 2017; Latta, Brothers, and Wilcock 2015; Phillips *et al.* 2014). In AD patients, microglia (CNS-specific macrophages) display higher activity

relative to control cells, and aggregate at higher concentrations near Aβ-plaques and NFTs when compared to healthy individuals (McGeer, Itagaki, and McGeer 1988). Transcriptomic analysis in a rodent model has even identified a specific microglia type associated with AD, conserved in both mice and humans (Keren-Shaul *et al.* 2017). Acute microglial activation plays a role in restoring brain homeostasis by removing dying cells, cellular debris (Sierra *et al.* 2010), and supporting neuronal survival (Giulian *et al.* 1994; Merlini *et al.* 2021). In-fact microglia play an active role in both neurodevelopment, neuroplasticity and neurogenesis, by stimulating growth factor release (Araki, Ikegaya, and Koyama 2021; Saw *et al.* 2020; Ueno *et al.* 2013) and synaptic pruning (Liu *et al.* 2021; Paolicelli *et al.* 2011)). However, prolonged or chronic microglial activation leads to the release of pro-inflammatory cytokines, such as interleukin-1β (IL-1β), interleukin-6 (IL-6) and tumour necrosis factor α (TNF-α) (Liddelow *et al.* 2017; Norden *et al.* 2016; Thakur *et al.* 2023). This 'reactive gliosis' can cause both general neuronal damage (Lull and Block 2010), and amyloid specific effects (Chun *et al.* 2018).

Longitudinal studies have shown that acute systemic inflammatory events elevate serum levels of proinflammatory cytokine TNF-α and a twofold acceleration in cognitive decline over a six-month period in participants with mild to severe dementia (Holmes *et al.* 2009). Furthermore, participants with consistently high baseline TNF-α levels exhibited a four-fold increase in the rate of cognitive decline. Subjects who had low levels of serum TNF-α throughout the study showed no measurable cognitive decline over the same period (Holmes *et al.* 2009). IL-6 overexpression has also been linked to memory deficits (Heyser *et al.* 1997; Wei *et al.* 2012; Zhao *et al.* 2024) and neuropathic pain (Chanda *et al.* 2025), with heightened participant IL-6 plasma-levels being associated with autism (Carpita *et al.* 2023), temporal lobe epilepsy (Peltola *et al.* 2023), schizophrenia and major depressive disorder (Frommberger *et al.* 1997; Yoshimura, Kishi, and Iwata 2019).

Outside of neurocentric evidence, some studies have shown that individuals with a history of certain autoimmune diseases and chronic infections, have a higher likelihood of developing AD (Diezma-Martín *et al.* 2024; Ramey *et al.* 2024). One larger nationwide cohort study assessing the relationship between all-cause-dementia, infection, and autoimmune diseases found that only infections had a dose-dependent association with increased dementia risk, suggesting that specific immune responses, rather than general systematic inflammation, contribute to neurocognitive decline (Janbek *et al.* 2023).

As with anti-viral treatment supporting the viral-hypothesis of AD (discussed below in section 1.3.5), substantial efforts have been made to assess the use of anti-inflammatories in reducing AD occurrence (Breitner *et al.* 2009; O'Bryant *et al.* 2018; Zandi and Breit-

ner 2001). The findings have been at best underwhelming. Phase III clinical trials of the non-steroidal anti-inflammatory (NSAID) drugs, naproxen and celecoxib, investigating their therapeutic efficacy in delaying AD onset were cancelled due to the drugs' failure to produce a benefit compared to placebo, while simultaneously increasing adverse event incidences (ADAPT Research Group 2007). Similarly phase III trials of lornoxicam were prematurely ended due to a lack of effect on cognitive decline (*EudraCT No. 2009-011098-34 (Lornoxicam Alzheimer Trial)-https://www.clinicaltrialsregister.eu/* 2025). One study, using negative binomial generalized linear mixed modelling of the Alzheimer's Disease Neuroimaging dataset (*Alzheimer's Disease Neuroimaging Initiative* 2025), was able to better assess commonly used NSAIDs and paracetamol in cognitive decline reduction (Rivers-Auty *et al.* 2020). Common medications, ibuprofen and aspirin were associated with higher baseline cognitive performance, but neither showed an effect on cognitive decline. Paracetamol was associated with an acceleration of cognitive decline, but the effect size was deemed negligible. Diclofenac alone was associated with a reduction in cognitive decline rate. As no other NSAID showed an effect, diclofenac's efficacy was unlikely due to common mechanisms such as COX inhibition.

1.3.5 Viral Activation Hypothesis

Since the early 1990s over 100 publications have proposed a connection between neural herpes simplex virus 1 (HSV-1) infection (reviewed extensively in (Itzhaki *et al.* 2016, 1997)), AD and/or ApoE-ε4. Transcriptome analysis of AD patient brain samples revealed significantly increased human herpes virus (HHV)-6A, -7, and HSV-1 latency-associated transcript (LAT) levels relative to controls. Not only were these findings replicated in three separate geographical cohorts, they specified HHV-6A & HHV-7 elevation towards AD progression, not "normal" age-related Aβ deposition or cognitive impairment. Readhead *et al.* (2018) (Readhead *et al.* 2018) were also able to relate increased viral levels in AD patients to NFT and Aβ plaque densities *via* a mechanism that may be dependent upon the ability of HHV-6A to downregulate miRNA-155 (Readhead *et al.* 2018). MiRNA-155 was identified *via* differential gene network analysis of preclinical AD samples and controls, as well as multiregional gene expression changes in clinical AD samples. This proposal was supported by the finding that offspring of APP/PS1 and miRNA-155 knockout mice developed an increased number and size of plaques compared to age-matched APP/PS1 animals. Further, this team's work highlighted changes in transcriptional regulators involved in AD risk and APP processing, *e.g.* PSEN1 and BACE1, possibly due to viral interference.

Comprehensive medical data on 99% of the Taiwanese population has been gathered for the National Health Insurance Research Database since its launch in 1995 (Tzeng *et al.* 2018). The information so far gathered by three separate studies has revealed that not only is there an increased incidence of dementia within herpes simplex virus (HSV)/varicellar zoster virus (VZV)-positive individuals over a period of 10, 5 or 6.2 years; The hazard ratio (HR), or ratio of the hazard rate of a given group over a set period of time as compared to a control group, of each study was 2.56 (Tzeng *et al.* 2018), 2.97 (Tsai *et al.* 2017), and 1.11 (Chen *et al.* 2018) respectively. Not only did the findings of Tzai *et al.* (2017) mirror HR results found by a previous study comparing HSV antibody presence in AD-specific risk (HR of 2.55), they also revealed that the use of antiherpetics during varicella zoster treatment was correlated with a decreased risk of developing dementia (Tsai *et al.* 2017). The duration of the anti-viral treatment affected the degree of AD risk reduction (adjusted HR 0.092 for anti-viral treatment, with medication courses greater than 30 days showing a greater decreased risk of dementia compared to treatment durations less than 30 days).

The possible mechanism(s) underlying herpes-AD association is/are still unclear. Eimer *et al.* (2018) have proposed that Aβ may act as an innate immune protein with antimicrobial activity such that *herpesviridae* may directly seed Aβ deposition and fibrilization (Eimer *et al.* 2018). Further, herpetic glycoproteins (Hgs) can initiate Aβ fibrilization one to two orders of magnitude faster than host brain glycosaminoglycans, with deposits sequestering HSV-1 and HHV-6 particles. Lathe & Haas (2017) investigated the expression of cellular receptors for HSV-1-specific Hgs within the brain and found that the adult human hippocampus has an increased expression of HgB and HgD receptor genes (Lathe and Haas 2017). As HSV-1 entry into cells requires the presence of multiple cell surface receptors, the increased expression of these two prime binding receptors may be indicative of a heightened HSV trophic ability of the hippocampus, which is the brain region often considered "ground-zero" for AD development.

HSV-1 appropriates APP into its protein retinue, but this is not without consequences as APP becomes mislocalised within HSV-1-infected cells, is overly proteolysed, and moves slower along transport pathways. These disruptions to physiological APP function could represent an early push towards amyloid pathology. Supporting this in the context of the other AD hypotheses, HSV-1 infection in mouse and rat neurons and glial cells induces Aβ accumulation, and synaptic dysfunction *via* increased cytosolic Ca^{2+} (Piacentini *et al.* 2011, 2015; Warwick and Hanani 2016). In human neuroblastoma cells, this HSV-1-induced calcium signalling requires IP_3R1 and the ER Ca^{2+} store (Zheng *et al.* 2014).

1.4 Traditional Models of AD

The decades of AD research presented above have relied heavily on disease model systems, most of which were animal models. These models can be broadly classified into spontaneous, interventional and genetically-engineered systems (Chen and Zhang 2022). Spontaneous pathological occurrence models, primarily non-human primates (NHPs), are limited due to the lack of a singular species presenting with the full histopathological and behavioural phenotype seen in humans. Additionally, their use is further restricted by the associated administrative difficulties, high costs, and zoonotic transmission risk (Geula, Nagykery, and Wu 2002; Jean *et al.* 2024; Li, Zhang, and Qin 2019). Interventional models aim to induce AD-like symptomatology in many different species through external insult or stimulation. These include, but are not limited to, centrally administered Aβ/tau (Clavaguera *et al.* 2009; Maurice, Lockhart, and Privat 1996; Mugantseva and Podolskii 2010), orally administered pharmacological compounds (Kumar, Dogra, and Prakash 2010; Nakayama and Sawada 2002), and peripherally administered drugs/toxins/cytokines intended to trigger systemic disease states (Ionov and Pushinskaya 2010; Maya, Prakash, and Goli 2018). Interventional models have been applied across various species, including rodents, canines, and zebrafish, though each presents distinct translational limitations. However, the majority of AD research has relied on genetically modified rodent models due to their cost-effectiveness and ease of manipulation.

1.4.1 Transgenic Rodents

As discussed previously (see section 1.1) less than 1% of all AD patients present with early onset familial AD (EOFAD), which is caused by the autosomal dominant inheritance of variant *APP*, *PSEN1*, or *PSEN2* genes. Neither wild-type mice nor rats endogenously develop amyloid plaques or tau tangles, even in advanced ageing. Normal *in vivo* concentrations of Aβ within rodent brains is estimated to be in the picomolar range, whereas it may reach nanomolar concentrations in the human AD brain (Teich, Patel, and Arancio 2013). Rodent Aβ also differs from human Aβ by three substitutions, and these are considered enough to prevent amyloid aggregation. Due to these factors, in order to develop a useful rodent model of AD, human EOFAD genes had to be transfected into the animals. Transgenic (TG) rodent models were developed with three general aims in mind (Zhong *et al.* 2024): 1) The presentation of the pathological hallmarks of AD (amyloid deposition, tau hyperphosphorylation, neuronal/synaptic degeneration). 2) The predictable progression of AD pathological features through brain areas that mimic patient progression. 3) Measurable cognitive decline.

Although mice were the first species to be developed as transgenic models of AD, purely in evolutionary terms, rats are superior experimental models as they are morphologically, physiologically and genetically closer to humans than mice (Gibbs *et al.* 2004; Jacob and Kwitek 2002; Lin 1995). Furthermore, in the context of research into behaviour and neurodegeneration, their more diverse and sophisticated behavioural repertoire and social dynamics (Whishaw *et al.* 2001), paired with their larger size (i.e. which facilitates the feasibility of intrathecal drug administration, repeated cerebrospinal fluid (CSF) sampling, *in vivo* and *ex vivo* electrophysiology, and neuroimaging (Tesson *et al.* 2005)) also makes their use preferable to that of mice. Like humans, rats also possess six tau isoforms (Hanes *et al.* 2009) and exhibit substantial ApoE amino acid sequence homology (McLean, Fukazawa, and Taylor 1983; Rajavashisth *et al.* 1985). However, rats at the time were, mid- to late 1990s, less amenable to transgenesis than mice. Rat single-cell embryos possessed less visible pronuclei and more flexible plasma and pronuclear membranes, making transgene injection more difficult (Charreau *et al.* 1996). Survival rates of injected embryos were lower (Charreau *et al.* 1996), and fewer tools for manipulation of the rat genome were readily available (Tesson *et al.* 2005). While a sizeable number of rat models were developed and studied, TG mouse models have dominated the field to this day.

1.4.1.1 Transgenic Mouse Models

The first TG mouse model of AD was developed in 1995 (Games *et al.* 1995), and since then, hundreds more have been generated (Polis and Samson 2024; Scearce-Levie, Sanchez, and Lewcock 2020; Zhong *et al.* 2024). Most of these involve overexpression of FAD-related APP mutations, alone or in combination with presenilin variants. Although MAPT mutations are not associated with AD, they have been incorporated into several models to induce tau pathology. More recent models attempt to minimise artefacts associated with overexpression by using gene-editing strategies such as knock-in (KI) and knock-out (KO) approaches (Saito *et al.* 2014; Xia *et al.* 2015).

Initial mouse AD models carried a single EOFAD mutation. The PDAPP mouse overexpress the 'Indiana' APP_{V717F} under the platelet-derived growth factor B-chain promoter, resulting in early cortical and hippocampal Aβ plaques, gliosis, synaptic deficits, and memory impairment (Games *et al.* 1995). Tg2576 mice express the 'Swedish' $APP_{K670N/M671L}$ under the PrP promoter and show widespread plaques and similar phenotypes (Hsiao *et al.* 1996). APP23 mice also carry the Swedish mutation but expressed the APP751 isoform under a Thy1 promoter, leading to more compact plaques, increased vascular amyloid, and regional neurodegeneration despite compara-

ble expression levels (Sturchler-Pierrat *et al.* 1997; Sturchler-Pierrat and Staufenbiel 2000).

Models combining multiple EOFAD mutations produced earlier and more severe phenotypes. For example, J20 mice express both Swedish and Indiana APP mutations (Mucke *et al.* 2000), while APP/PS1 mice expressing pairs of mutant APP and PSEN1 variants are widely used. Phenotypes vary by promoter and mutation. For example, $APP_{K670N/M671L}$/$PS1_{L166P}$ mice develop plaques by six weeks (Radde *et al.* 2006), whereas $APP_{K670N/M671L}$/$PS1_{M146L}$ mice take six months to do so (Holcomb *et al.* 1998). The 5xFAD model, combining five mutations ($APP_{K670N/M671L}$, APP_{I716V}, APP_{V7171}, $PSEN1_{M146L}$, and $PSEN1_{L286V}$), shows intraneuronal Aβ accumulation by six weeks and extracellular plaques by two months (Oakley *et al.* 2006). In general, these models exhibit robust plaque pathology, gliosis, synaptic dysfunction, and cognitive deficits particularly in spatial memory tasks. However, cognitive decline typically occurs alongside early plaque formation, in contrast to the delayed clinical onset in human AD. A further limitation is their lack of widespread neurodegeneration and atrophy. When present, it is usually restricted to older animals and specific brain regions. While several models exhibit soluble oligomeric hyperphosphorylated tau, none develop authentic NFTs (Oakley *et al.* 2006; Radde *et al.* 2006; Sturchler-Pierrat *et al.* 1997; Tomiyama *et al.* 2010). This likely reflects the differences in tau biology in that mouse tau shares only 88% homology with human tau and lacks 3R isoforms. Even when all six human tau isoforms are expressed, NFTs do not form unless endogenous mouse tau is removed (Andorfer *et al.* 2003). In contrast, tangles readily form in mice expressing mutant human tau (e.g., P301L, P301S), which also exhibit neurodegeneration and motor deficits (Götz and Ittner 2008; Lewis *et al.* 2001, 2000; Santacruz *et al.* 2005). However, these mutations are not present in AD, and the resulting phenotypes are therefore distinct from the human condition.

A limited number of models co-express both plaques and tangles, although consistent dual pathology is difficult to achieve. Of these, the triple-transgenic (3xTG) mouse (containing the $APP_{K595N/M596L}$, $PSEN1_{M146V}$, and $MAPT_{P301L}$ mutations) remains the most widely used. These mice develop intraneuronal Aβ by 3–4 months, plaques by 6 months, and NFTs by 12 months (Oddo *et al.* 2003). Additional features include localised neurodegeneration, synaptic impairment, and cognitive decline. Neurons from 3xTg mice exhibit disrupted calcium signalling, reversible via calcineurin inhibition or mitochondrial calcium uniporter KO (Lopez *et al.* 2008; Smith *et al.* 2005; Wang *et al.* 2024b; Zeng *et al.* 2024). Nevertheless, the model still relies upon overexpression of mutant human proteins, with mature pathology appearing relatively late and remaining less extensive than in human AD.

KI models aim to overcome these limitations by introducing EOFAD mutations directly into the endogenous mouse APP locus, preserving normal gene expression and spatiotemporal regulation. For instance, KI of Swedish ($APP_{K595N/M596L}$), London (APP_{V717I}), and Dutch (APP_{E693Q}) mutations only leads to plaques when crossed with $PS1_{M146V}$ mice (Li *et al.* 2014). Swedish/Iberian ($APP_{K595N/M596L}$/APP_{I716F}) KI mice develop plaques by 6 months and cognitive deficits by 18 months, while adding the Arctic (APP_{E693G}) mutation accelerates onset to 2 months (Saito *et al.* 2014). Although more physiological, these models still rely on multiple EOFAD mutations and do not recapitulate the polygenic and sporadic nature of LOAD.

1.4.2 Non-human Primates (NHPs)

Several NHP species develop spontaneous AD-like features with age, including Aβ accumulation, tau hyperphosphorylation, and mild cognitive decline. However, no single species fully recapitulates the human disease pathology (Isidro 2024; Kumar *et al.* 2018). Despite their biological proximity to humans and 100% Aβ sequence homology, the use of NHPs in AD research is constrained by ethical considerations, high costs, low reproductive rates, and zoonotic risks (Braidy *et al.* 2015; Camus *et al.* 2015; Inestrosa *et al.* 2005).

Among great apes (chimpanzees, gorillas, orangutans), aged individuals exhibit diffuse amyloid plaque formation and vascular Aβ deposition, but tauopathy is rare. Only focal tau phosphorylation has been observed, with NFTs reported in a minority of chimpanzees, often alongside other risk factors such as stroke or metabolic dysfunction (Edler *et al.* 2017; Perez *et al.* 2013, 2016).

Old world monkeys, particularly rhesus macaques, show consistent age-related Aβ accumulation and plaque deposition, primarily within the cortex as a mix of diffuse and compact plaques (Härtig *et al.* 1997; Rosen, Walker, and Levine 2011). Tau pathology is absent in rhesus monkeys but has been observed in the hippocampi of aged baboons (Schultz *et al.* 2000). Vervets show parenchymal and vascular Aβ, gliosis, and dystrophic neurites with occasional tau reactivity but no NFTs (Frost *et al.* 2013; Kalinin *et al.* 2013). New world monkeys, such as squirrel monkeys, also accumulate Aβ, especially in vasculature, and express a broad range of human-like Aβ isoforms. However, no mature tau pathology is seen even in aged individuals (Rosen *et al.* 2016; Walker *et al.* 1990). The gray mouse lemur presents with early cortical plaque formation, intraneuronal tau, and age-related cortical atrophy that correlates with cognitive decline,

making it an interesting small-bodied model for preclinical studies (Bons *et al.* 1994; Kraska *et al.* 2011).

1.4.3 Other Mammals

Some other mammals, notably dogs and the South American rodent *Octodon degus*, develop age-related AD-like pathology. Dogs share an identical Aβ sequence with humans and develop diffuse cortical plaques and vascular deposits from around 8–9 years of age (Schmidt *et al.* 2015; Schütt *et al.* 2016). Though compact plaques and tau pathology are rare, some demented dogs exhibit soluble oligomeric tau, increased phosphorylated tau, and synaptic dysfunction (Smolek *et al.* 2016). Dogs also show measurable cognitive decline, particularly in memory and executive function, which has been correlated with Aβ burden in some studies (DeBoer *et al.* 2014). Their long preclinical phase and spontaneous pathology have made them valuable for therapeutic testing, though their long lifespan and inter-individual variability limit scalability.

Octodon degus shows high Aβ sequence homology to humans (with a single substitution), and some studies report age-related Aβ accumulation, tau pathology, gliosis, and cognitive impairment (Braidy *et al.* 2015; Salazar *et al.* 2016). However, findings are inconsistent across studies, raising concerns about this particular proposed model's reliability (Steffen *et al.* 2016).

Components of AD-like pathology have also been reported in wild mammals such as bears (Lucot *et al.* 2022), sea lions (Takaichi *et al.* 2021), and dolphins (Vacher *et al.* 2023), though these species are not used experimentally. Feline cognitive dysfunction, an age-related neurodegenerative condition in domestic cats, is emerging as a potential AD model (Zadik-Weiss *et al.* 2020). While feline Aβ aggregates differ structurally from human counterparts (Gunn-Moore 2011), tau aggregation appears to follow a similar anatomical progression to that seen in human AD (Fiock *et al.* 2020; Poncelet *et al.* 2019).

1.4.4 Invertebrates

Invertebrate models such as *Drosophila melanogaster* and *Caenorhabditis elegans*, as well as lower vertebrates like zebrafish, have been widely used in genetically engineered models of AD. These organisms are not suitable as physiological models due to low genetic homology, simplified nervous systems, and lack of endogenous Aβ expression (Alexander, Marfil, and Li 2014; Fernandez-Funez, de Mena, and Rincon-Limas

2015). Nonetheless, they express orthologues of AD-relevant genes (*e.g.*, APP, PSEN1, BACE1, MAPT), and are easily manipulated to express human transgenes (Alexander, Marfil, and Li 2014; Fernandez-Funez, de Mena, and Rincon-Limas 2015; Paquet *et al.* 2009).

Their main advantages include low cost, short lifespan, ease of handling, and suitability for high-throughput genetic or drug screening. For example, transgenic *Drosophila* models have been instrumental in identifying drugs that modify tau toxicity (Hannan *et al.* 2016). However, these models lack conserved cellular pathways and human-specific interactors and thus require validation in more biologically relevant systems.

1.5 Human Stem Cell Technology

In 2006, Takahashi and Yamanaka reported that terminally differentiated mouse fibroblasts could be reprogrammed into a pluripotent state using retroviral delivery of four transcription factors: Oct4, Sox2, Klf4, and c-Myc (Takahashi and Yamanaka 2006). The reprogramming factors have since become widely known as the OSKM or "Yamanaka factors". These induced pluripotent stem cells (iPSC) exhibited transcriptional and epigenetic profiles, as well as developmental potential, closely resembling that of embryonic stem cells (ESCs). A year later, this methodology was extended to human fibroblasts by two independent groups. Yamanaka and colleagues applied the same OSKM factors (Takahashi *et al.* 2007), while Thomson and team used a distinct set comprising OCT4, SOX2, NANOG, and LIN28 (Yu *et al.* 2007), building on their prior work on the isolating of human ESCs (Thomson *et al.* 1998).

Since their introduction, human iPSC technologies have been developed and applied extensively across multiple domains including regenerative medicine, stem cell biology, drug screening, and *in vitro* disease modeling. Patient-derived iPSC lines have been used to generate disease-relevant cell types, enabling phenotypic studies of neurodegenerative, cardiovascular, and metabolic disorders, as well as toxicity profiling of candidate compounds (Mack *et al.* 2014; Tiscornia, Vivas, and Belmonte 2011). iPSCs offer several advantages over traditional screening platforms as they are of human origin, clonally expandable, capable of directed differentiation into ectodermal, mesodermal, and endodermal derivatives, and they do not raise the ethical concerns associated with human ESC usage (Cerneckis, Cai, and Shi 2024). The utility of iPSCs has been significantly enhanced by the advent of genome editing tools, particularly the CRISPR/Cas9 system, which permits the generation of isogenic control and mutant lines for comparative analysis (Bassett 2017). Furthermore, integration with advanced cell culture platforms, including organoids and scaffold-based systems, has led to the development of 3D models incorporating multiple, interacting cell types (Centeno, Cimarosti, and Bithell 2018; Edmondson *et al.* 2014; Shah *et al.* 2023). These approaches are increasingly applied to disease modelling efforts in contexts where tissue-level complexity and spatial organization are relevant to phenotype; that is to say all physiology.

1.5.1 Disease Modelling

Human iPSC models have begun to address the key challenges in AD research, including disease heterogeneity, limited therapeutic targets beyond Aβ and tau, and a lack of patient-specific model systems. Differentiation of iPSCs into neuronal lineages is typically achieved by directing cells through neuroectodermal progenitor states using

defined developmental cues, most commonly *via* dual-SMAD inhibition and region specific patterning signals that recapitulate the *in vitro* developmental process. By enabling the generation of human neurons and glial cells from genetically diverse individuals, including those with sporadic LOAD, human iPSCs facilitate the study of clinically relevant phenotypic variation (Haidar *et al.* 2024). Human iPSC-based platforms have accelerated drug screening through the identification of disease-relevant molecular pathways, and the provision of a source of human neurons for biomarker discovery. iPSC-derived neurons have validated the correlations previously observed in animal models between oxidative stress, impaired autophagy, and lysosomal dysfunction, and the cerebrospinal fluid (CSF) biomarkers phosphorylated tau and altered Aβ42/40 ratios (Birnbaum *et al.* 2018; Mustaly-Kalimi *et al.* 2022; Nieweg *et al.* 2015). In addition to classical protein markers, candidate biomarkers such as astrocyte-secreted miRNAs and lipid metabolites have also emerged from iPSC-based studies (Feringa *et al.* 2023; Garcia *et al.* 2021).

Despite these advantages, iPSC models have notable limitations. Reprogramming to pluripotency erases epigenetic signatures acquired during aging (Papp and Plath 2011; Sardo *et al.* 2017), limiting their capacity to recapitulate age-dependent features of LOAD. Direct reprogramming, or transdifferentiation, has been proposed as an alternative method that preserves age-related epigenetic information by converting somatic cells directly into functional neurons or glia, bypassing the pluripotent state (Mertens *et al.* 2015). Conventional 2D cultures also lack the structural and cellular complexity of the human brain. In particular, they fail to capture multicellular interactions, such as neuron-glia–microglia cross-talk, as well as features of the vascular niche and immune infiltration, which are increasingly implicated in AD pathology (Kelley and Pașca 2022). This limits their applicability in modelling neurovascular dysfunction or inflammation-driven degeneration.

To address these limitations, 3D organoid systems have been developed (Adlakha 2023). These self-organising neural tissues can model aspects of FAD pathology, including Aβ accumulation, tau hyperphosphorylation, and regional atrophy, with greater fidelity than 2D cultures (Choe *et al.* 2024). Vascularised organoids co-cultured with microglia and endothelial cells enable the study of blood-brain barrier breakdown and immune cell infiltration (Kistemaker *et al.* 2025). When combined with CRISPR-based perturbation screens, these platforms allow systematic interrogation of genetic risk factors and pathway-specific drug candidates. Nonetheless, modelling the polygenic and multifactorial nature of LOAD remains a challenge. Future studies may require integrated organoid-vascular co-cultures, longitudinal phenotyping, and multi-omics characterisation to capture the full complexity of disease onset and progression (Gulati

et al. 2020).

A recent bibliometric analysis suggests a thematic shift in iPSC-based AD research, with an increasing focus on inflammation, microglial biology, astrocyte responses, ApoE, and tau (Sun *et al.* 2025). Tau-directed targetted antibody therapies, including semorinemab and davunetide, have been tested in iPSC-derived neuronal models for efficacy and mechanistic specificity (Parra Bravo *et al.* 2024; Teng *et al.* 2022). Studies of TREM2-variant microglia derived from patient iPSCs have revealed altered phagocytic capacity, inflammatory signalling, and metabolic dysregulation, supporting their use in anti-inflammatory drug development (Long *et al.* 2024; Penney *et al.* 2024). Gene-editing approaches targeting ApoE4, and pharmacological interventions affecting astrocytic lipid handling, have also been explored in iPSC-derived glia (van der Kant 2022).

1.6 Thesis Hypothesis & Aims

The doctoral work presented within this thesis sought to achieve the following:

- Generate induced pluripotent stem cells (iPSC) derived human cell & tissue models of nervous tissue.
- Validate the use of iPSC-derived human cell and tissue models of nervous tissue to conduct AD focussed research.
- Use these human cellular and tissue models to investigate the pathophysiological state of an AD-patient derived cell line.
- Conduct a systematic review of the existing evidence for alternative aetiological hypothesis of AD.

This thesis is structured to best communicate the pursuit of these aims. As a large body of the work conducted during this doctoral project was method refinement and development, Chapter 2 is written in part as a manual, for all methods described within the thesis. Chapter 3 presents evidence on the successful and unsuccessful generation of culture systems, and reflects on the ability of these iPSC-derived methods to completely replace the need for animals in AD research. Chapter 4 presents the results of all comparative physiological investigations carried out on iPSC-derived culture products between a healthy control, and an AD patient-derived cell line, expressing the PSEN1 mutation, M139V. Chapter 5 consists of a systematic review, investigating the existing primary data of alterations to the human neural intracellular trafficking system following exposure to herpes viruses. Chapter 6 summarises the findings and the potential impact of this work as a whole.

2.1 Cell & Tissue Culture

All cell and tissue culture was performed in a UV-sterilised level 2 laminar flow hood, using equipment sterilised with 70% ethanol. All media and reagents were either sterile or sterile-filtered, and unless otherwise stated, all procedures were carried out without antibiotic supplementation. Strict aseptic technique was maintained throughout to avoid contamination. All cells and tissues were maintained in a humidified incubator at 37°C and 5% CO_2. Solutions were pre-warmed to 15 - 21°C prior to use.

2.1.1 Cell Lines

As the focus of this doctoral project was on pre-clinical AD pathophysiology, and used techniques primarily based on developmental neurology, a cell line with a confirmed early pathological phenotype within our pathway of interest (intracellular calcium handling) was essential. The control RBi001-A, and mutant presenilin STBCi012-C iPSC lines were obtained from the European Bank for Induced pluripotent Stem Cells (ebisc.org). The control CaCntrl iPSC line was kindly shared with us by Professor Selina Wray of University College London (Table 2.1). All lines were chosen for their predefined ability to undergo self-directed organoidogenisis (Arber *et al.* 2019; Lancaster and Knoblich 2014). The STBCi012-C $PSEN1_{M139V}$ cell line (heretofore referred to as PSN1) was chosen as our AD model line because its PSEN1 mutation at residue 139 lies just seven amino acids upstream of, and withing the same transmembrane domain as, the $PSEN1_{M146V}$ mutation that is expressed in the triple-transgenic (3xTG) AD mouse model, which we, and others have shown disrupts calcium homeostasis in neurons (Kaar 2019; Nelson *et al.* 2010).

Table 2.1: **Characterisation of Cell Lines**

Cell Line	Pathology	Sex	Age of Onset	Age of Biopsy	APOE Genotype	Origin
CaCntrl	Cognitively normal	M	-	78	3/3	Prof Selina Wray
RBi001-a	Cognitively normal	M	-	45 - 49	3/3	EBiSC
STBCi012-C	PSEN1 M139V	F	34	45	2/3	EBiSC

2.1.2 Culture System Design

All of the culture systems utilised within the studies described in this thesis derive sequentially from the maintenance and differentiation of iPSCs. Each subsequent culture utilises the product of the one before. The relatedness of each system is depicted in Figure 2.1. A full list of culture system products and the target cellular sub-type being modelled is shown in Table 2.2.

Established culture protocols (STEMCELL Technologies, Vancouver, Canada) were found to be generally effective. When needed or beneficial, modifications based on other published methodologies (individually cited where relevant) were implemented.

Table 2.2: **Culture System products and corresponding cell developmental stages**

Product Name	**Days in Culture**	**Modelled Cell Stage**
iPSC	*NA*	Embryonic stem cells
NPC "Stock"	*NA*	Embryonic CNS progenitor cells
NPC "Coverslip Culture"	1 - 14	Adult neural stem cell reserve / immature neurons
DGN	31- 46	Mature hippocampal dentate gyrus cells
Embryoid body	1 - 4	Gastrula
Cerebroid	45 -75	1st trimester foetal brain
ALI-CO	74 +	Maturing adult neural circuitry

*A*bbreviations: Induced pluripotent stem cells (iPSC), neural progenitor cell (NPC), dentate gyrus-like neurons (DGN), air-liquid interface cerebral organoid (ALI-CO).

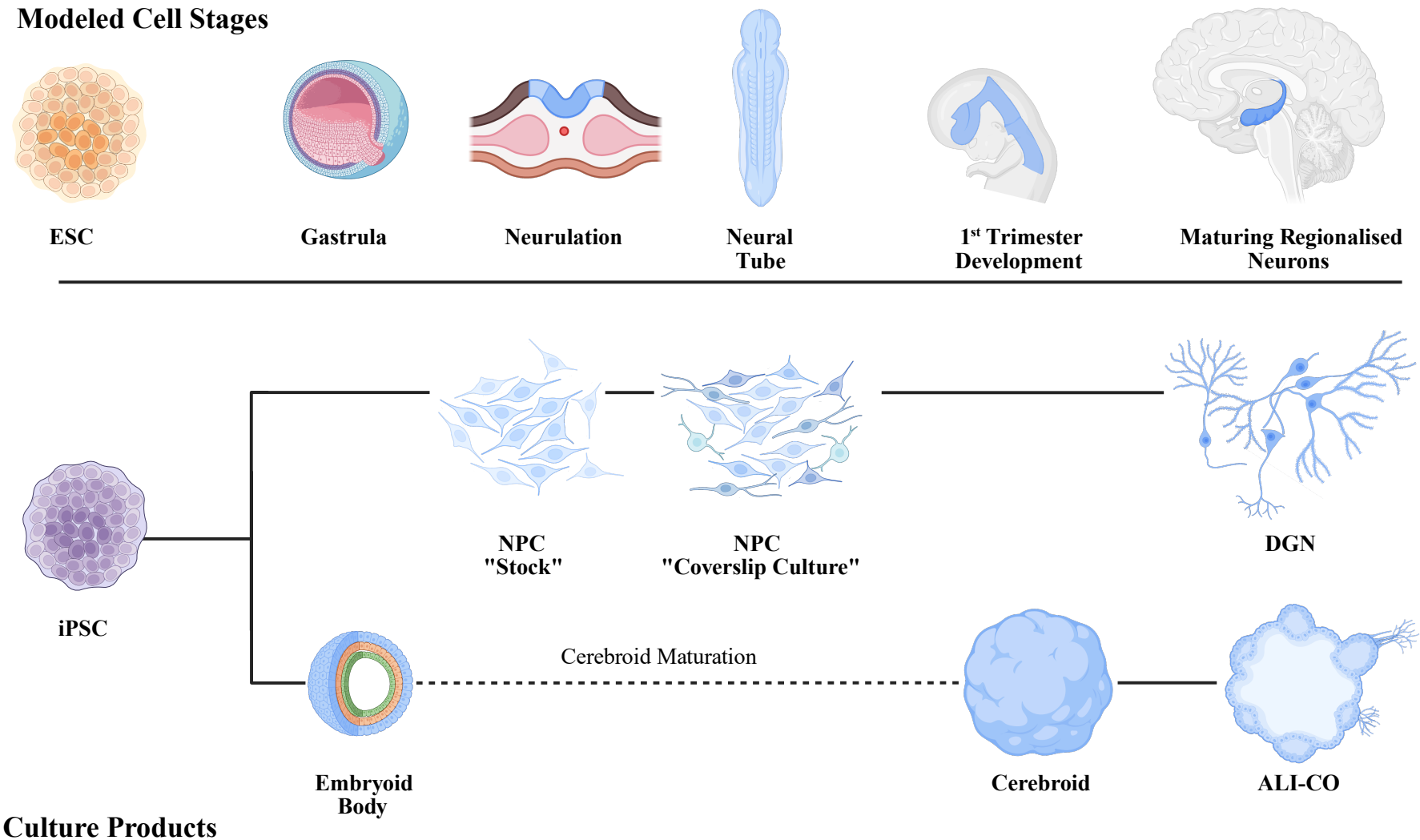

Figure 2.1: **Diagram of culture system relatedness and modelled developmental stages.** All cell culture products used in this thesis derive from a core iPSC culture. The 2D systems proceed through NPC cultures to yield DGNs, modelling post-mitotic hippocampal cell development. The 3D systems mature organoid cultures through embryoid body formation, leading to cerebroid maturation and following slicing and re-culturing to air-liquid interface cerebral organoid (ALI-CO) cultures, which model maturing neural circuit outgrowth. Modelled developmental stages are shown above the corresponding culture products. Created with BioRender.com.

2.2 Core Laboratory Materials

The core laboratory equipment, materials and reagents used throughout this doctoral project for the production, maintenance and fixation of biological samples are listed here. Material components used during interventional experiments (*e.g.* Ca^{2+} imaging, metabolic analysis), and specialist culture components are listed separately in their relevant sections.

2.2.1 Core Equipment

- Sterile laminar flow hood, HEPA-filtered air.
- Sterile dissection hood, HEPA-filtered air.
- Incubator, controlled 5% CO_2, humidified (New Brunswick Scientific, Edison, NJ, USA).
- Benchtop Shaker (INFORS HT, Bottmingen, Switzerland).
- Inverted microscope, phase contrast, with a long working distance objective (Olympus, Tokyo, Japan).
- Swinging bucket centrifuge.
- Water bath.
- Osmometer.
- Haemocytometer.
- Vibratome (Camden Instruments, Leicestershire, UK).
- Nalgene® Mr. Frosty Freezing container (Sigma-Aldrich).
- Liquid nitrogen (LN_2) vapour tank.
- -80°C freezer.
- -20°C freezer.
- Refrigerator (2 - 8°C).
- Fine and course dissection tools.
- Assorted pipettes (and appropriate pipette tips).
- Pipette controller (Accumax Lab Devices, Gandhinagar, India).

2.2.2 Core Materials

- 6-well cell culture plate (Corning, Flintshire, UK).
- 6-well ultra-low adherence cell culture plate (Corning).
- 24-well ultra-low adherence cell culture plate (Corning).
- 96-well ultra-low adherence u-bottom cell culture plate (Corning).
- 35 mm cell culture dish (Merk Sigma Aldrich, Wicklow, Ireland).
- 145 mm cell culture dish (Merk Sigma Aldrich).
- 13 mm glass coverslips (TAAB Laboratories Equipment, Berkshire, UK).
- 15- and 50-mL sterile polypropylene (PP) centrifuge tubes (Fisher Scientific).
- 150 mm Pasteur pipette (Avantor, Radnor, PA, USA).
- 3.5 mL Plastic transfer pipette (Sarstedt, Nümbrecht, Germany).
- Cell Scraper (Merk Sigma Aldrich).
- Nalgene® Cryo Vials (Merk Sigma Aldrich).

2.2.3 Core Reagents

- Isopropanol (Merk Sigma Aldrich).
- Ethanol (Merk Sigma Aldrich).
- Corning® Matrigel® hESC-Qualified Matrix (Fisher Scientific).
- StableCell™ DMEM/F12 (Merk Sigma Aldrich).
- DMEM/F-12 with 15 mM HEPES (Merk Sigma Aldrich).
- D-phosphate-buffered saline (PBS) (Without Ca^{2+} and Mg^{2+})(Merk Sigma Aldrich).
- PBS Tablets (Merk Sigma Aldrich).
- Trypan Blue (ThermoFisher Scientific).
- Y-27632 ROCK Inhibitor (STEMCELL Technologies).
- Poly-L-Ornithine (Merk Sigma Aldrich).
- Fluoroshield Mounting Medium with DAPI (Abcam, Cambridge, UK).

2.3 Induced Pluripotent Stem Cell (iPSC) Culture

iPSCs are derived from donated somatic cells transduced with stem cell-associated genes commonly referred to as Yamanaka factors (see section 1.5) (Takahashi and Yamanaka 2016). Upon successful reprogramming, iPSCs form colonies that mimic ESC morphology, pluripotency and mitotic activity (Chatterjee *et al.* 2016). These colonies expand continuously across adherent surfaces to fill their given culture vessel. Before a stem cell monolayer can become confluent, they are detached from their cultureware, broken into smaller colonies, and re-seeded into a new vessel. This process, known as passaging or splitting, is also used to track the age of the cell line. While iPSCs have the capacity for indefinite propagation, the risk of genetic drift or mutation increases with higher passage numbers (Popp *et al.* 2018; Volpato and Webber 2020), but the magnitude of this risk is still under investigation (Kosanke *et al.* 2021). Culture health is typically determined by the percentage of differentiated cells present relative to total biomass within the culture vessel (Rivera *et al.* 2020). Cell differentiation needs to be minimised in order to ensure the continued self-renewal of stem cells and to avoid later experimental contamination with unwanted cell lineages (see Fig. 2.2). iPSC colonies are cryopreserved to maintain a stock of healthy cells between experiments. How each of these methods were performed during this thesis is explained below.

2.3.1 iPSC Source Manual & Materials

The following iPSC protocols were derived from the STEMCELL Technologies "Maintenance of Human Pluripotent Stem Cells in mTeSR™1" Technical Manual. Protocol specific materials and reagents are listed in table 2.3.

Table 2.3: **iPSC Materials**

Category	Material	Vendor	Catalogue
Culture Media	mTeSR™ Plus Basal Medium	STEMCELL Technologies	#100-0274
	mTeSR™ Plus 5X Supplement		#100-0275
Passaging Reagents	ReLeSR™		#100-0484
	Gentle Cell Dissociation Reagent		#100-0485
Cryopreservation Media	mFreSR™		#05855

2.3.2 iPSC Maintenance

All iPSCs were cultured in "feeder-free" conditions. In the absence of a feeder-cell layer (most commonly mitotically inactivated mouse-derived fibroblasts (Thomson *et al.* 1998)), Matrigel extracellular matrix provided iPSCs with required extracellular protein components and a viable attachment surface. 6-well plates (9.6 cm^2 culture area) were coated with Matrigel diluted 1:100 in StableCell™ DMEM/F12 and kept (for a minimum) overnight to polymerise at 37°C prior to use. Cells were maintained in mTeSR™ Plus Basal Medium supplemented with mTeSR™ Plus 5X Supplement with complete media changes every other day to avoid nutrient deprivation and build-up of toxic metabolites. iPSC colony quality and confluence were assessed morphologically using an inverted bright field microscope (Fig. 2.3). Cultures were split every 5 - 8 days when total well confluence was >80%.

Cell passaging;

- If cell differentiation within a culture was below 5% (i.e. a high quality culture), the mTeSR™ Plus media was aspirated, and cells then incubated in 1 mL/well Gentle Cell Dissociation Reagent (GCDR) at room temperature for 8 minutes. GCDR, a non-enzymatic solution designed to dissociate iPSCs with minimal stress to colonies. Upon removal of GCDR, 1 mL/well of complete mTeSR™ Plus was added. Colonies were gently detached by the force of media addition. Disaggregated colonies were immediately replated at a split ratio between 1:4 to 1:12, meaning colonies from one well were transferred to four to twelve new wells. GCDR was used to ensure the maximal yield of high-quality iPSCs while minimising mechanical stress and disruption to the colonies.

- If cell differentiation was above 5%, determined by visual inspection (see Fig 2.2 for examples of iPSC differentiation), media was aspirated, cultures were washed once with D-PBS (without Ca^{2+} and Mg^{2+}) and then incubated at 37°C for 5 minutes in a thin film of ReLeSR™, an enzyme-free reagent used to selectively detach undifferentiated ESC and iPSC while leaving differentiated cells attached to the plate. The use of ReLeSR™ mitigated the need for manual scraping of differentiated regions under a microscope, risking culture contamination. iPSC colonies were detached by firmly tapping each side of the plate for a total of 60 seconds. 1 mL/well of complete mTeSR™ Plus media was added to suspend disaggregated colonies, which were immediately replated at a split ratio of 1:1 to 1:3 wells. Lower split ratios were used to rescue cultures with excessive differentiation.

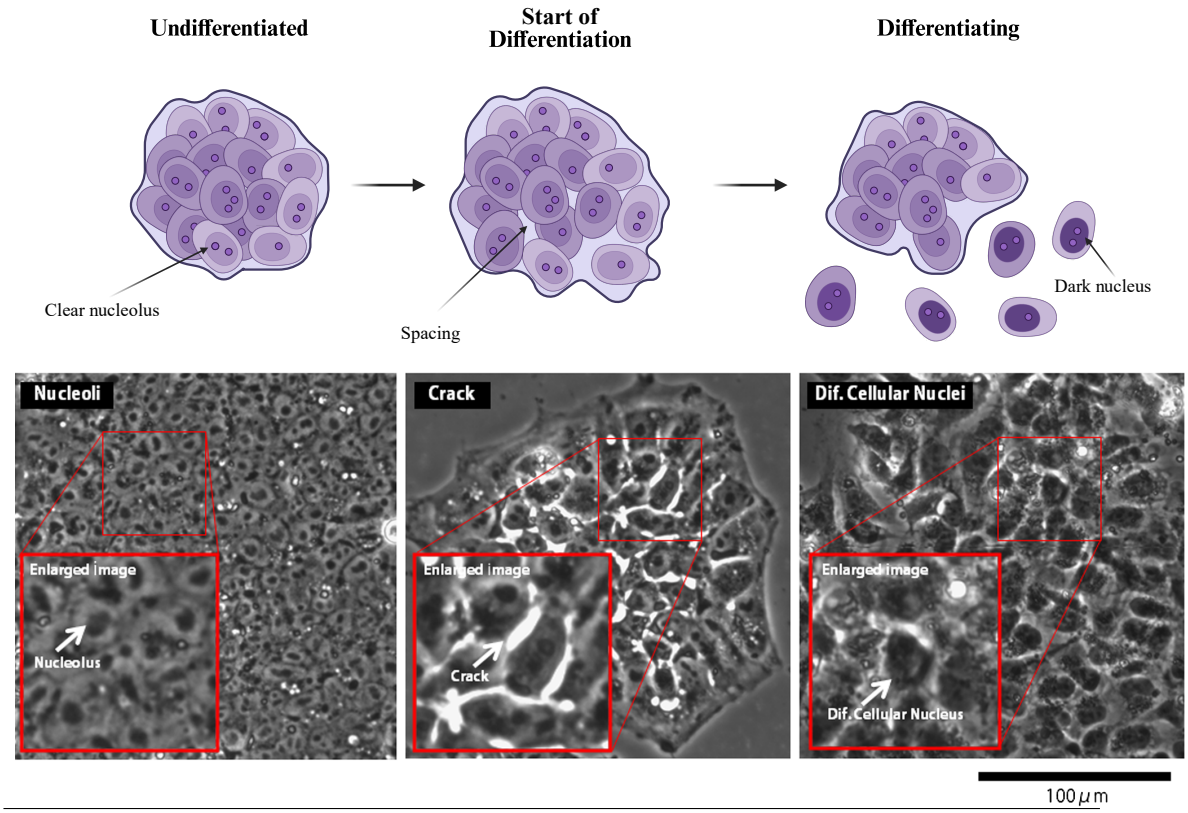

Figure 2.2: **Morphological changes of iPSCs during differentiation. Above:** Cartoon representation of typical morphological changes in iPSCs when differentiation begins to occur. Created with BioRender.com. **Below:** Brightfield images of typical morphological changes in iPSCs undergoing differentiation. Images taken from (Wakui *et al.* 2017) were captured using a 10x objective lens.

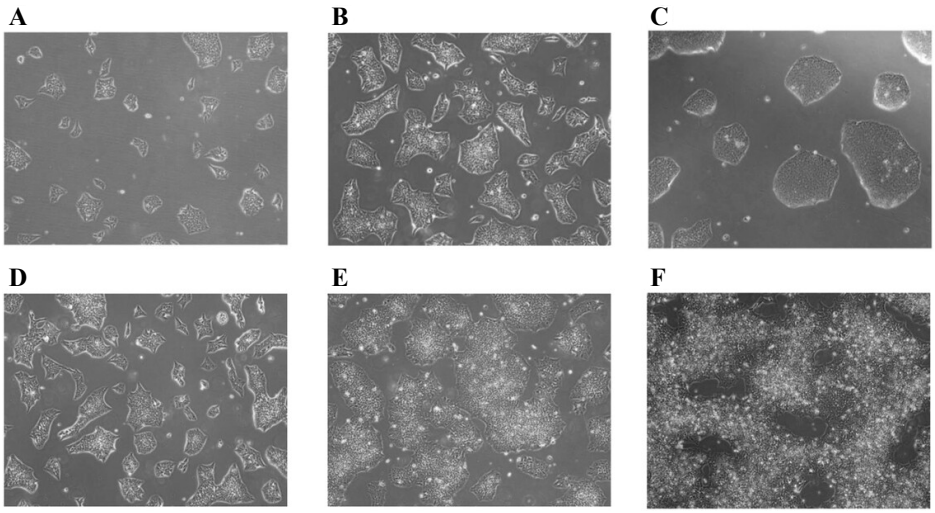

Figure 2.3: **Confluency of iPSC cultures.** Representative images of **A:** small- and medium-sized iPSC colonies. **B, C:** medium- and large-sized iPSC colonies, **D:** an iPSC culture at 40% confluence, **E:** an iPSC culture at 60%-75% confluence, and **F:** an overgrown iPSC culture. 10× magnification. Images taken from (Rivera *et al.* 2020).

2.3.3 iPSC Cryopreservation

Cells were cryopreserved in mFreSR™ media and stored in liquid nitrogen. Following GCDR dissociation (as only high quality cultures were stored) described above, cells were spun down for 5 minutes at 250 relative centrifugal force (rcf). The cell pellet was resuspended in 2 mL/well cold (2 - 8°C) mFreSR™ and transferred into labelled cryovials. An isopropanol filled "Mr. Frosty" freezing container was used to achieve vial cooling at -1°C/minute within a -80°C freezer. After 24 hours vials were immersed in liquid nitrogen for long term storage.

2.3.4 iPSC Vial Thaw

Cryopreserved iPSC vials were rapidly thawed in a 37°C water bath. Cell aggregates were moved to a 15 mL centrifuge tube and 11 mL of complete mTESR™ Plus medium was added drop wise (to avoid excessive osmotic stress) before cells were spun down for 5 minutes at 250 rcf. The pellet was then resuspended in 1 mL fresh mTESR™ Plus supplemented with 10 µM Y-27632 Rho-associated, coiled-coil containing protein kinase (ROCK) inhibitor to reduce dissociation-induced apoptosis (anoikis). 0.5 mL/well of cell suspension was then plated on Matrigel-coated wells pre-filled with 2.5 mL of complete mTESR™ Plus.

2.4 Neural Progenitor Cell (NPC) Culture

To reduce the time required to culture functional neurons directly from iPSCs, a 'checkpoint' differentiation to neural progenitor cells (NPCs) was conducted. These multipotent cells can still be expanded, frozen and stored like iPSCs, but can only be further differentiated into neural lineage cell types.

2.4.1 NPC Source Manual & Materials

The following NPC protocol was derived from the STEMCELL Technologies "Generation and Culture of Neural Progenitor Cells Using the STEMdiff™ Neural System" Technical Manual. Protocol-specific materials and reagents are listed in table 2.4 below.

Table 2.4: **NPC Materials**

Category	Material	Vendor	Catalogue
Culture Media	STEMdiff™ Neural Induction Medium	STEMCELL Technologies	#05835
	STEMdiff™ SMADi Neural Induction Supplement		#08580
	STEMdiff™ Neural Progenitor Medium		#05833
Passaging Reagents	ACCUTASE™		#07920
	Gentle Cell Dissociation Reagent		#100-0485
Cryopreservation Media	STEMdiff™ Neural Progenitor Freezing Medium		# 05838

2.4.2 NPC Induction

NPCs were derived from iPSCs using the STEMCELL Technologies STEMdiff™ SMADi Neural Induction Kit and utilising a monolayer culture system. High quality iPSC cultures, as defined by passaging guidelines in section 2.3.2, were prepared for passaging using GCDR disassociation as described in section 2.3. The collected aggregates were triturated using a 1 mL serological pipette until a cellular suspension was achieved. A count of viable cells was made using Trypan Blue and a haemocytometer. The cell suspension was then spun down at 250 rcf, resuspended in STEMdiff™ Neural Induction Medium supplemented with SMADi and 10 µM Y-27632, and plated on preprepared Matrigel-coated plates at a cell density of 2 x 10^5 cells/cm^2.

NPC induction cultures were maintained with daily full-media changes with SMADi supplemented STEMdiff™ Neural Induction Medium at 37°C. Passage two was carried out between days 6 - 9 post-plating, with passage three carried out 7 days later. Multiple passages are conducted to ensure a pure NPC population within the cultue. iPSC induction to NPC state, and overall passage preparedness, were judged using an inverted brightfield microscope (10x objective, phase contrast filter). Examples of desired morphology iPSCs and NPCs are shorn in Figure 2.4.

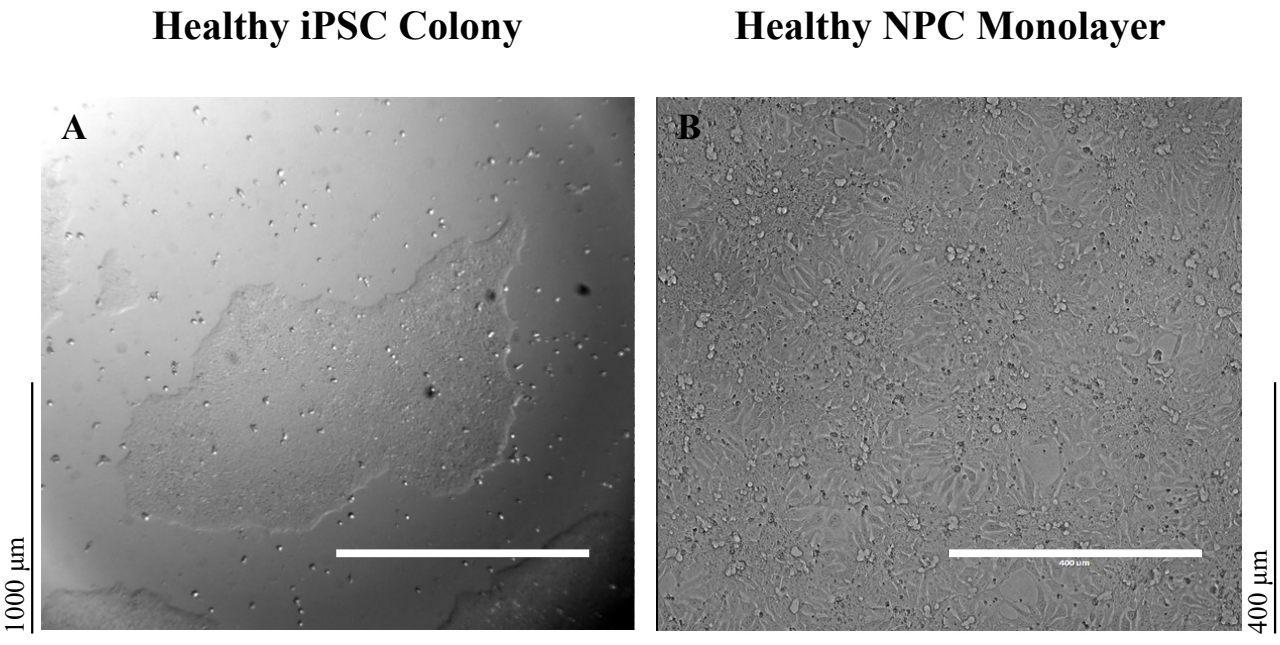

Figure 2.4: **Brightfield images of iPSCs and NPCs.** Representative images of **A** Healthy iPSCs - defined edges, solid colonies, and **B**: Healthy NPCs - single cells, elongated bodies. Images captured at 4x and 10 magnification, scale bars denote 1000 µm and 400 µm.

2.4.3 NPC Maintenance

Following induction, NPC cultures were maintained on Matrigel-coated plates (as described in section 2.3) in 2 mL/well STEMdiff™ Neural Progenitor Medium supplemented with STEMdiff™ Supplement A and STEMdiff™Supplement B (henceforth referred to as complete STEMdiff™ Neural Progenitor Medium). A full media change was made every other day.

For passaging, cells were incubated with 1 mL/well of ACCUTASE™, a gentle, enzyme-based cell detachment solution, for 7 minutes at 37°C. ACCUTASE™ preserves surface proteins and is commonly used for dissociating adherent cells without compromising viability. A minimum cell density of 1.25 x 10^5 cells/cm^2 was maintained to ensure NPC survival and to reduce spontaneous differentiation at low densities.

2.4.4 NPC Cryopreservation

Cells were cryopreserved, for use in later experiments, in STEMdiff™ Neural Progenitor Freezing Medium and stored in liquid nitrogen. Following ACCUTASE™ disassociation, cells were spun down for 5 minutes at 250 rcf. The resulting pellet was resuspended at 2 x 10^6 cells/mL (2 - 8°C) in cold STEMdiff™ Neural Progenitor Freezing Medium and 1 mL of cell suspension was transferred into each cryovial. An isopropanol-filled "Mr. Frosty" was used to achieve vial cooling at -1°C/minute within a -80°C freezer. After 24 hours, vials were moved to liquid nitrogen for long term storage.

2.4.5 NPC Vial Thaw

Like iPSCs, cryopreserved NPC vials were rapidly thawed in a 37°C water bath. Cells were moved to a 15 mL centrifuge tube and 11 mL of warm DMEM/F-12 containing 15 mM HEPES was added drop wise. Cells were then centrifuged for 5 minutes at 250 rcf. The cell pellet was then resuspended in 1 mL complete STEMdiff™ Neural Progenitor Medium containing 10 µM Y-27632 ROCK inhibitor and the cellular suspension plated in one well of a Matrigel-coated 6-well plate pre-filled with 2 mL of complete STEMdiff™ Neural Progenitor Medium.

2.4.6 NPC Coverslip Culture

To facilitate calcium imaging and immunocytochemistry experiments NPCs were cultured on 13 mm glass coverslips using a modified protocol (Kaar 2019), detailed below.

2.4.6.1 Coverslip Preparation

13 mm glass coverslips were sterilised in a 35 mm cell culture dish containing 2 mL of 70% ethanol. Coverslips were then placed upright in 35 mm cell culture dishes, two slips per dish, to air dry. Dry slips were then placed horizontally within the dish and eight individual 35 mm dishes were placed in a larger 145 mm cell culture dish for ease of handling.

Sterile (washed with 70% ethanol) glass coverslips were coated with Poly-L-ornithine (PLO) solution (100 mL, 15 mg/mL in sterile PBS), to facilitate cell-to-glass adhesion, for two hours at room temperature within the laminar flow hood. A 145 mm holding dish lid was used to cover the dishes to reduce evaporation. After incubation, the PLO was aspirated and all slips were washed twice with PBS, and maintained in PBS until ready for NPC plating.

2.4.6.2 Coverslip Plating

NPCs were disassociated with ACCUTASE™, as described in section 2.4, and resuspended at a cell density of 1 x 10^6 cells/mL in complete STEMdiff™ Neural Progenitor Medium containing 10 µM Y-27632 ROCK inhibitor. PBS was aspirated from prepared PLO coverslips, and NPCs were seeded drop-wise to the centre of each coverslip using a flame-polished Pasteur pipette. The culture dishes were then covered and left to allow cell attachment for one hour at 37°C in 5% CO_2. 2 mL of complete STEMdiff™ Neural Progenitor Medium was added to each 35 mm cell culture dish, and all coverslips were inverted (cells facing towards the base of the dish, not towards the media) using flame sterilised forceps to limit oxygen diffusion and thereby establish a hypoxic microenvironment for the cells.

2.5 Mature Human-derived Neuronal Culture

To generate physiologically relevant mature neurons resembling neural cells of the human dentate gyrus, terminal differentiation was induced from NPCs. These mature neurons are post-mitotic, no longer capable of expansion and cannot be cryopreserved, distinguishing them from their iPSC and NPC progenitors. Unlike traditional three-dimensional neurosphere-based methods, the approach used here maintained all culture steps in two-dimensions and avoided the need for neurosphere formation. This enabled a more consistent and scalable protocol for downstream functional assays.

2.5.1 MatNeuro Source Manual & Materials

The composition of DGNeuron Media (Table 2.5 and details of individual components listed in Table 2.6) was based on induction protocols described by Yu et al. (2014) (Yu *et al.* 2014) and Vőfély et al. (2018) (Vőfély *et al.* 2018).

Table 2.5: **DGNeuron Media Composition**

Component	Concentration
BrainPhys Neuro	-
NeuroCult SM1	2%
N2-A	1%
IBMX	110 µg/mL
Ascorbic acid	200 nM
BDNF	20 ng/mL
Laminin	1 µg/mL
Wnt3a	20 ng/mL

Table 2.6: **DGNeuron Media Materials**

Category	Material	Vendor	Catalogue
Culture Media	BrainPhys™ Neuronal Media	STEMCELL Technologies	#05790
Readymade Supplements	NeuroCult™ SM1 Neuronal Supplement		#05711
	N2 Supplement-A		#07152
cAMP enhancer	IBMX		#72764
Antioxidant	Ascorbic Acid	Merk	A4403
Recombinant Proteins	BDNF	R&D Systems	248-BDB
	Laminin 1		3400-010
	Wnt3a		5036-WN

2.5.2 Dentate Gyrus Mature Neuron Induction

Coverslips were prepared prior to culturing as in section 2.4.6. On culture Day 0 healthy NPCs were disassociated with ACCUTASE™, as described in section 2.4.3, and resuspended at a cell density of 1 x 10^6 cells/mL in complete STEMdiff™ Neural Progenitor Medium containing 10 µM Y-27632 ROCK inhibitor. NPCs were seeded onto prepared PLO coverslips at a cell density of 2 x 10^4 cells/cm^2. Culture dishes were covered, and incubated for one hour at 37°C in 5% CO_2. 1 mL of complete STEMdiff™ Neural Progenitor Medium was added to each 35 mm cell culture dish (each containing two coverslips), and returned to the incubator over night.

Visual assessment of seeded NPC health on culture Day 2 was conducted to ensure cell survival prior to further DGN induction. 0.5 mL of STEMdiff™ Neural Progenitor Medium was aspirated from viable DGN culture dishes, and replaced with 0.5 mL of "DGNeuron Media" (for full DGNeuron Media Composition, see Table 2.5). DGNs were maintained for three weeks with half media changes of DGNeuron Media every 3 - 4 days. After 21 days Wnt3a was removed from the DGNeuron Media, and DGNs were cultured for a further 7 - 14 days as before, prior to experimentation.

2.6 iPSC-derived Cerebroid Culture

Cerebral organoids (cerebroids) were derived from iPSCs using the STEMCELL Technologies STEMdiff™ Cerebral Organoid Kit, based on the formulation published by Dr Madeline Lancaster and colleagues (Lancaster and Knoblich 2014; Lancaster *et al.* 2013). Generation of cerebroids followed a day based timeline, as shown in figure 2.5.

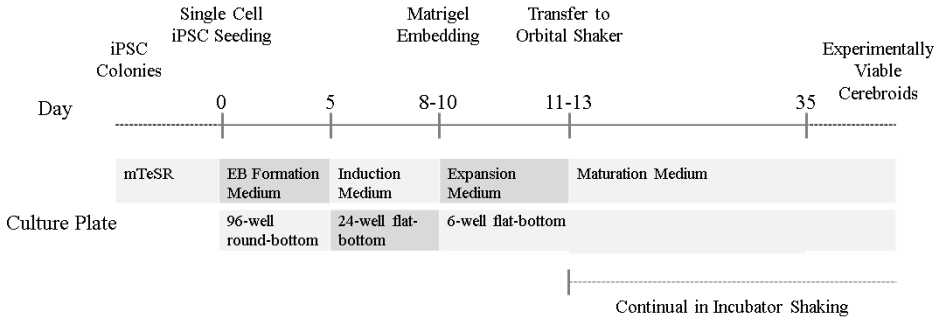

Figure 2.5: **Cerebroid Generation Timeline.** Schematic overview of the cerebroid differentiation protocol from human induced pluripotent stem cells (iPSCs). Single iPSC colonies were dissociated and seeded as single cells (Day 0) in mTeSR medium in 96-well round-bottom plates to promote embryoid body (EB) formation. On Day 5, EBs were transferred to induction medium in 24-well flat-bottom plates. Between Days 8–10, neural epithelium enriched EBs were embedded in Matrigel and transferred to expansion medium in 6-well flat-bottom plates. From Days 11–13 onward, cultures were maintained in maturation medium and placed on an orbital shaker to enhance nutrient diffusion and tissue growth. Organoids were considered experimentally viable from approximately Day 35. Cultures were maintained under continuous shaking within a humidified incubator following transfer to the orbital shaker.

2.6.1 Cerebroid Source Manual & Materials

Protocol-specific materials and reagents are listed in Table 2.7 below. Reagent preparation for all cerebroid media is described in Table 2.8. Additions and alterations to the STEMdiff protocol were made based on in-lab validation and optimisation and discussion with Dr Christopher Lovejoy, University College London.

Table 2.7: **Cerebroid Materials**

Category	Material	Vendor	Catalogue
Culture Media	STEMdiff™ Cerebral Organoid Basal Medium 1	STEMCELL Technologies	#08572
	STEMdiff™ Cerebral Organoid Basal Medium 2		#08573
	STEMdiff™ Cerebral Organoid Supplement A		#08574
	STEMdiff™ Cerebral Organoid Supplement B		#08575
	STEMdiff™ Cerebral Organoid Supplement C		#08576
	STEMdiff™ Cerebral Organoid Supplement D		#08577
	STEMdiff™ Cerebral Organoid Supplement E		#08578
Culture Plasticware	Corning® 96-well round-bottom ultra-low attachment microplate	Corning	#7007
	Costar® 24-well ultra-low attachment plate		#3473
	Costar® 6-well ultra-low attachment plate		#3471

Table 2.8: **STEMdiff™ Cerebral Organoid Media Preparation**

Medium	**Component**	**mL**
EB Formation Medium	STEMdiff™ Cerebral Organoid Basal Medium 1	40
	STEMdiff™ Cerebral Organoid Supplement A	10
Induction Medium	STEMdiff™ Cerebral Organoid Basal Medium 1	49.5
	STEMdiff™ Cerebral Organoid Supplement B	0.5
Expansion Medium	STEMdiff™ Cerebral Organoid Basal Medium 2	24.25
	STEMdiff™ Cerebral Organoid Supplement C	0.25
	STEMdiff™ Cerebral Organoid Supplement D	0.5
Maturation Medium	STEMdiff™ Cerebral Organoid Basal Medium 2	49
	STEMdiff™ Cerebral Organoid Supplement E	1

2.6.2 Cerebroid Generation

On generation day 0, high quality iPSC cultures were prepared for passaging using GCDR dissociation as described in section 2.3. The collected aggregates were triturated using a 1 mL serological pipette until a single cell suspension was achieved. A count of viable cells was made using Trypan Blue and a haemocytometer. The cell suspension was then spun down at 250 rcf, resuspended in embryoid body (EB) Formation Medium supplemented with 10 µM Y-27632, at a viable cell density of 9 x 10^4 cells/mL. 150 µL of cell suspension was seeded into each well of a 96-well round-bottom ultra-low attachment plate. On day 3, an additional 200 µL of EB Formation Medium was added to each well.

On day 5, two EBs were moved to one well of a 24-well ultra-low attachment plate containing 0.5 mL of Induction Medium to facilitate epitheliochorial induction. On day 7 an additional 0.5 mL of Induction Medium was added.

On days 8 - 10 (depending on cerebroid morphology), cerebroids were embedded in matrigel for expansion. Cerebroids were placed onto an embedding surface (dimpled parafilm), and excess Induction Medium was removed. Using cold pipette tips chilled at -20°C to avoid gel polymerisation, 10 µL of liquid matrigel was placed onto each cerebroid and, using a fresh tip, the cerebroid was positioned into the centre of the drop. The embedding surface containing at most 16 cerebroids was placed in the incubator at 37°C for at least 30 minutes to allow the matrigel to polymerise. All cerebroids were then washed into 1 well of a 6-Well Ultra-Low Adherent plate and suspended in 3 mL of Expansion Medium. An upper limit of 16 cerebroids per embedding sheet was used because this number balanced practical handling and experimental integrity. Specifically, 16 organoids could be embedded, polymerized, and transferred without risking desiccation when media was removed from one while processing others. Additionally, the physical size of the embedding surface with 16 organoids remained manageable for washing into a single well of a 6-well Ultra-Low Attachment plate. Lastly, exceeding 16 cerebroids per well increased the risk of organoid fusion or competition for nutrients, potentially compromising culture health and experimental consistency.

On day 11 - 13, following formation of neuroepithelial buds, generation was considered complete and cerebroids were maintained in 3 mL Maturation Medium with continual shaking within the incubator. Media changes were carried out every Monday, Wednesday and Friday, with an extra millilitre of media added per well on Fridays. As cerebroids matured, they were separated into more wells, to ensure over consumption of media did not occur.

2.7 Air-Liquid Interface Cerebral Organoid (ALI-CO) Culture

Cerebroids recapitulate *in vivo* cortical structural developmental for approximately 90 days. However, without co-developing vasculature, later-stage cell types do develop, but without appropriate spacial organisation, and with limited external cues to drive maturation. To stimulate further neuronal maturation, including axonal outgrowth, an alternative protocol was used where cerebroids were sliced and re-cultured at the air-liquid interface (Giandomenico *et al.* 2019).

ALI-COs were produced by embedding day 60 or older cerebroids in agarose (10% in DMEM) using a Peel-A-Way embedding mold (Merk Sigma Aldrich). Gels were secured to the mounting block using cyanoacrylate super glue, submerged in chilled (0°C) "cutting solution" (see table 2.9 for solution composition) and sliced to a thickness of 200 µm using a 5100mz Campden vibratome.

Slices were placed on Millicell-CM cell culture inserts (Merk Sigma Aldrich, #PICM0RG50) in a six-well plate and equilibrated for 1 h at 37°C in serum-supplemented slice culture medium (DMEM, 10% FBS, 0.5% (w/v) glucose, supplemented with 1% penicillin–streptomycin). Following the equilibration period, the media was replaced with serum-free slice culture medium (NeuroCult NS-A Basal Medium (Stem Cell Technologies, #05750), 2% (v/v) B-27 supplement (Themo Fisher Scientific, #17504044), 0.5% (w/v) glucose, 1% (v/v) Glutamax (Termo Fisher Scientific, #35050061) supplemented with antibiotic–antimycotic (Thermo Fisher Scientific, #15240062). ALI-CO cultures were maintained at 37°C and 5% CO_2 with daily media changes. Media was provided only below the filter insert so that sections stayed at the interface and were not submerged.

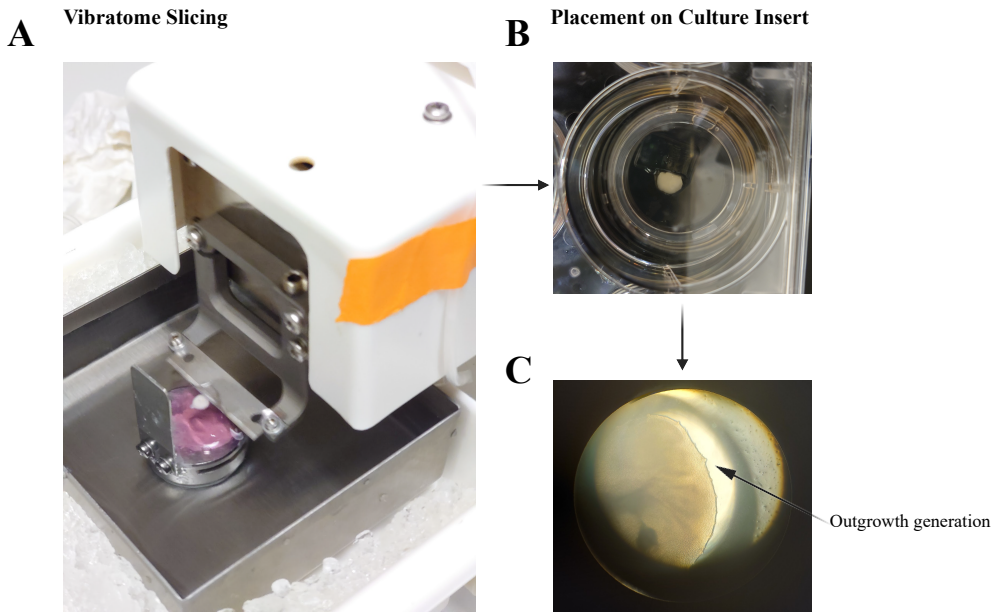

Figure 2.6: **Schematic of ALI-CO culture Generation.** Representative images of **A:** vibratome slicing of live cerebroid embedded in agarose gel, **B:** placement of the cerebroid slice on the culture insert, and **C:** neuronal outgrowth during ALI-CO culture. Images were taken with a phone camera.

Table 2.9: **Cutting Solution Preparations**

Component	mM	MW	g/Litre
$C_7H_{17}NO_5$	92.00	195.22	17.96
KCl	2.50	74.55	0.19
NaH_2PO_4	1.20	120.00	0.16
$NaHCO_3$	35.00	84.01	2.94
$C_8H_{18}N_2O_4S$	20.00	238.31	4.77
$C_6H_{12}O_6$	20.00	180.20	3.60
$C_6H_{706}Na$	5.00	198.00	0.88
$SC(NH_2)_2$	2.00	76.12	0.15
$C_3H_3NaO_3$	3.00	110.04	0.33
$MgSO_4 \cdot 7H_{20}$	10.00	246.48	2.46
$CaCl_2 \cdot 2H_{20}$	0.50	147.01	0.74

- Osmolarity corrected to 300 - 310 mOsm with sucrose
- pH balanced 7.3 - 7.4

2.8 Calcium Imaging

2.8.1 Core Imaging Design

Intracellular calcium measurements from target culture products were conducted using a conventional fluorescence imaging system consisting of an upright fluorescent microscope (Olympus BX51WI) paired with a bright light source (Olympus TH4-200), monochromator (Cairn Optoscan), integrating camera (Hamamatsu ORCA-ER), DAQ device (USB6229) and frame grabber. All experiments were conducted in a perfusion bath maintaining 2 mL/minute superfusion of either HEPES buffered saline solution (HBSS) or artificial cerebrospinal fluid (aCSF) on the given product (for full solution composition, see tables 2.10 and 2.11). The open source imaging software, Winfluor (John Dempster, University of Strathclyde, Scotland) was used for image acquisition.

Prior to calcium imaging experiments cells/tissues were washed of culture media using the appropriate saline solution and loaded for one hour in the dark at room temperature with the intensiometric cell-permeable calcium indicator, Calbryte™ 520 AM (AAT Bioquest, Pleasanton, CA, USA; excitation/emission maxima $\approx$ 495/520 nm)(DGNs: 2 µM in HBSS | NPCs: 4 µM in HBSS | tissues: 8 µM in aCSF). Dye loaded samples were mounted into the superfusion bath and imaged using 20x and/or 40x objective magnification where appropriate.

Table 2.10: **HBSS Solution Preparations**

Component	**mM**	**MW**	**g/Litre**
NaCl	130.00	58.44	7.59
KCl	5.40	74.55	0.40
$C_8H_{18}N_2O_4S$	10.00	238.31	2.38
$C_6H_{12}O_6$	10.00	180.20	1.80
$MgSO_4 \cdot 7H_{20}$	1.00	246.48	0.25
$CaCl_2 \cdot 2H_{20}$	2.00	147.01	0.29

- Osmolarity corrected to 330 - 340 mOsm with sucrose
- pH balanced 7.3 - 7.4

Table 2.11: **aCSF Solution Preparations**

Component	**mM**	**MW**	**g/Litre**
NaCl	124.00	58.44	7.25
KCl	2.50	74.55	0.19
NaH_2PO_4	1.20	120.00	0.16
$NaHCO_3$	24.00	84.01	2.02
$C_8H_{18}N_2O_4S$	5.00	238.31	1.19
$C_6H_{12}O_6$	12.50	180.20	2.25
$MgSO_4 \cdot 7H_{20}$	2.00	246.48	0.49
$CaCl_2 \cdot 2H_{20}$	2.00	147.01	0.29

- Osmolarity corrected to 330 - 340 mOsm with sucrose
- pH balanced 7.3 - 7.4

2.8.2 Calcium Imaging Experimental Design

A priori power analysis was conducted to determine minimum sample number required for comparative analysis between cell lines, using G*Power (Faul *et al.* 2009). Minimum effect size (d) for differences in calcium handling between control and presenilin mutant cells was determined from results presented in previous work (Kaar 2019; Nelson *et al.* 2010). The smallest d taken from these studies was 3.19, considered to be extremely large using Cohen's (1988) criteria (Cohen 2013).

d = 0.5 was chosen, so as to accurately recognise medium size effects. With an α = 0.05 and power = 0.80, the projected minimum sample size needed with this effect size for comparison of two independent means was n = 64 per group.

To this end, all calcium imaging studies were carried out with a minimum of 64 cells/regions of interest from at least three different experiments/coverslips from at least three separate cultures, per group. The actual post-hoc power of each analysis is included with their results. Collated n numbers for each study are presented as "x cells/ROI's – from y experiments/coverslips – from z cultures".

2.8.3 Calcium Data Analysis

Images acquired using Winfluor software were analysed using a classic "Manual" technique, target cells were identified by the experimenter and region of interest (ROI)s were drawn by hand on the image sequences within Winlfuor. Background fluorescence intensity was subtracted from all ROI pixels. Text files containing the average pixel fluorescence values per ROI (arbitrary fluorescence units (A.F.U.)) vs time (seconds) were exported from Winfluor, imported into GraphPad Prism (v10.0), and analysed as XY line graphs. Fluorescence traces were expressed as $\Delta F/F_0$, where F_0 was defined as the mean baseline fluorescence calculated from the 50 frames preceding the inflection event. Area under the curve values were calculated from baseline-corrected $\Delta F/F_0$ traces over the defined response period using the default integration settings in GraphPad Prism. Statistical analyses were selected based on experimental design and data distribution and are reported alongside the corresponding results.

2.9 Metabolic Analysis

2.9.1 Seahorse Analysis

The Seahorse XF system is a real-time metabolic flux analysis platform designed to quantify cellular bioenergetic function by measuring oxygen consumption and proton production rates in live cells (Yoo *et al.* 2024). By interrogating mitochondrial respiration and glycolytic activity under defined perturbations, it enables functional assessment of cellular metabolic states.

Mitochondrial function within self-directed differentiating NPCs was assessed using the Seahorse XF96 Analyzer (Agilent, Santa Clara, CA, USA). Solid-state sensors simultaneously measure both oxygen consumption rate (OCR) and extracellular acidification rate (ECAR) in response to sequential addition of respiration modulators (Plitzko and Loesgen 2018). OCR is the rate of the decrease of oxygen concentration in the assay medium and, therefore, it is an indicator of mitochondrial respiration (Plitzko and Loesgen 2018). ECAR corresponds to the rate of increase in proton concentration (or decrease in pH) in the assay medium and, therefore, is a measure of the rate of glycolysis (Plitzko and Loesgen 2018). Unless otherwise stated, or if techniques are referenced from another methods section, all equipment and reagents used in the Seahorse analysis experiments came from Agilent Technologies.

The Cell Mito Stress Test Kit (Agilent) was used to measure basal respiration, ATP-linked respiration, proton leak, maximal respiration, spare respiratory capacity, and non-mitochondrial respiration of NPC lines. Baseline OCR and ECAR are recorded prior to drug additions to establish basal respiration. Injection of oligomycin, a specific inhibitor of the F_1F_o-ATP synthase blocks proton flow through ATP synthase, causing OCR to drop, and ECAR to rise. The magnitude of this decrease corresponded to ATP-linked respiration, while the remaining OCR is considered proton leak. The rise in ECAR is considered maximal glycolysis. carbonyl cyanide-4 (trifluoromethoxy) phenylhydrazone (FCCP), a protonophore uncoupler, collapses the mitochondrial proton gradient, driving maximal electron transport and OCR, this peak rate defines maximal respiratory capacity. The difference between maximal and basal OCR yields the spare respiratory capacity. Finally, addition of rotenone (complex I inhibitor) together with antimycin A (complex III inhibitor) fully shut down mitochondrial electron transport, revealing non-mitochondrial OCR as the residual signal. (see Fig. 2.7).

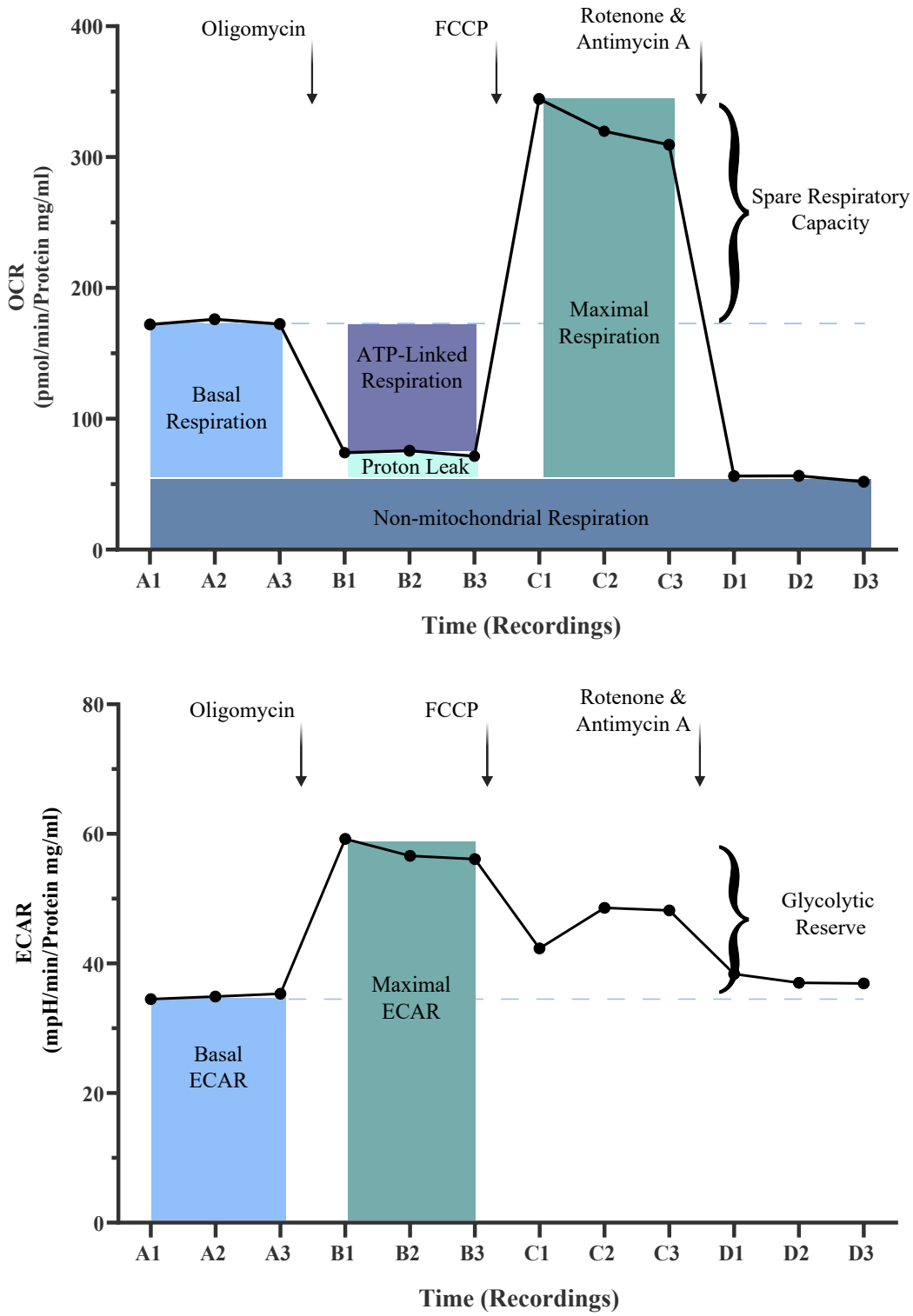

Figure 2.7: **Seahorse XF96 Mito Stress Test Experimental Profile.** Representative traces illustrating sequential measurements (A1 - D3) of **Above:** OCR and **Below:** ECAR. Bioenergetic measures are calculated based on the changes in readings between injections of intervals oligomycin, FCCP, and rotenone & antimycin. Trace schematic adapted from materials provided by Agilent Technologies.

2.9.1.1 Seahorse Experimental Preparation

7 days prior to Seahorse experiments, a Seahorse XFe96/XF Pro PDL Cell Culture Microplate (96-well) was coated in PLO solution (see section 2.4.6.1). As in section 2.4.6.2, NPCs were split with ACCUTASE™ and suspended in complete STEMdiff™ Neural Progenitor Medium containing 10 μM Y-27632 ROCK inhibitor. NPCs were seeded at an optimal density of 5 x 10^4 cells/well (determined experimentally as being sufficient to resolve differences in metabolic measures) and returned to incubator. 1 day prior to experiments, all wells received a half media change of complete STEMdiff™ Neural Progenitor Medium to avoid cell dislodging cells. When assessing inhibition of RyR-mediated calcium release (see section 4.2.6), target intervention wells media change contained 10 μM of dantrolene. The evening prior to the experimental work, the experimental sensor cartridge was hydrated in Seahorse XF Calibrant at 37°C in the non-CO_2 incubator, and the Seahorse XF96 Analyzer was turned on to reach operational temperature overnight.

On the day of the assay, NPCs were washed and incubated in XF Seahorse Base Medium DMEM supplemented with 1 mM sodium pyruvate, 10 mM glucose, and 2 mM L-glutamine. OCR and ECAR were measured over time under basal conditions, following experimental intervention (2 μM NMDA), and after the addition of the mitochondrial inhibitors (2.5 μM oligomycin, 2 μM FCCP and 0.5 μM rotenone/antimycin). At the end of experiments all media was aspirated, 20 μL of radioimmunoprecipitation assay buffer (RIPA) was added to each well to lyse cells, the plate was sealed in parafilm, and frozen at -20°C for later protein concentration determination (see section 2.9.2). Total experimental run time was 1 hour 33 minutes and data were exported using the Seahorse Wave 2.4 XF-96 software. For full protocol description see Table 2.12 below.

Table 2.12: **Mito Stress Test Experimental Run Protocol**

Command	**Duration (min)**	**Port**	**Drug**
Calibrate			
Equilibrate	12		
Mix - Measure (x 3)	6		
Inject		A	NMDA or Base Medium DMEM
Mix - Measure (x 3)	6		
Inject		B	Oligomycin
Mix - Measure (x 3)	6		
Inject		C	FCCP
Mix - Measure (x 3)	6		
Inject		D	Rotenone/Antimycin
Mix - Measure (x 3)	6		
End Protocol			

2.9.2 BCA Protein Assay Data Normalisation

The bicinchoninic acid (BCA) assay was used to determine sample total protein concentration for normalisation of Seahorse data. Pierce™ BCA Protein Assay Kits were used (ThermoFisher Scientific). Bovine serum albumin (BSA) protein standards of 1500, 1000, 750, 500, 250, 125, 25, and 5 μg/mL were made in RIPA. 50 parts reagent A was mixed with 1 part reagent B to make BCA working reagent. 10 μL of each standard and sample were loaded in duplicate into a 96-well plate. 200 μL of working reagent was added to each experimental well. The plate was incubated in the dark at 37°C with gentle rocking. A plate reader (SpectraMax M3, Molecular Devices) measured well absorbance at 562 nm. Sample protein concentrations were calculated from the standard curve generated using the absorbance readings from the standards. All subsequent seahorse data analysis was conducted on normalised data.

2.9.3 OCR Statistical Analysis

Analysis of OCR data collected using the Agilent Seahorse mitochondrial stress test assess absolute differences in the natural scale of six pre-defined bioenergetic measures (see Table 2.13). Within this thesis, Seahorse data were analysed using the OCR-Stats methodology described by Yépez *et al.,* 2018 (Yépez *et al.* 2018). Bioenergetic measurements based on differences in the logarithmic scale (see Table 2.13) were assessed using linear regression models to determine statistical significance between sample groups. Analysis, including automated outlier detection, was conducted in RStudio (v R-4.2.1) using code sourced from the Gagneur Lab Git repository.

Table 2.13: **OCR-Stats Definitions**

Traditional Bioenergetic Measures	**Ratiometric Measure**	**Metric**	**Definition**
Basal respiration: OCR_1 - OCR_4	E/I-proportion	$\frac{OCR_1 - OCR_4}{OCR_1} = 1 - exp(\theta_{Ei} - \theta_I)$	Proportion of OCR in the ETC with respect to the initial OCR
ATP-linked respiration: OCR_1 - OCR_2	A/I-proportion	$\frac{OCR_1 - OCR_2}{OCR_1} = 1 - exp(\theta_{Ai} - \theta_I)$	Proportion of OCR driven by ATPase proton pumping with respect to the initial OCR
Proton leak: OCR_2 - OCR_4	E/Ai-proportion	$\frac{OCR_2 - OCR_4}{OCR_2} = 1 - exp(\theta_{Ei} - \theta_{Ai})$	Proportion of OCR in the ETC, not driven by ATPase proton pumping, with respect to all non ATPase driven OCR
Spare respiratory capacity: OCR_3 - OCR_1	M/I-fold change	$\frac{OCR_3}{OCR_1} = exp(\theta_M - \theta_I)$	Ratio between maximal OCR and initial OCR
Maximal respiration: OCR_3 - OCR_4	M/Ei-fold change	$\frac{OCR_3}{OCR_4} = exp(\theta_M - \theta_{Ei})$	Ratio between maximal OCR and non-ETC driven OCR
Non-mitochondrial respiration: OCR_4	*NA*	*NA*	Not defined as a ratio

- OCR_i and θ_i correspond to the expected OCR value on the time interval i in the natural and logarithmic scale, respectively.
- Table modified from Table 1, Yépez *et al.,* 2018.

2.9.4 Resipher Live Tracking of Neural Progenitor Cell Respiration

The Lucid Scientific Resipher system (Lucid Scientific, Atlanta, GA, USA) was used to assesses differences in cell line metabolic behaviours during the transition from NPC to DGN. Similar to the Seahorse experiments, Resipher uses micro LED probes to detect O_2 concentrations within a cell culture well. Unlike the Seahorse system, Resipher probes move up and down within the well (see Figure 2.8). This allows for active-scanning of the oxygen gradient above the sample and reduces the effect of external variables (humidity, atmospheric pressure) on measurement accuracy. The in-incubator nature of the Resipher experiment also allows for monitoring of cellular respiration over a longer time period (days - weeks).

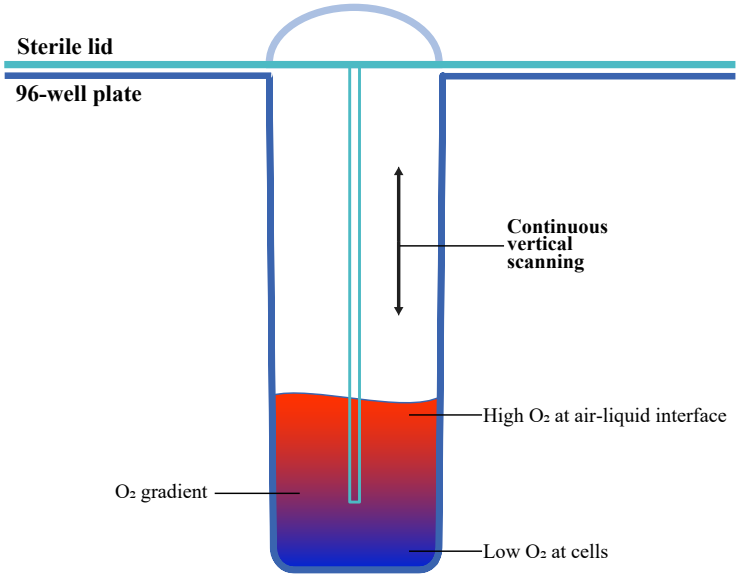

Figure 2.8: **Schematic of Resipher probe operation for oxygen gradient detection.** The Resipher system employs a vertically mobile micro-LED probe that continuously scans the oxygen gradient within a culture well, from the air–liquid interface to the cell layer.

As in section 2.9.1.1, NPCs were dissociated with ACCUTASE™ and seeded on PLO coated plasticware. On experimental day 0, NPCs were seeded in 100 µL complete STEMdiff™ Neural Progenitor Medium containing 10 µM Y-27632 ROCK inhibitor, at 5.7 x 10^3 cells/cm^2 on a 96-well Nunclon™ culture plate. On day 1, well media and non-attached cells were aspirated and replaced with 100 µL Y-27632 free complete STEMdiff™ Neural Progenitor Medium. Following media replacement the

Resipher probe lid (Fig. 2.9 A) was placed on-top of the cell plate, returned to the incubator, and connected to the Resipher plate sensor. Baseline OCR readings were taken from days 1 - 4. On experimental day 4, sample well media was replaced with 0.3 mL of DGNeuron media containing Wnt or complete STEMdiff™ Neural Progenitor Medium, with recordings lasting for a further 4 days. Readings from Resipher experiments were automatically uploaded to the Lucid Lab web application (*Lucid Lab https://lab.lucidsci.com/* 2025). Experimental traces (Figure 2.9 C) were taken from Lucid Lab and analysed using GraphPad Prism.

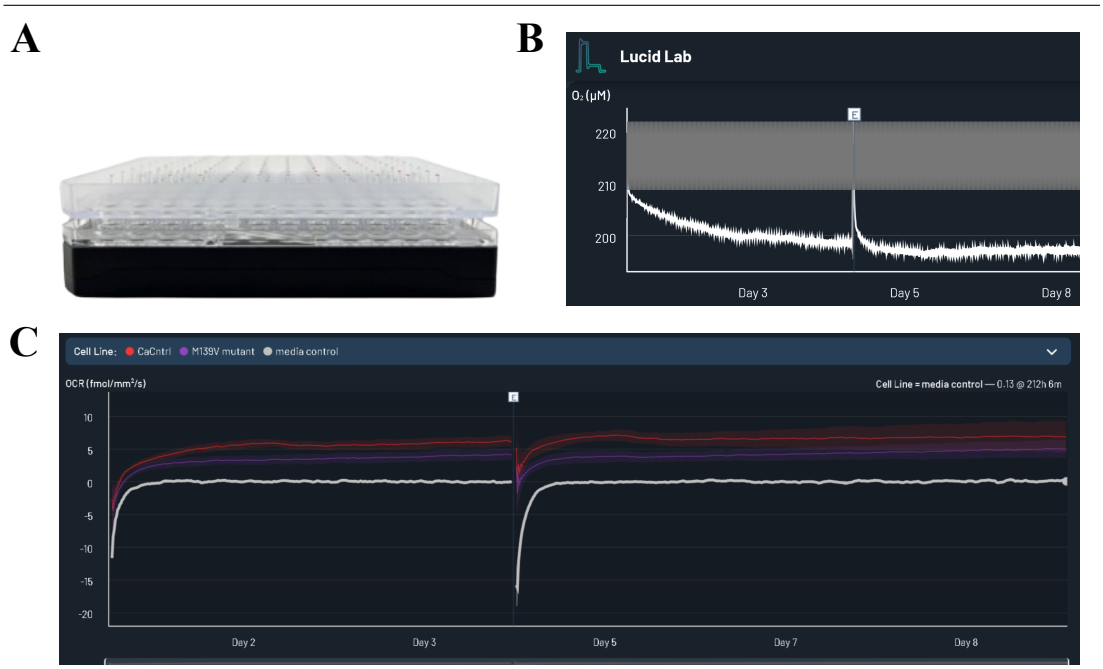

Figure 2.9: **Resipher components and experimental outputs.** Images of **A:** the inverted sensor lid and sensor unit. **B:** Example live (O_2 displayed in software. **C:** Example of full in-incubator OCR tracking data in Lucid Lab softwar.

2.10 Immunofluorescent labelling

2.10.1 Immunocytochemistry

To facilitate characterisation of cells post calcium imaging experiments, NPCs and DGNs cultured on glass coverslips were immunocytochemically labelled. Using a slightly modified version of the protocol described by Marchenko & Flanagan (2007) (Marchenko and Flanagan 2007), NPCs were washed three times with PBS prior to 15-minute fixation in 4% (w/v) paraformaldehyde (PFA) solution made in PBS (see Table 2.14 for full 4% PFA fixative preparation). Following washing with PBS (5 minutes x 3), coverslips were moved to PFA-free 35 mm cell culture dishes, and simultaneously permeabilised and blocked for non-specific epitope binding for one hour at room temperature with a PBS based buffer solution containing 10% (v/v) fetal bovine serum, 1% (w/v) bovine serum albumin, and 0.1% (v/v) Triton-X 100.

Primary and secondary antibody solutions were prepared in the same blocking buffer described above, with or without permeabilisation agent, depending on target epitope accessibility (see Table 2.15 for final working concentrations). In order to immunolabel cells correctly, 15 ul of primary antibody solution and 25 ul of secondary antibody solution were required per 13 mm coverslip.

Coverslips were incubated in primary antibody solution overnight at 4°C by inverting the coverslip (fixed cells facing down) onto a drop (15 µl) of primary antibody solution on a metal plate covered with parafilm. A second sheet of parafilm was placed over the entire construct to prevent evaporation of solutions. Coverslips were then returned to 35 mm cell culture dishes for three, five minute, PBS washes. For secondary antibody incubation, coverslips were again inverted and placed onto a drop of secondary antibody solution (25 µl) on fresh parafilm, sealed, and incubated in the dark, for one hour at room temperature. Following repeated PBS washes (as described previously), coverslips were mounted on 25 x 75 mm microscope slides, with Fluoroshield DAPI-containing antifade mounting solution. To avoid crystal formation, and later image disruption, the back (fixed-cell free) side of coverslips were briefly washed with deionised water, directly before microscope slide mounting. Mounted slides were left to cure overnight in the dark at room temperature and stored at 4°C.

For a full list of all antibodies used, their concentrations and their targets see Table 2.15.

Table 2.14: **4% Paraformaldehyde Fixative preparation (Marchenko & Flanagan, 2007)**

Reagents and steps	For 100 mL of fixative
Deionised Water	75 mL
Paraformaldehyde	4 g
5N NaOH, added dropwise until solution clears	As needed
10X PBS	10 mL
1M $MgCL_2$	0.5 mL
Sucrose	4 g
1N HCl, titrate to pH 7.4	As needed
Deionised Water	Bring to 100 mL

- Filter prior to use.
- Store at 4°C for up to 1 week.
- Warm to 37°C before use

Table 2.15: **Immunocytochemical reagents and their targets**

Antigen	Host	Clonality	Supplier	Working Concentration
MAP2	Rabbit	Polyclonal	Abcam	4 µg/mL
βIII-Tubulin	Rabbit	Polyclonal	Abcam	4 µg/mL
Nestin	Rabbit	Monoclonal	Abcam	4 µg/mL
SOX2	Goat	Polyclonal	R&D Systems	8 µg/mL
PROX1	Rabbit	Monoclonal	Abcam	4 µg/mL
FOXG1	Rabbit	Monoclonal	Abcam	3 µg/mL
TBR1	Rabbit	Monoclonal	Abcam	1 µg/mL
DAPI	*NA*	Nuclear Stain	R&D Systems	1 µg/mL
Hoechst 33342	*NA*	Nuclear Stain	Cell Signalling Technology	1 µg/mL
Sytox DeepRed	*NA*	Nuclear Stain	Thermofisher	0.5 µM
Goat IgG	Donkey	FITC-conjugated	Thermofisher	10 µg/mL
Rabbit IgG	Donkey	TRITC-conjugated	Jackson Research	7.5 µg/mL

2.10.2 Confocal Microscopy

Fluorescence imaging of fixed, immunolabelled coverslips was performed using a laser-scanning confocal microscope (Olympus Fluoview FV10i, Department of Pharmacology & Therapeutics, University College Cork, Cork, Ireland). Fluorophore-specific laser lines and detector gain/saturation settings were optimised per antibody and kept constant across all samples within a given experimental group. Imaging was carried out under matched acquisition parameters to ensure comparability between biological replicates. Confocal fluorescence lifetime imaging microscopy (FLIM) of live and fixed samples was performed using a Leica Stellaris 8 Falcon FLIM microscope (Ghent Light Microscopy CORE, Ghent University, Ghent, Belgium). Fiji ImageJ software was used to visualize and anaylse images.

2.10.3 3D Sample Fixation & Labelling

Three dimensional tissue samples present unique issues when it comes to imaging. To reliably image fixed 3D tissues, without destroying the sample in the process, they underwent additional "SHIELD" stabilization to harsh conditions via intramolecular epoxide linkages to prevent degradation (SHIELD) fixation, delipidisation, and actively controlled "eFlash" antibody staining. The "Single-cell and Cytoarchitecture analysis of Organoids using Unbiased Techniques (SCOUT) Analysis Pipeline" designed for multiscale 3D phenotyping of human cerebroids by the Chung Lab (Albanese *et al.* 2020) was adapted for use in this thesis with the help of Dr Keith Siew and Dr Ben Walsh of University College London. Time working in the Walsh Lab was funded by a Company of Biologists Travel Fellowship.

SHIELD fixation and eFlash staining both work on the principle of uniform diffusion of an inactive agent throughout the tissue and subsequent activation of the fixation/staining. Both techniques are described in full in Park *et al.*, 2019 (Park *et al.* 2019) and Yun *et al.*, 2019 (Yun *et al.* 2019). SHIELD polyepoxide reactivity is suppressed at 4°C, pH 7.4, and increased tenfold at 37°C, pH 10. As opposed to PFA fixation, SHIELD fixation enhances the stability of protein tertiary structure, and preserves tissue architecture and endogenous fluorescence under harsher chemical/thermal conditions, without impeding antigen accessibility. Many immunolabelling probes have weak binding affinity in the presence of high concentrations of bile salts and a basic pH. The eFlash technique uses stochastic electrotransport to simultaneously disperse target inactive probes rapidly and to gradually acidify sample solution by electrocatalytic oxidation. Pairing this with the selective removal of bile salts from the eFlasg antibody cocktail via nanoporous membrane, the "SmartLabel" device uses the eFlash technique to control the high-

quality uniform immunolabelling of the whole 3D tissues. The following protocols were derived from the LifeCanvas Technologies "Full Active Pipeline Protocol V2.7". Protocol specific reagents are listed in table 2.19 below.

2.10.3.1 Cerebroid SHIELD Fixation

Cerebroids were washed three times with PBS, prior to a 30-minute fixation with freshly prepared 4% PFA in PBS at room temperature on a shaker. After fixation cerebroids were again washed three times in PBS, transferred into ice cold modified "SHIELD OFF" solution, which contains inactive epoxy diffusing throughout the sample (Table 2.16), and incubated for 48 hours at 4°C with light shaking. Subsequently, samples were transferred directly to "SHIELD ON" solution, which alkalised the sample, activating epoxy cross-linking, and were incubated for a further 24 hours at 37°C with light shaking.

Table 2.16: **Modified SHIELD OFF Solution Preparation**

Reagent	Percentage	Volume for 20 mL Solution
De-Ionised Water	59.375 %	11.875 mL
SHIELD Buffer	25 %	5 mL
SHIELD Epoxy	15.625 %	3.123 mL

2.10.3.2 Cerebroid Delipidation

Cerebroids are small and delicate, mounting in 1-3% agarose mould prior to delipidaton ensures samples can be reliably handled throughout the rest of the analysis pipeline.

SHIELD fixed cerebroids were washed extensively with PBS for 8 hours, cleared in 0.2 M SDS (Delipidation Buffer) for 48 hour at 55°C while shaking in EasyClear system (LifeCanvas Technologies), and washed in PBST (PBS, 0.1% Triton X-100, 0.02% sodium azide) for 24 hours. Lipid cleared cerebroids could be stored in PBST at 4°C.

2.10.3.3 Cerebroid Immunohistochemistry with SmartLabel Device

Prior to labelling, cleared cerebroids were equilibrated overnight in "Primary Sample Buffer" at room temperature with light shaking. Sample Buffer was refreshed and incubated for a further 3 hours. All antibody cocktails were prepared in 1 mL Sample Buffer. For full list of antibodies used in cerebroid staining see Table 2.17.

The SmartLabel system, designed for the eFlash technique, was rinsed thoroughly a minimum of 3 times with de-ionised water. The Sample Cup was washed sequentially in de-ionised water and fresh Sample Buffer. Agarose mounted cerebroids were placed in the Sample Cup and fully submerged in 3 mL Sample Buffer and 1 mL antibody cocktail. The Sample Cup was placed into the Labelling Chamber, the system filled with Labelling buffer, and operated at the conditions described in table 2.18. Completed samples were washed in PBS and stored in the dark prior to use.

Table 2.17: **eFlash Compatible Antibodies/Stains**

Antigen	**Host**	**Clonality**	**Supplier**	**Working Concentration**
SOX2	Goat	Polyclonal	R&D Systems	1 µg/mL
TBR1	Rabbit	Monoclonal	Cell Signalling Technologies	2 µg/mL
SYTOX Red	*NA*	Stain	ThermoFisher Scientific	5 µM

Table 2.18: **SmartLabel Settings**

Setting	**Value**
Voltage	90 V
Current Limit	1000 mA
Temperature	25°C
Rotation Speed	00.1 RPM
Timer	21 hours

Table 2.19: **Fixation & Labelling Materials**

Category	Material	Vendor
SHIELD Fixation	SHIELD-Epoxy Solution	LifeCanvas Technologies
	SHIELD-Buffer Solution	
	SHIELD-On Buffer Solution	
Delipidation	EasyClear Delipidation Buffer	
eFlash Staining	Primary Sample Buffer	
	Labelling Buffer	
Refractive Index Matching	EasyIndex	

2.10.3.4 Index Matching & Mounting

All samples were refractive index matched in EasyIndex (LifeCanvas Tachnologies) for a minimum of 16 hours at 37°C with light shaking. For mesoSPIM imaging, labelled cerebroids were mounted in custom cuvette moulds in 0.9% low melting point agarose made in PBS prior to refractive index matching.

2.10.4 Multiscale 3D Cerebroid Phenotyping

Current analysis of organoid tissues relies heavily on single-cell transcriptomics and 2D histology. While large amounts of new data can be extracted with these methods they do not take advantage of the primary benefit of organoid culture, the self-assembly of cells in 3D is not being mined fully. By pairing mesoSPIM light sheet microscopy with the Single-cell and Cytoarchitecture analysis of Organoids using Unbiased Techniques (SCOUT) computational pipeline (Albanese *et al.* 2020) we attempted to perform quantitative analysis of intact whole cerebroids.

2.10.4.1 mesoSPIM Imaging

All mesoSPIM imaging was conducted at the Sainsbury Wellcome Centre Advanced Microscopy Unit (London, UK), with assistance from Dr Rob Campbell and Dr Peter Gordon. Stained and refractive index-matched cerebroids, prepared as described

in section 2.10.3.4, were imaged using a custom-built mesoscale selective plane illumination microscope mesoSPIM v5.1 (Voigt *et al.,* 2019, www.mesospim.org)(see Fig. 2.10), which offers advantages over standard confocal microscopy, such as more rapid volumetric imaging of larger samples with reduced photobleaching. Tissues were imaged using 647 nm, 561 nm, and 488 nm excitation, while the emission signal was acquired at 2x zoom (2,048 x 2,048 pixels, 3.26 µm pixel size) with 10 µm optical sections.

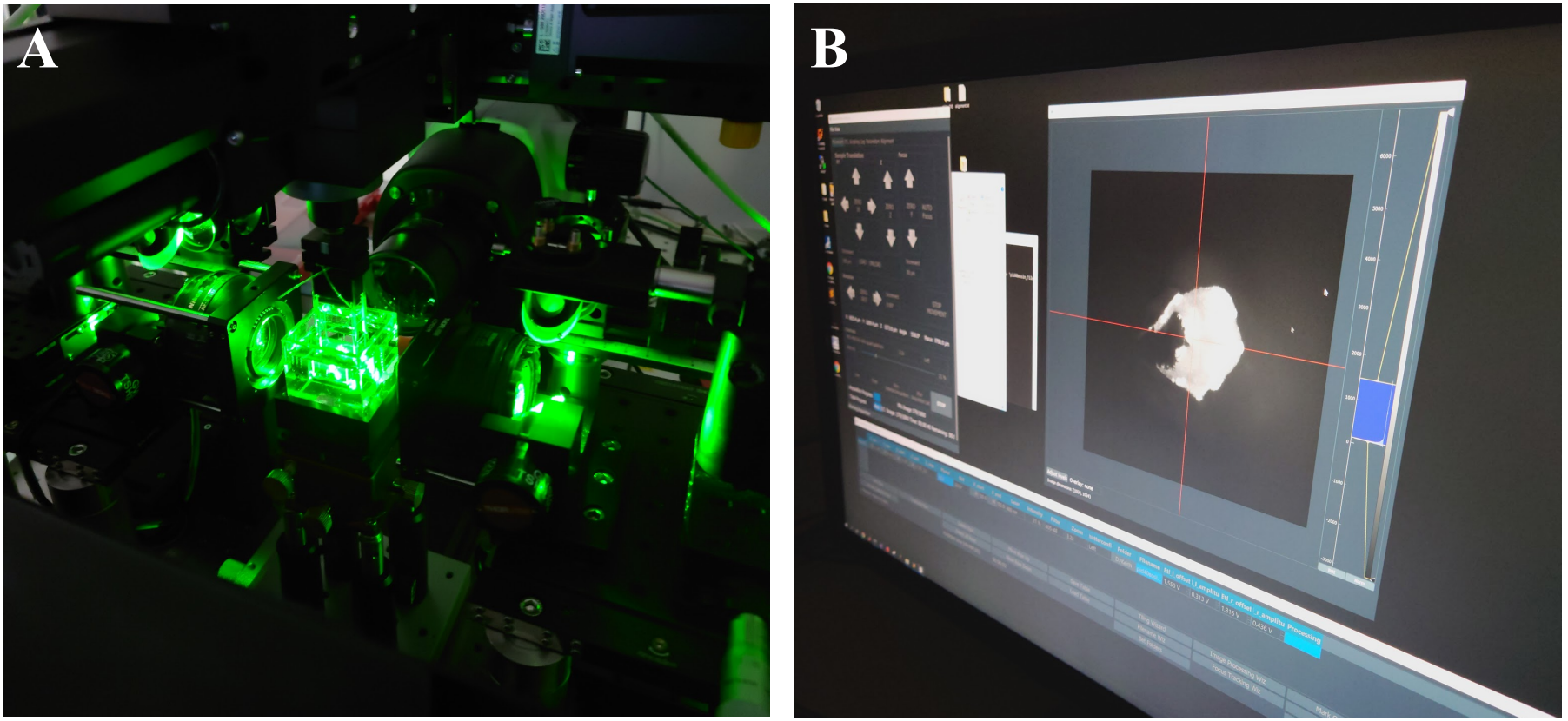

Figure 2.10: **mesoSPIM v5.1.** Images of custom built light sheet microscope. **A:** Laser illumination of mounted sample. **B:** Software rendering volumetric image in real-time during imaging. Images taken with a phone camera.

DEVELOPMENT OF HUMAN NEURAL TISSUE FOR EXPLORATION OF CELLULAR CHANGES ASSOCIATED WITH ALZHEIMER'S DISEASE

3.1 Introduction

Human brain development begins with neurulation of the embryonic ectoderm and unfolds over roughly 20 to 25 years (Jiang and Nardelli 2016). This extended maturation requires the temporally and spatially controlled production of diverse neural and non-neural cell types (Li *et al.* 2023b), as well as the establishment of accurate synaptic connections and efficient intercellular communication to coordinate behaviour, perception and higher cognitive functions (Huttenlocher and Dabholkar 1997; Petanjek *et al.* 2011). Our ability to study this organogenesis has tracked technological advances. Early histological innovations, such as tissue fixation and microtomy let His, Cajal, and colleagues capture early human cellular morphology and identify unique cell types (de Castro and Merchán 2016). Microscopy of developing neural tissue revealed primate neocortical progenitors (Rakic 1971) and mapped human synapse formation (Huttenlocher 1979). *Ex vivo* culture of foetal cells enabled live analysis and the directed differentiation of neurons and glia *in vitro* (Hansen *et al.* 2013; Krencik and Zhang 2011; Zhang *et al.* 2001). iPSC reprogramming opened the door to patient-specific neural models (Takahashi and Yamanaka 2006)(see section 1.5), and finally, organoid technology has made human organogenesis accessible and visible in the lab (Kelley and Pașca 2022; Lancaster *et al.* 2013). So, this evolution of technology has facilitated advances in the field of neuroscience and clinical medicine as a whole.

3.1.1 iPSC-derived human neuronal tissue (2D and 3D)

iPSC technology has been instrumental in studying human neurodevelopment and *in vivo* cell function, but its utility is also informed by the dimensional structure of the culture systems that can be derived from stem cells. Early cortical models used 2D cultures: NPCs derived from pseudo-monolayer iPSCs formed flattened neural rosettes on planar surfaces, exhibiting lumen-like structures and characteristic neural migration patterns (Shi *et al.* 2012; Wilson and Stice 2006). However, the 2D systems lack the three-dimensional microenvironment that is critical to the complex signalling that underpins human brain function. This is of particular relevance to the hippocampal formation, the brain region where declarative memories are laid down and consolidated. Pathologically, the hippocampus is one of the regions first affected in AD, a factor

which accounts for one of the most prominent features of AD, declarative memory loss (Heneka *et al.* 2024). With the goal of creating a human-derived experimental model, that is more faithful to human brain tissue and structure, advances that have been made in the development of 3D cerebroids are promising. During this development, 3D cerebroids generate neuroepithelium and then recapitulate *in vivo* neurogenesis by allowing neural tube-like structures (neural rosette equivalents) to form and expand either in suspension, or embedded within an extracellular matrix (Jain *et al.* 2025; Lancaster *et al.* 2013). The ability to study the development of cerebroids both temporally and in three dimensions benefits our understanding of both physiological and pathophysiological neurodevelopment, as it is now possible to observe the cells as they develop their own orientation and spatial relations.

3.1.2 Stem cell-derived models investigating AD-related neuronal pathophysiology

Excitingly, distinctive *in vitro* iPSC-derived experimental models are emerging (Kelley and Pașca 2022), which promise to complement extant animal models in AD research. At its core, iPSC-derived human culture systems represent a technology, a dynamic collection of tools, techniques, and materials that offer immense value to medical research. Initially developed by stem cell biologists, the utilization of this technology has experienced exponential growth, particularly under the purview of geneticists (Klompstra, Yoon, and Koo 2025; Sato *et al.* 2009). The obvious advantage to using human-derived neurophysiological experimental models is the opportunity to develop models of specific neuropathologies. For example, it is possible to recapitulate both genetic and sporadic AD-linked neuronal and glial phenotypes in cerebroids derived from iPSCs from early- and late-onset AD patients, respectively. Recapitulated phenotypes have included altered Aβ42/40 ratios, tau phosphorylation, oxidative stress, and lysosomal dysfunction. Others have applied this system to enable high-throughput screening of drug candidates and biomarkers (Birnbaum *et al.* 2018; Haidar *et al.* 2024; Nieweg *et al.* 2015).

With the goal of more accurately recapitulating human physiology and pathophysiology, we sought to establish, validate and advance the use of human iPSC-derived cultures for the study of healthy neurophysiology and pathological changes associated with neurodegenerative diseases, specifically AD.

3.1.3 Chapter Hypothesis and Aims

We hypothesised that the use of both 2D and 3D human iPSC-derived neuronal cultures could more accurately recapitulate human physiology and pathophysiology, and provide a better framework for replicating studies conducted on animal models of AD. To facilitate this, the aims of this chapter were as follows:

1. To generate NPCs, novel 2D DGNs, and 3D cerebroids from iPSC lines, including from a patient with the familial Alzheimer's disease presenilin1 mutation M139V.
2. To characterise the function and morphology of 2D and 3D human iPSC-derived culture products in order to asses their viability for the replication of previous experiments in AD animal models.

Techniques used:

1. Induced pluripotent stem cell culture (2.3)
2. Neural progenitor cell culture (2.4).
3. Neural progenitor cell coverslip culture (2.4.6).
4. Dentate gyrus mature neuron induction (2.5.2).
5. Cerebral organoid culture (2.6)
6. Air-liquid interface cerebral organoid culture (ALICO) (2.7)
7. Perfusion bath calcium imaging (2.8).
8. Real time oxygen consumption rate recording (2.9.4).
9. Immunohistochemistry and immunocytochemistry (2.10).

3.2 Results

To facilitate the 2D culture of human neural lineage cells, NPCs were generated from two healthy control iPSC lines and one FAD line (PSEN1 M139V) using a version of the protocol described in Section 2.4 of this thesis (Chambers *et al.* 2009) (For full cell line information see Table 2.1). The primary practical benefit of expanding NPC cultures is the ability to introduce a differentiation 'checkpoint' after approximately 21 days (illustrated in Fig. 3.1). At this point, cells are a stable progenitor population committed to the neural lineage differentiation that can be cryopreserved. This approach allows a large biomass to be established before the selection and initiation of more specialised, shorter neuronal maturation protocols.

3.2.1 Generation of human NPC cultures

NPCs were generated in 2D culture from the control iPSC lines RBi001a ($n_{inductions} = 2$) and CaCntrl ($n_{inductions} = 2$), and one FAD line ($PSEN1_{M139V}$) ($n_{inductions} = 2$). Establishing human NPC cultures in 2D enabled the rapid expansion of a large, uniform cell population prior to neuronal maturation using a standardised and validated NPC induction protocol (Fig. 3.1).

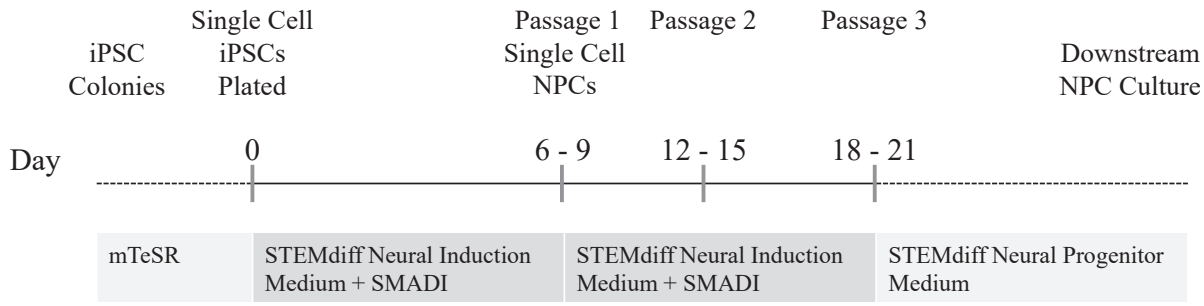

Figure 3.1: **Simplified schematic of neural progenitor cell (NPC) induction protocol.** The figure above illustrates the key steps involved in generating NPCs from iPSCs. The protocol was used for iPSCs from healthy donors (RBi001a and CaCntrl) and a patient with FAD ($PSEN1_{M139V}$).

To validate the success of this protocol, the impact of biophysical cues on iPSCs as they progressed through NPC induction was monitored using phase-contrast microscopy (Fig. 3.2). From day 1 to day 6, single-cell monolayers of iPSCs were exposed to inhibitors of the SMAD signalling pathway (Noggin and SB431542) to drive cells towards differentiation into NPCs. On visual inspection, initial iPSCs seeded as single

cells displayed non-uniform cell shapes, and unclear boundaries between cells (Fig. 3.2A, indicated by arrow). These single cells try to reform colonies, the preferred state of iPSCs (Fig. 3.2B, indicated by circle), which could be observed when the larger denser cell clumps bent light into a bright shine (Fig. 3.2B, indicated by arrow). After the first NPC passage, elongated cells, with more defined boundaries become more common (Fig. 3.2C, indicated by arrows), and the density of colony-like shapes reduce (Fig. 3.2D, indicated by arrows) as cells no longer need the colony structure. Following the second NPC passage, elongated (rectangular) cells with clearly defined cell borders are visible (Fig. 3.2E, indicated by arrows). Cells become densely packed in a true 2D monolayer (Fig. 3.2F), consistent with the development of a stable NPC culture.

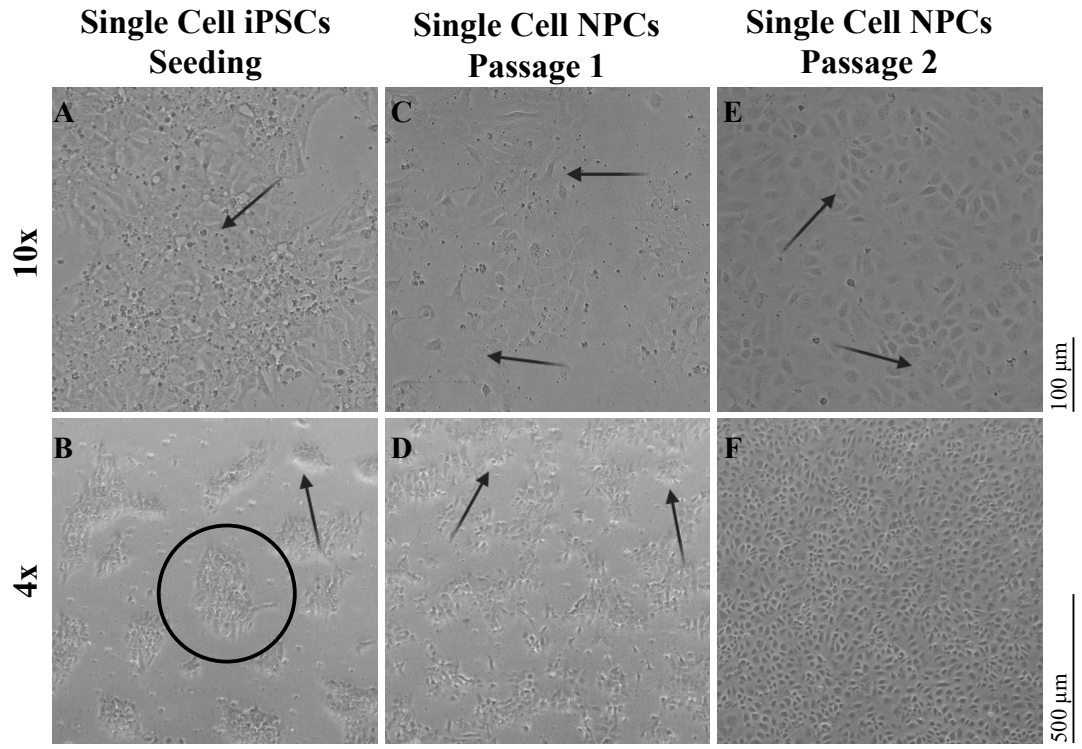

Figure 3.2: **Morphological changes observed during NPC induction.** Phase contrast images of the morphological changes in iPSCs seeded as single cells on **A B**: day one of initial seeding, **C, D**: day one following single cell NPC passage 1, and **E, F**: day one following NPC passage 2. Images captured at 4x and 10 magnification, scale bars denote 100 µm and 500 µm.

After three weeks, and three passages, cultures containing densely packed, morphologically homogenous cells were considered viable NPCs, and the induction media was

replaced with STEMdiff Neural Progenitor Medium (Fig. 3.1). From this point, cells were sub-selected for subsequent, shorter-term neuronal differentiation protocols. Stock NPCs were maintained as dense cultures on Matrigel. If stock cultures showed increased cellular maturation, such as axonal or dendritic elongation and/or the formation of round granular cell bodies, they were discarded.

3.2.2 NPCs express maturing neuronal cytoskeletal proteins

In addition to morphological cues of maturation into NPCs, as evident under brightfield illumination, immunofluorescently-labelled protein expression also provided evidence of differentiation of iPSCs into a neuronal lineage. To confirm these changes, cultured NPCs (see Section 2.4.6) at d4 and d12 (CaCntrl d4 $n_{coversilps} = 8$, $n_{cultures} = 4$, d12 $n_{coverslips} = 4$, $n_{cultures} = 1$; PSN1 d4 $n_{coverslips} = 3$, $n_{cultures} = 1$, d12 $n_{coverslips} = 4$, $n_{cultures} = 1$) were fixed and immunofluorescently stained using monoclonal antibodies targetting markers of neural identity (as described in methods section 2.10). The expected time period for iPSCs to transition to NPCs is from 6 to 14 days (Chambers *et al.* 2009). Hence, we compared d4 cells, which are likely to have iPSC traits, to d12 cells, which are likely to have been driven towards NPCs.

Expression of the transcription factor SRY-box transcription factor 2 (SOX2) was used to confirm the presence of pluri/multipotent stem cells. In this context, SOX2 was expected in both undifferentiated stem cells (d4) and neural progenitor cells (d12). SOX2 can be both nuclear and cytosolic (Schaefer *et al.* 2024). Indeed, diffuse SOX2 labelling was observed throughout the cell bodies of cells at d4, both in the cytosol and the nucleus (Fig. 3.3A, green labelling, indicated by white arrow). Interestingly, by d12, along with morphological changes in the developing NPCs, expression of SOX2 also appeared different. Labelling was predominantly outside of the nucleus in the cellular cytosol (Fig. 3.3D and D1 magnified image, nucleus indicated by white arrow) suggesting a change of protein function over time.

Co-expression of SOX2 with other markers of neural lineage was explored in an attempt to confirm cell differentiation. The cytoskeletal proteins nestin, βIII-tubulin (also referred to as Tuj1) and MAP2 are commonly used to define the degree of neuronal differentiation (Garavaglia *et al.* 2010; Liu *et al.* 2013). βIII-tubulin is a major microtubule protein expressed in post-mitotic neurons. Surprisingly, βIII-tubulin was present in both d4 and d12 cells (Fig. 3.3B, E). Consistent with its function as a cytoskeletal protein, labelling was strong in the developing processes of these cells (Fig. 3.3B, E, red labelling, indicated by arrows). Moreover, when the post-mitotic neuronal marker

was dual-labelled with SOX2, the label for pluripotent stem cells, there was no evidence of co-expression, with both markers localized to regions specific to their proteins (cell body for SOX2 and the processes for βIII-tubulin) (See merged image, Fig. 3.3C1, F1, indicated by white arrows). Nonetheless, expression of both markers in the same cells confirms that at 4 and 12 days in culture, the cells were of mixed neuronal lineage (Fig. 3.3C, F).

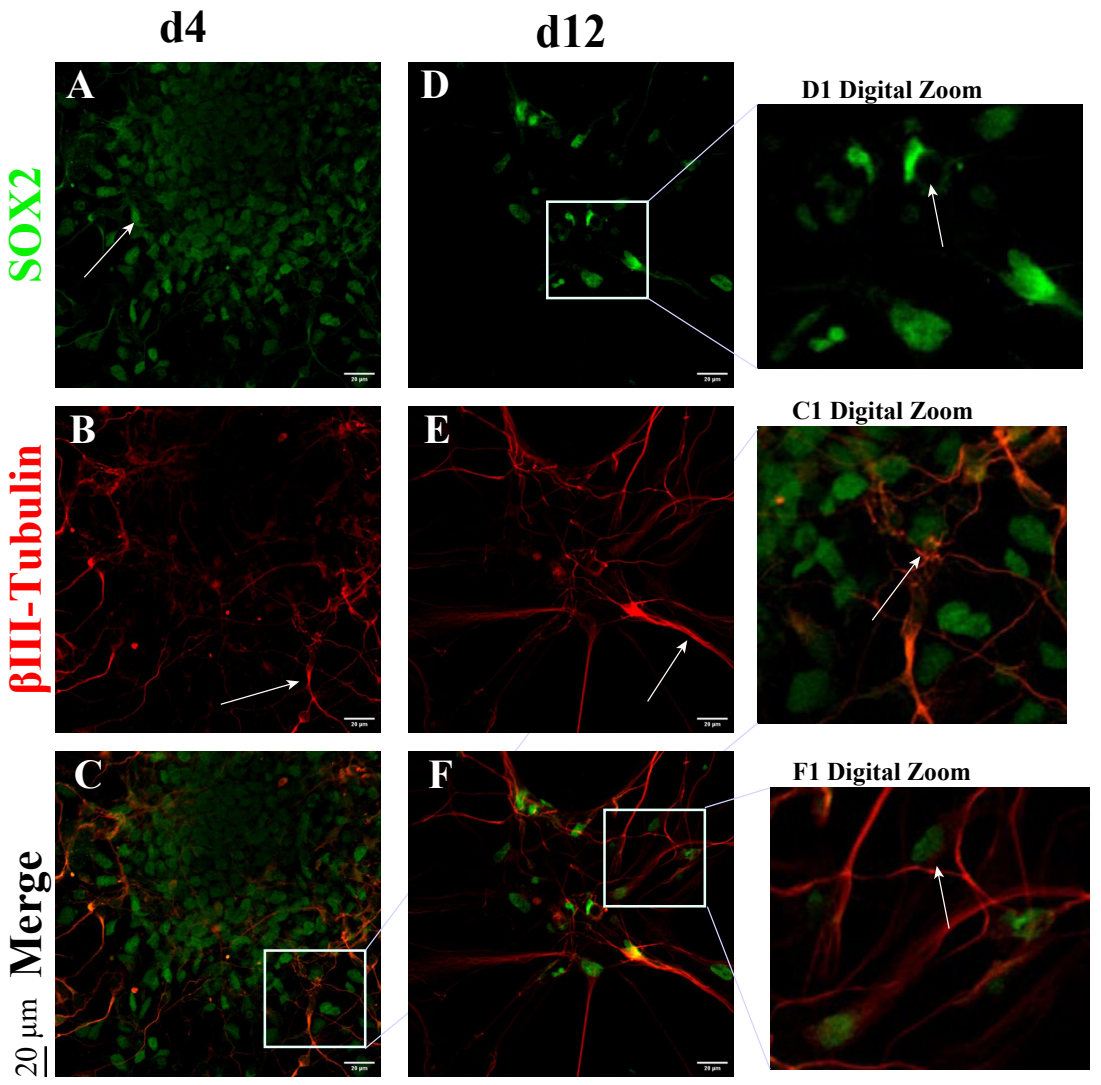

Figure 3.3: **NPC cultures express both SOX2 and βIII-tubulin.** Representative confocal florescent images of NPCs at **A-C**:4 and **D-IF** 12 days post-coverslip culture, generated from control CaCntrl and fAD PSN1 iPSC lines. Cells were stained for **A, D:** SOX2 and **B,E** βIII-tubulin. Both channels were merged **C, F:** and some images have an accompanying digital zoom to visualise sites of interest. White arrows indicate, **A** nuclear and cytoplasmic labelling, **B, E** cell process labelling, **D1:** stain free nuclei, and **C1, F1:** the compartment specific separation of labels. Scale bar denotes 20 µm.

Independent of SOX2, co-labelling of Nestin and MAP2 on d12 cells (PSN1 d12 $n_{coverslips} = 6$, $n_{culture} = 1$) is shown in Fig. 3.4. Nestin is an intermediate filament protein highly expressed during early stages of proliferative neuronal development. It was detected in a filamentous pattern throughout the d12 cells (Fig. 3.4A green labelling). Nestin is reported to be strongly expressed in axons (Bott *et al.* 2019), consistent with the labelling pattern observed here (Fig. 3.4A, indicated by arrow). Microtubule associated protein 2 (MAP2) is a protein that binds to and stabilises microtubules in mature neurons and is specifically expressed in dendritic structures. It serves as a reliable marker of neuronal differentiation. As stem cells differentiate, they begin to express MAP2, reflecting the acquisition of mature neuronal features. In agreement with this developmental transition, MAP2 labelling was evident at d12 (Fig. 3.4B red labelling). As expected, labelling was particularly strong in cellular processes (Fig. 3.4B, indicated by arrows) which were in contact with, and emerging from, Nestin-positive structures (Fig. 3.4C, digital zoom, indicated by arrows). This cytoskeletal reorganisation supports the assertion that iPSCs were transitioning of these cells from pluripotent iPSCs to NPCs.

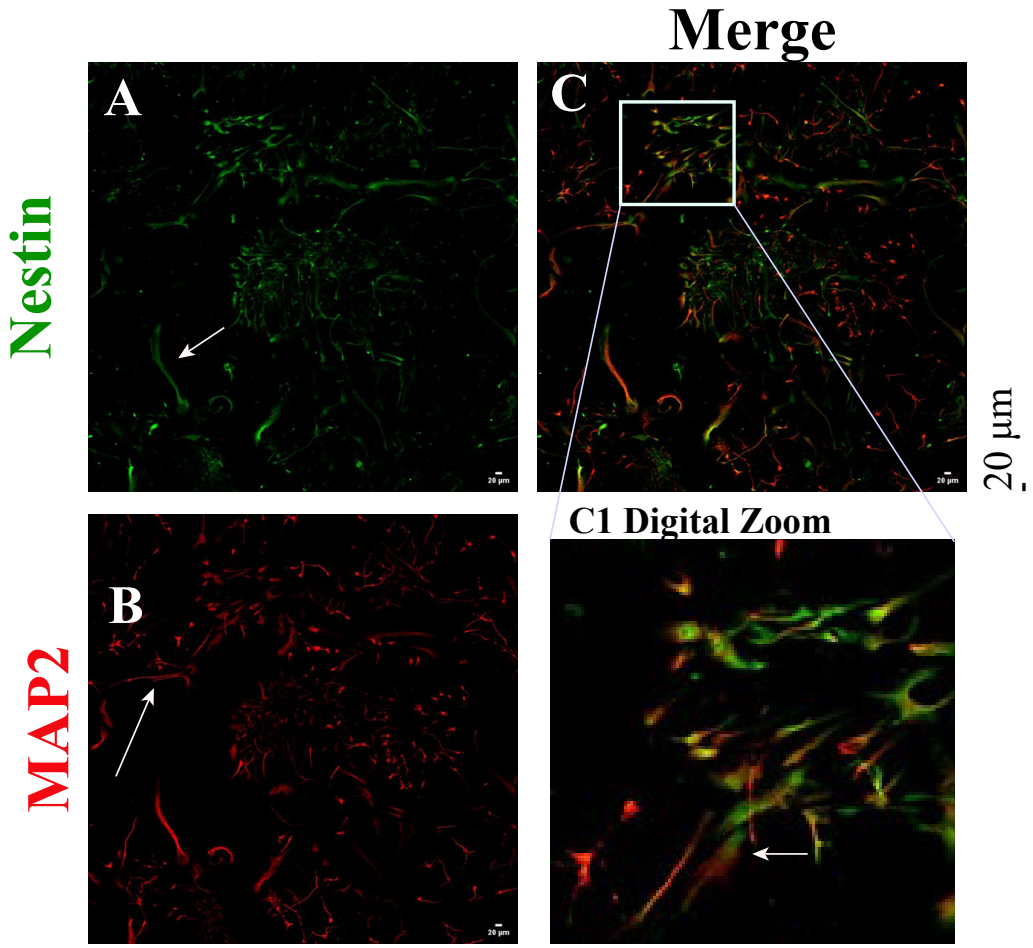

Figure 3.4: **NPC cultures express both Nestin and MAP2 cytoskeletal proteins.** Representative confocal florescent images of NPCs at 12 days post-coverslip culture, generated from the fAD mutant PSN1 iPSC lines. Cells were stained for **A:** Nestin and **B:** MAP2. **C:** The overlay of both channels is further enhanced by digital zoom. White arrows denote cell filaments of interest. Scale bar denotes 20 µm.

3.2.3 Neural progenitor culture products exhibit physiological functionality

Having confirmed morphological characteristics that were consistent with the development of iPSCs into NPCs, we then examined the physiological function of d4 - d13 NPCs. Consistent with these NPCs having intact neurophysiological responses, HBSS containing elevated K^+ (50 mM, 30 seconds), which depolarizes cell membranes and thereby opens VGCCs on the neural plasma membrane induced robust increases in intracellular calcium (Fig. 3.5A, B) from baseline (Wilcoxon matched-pairs signed-rank test; CaCntrl $n_{cells} = 79$, $n_{experiments} = 10$, $n_{cultures} = 4$; $W = 3160$; $p < 0.001$), with a median difference of 13.15 arbitrary fluorescence units (A.F.U.)(95.78% CI 9.49 to 14.21).

As expected for cells lacking functional group 1 mGluRs, only 8.8% $\pm$ 3.2% of K^+-responsive NPCs ($n_{cells\ responding} = 3$, $n_{cells\ total} = 46$, $n_{experiments} = 4$, $n_{cultures} = 2$; mean $\pm$ SEM) responded to the specific I-mGluR agonist, S-dihydroxyphenylglycine (DHPG) (50 μM, 120 seconds), with an increase in intracellular calcium (Fig. 3.5C, D).

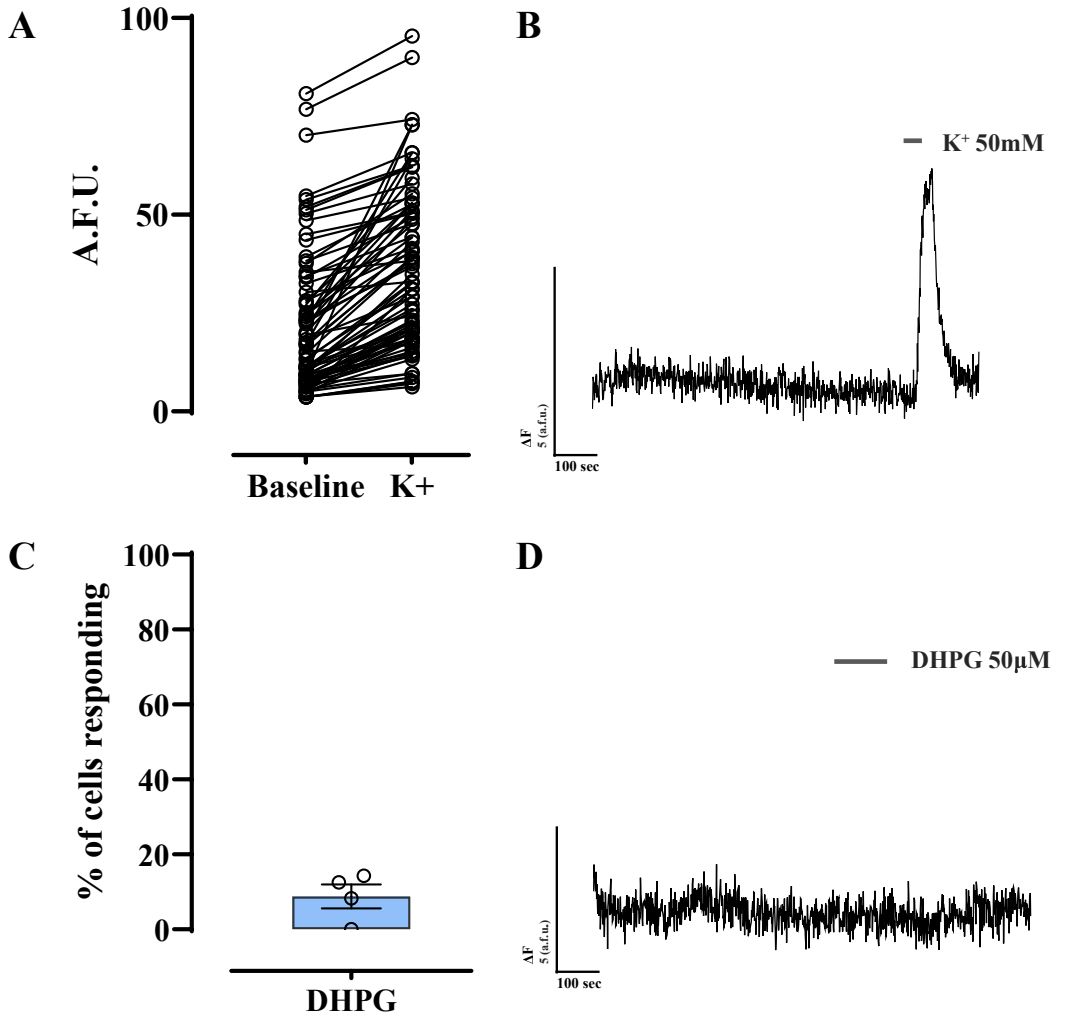

Figure 3.5: **NPCs exhibit physiological stimulus-evoked Ca^{2+} responses. A:** Paired scatter plot of baseline vs. K^+-evoked intracellular Ca^{2+} fluorescence. Lines connect measurements from the same cell. **C:** Bar plot (bar = mean +/- SEM) of percentage of confirmed K^+-responsive NPCs responding to S-DHPG (50 µM). Individual experiment values denoted as open circles. Representative single-cell ΔF traces of typical NPC Ca^{2+} transients in response to **B:** 30 second application of 50 mM K^+, and **D:** 120 second application of S-DHPG (50 µM). Scale bars denote 100 seconds and 5 A.F.U.: arbitrary fluorescence units.

3.2.4 Generation of human-derived mature dentate gyrus-like neuronal cultures

With the goal of using human dentate gyrus (DG)-like mature neurons to facilitate cell type- and species-specific investigations of AD hypotheses, NPCs from two healthy control donors (RBi001a and CaCntrl) and a donor with FAD ($PSEN1_{M139V}$), were used to generate human-derived DGNs cells. Using a protocol designed in-house, based on previous work (described fully in Section 2.5 of this thesis (Vőfély *et al.* 2018; Yu *et al.* 2014)), NPCs were prepared as neural progenitor coverslip cultures (NPCC)s and then exposed to our DG induction media to induce differentiation.

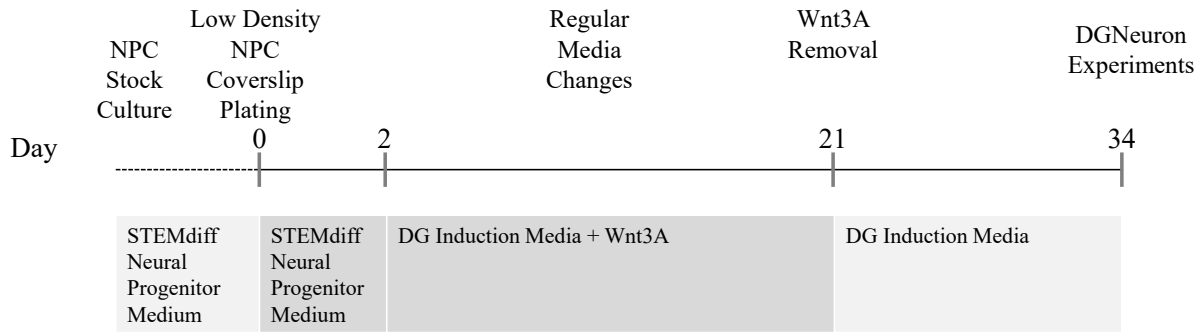

Figure 3.6: **Simplified schematic of dentate gyrus like neuronal (DGN) culture protocol.** The figure above illustrates the key steps involved in generating DGNs from NPCs. The protocol was used for NPCs from healthy donors (RBi001a and CaCntrl) and a patient with FAD ($PSEN1_{M139V}$).

3.2.4.1 DGNs display desired mature morphology over extended differentiation

NPCs seeded at low densities (2 x 10^4 cells/cm^2) on glass coverslips were exposed to DG induction media containing Wnt3A (Fig. 3.6) a protein important in neuronal differentiation, axon guidance, and neuroprotection (Munji *et al.* 2011). NPCs began to differentiate into maturing neurons 6 days into the DGN protocol, as confirmed by monitoring the morphological changes using phase contrast microscopy.

Within 6 days of culture, NPCs had developed long projections (indicated by arrows, Fig. 3.7A). Differentiating cells were maintained for over 40 days in culture. During this time, they continued to develop mature neuronal networks, distinct granular cell bodies (indicated by arrows, Fig. 3.7B) and long large processes that were morphologically similar to dendrites and axons (indicated by arrows, Fig. 3.7C). As is commonly noted in neural culture methods (Banker and Cowan 1977; Brewer and Cotman 1989), increased evidence of cell death was observed over time. However, we noted that neuronal cell survival was greatest in cells that had formed denser cell clusters networks (cluster indicated by circle, Fig. 3.7C). No visual differences in growth between cell lines were observed.

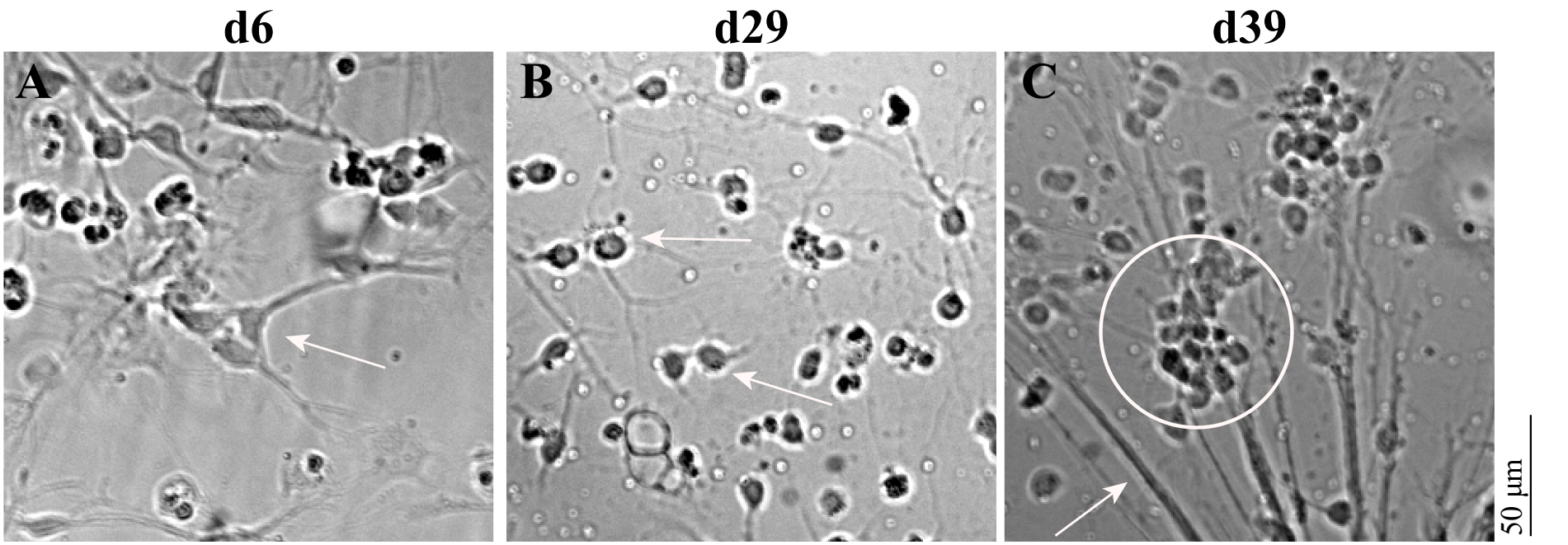

Figure 3.7: **Morphological changes of mature dentate gyrus-like neuron differentiation.** Phase contrast images of RBi001a NPCs and DGNs from experimental days **A:** 6, **B:** 29 and **39**. **A:** White arrow highlights cells with processes, but not round granular cell bodies. **B:** White arrows indicate round granular cell bodies. **C:** White arrow indicates large mature neuronal process. White circle highlights surviving neurons clustered together along processes. Images taken using inverted phase contrast microscope. All images taken at 20x magnification, and equally digitally zoomed. Scale bar denotes 50 µm.

3.2.4.2 DGNs display markers of mature neurons over extended differentiation

To confirm successful differentiation of NPCs into DGN, cultures from the healthy control CaCntrl and PSN1 cell lines were fixed at d14, and d35-38 and stained for PROX1 (Fig. 3.8A), which labels post-mitotic DG granular cells (Stergiopoulos, Elkouris, and Politis 2015) (CaCntrl d14 $n_{images} = 13$, $n_{coverslips} = 3$, $n_{cultures} = 1$; CaCntrl d35 $n_{images} = 10$, $n_{coverslips} = 3$, $n_{cultures} = 1$; PSN1 d14 $n_{images} = 17$, $n_{coverslips} = 4$, $n_{cultures} = 1$; PSN1 d38 $n_{images} = 6$, $n_{coverslips} = 3$, $n_{cultures} = 1$). Punctate PROX1 labelling was evident in the cell bodies of d14 DGNs, with a weaker signal extending into the processes of the cells. By d35 (CaCntrl) and d38 (PSN1), the cytosolic compartment still possessed the strongest signal of the whole cell, with a steady increase in signal intensity, reflecting protein expression, in both cell lines over time (Fig. 3.8B)(CaCntrl d14 ($n_{cells} = 84$) vs d35 ($n_{cells} = 39$), Mann-Whitney 1458.02, [1172.21, 1884.65] vs. 2157.95, [1431.10, 2802.72] A.U., U =905, $p < 0.0001$; PSN1 d14 ($n_{cells} = 114$) vs. d38 ($n_{cells} = 17$), Mann-Whitney 1230.67, [1026.20, 1402.60] vs. 1636.42, [1315.06, 2280.99] A.U., U =358, $p < 0.0001$).

While PROX1 label intensity was significantly lower in PSN1 DGNs at d14 (CaCntrl d14 ($n_{cells} = 84$) vs. PSN1 d14 ($n_{cells} = 114$), Mann-Whitney 1458.02, [1172.21, 1884.65] vs. 1230.67, [1026.20, 1402.60] A.U., U =2871, $p < 0.0001$), the cell line difference was no longer statistically significant between the older DGNs (CaCntrl d35 ($n_{cells} = 39$) vs. PSN1 d38 ($n_{cells} = 17$), Mann-Whitney 2157.95, [1431.10, 2802.72] vs. 1636.42, [1315.06, 2280.99] A.U., U = 250m, $p = 0.1502$).

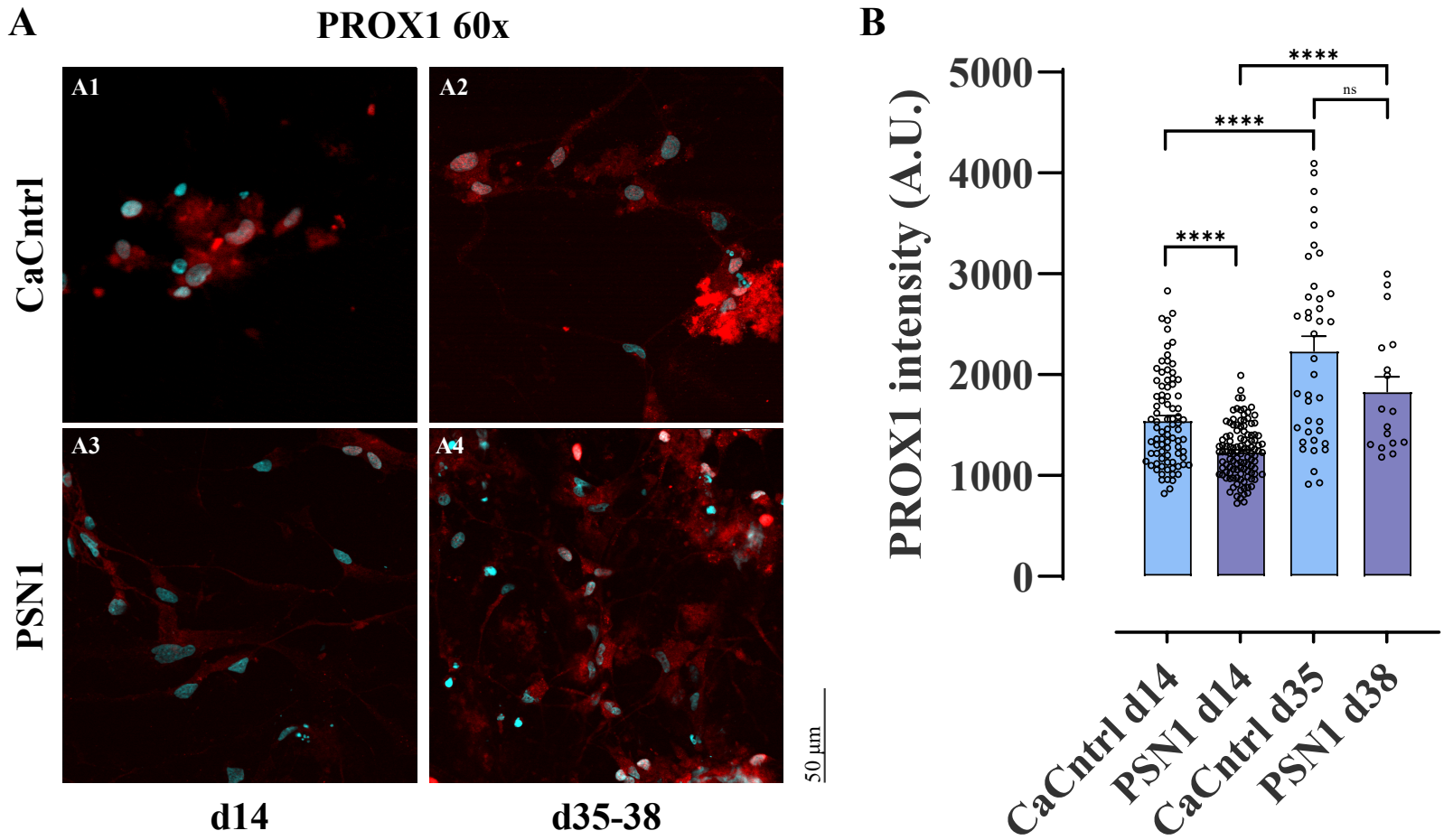

Figure 3.8: **PROX1 expression increases in DGNs over time.** **A**: Confocal images of PROX1 immunolabelling (red) DGNs. Images are representative of the cell lines CaCntrl at days **A1**: 14 & **A2**: 35, and PSN1 at days **A3**: 14, & **A4**: 38 in DGN culture. Images captured at 60x magnification. Scale bar denotes 50 µm. **B:** Bar plots (bar = mean +/- SEM) of PROX1 signal intensity A.U. (arbitrary units) of individuals DGN cells, confirmed by DAPI nuclear staining. Individual cell values (CaCntrl d14 $n_{cells} = 84$, d35 $n_{cells} = 39$, PSN1 d14 $n_{cells} = 114$, d38 $n_{cells} = 17$) denoted as open circles, **** indicate $p < 0.0001$.

3.2.4.3 DGNs exhibit mature physiological functionality

Consistent with DGNs possessing intact neurophysiological responses, K^+ containing HBSS (50 mM, 30 seconds) induced robust increases in intracellular calcium fluorescence (Fig. 3.9 B) in d31 - d38 DGN cultures (RBi001a $n_{cells} = 13$, $n_{experiments} = 1$, $n_{cultures} = 1$; PSN1 $n_{cells} = 26$, $n_{experiments} = 3$, $n_{cultures} = 1$).

As expected for mature neuronal cells containing functional group 1 mGluRs, 84.9% $\pm$ 0.8% of PSEN1 ($n_{cells\ responding} = 22$, $n_{cells\ total} = 26$, $n_{experiments} = 3$, $n_{cultures} = 1$; 33 to 38 days in culture; mean $\pm$ SEM) and 84.6% of RBi001a ($n_{cells\ responding} = 11$, $n_{cells\ total} = 13$, $n_{experiments} = 1$, $n_{cultures} = 1$; 31 days in culture) K^+-responsive DGNs responded to the specific I-mGluR agonist S-DHPG (50 µM, 120 seconds), with an increase in intracellular calcium levels (Fig. 3.5 C, D). RBi001a cells had a median difference of 4.16 A.F.U. (Wilcoxon matched-pairs signed-rank tests; 96.14% CI 2.98 to 5.32; $n_{cells} = 12$, $n_{experiments} = 1$, $n_{cultures} = 1$; $W = 78$; $p = 0.0005$), and PSN1 cells had a median difference of 4.52 A.F.U. (Wilcoxon matched-pairs signed-rank tests; 98.3% CI 3.32 to 6.52; $n_{cells} = 22$, $n_{experiments} = 3$, $n_{cultures} = 1$; $W = 253$; $p < 0.0001$) from baseline to peak calcium fluorescence.

Single experimental assessments of DHPG sensitivity in K^+-responsive RBi001a and PSN1 NPCs demonstrated 8.3% ($n_{cells\ responding} = 1$, $n_{cells\ total} = 12$, $n_{experiments} = 1$; 14 days in culture) and 13.04% ($n_{cells\ responding} = 3$, $n_{cells\ total} = 23$, $n_{experiments} = 1$; 6 days in culture) of cells responding respectively. These values fall close to the range of responding CaCntrl NPCs determined in section 3.2.3.

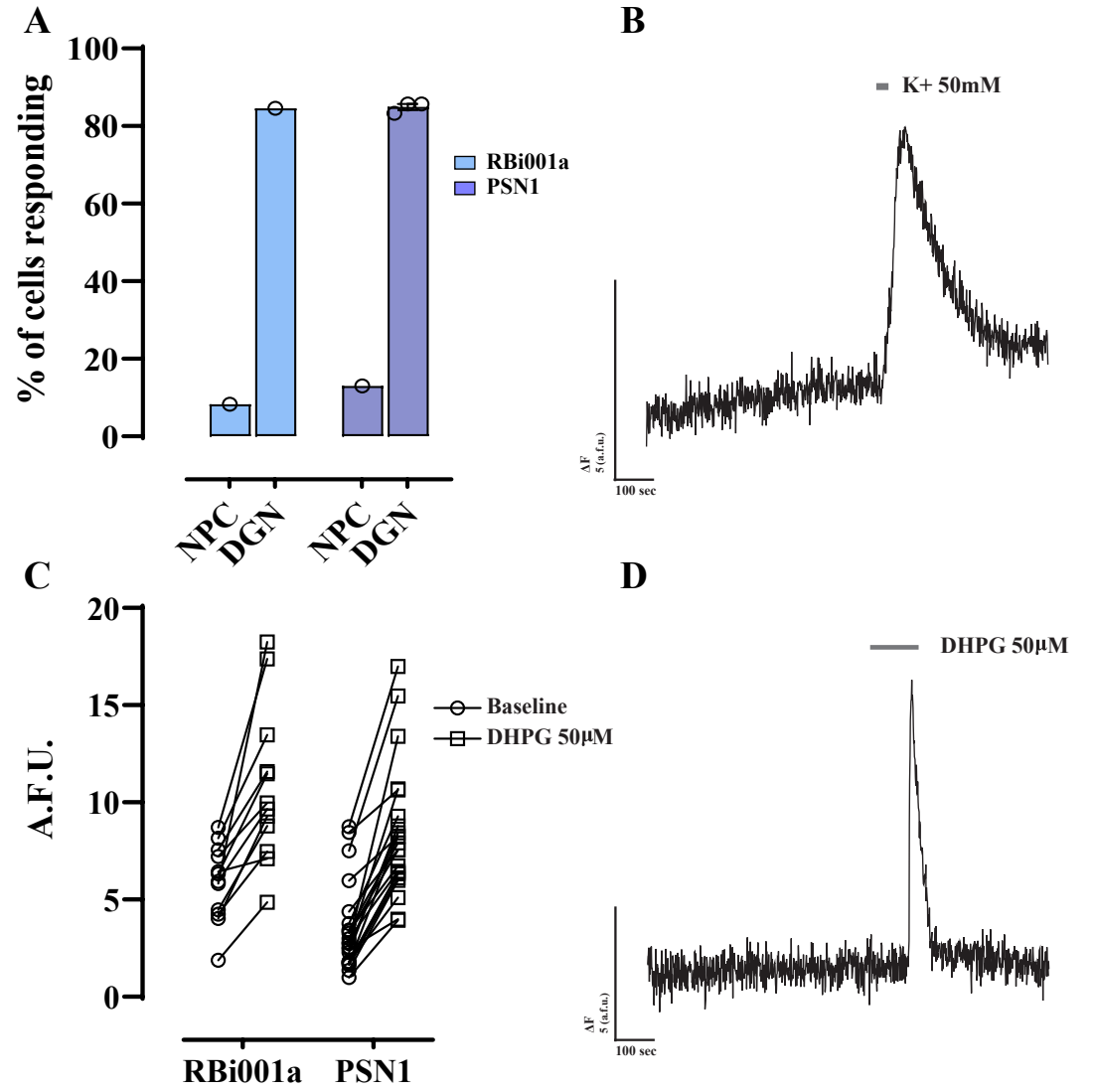

Figure 3.9: **DGNs exhibit physiological stimulus-evoked Ca^{2+} responses. A:** Grouped bar plots (bar = mean +/- SEM) of the percentage of confirmed K^+-responsive cells within an experiment responding to S-DHPG (50 µM). NPCs and DGNs were derived from a healthy control iPSC line (RBi001a), and an iPSC line containing the $PSEN1_{M139V}$ mutation (PSN1). Individual experiment values denoted as open circles. **C:** Paired scatter plot of baseline vs. DHPG-evoked intracellular Ca^{2+} fluorescence in RBi001a and PSN1 DGNs. Lines connect measurements from the same cell. Representative single-cell ΔF traces of typical DGN Ca^{2+} transients in response to **B:** 30 second application of 50 mM K^+, and **D:** 120 second application of S-DHPG (50 µM). Scale bars denote 100 seconds and 5 A.F.U.: arbitrary fluorescence units.

3.2.4.4 Altered oxygen consumption rate indicates a shift from proliferating NPCs to non-proliferating DGNs

Further physiological assessments of the development of DGNs was conducted using real-time in-incubator recording of the cellular oxygen consumption rate (OCR), which was used as a read-out of cellular mitochondiral respiration during the shift from NPCs to DGN. Healthy control (CaCntrl) and FAD patient ($PSEN1_{M139V}$) NPCs were monitored for 210 hours (8.7 days). As described in section 2.9.4, 1.7 x 10^4 NPCs were seeded per well of a 96-well plate in complete STEMdiff™ Neural Progenitor Medium. Each well was monitored individually.

Following a 90 hour long assessment of basal metabolic activity (presented in section 4.2.5), well media was changed and NPCs were monitored for a further 96 hours (4 days, time before another media change would be required). Wells that were refreshed with 0.3 mL complete STEMdiff™ Neural Progenitor Medium, to prevent further differentiation, exhibited increased oxygen consumption over the recording period (Fig. 3.10, Basal Media: CaCntrl $n_{wells} = 6$, $PSEN1_{M139V}$ $n_{wells} = 6$). This is consistent with the increased oxygen requirements of a growing number of proliferating cells, and a continuation of the behaviour seen in all cells prior to any media changes (see Fig. 4.8). Wells refreshed with 0.3 mL DG induction media exhibited a stabilising oxygen consumption profile over the time period of recording (Fig. 3.10, DGN Media: CaCntrl $n_{wells} = 6$, $PSEN1_{M139V}$ $n_{wells} = 5$), which is consistent with non-proliferating post-mitotic cells (Dranka *et al.* 2011).

By 96 hours post-stimulation the developing DGNs had reduced oxygen consumption (0.61 ± 0.04 units; $n_{wells} = 11$) compared to the NPCs (0.97 ± 0.09 units; $n_{wells} = 12$; Unpaired two-tailed Student's t test; p = 0.0221; units = $\left(\text{fmol } O_2 \cdot \text{mL} \cdot \text{mm}^{-2} \cdot \text{s}^{-1} \cdot \mu\text{g}^{-1} \text{ Protein}\right)$).

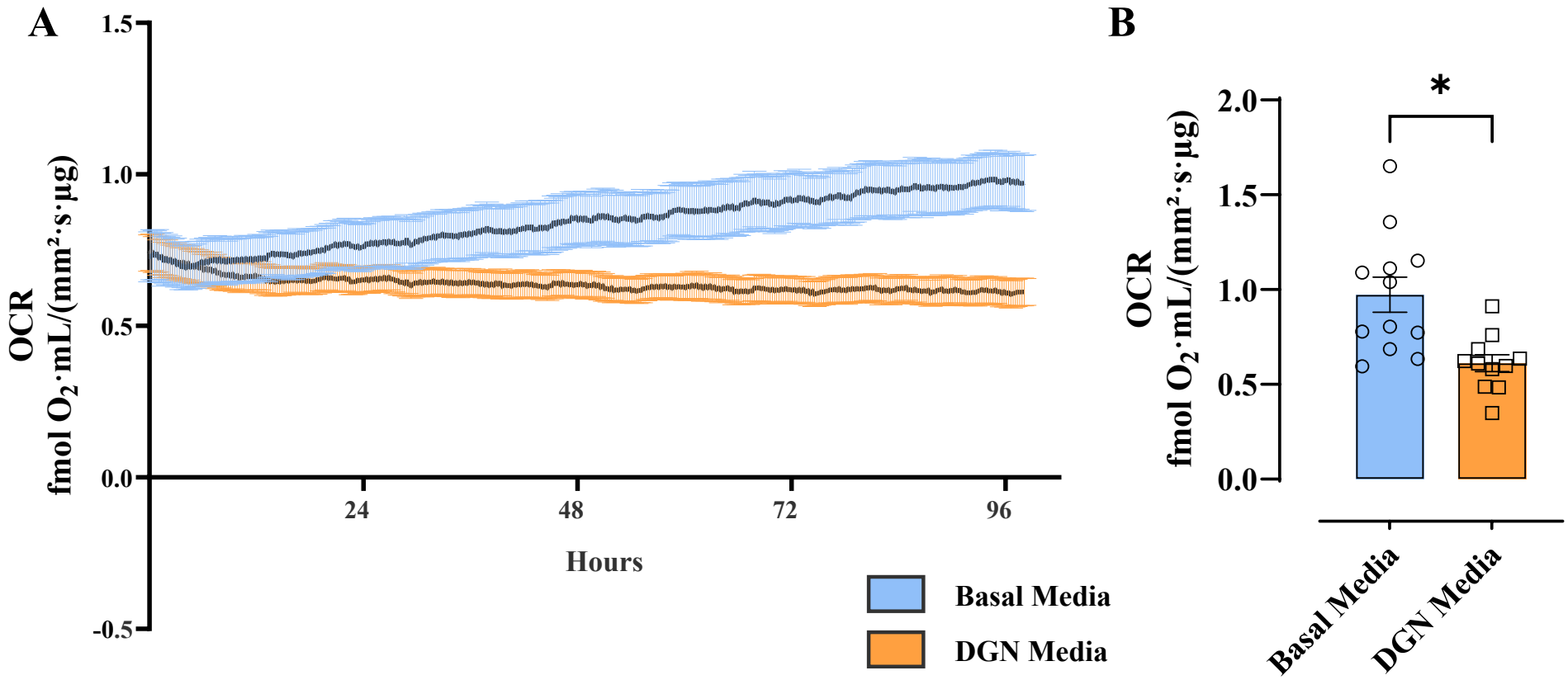

Figure 3.10: **Real-time recording of change in OCR in response to DGN media. A:** Traces illustrating continual measures of oxygen consumption rate (OCR) over a period of 96 hours in basal (blue) and DGN (orange) media. **B:** Bar plot illustrating OCR between media conditions at 96 hours post media change. Cells maintained in a standard cell culture incubator. Data represent normalized and grouped measurements across parallel well replicates (Basal Media CaCntrl $n_{wells} = 6$, $\text{PSEN1}_{\text{M139V}}$ $n_{wells} = 6$, vs DGN Media CaCntrl $n_{wells} = 6$, $\text{PSEN1}_{\text{M139V}}$ $n_{wells} = 5$), normalised to well protein, OCR units = $\left(\text{fmol O}_2 \cdot \text{mL} \cdot \text{mm}^{-2} \cdot \text{s}^{-1} \cdot \mu\text{g}^{-1} \text{ Protein}\right)$. Data are presented as mean±SEM, * indicates $p < 0.05$.

3.2.5 Generation and maturation of cerebroid cultures

Whilst 2D cell models have many benefits, such as the simplicity of use, relative cost, and homogeneity of culture (Centeno, Cimarosti, and Bithell 2018), they lack the 3D cytoarchitecture that is critical to the functionality of many brain regions. Therefore, the next step in establishing human-derived cellular models for exploration of the pathophysiological changes associated with AD was the development of 3D cerebral organoids, or cerebroids. In our study, cerebroids were generated in batches, from control iPSC lines RBi001a ($n_{batch} = 10, n_{success} = 4$) and CaCntrl ($n_{batch} = 8, n_{success} = 7$), and one FAD line ($PSEN1_{M139V}$) ($n_{batch} = 7, n_{success} = 7$) using a modified version of the protocol described in section 2.6. A batch was considered successful if any viable neural-like tissue (determined by brightfield morphology, or immunofluorescent labelling of neural marker proteins, or the presence of neural like behaviour was observed *via* calcium imaging, after 30 days in culture).

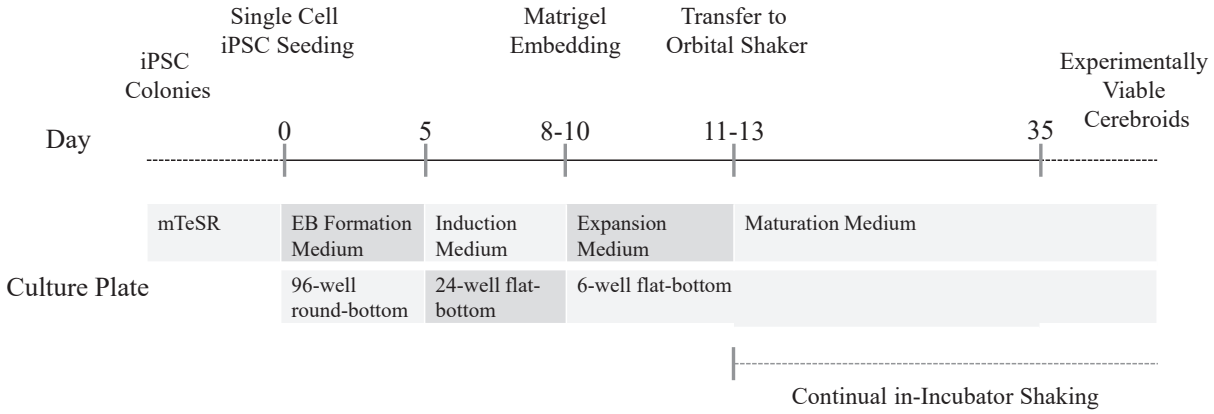

Figure 3.11: **Simplified schematic of cerebral organoid culture protocol.** The figure above illustrates the key steps involved in generating cerebroids from iPSCs. The protocol was used for iPSCs from healthy donors (RBi001a and CaCntrl) and a patient with FAD ($PSEN1_{M139V}$).

3.2.5.1 Cerebroid cultures displayed stepwise morphological development into immature brain tissue

Development of cerebroids from human-derived iPSCs (two healthy donors and one AD donor) progressed in a stepwise fashion. iPSCs seeded in round-bottomed ultra-low-attachment plates aggregated to form compact embryoid bodies by day 1. Each embryoid body was spherical, with a defined edge, floated as a cohesive unit and remained intact when the plate was gently agitated (Fig. 3.12A). Cell debris, and non-incorporated cell masses were sometimes visible prior to total media changes.

From day 5 onwards, embryoid bodies further enlarged (Fig. 3.12A-B), and differentiation to neuroepithelium could be observed *via* a change in the optical properties (clear bright) of the tissue edges (Fig. 3.12C, indicated by arrows). As cells differentiate, their optical properties change due to changes in tissue ultrastructure and biochemical content (Martins *et al.* 2023). Embryoid bodies that failed to show neuroepithelium or showed regions of single cells undergoing more rapid differentiation (outgrowths, or migration from the tissue) were discarded at this stage, as they would have an insufficient pool of neuroprogenitor cells to facilitate the expansion of a reproducible cerebroid.

By day 13, embryoid bodies exhibited neural-tube like structures (Fig. 3.12D, indicated by arrows and drawn dashed line) that act as the neural progenitor source for subsequent development. This is the development point at which they are considered to be cerebroids (Lancaster and Knoblich 2014; Pașca *et al.* 2025). Both the total cerebroids and the neural-tube like structures contained within them continued to increase in size in culture however. The density of the cerebroids (determined visually by the opacity of the tissue) continued to increase as the 3D nature of the tissue model increased in complexity. Development was consistent in each of the cell lines, with no obvious differences observed.

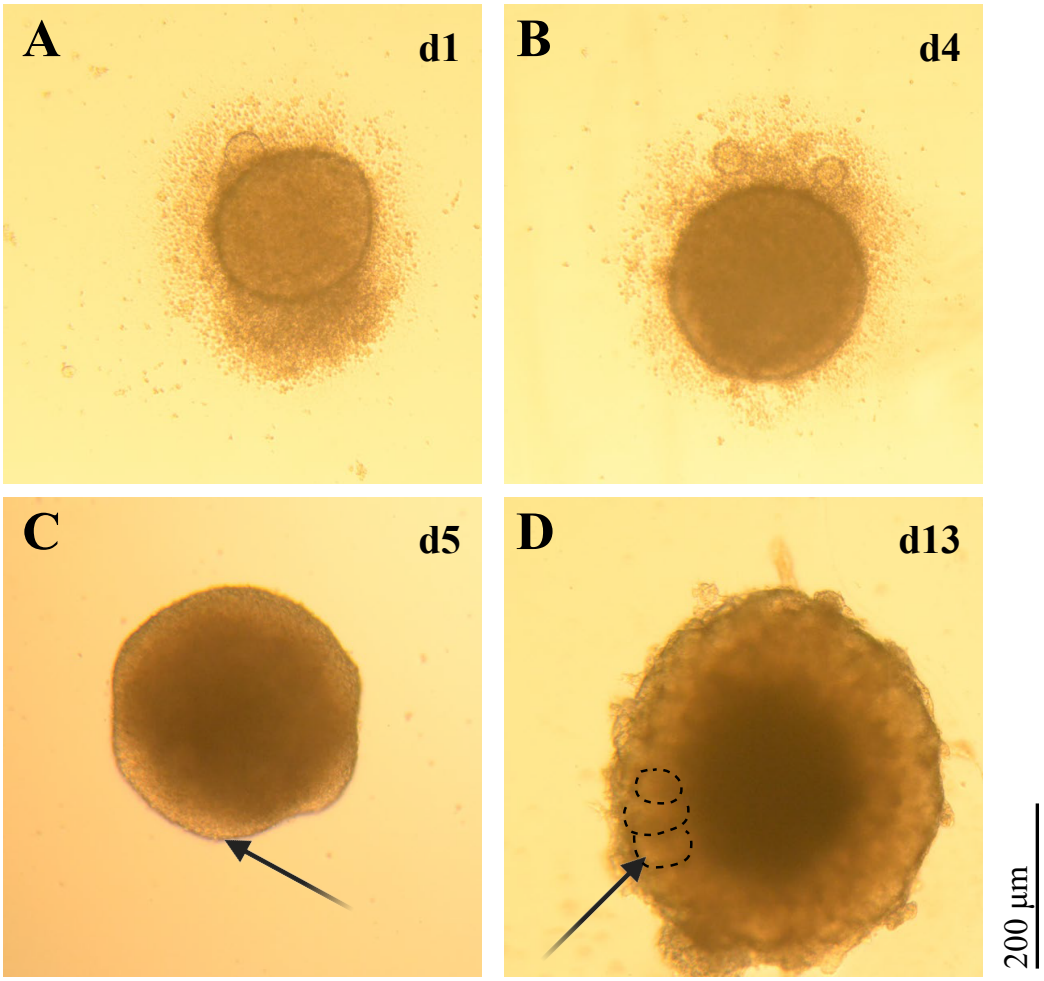

Figure 3.12: **Cerebral organoid morphology develops over time.** Phase contrast images of cerebroids developing from healthy control iPSCs (RBi001a) from experimental days 1 - 13, demonstrating embryoid body formation(**A:** d1, **B:** d4), formation of neuroepithelium (**C:** d5) the transparent cell border indicated by an arrow, and development of neural tube-like structures, indicated by arrows (**D:** d13). Images taken using a phase microscope utilising a camera down the lens. Images taken at 5x objective magnification. Scale bar denotes 200 µm.

3.2.5.2 Cerebroids expressed proteins for multiple developmental stages and structures

To confirm the successful differentiation of iPSCs into the neuronal lineage within the embryoid bodies, thereby forming cerebroids, we performed multiple immunolabelling and microscopy techniques on cerebroids >30 days in culture. This timepoint was selected based on prior reports indicating, that by this stage, the tissues should exhibit sufficient structural (e.g., cortical layering) and cellular (e.g., early neurogenesis) maturity to model aspects of human neurodevelopment (Lancaster 2024; Pașca *et al.* 2025).

Initial immunolabelling and confocal imaging for βIII-tubulin, a cytoskeletal protein specific to immature neurons, revealed widespread expression throughout the tissue (Fig. 3.13 red labelling, healthy RBi001a, $n_{cerebroids} = 4$, $n_{batch} = 2$, 152 and 159 days in culture). Counterstaining with the nuclear marker DAPI (cyan) supported the cytoplasmic localisation of βIII-tubulin along extended neuronal processes (Fig. 3.13B). βIII-tubulin expression appeared stronger towards the periphery of the cerebroid (Fig. 3.13A), suggesting increased neuronal maturation in outer regions. Additionally, tissue architecture and cellular arrangement could also be observed by the alignment of DAPI-stained nuclei (Fig. 3.13C, arranged in parallel together, perpendicular to the dashed white line drawn).

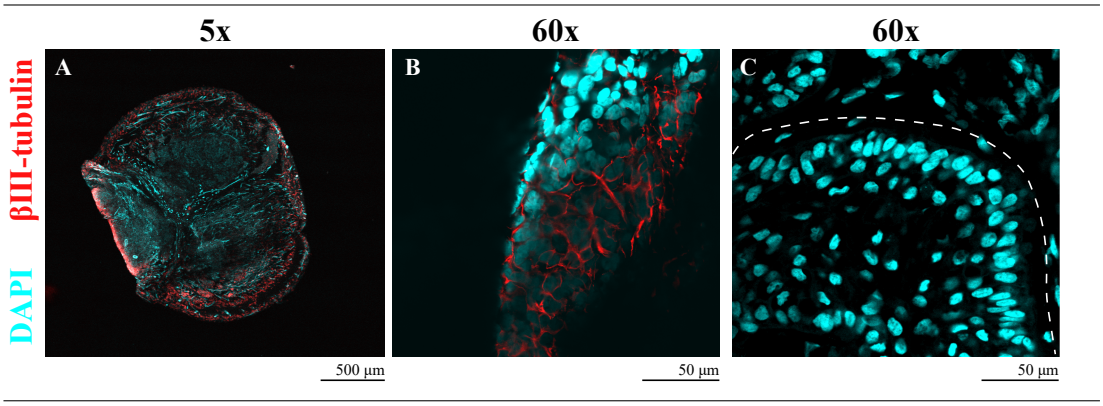

Figure 3.13: **βIII-tubulin expression confirms cerebroid neural identity.** Confocal images of DAPI (cyan) and βIII-tubulin (red) in cerebroid slices. Representative images from RBi001a (healthy control) cerebroids, fixed after 152 days in culture. **A:** 5x magnification map image of whole tissue section, scale bar denotes 500 µm. **B:** 60x magnification image of tissue periphery highlighting βIII-tubulin in long neuronal processes. **C:** 60x magnification image highlighting the self-directed cellular arrangement within the tissue. White dashed line drawn to emphasise nuclear alignment. Scale bar for 60x images denotes 50 µm.

Widefield fluorescence imaging for PAX6, a neural progenitor cell protein, demonstrated clear labelling across the tissues, indicating that cells within the cerebroids were of a neuronal lineage (Fig. 3.14 red labelling, CaCntrl, $n_{cerebroids} = 2$, $n_{batch} = 1$, 44 days in culture). Co-labelling for MAP2 (Fig. 3.14A green labelling), a cytoskeletal protein expressed in post-mitotic maturing neurons, and Hoechst 33342 (HXT, Fig. 3.14 blue staining), a nuclear dye, revealed spatial organisation reminiscent of *in vivo* neurodevelopment (Zhang *et al.* 2001). Notably, HXT- and PAX6-positive cells were arranged in a circular columnar structure around a central lumen (Fig. 3.14B, example outlined with white dashed line), forming a 'neural rosette', so named for its rose-like morphology and regarded as the *in vitro* equivalent of the neural tube. Stronger MAP2 labelling was observed radially beyond the rosette (Fig. 3.14A, white dashed lines indicate the inner and outer edges of the ventricle), consistent with the migration of progenitor cells beyond the subventricular zone before neuronal maturation (Yamashita *et al.* 2006).

Immunolabelling for Nestin (red), a cytoskeletal protein specific to neural progenitor cells, and FOXG1 (green), a forebrain-specific transcription factor (Hettige *et al.* 2022), confirmed the expression of both markers in cerebroids (de-convoluted widefield fluorescence imaging, Fig. 3.15A $n_{cerebroids} = 2$, $n_{batch} = 1$, 44 days in culture). Although strong co-localisation was observed (yellow signal), FOXG1 showed a more intense signal within cell bodies near the rosette lumen (outlined by a white dashed circle), consistent with its nuclear localisation. In contrast, Nestin labelling appeared as thin cytoskeletal filaments between cells. Fluorescence Lifetime Imaging Microscopy (FLIM) on the same samples further enhanced the specificity of the FOXG1 signal (Confocal FLIM imaging, Fig. 3.15 B). By capturing differences in fluorescence lifetime (visualised as a colour gradient), FLIM enabled clear separation of the FOXG1 signal from background autofluorescence within the same emission channel, thereby improving detection of this transcription factor.

Lastly, live labelling of whole cerebroids with cholera toxin subunit B conjugated to Rhodamine Red™-X (CTX), a non-toxic tracer commonly used for neuronal tracing (Luppi *et al.* 1987), confirmed the presence of mature neuronal cells on the periphery of the cerebroids (Fig. 3.15, RBi001a $n_{cerebroids} = 3$, $n_{batch} = 1$, 152 days in culture). Both signal intensity (Fig. 3.15A) and fluorescence lifetime (Fig. 3.15B) demonstrated strong CTX labelling in the perinuclear region of numerous cells. As expected however, CTX was unable to penetrate deeper into the cerebroid's developmental core.

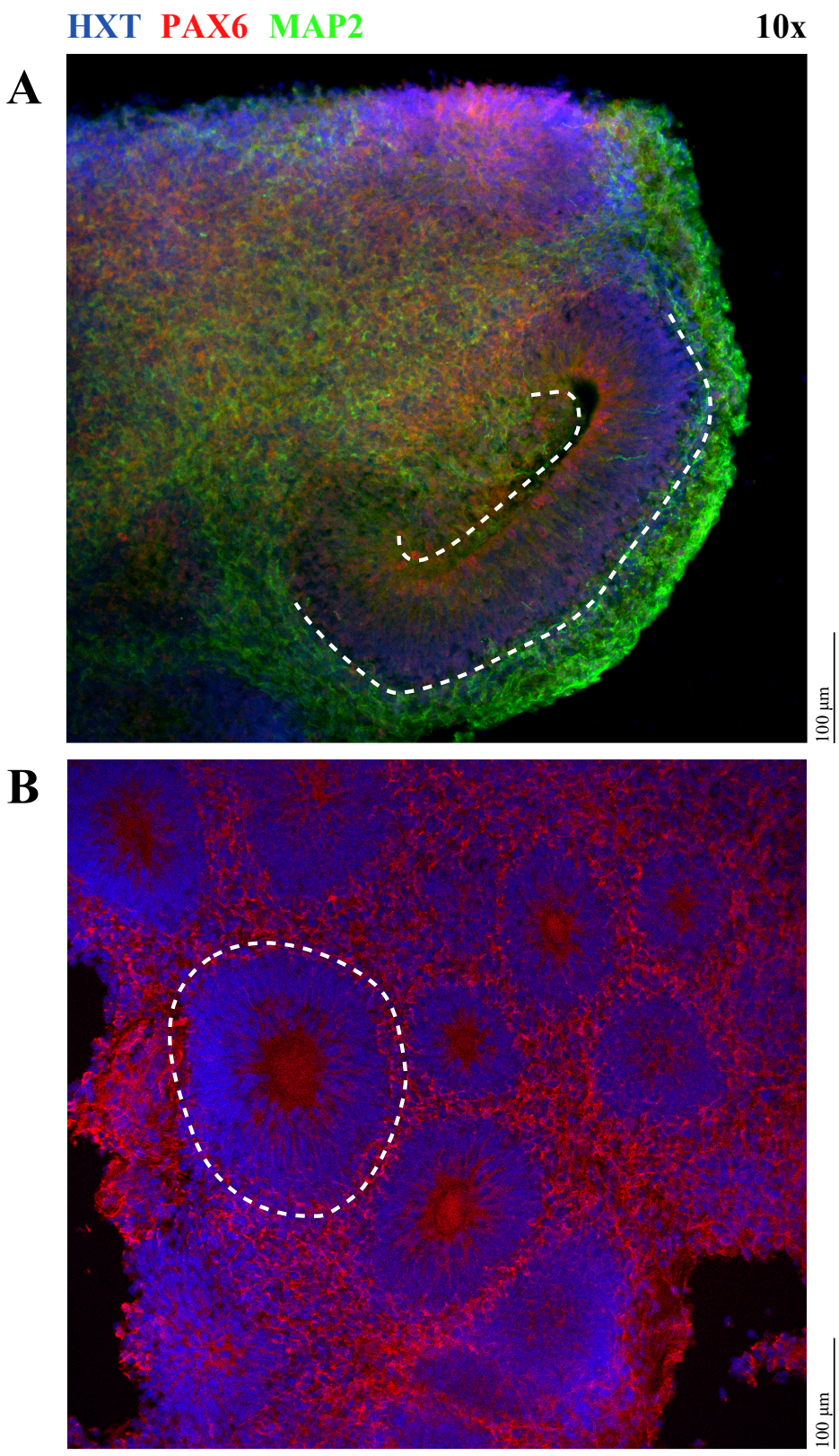

Figure 3.14: **PAX6 and MAP2 expression outline developmental structure within cerebroids.** Widefield fluorescence images of Hoechst 33342 (HXT, blue), PAX6 (red) and MAP2 (green, image A only) in cerebroid slices. Representative images from CaCntrl healthy control cerebroids, fixed on day 44 in culture. **A:** White dashed lines emphasise the expanding sub-ventricular zone. **B:** White dashed line drawn shows total 'neural rosette' structure which forms the proliferative region within cerebroids upon expansion. Images taken at 10x magnification. Scale bar denotes 100 µm.

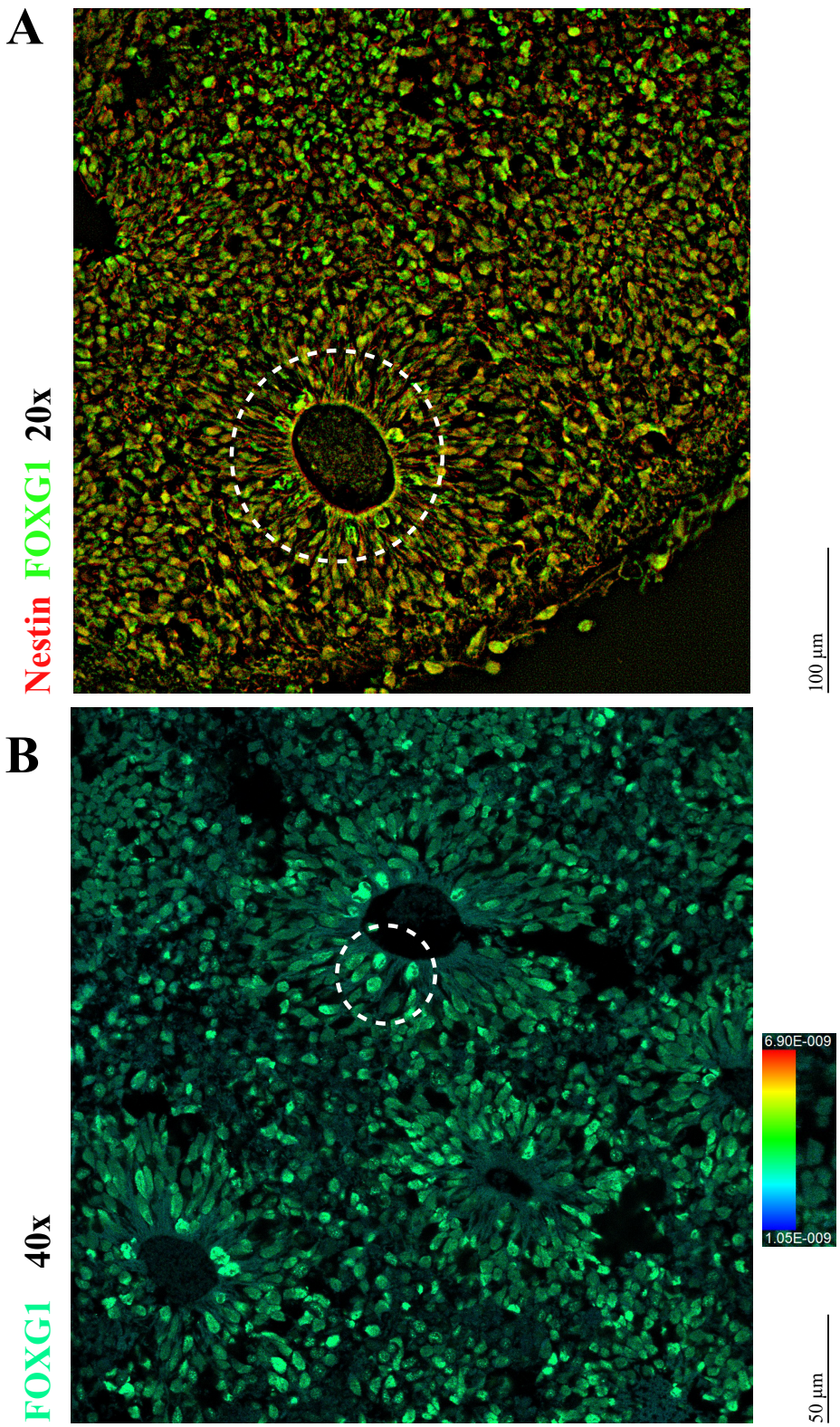

Figure 3.15: **FOXG1 and Nestin expression confirm forebrain neural identity.** Representative images from RBi001a (healthy control) cerebroid, fixed on day 152 in culture. **A:** De-convoluted widefield fluorescence image of Nestin (red) and FOXG1 (green) in cerebroid slice. Neural rosette ventricle outlined with white dashed circle. Image taken at 20x magnification. Scale bar denotes 100 µm. **B:** Confocal FLIM image of FOXG1 labelling in a cerebroid slice. FOXG1-positive cell bodies, and shorter lifetime highlighted with white dashed circle. Images taken at 40x magnification. Scale bar denotes 50 µm. Colour bar denotes fluorescence lifetime from 1.05^{-9} to 6.90^{-9} seconds.

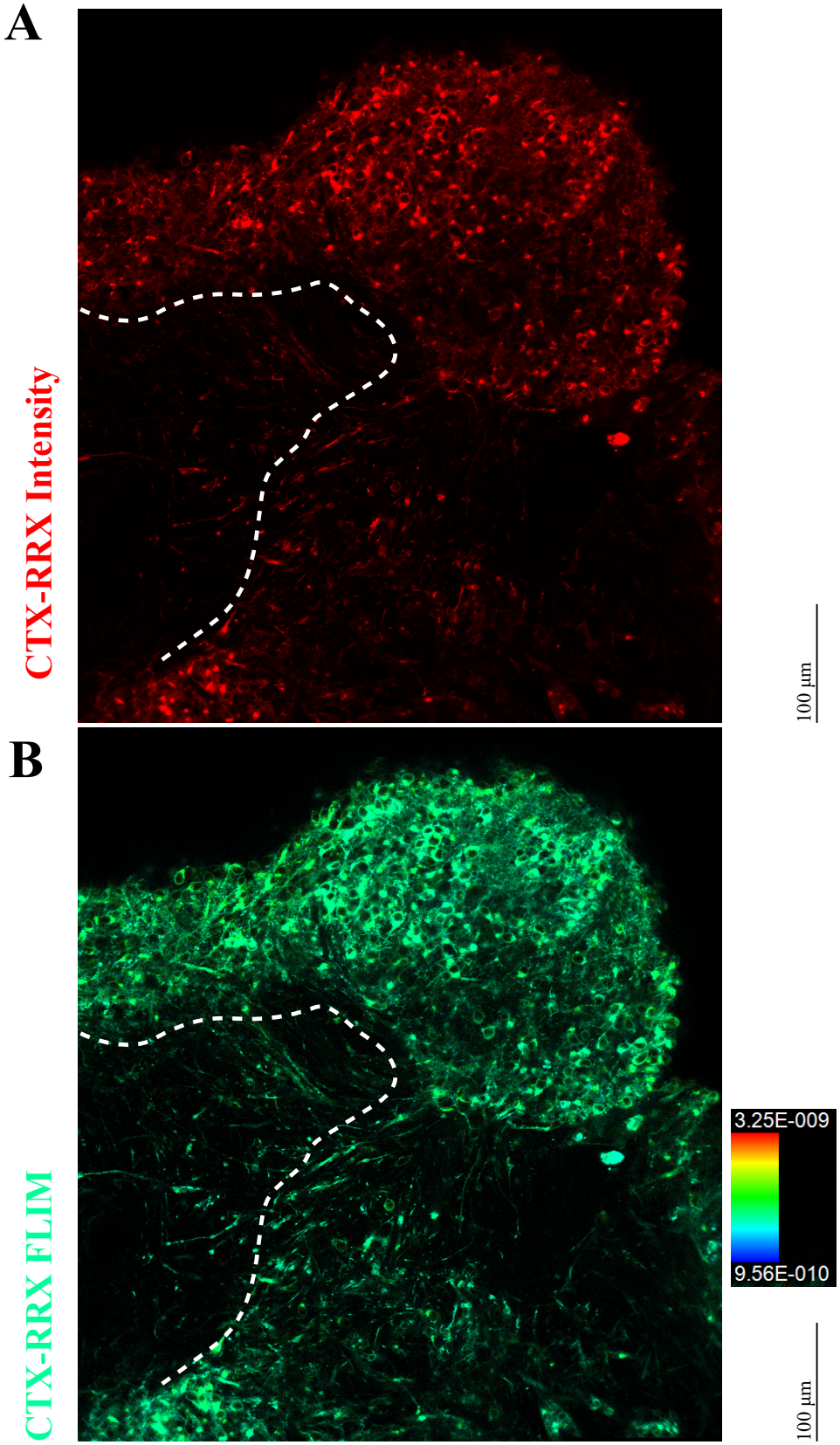

Figure 3.16: **Live FLIM imaging of cerebroids.** Live FLIM confocal images of cholera toxin Rhodamine Red™-X labelling in whole cerebroids. Representative images of an RBi001a(healthy control) cerebroid, stained live overnight at day 152 in culture. Images show **A:** fluorescence intensity and **B:** fluorescence lifetime. White dashed line drawn to visualise inner progenitor cell region not accessed by CTX. Scale bar denotes 100 µm. Colour bar denotes fluorescence lifetime from 9.56^{-10} to 3.25^{-9} seconds.

3.2.5.3 Calcium Imaging in Cerebroids

When loaded with the calcium indicator Calbryte™ 520 AM (8 µM in aCSF for one hour), unstimulated cerebroid slices (see section 2.7 for preparation) displayed spontaneous cell activity (PSN1 $n_{experiments} = 8$, $n_{organoids} = 3$, 38 to 42 days in culture; RBi001a $n_{experiments} = 6$, $n_{organoids} = 4$, 68 to 145 days in culture). However, individual active cells were often difficult to resolve and record. Therefore in an attempt to enhance the ability to identify and record from mature neurons at the tissue periphery, we next cultured cerebroid (PSN1 $n_{organoids} = 3$, 69 days in culture) slices at the air–liquid (ALI-CO) interface for 72 to 78 days prior to calcium imaging (full methods in section 2.7).

ALI-CO slice cells responded to a 120 second superfusion of S-DHPG (50-µM) (PSN1 $n_{cells} = 5$, $n_{experiments} = 4$, $n_{organoids} = 3$; 141 to 147 total days in culture), an agonist of mGluR1 and mGluR5 receptors, with a robust calcium response (mean difference from baseline 8.57 ± 1.65 A.F.U; Paired two-tailed Student's t test; $p = 0.0065$; Fig. 3.17). These data suggest that the cerebroids were viable and had developed physiological responses consistent with a maturing neuronal network.

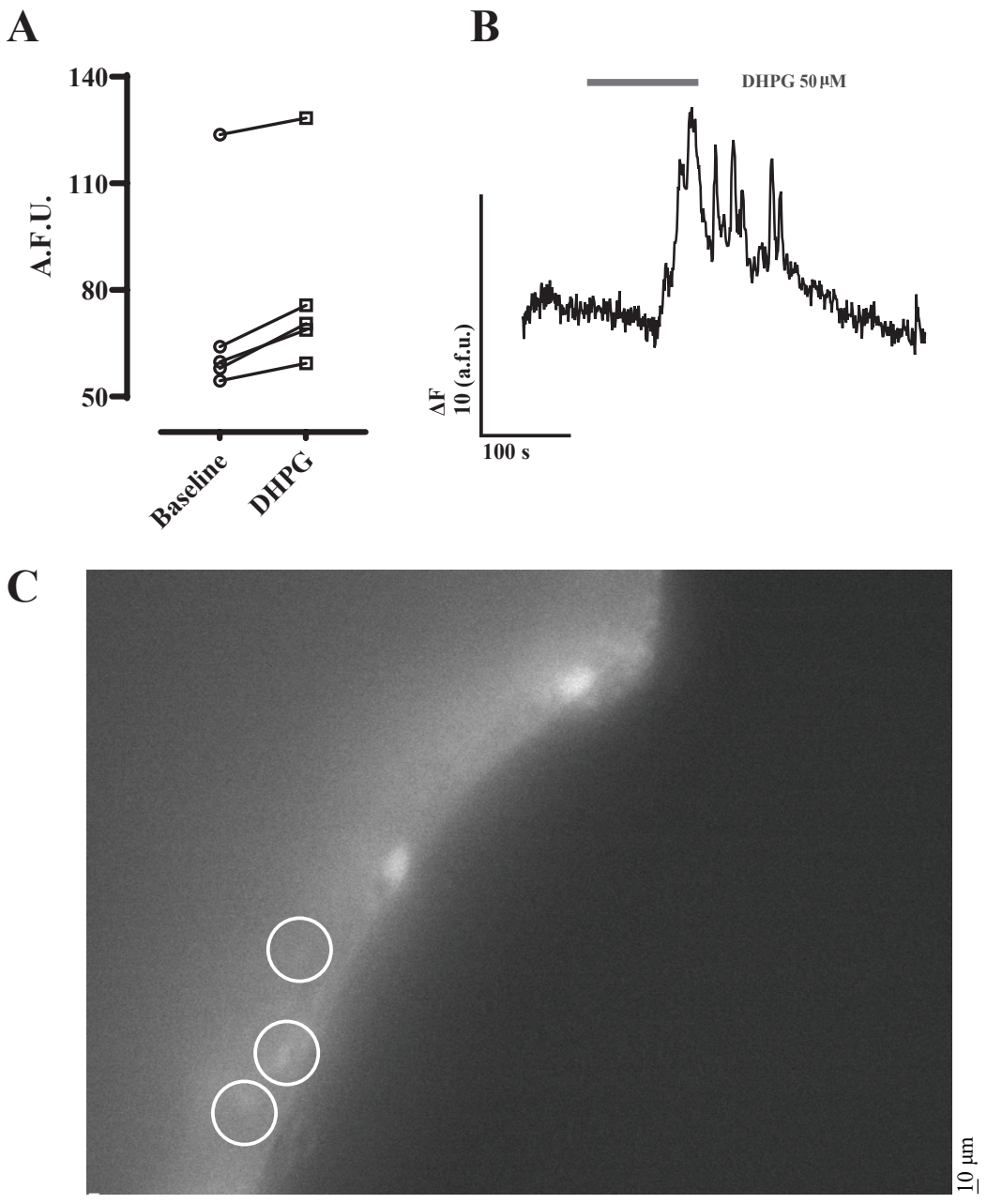

Figure 3.17: **ALI-CO cells exhibit physiological stimulus-evoked Ca^{2+} responses. A:** Paired scatter plot of baseline vs. DHPG-evoked intracellular Ca^{2+} fluorescence in ALI-COs slices. Lines connect measurements from the same cell. **B:** Representative single cell ΔF trace of typical DGN Ca^{2+} transients in response to 120 second application of S-DHPG (50 µM). Scale bars denote 100 seconds and 10 A.F.U.: arbitrary fluorescence units. **C**: Calcium fluorescence image of cells within ALI-CO responding to S-DHPG (50 µM). Active cells are highlighted by white rings. Scale bar denotes 10 µm.

3.2.5.4 Cerebroid optical clearing and volumetric imaging

To maximise our understanding of 3D organoid development, significant efforts were applied to image the entire cerebroid in full 3D. The "SHIELD" fixation and delipidisation technique developed by Harvard's Chung Lab (Albanese *et al.* 2020) was used to improve fixation and optical clearing of the 3D structure (see full description in section 2.10.3). To conduct 3D tissue compatible immuno labeling and volumetric imaging, work was conducted at University College London, in collaboration with Dr Keith Siew.

Cerebroids required structural support to survive both the optical clearing, and the eFlash smart staining processes. A protocol for the reproducible handling and embedding of SHIELD fixed organoids was devised using cut 1 ml syringes and warm 1-3% agarose gel layered carefully to prevent tissue contact with the plastic surface (described in section 2.10.3.2, Fig. 3.18A, embedded organoid highlighted with black arrow). These gels allowed for handling of the tissues with forceps, without damaging the cerebroid surface (Fig. 3.18B, gel cylinder visible around uncleared cerebroids). The process did not impair lipid clearing of the tissues, and could also be refractive index matched for volumetric imaging. Their primary use was to protect the cerebroids when loaded into 'mesh bags' (Fig. 3.18C, cleared cerebroid in gel highlighted with white arrow, next to eFlash staining sample mesh bag). Volumetric labelling and imaging was initially designed for slightly larger, more rigid tissues, that are not as sensitive to physical damage as neural organoids.

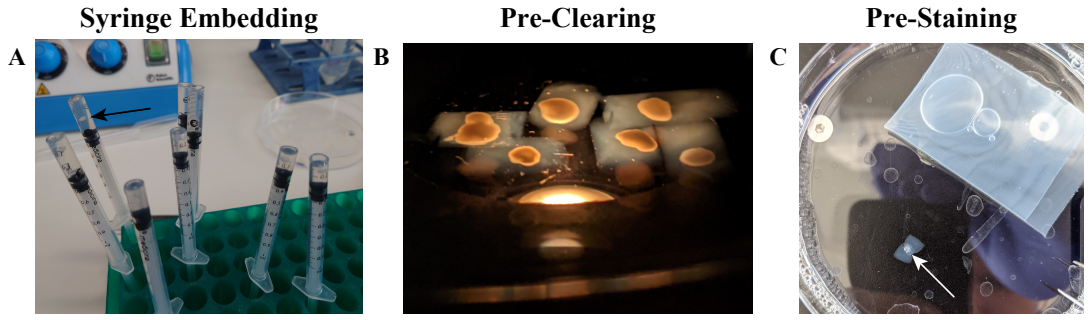

Figure 3.18: **Example images of cerebroid embedding and handling for volumetric imaging. A:** Cerebroids collected and embedded using cut syringe method. Cerebroid highlighted with black arrow. **B:** Collection of embedded fixed cerebroids prior to lipid clearing. Bench-top microscope lamp was used to visualise the gel, and to assess the integrity of the embedding. **C:** Lipid cleared, embedded cerebroid ready to be loaded into a mesh sample bag, for eFlash smart staining. Organoid highlighted with white arrow.

Although gel embedding provided sufficient protection for lipid clearing and organoid storage, the eFlash staining protocol remained too harsh to preserve tissue integrity. Nonetheless, imaging was attempted using a custom-built mesoscale selective plane illumination microscope (mesoSPIM v5.1; see section 2.10.4.1). Cerebroids were stained with the stem cell marker SOX2 (green), the postmitotic cortical neuron marker TBR1 (red), and the nuclear dye Sytox DeepRed (blue), and subsequently imaged in 3D (Fig. 3.19). These markers were selected in order to enable the identification of individual cell types by comparing the relative signal intensities of SOX2 and TBR1 in proximity to Sytox DeepRed-positive nuclei. However, tissue collapse following the eFlash procedure precluded the acquisition of structurally intact whole-tissue 3D images.



Figure 3.19: **Example volumetric image of optically cleared and stained cerebroids.** MesoSpim Lightsheet volumetric image of a SHIELD fixed, lipid cleared, eFlash stained cerebroid. Cerebroids were immunostained for SOX2 (green), TBR1 (red), and Sytox DeepRed (blue) for nuclei. No cerebroids maintained shape to allow successful imaging. The tissue collapsed within its gel mould (original cerebroid shape maintained in mould highlighted with white arrow), but still shows positive SOX2 (indicated with black arrow) and TBR1 signals. Movement artefacts precluded cell level resolution during imaging.

3.3 Discussion

There remains a widespread reliance on transgenic mouse models in traditional physiological research, despite species-specific differences that limit their translational relevance to human neurobiology. We sought to leverage recent advancements in stem cell research to address the need for easily applicable and effective neural culture protocols derived from human tissue.

Using iPSC culture as a starting point, we demonstrated the feasibility of generating and maintaining viable, expandable stocks of human NPCs that exhibited robust expression of canonical NPC markers such as nestin and SOX2 (Bott *et al.* 2019; Graham *et al.* 2003). Notably, when seeded at low densities, these cells retained their intrinsic capacity for spontaneous differentiation into mature neural lineages, as seen by the expression of βIII-tubulin and MAP2 (Garavaglia *et al.* 2010; Liu *et al.* 2013). This property enabled their use in multiple experimental systems, including perfusion bath calcium imaging, immunocytochemistry and Seahorse MitoStress Test analyses, without the need for expensive targeted media components or specialised cultureware.

Since its initial demonstration in 2009, the dual SMAD inhibition approach to neuroectoderm induction we employed has become a staple of iPSC-based neuroresearch (Chambers *et al.* 2009; Telias 2023; Wei *et al.* 2019). In the last five years, however, newer publications have explored the nuances of NPC subtype specification and the importance of additional morphogen gradients, such as Wnt-inhibition, required for reproducible differentiations (Kim *et al.* 2021; Rosebrock *et al.* 2022). While our data confirm the neural identity of culture products, we did not investigate subtype specification. Nevertheless, subsequent work building upon the methodological and experimental design frameworks developed during the course of this work, has investigated and underscored the importance of homogenous NPC subtype generation in omics-based research (Hamerlinck *et al.* 2025).

We have described a streamlined protocol for the production of 2D human-derived dentate-gyrus-like neurons from neural progenitor cells that remain viable for up to 40 days post-plating (section 3.2.4). In contrast to earlier hippocampal differentiation strategies that required neurosphere formation and continuous, uninterrupted differentiation phases, our approach eliminated the neurosphere stage and introduced defined cryopreservation checkpoints at the neural progenitor stage. This modification permits the pausing and banking of differentiation-ready populations, thereby decoupling progenitor expansion from downstream neuronal maturation. By removing the requirement for prolonged continuous culture and reducing reliance on extended patterning phases,

the protocol increases experimental flexibility, improves batch consistency, and lowers logistical burden. Cells from such cultures display normal morphology, physiology, and metabolic behaviours consistent with granule cells from dentate gyrus tissue (Kaar, Weir, and Rae 2024). Within our lab, this protocol has already been used in two undergraduate Honours bachelor research projects, where it enabled the investigation of differences in IP_3R, stromal interaction molecule (STIM), and Orai expression between healthy control and presenilin-mutant iPSC-derived lines. Collectively, these refinements convert what was previously a continuous and labour-intensive differentiation process into a modular, scalable workflow suitable for longitudinal and comparative studies.

Although the initial objectives of this project included the identification and comparison of overt AD-like phenotypes between PSEN1-mutant and control lines within these culture systems, systematic comparative analyses were not pursued to completion within the time-frame of this thesis. A combination of experimental attrition, variability in differentiation efficiency, and technical limitations in early-stage optimisation experiments reduced the number of high-quality replicates available for rigorous statistical comparison. While preliminary data suggested more potential genotype-associated differences, the resulting sample sizes were insufficient to support robust conclusions. Importantly, we elected not to compensate for low cerebroid numbers through excessive data manipulation, over-correction, or selective reporting. Instead, emphasis was placed on refining and stabilising the culture systems to ensure that future comparative analyses could be conducted with appropriate statistical power and reproducibility.

Future refinement and optimisation of the protocol would benefit from transcriptomic profiling of the cultures and comparison with publicly available RNA sequencing data from human dentate gyrus tissue (Ramnauth *et al.* 2025). This would enable a more accurate assessment and confirmation of regional identity and maturity. In the wider field, 3D brain organoids and patterned spheroids have shown promise in generating spatially distinct hippocampal tissue, including the dentate gyrus and *cornu ammonis* (CA) subregions. These models, however, are still often limited by low reproducibility, extended culture durations, and high cellular heterogeneity (Jacob *et al.* 2020; Pomeshchik *et al.* 2020; Sakaguchi *et al.* 2015). More recently, research efforts have begun to shift to 'assembloid' culture systems, which aim to recapitulate classical unidirectional connectivity, such as projections from the olfactory cortex projecting to the DG, and from the DG to the CA3 region (Wu *et al.* 2024). These systems require the parallel generation and maturation of organoids from specific subregions, followed by their fusion and prolonged co-culture (Kanton and Paşca 2022). Within this context, improved versions of simplified 2D systems like ours may offer a short-term pilot platform for probing

early-stage projection dynamics and neuronal responsiveness, without the prolonged culture durations and cellular variability of the 3D systems.

The presence of nestin, MAP2, βIII-tubulin, and TBR1 antibody markers is consistent with successful differentiation of iPSC cell lines into cerebroids (Albanese *et al.* 2020; Lancaster and Knoblich 2014). These data confirm the successful differentiation of a mixed central nervous system-like cytoarchitecture, with the capacity for continual differentiation (progenitor cell populations) and regional maturation (outer post-mitotic populations). Moreover, the spatially distinct locations of each marker highlighted the self-organised and structured nature of these 3D cultures. Expression of FOXG1 within the rosettes further confirmed the forebrain-specific cortical identity of generated organoids (Hettige *et al.* 2022). Live labelling with CTX further validated the presence of mature, functionally-active neurons in the outer regions of the organoids, consistent with CTX-B uptake by mature neuronal membranes (Alisky, van de Wetering, and Davidson 2002; Giandomenico *et al.* 2019).

These findings align with an ever-growing body of literature demonstrating the capacity of 3D organoid culture systems to self-pattern along major neurodevelopmental trajectories (Lee and Sun 2022; Pașca *et al.* 2025). Traditional organoid models, including ours, have shown the potential to generate the full gamut of brain regions. However, most protocols are still hampered by high variability and low reproducibility between culture batches (Andrews and Kriegstein 2022; Urrestizala-Arenaza *et al.* 2024). Encouragingly, recent efforts to standardise system nomenclature (Pașca *et al.* 2022), characterisation procedures (Sandoval *et al.* 2024), and cross-site cell line selection (Glass *et al.* 2024) have begun to move the field in a more reproducible and rigorous direction.

As with the DGN cultures, the implementation of multi-omic analyses would substantially strengthen future cerebroid-based research. In this regard, the recently published Human Neural Organoid Cell Atlas (HNOCA) offers a valuable resource, enabling researchers to benchmark organoid-derived cell populations against reference datasets from other organoid systems, rather than relying exclusively on primary foetal tissue comparisons (He *et al.* 2024). Additionally, the generalisability of findings from cerebroid-based research can be improved by 'village-in-a-dish' and 'chimeroid' approaches.

The 'village-in-a-dish' method involves co-culturing multiple genetically distinct iPSC lines within a single differentiation experiment, allowing for simultaneous, internally controlled comparisons across genotypes under identical conditions (Neavin *et al.* 2023). This strategy mitigates batch effects and enhances the detection of disease- or genotype-

specific phenotypes. Similarly, 'chimeroid' cultures, generated by mixing cells from separate iPSC lines prior to differentiation, enable the investigation of lineage- and cell-type-specific phenotypes at single-cell resolution (Antón-Bolaños *et al.* 2024). Our iPSC-derived culture systems were originally based on traditional cohort-control designs, which compare groups based on clinical diagnoses. However, it is now widely recognised, that this approach has contributed to a widespread statistical 'power failure' in neuroscience (Button *et al.* 2013; Nord *et al.* 2017). To address this, the use of multiple isogenic iPSC pairs is recommended (Brunner *et al.* 2023). While generating cerebroid cultures at such a scale is often financially and practically unfeasible, 'village-in-a-dish' and 'chimeroids' approaches offer viable and scalable alternatives.

We explored the use of cerebroid slices for bulk calcium imaging, with the aim of developing a human neuron-specific alternative to traditional rodent brain slice preparations. While technically feasible, this approach presented several limitations. For example, slices required extended ALI-CO culturing prior to imaging, and even after this maturation period, cells exhibiting discernable calcium activity were largely restricted to the periphery of the tissue and lacked clear structural organisation (Fig. 3.17B). Moreover, identification of stimulus-responsive-cells was not possible prior to pharmacological stimulation (with S-DHPG), preventing targeted selection of the imaging field to maximise responsive cell inclusion. Despite these limitations however, with further refinement, this platform could offer a human-derived model to match rodent-derived brain slices for neurophysiological studies.

More recently, several advances have addressed these challenges associated with calcium imaging in human cerebroid systems. These include the use of iPSCs lines engineered to express genetically encoded calcium indicators, which enable continuous, cell-type-specific monitoring of intracellular calcium dynamics without the need for dye loading (Oliva *et al.* 2024). Another strategy involves the application of dye-based calcium imaging to more mature ALI-CO cultures, where extended differentiation and attachment promote improved neuronal organisation and enhanced signal fidelity (Tang *et al.* 2023). Finally, some studies within the organoid field have circumvented the limitations of calcium imaging by employing direct electrophysiological recordings *via* multi-electrode arrays, which allow for real-time, high resolution detection of network level neuronal activity without relying on calcium as a proxy signal (Sharf *et al.* 2022). From a traditional physiological perspective, however, we propose that combining calcium imaging with electrophysiological measurements offers a more holistic view of neuronal activity than electrophysiology alone.

While efforts to fully optimize the optical clearing and volumetric imaging cerebroid

protocol continue, we were able to render tissues optically clear and detect positive immunofluorescent labelling within them. However, we were unable to maintain the cerebroid structural integrity during the labelling-pipeline that was required to facilitate complete volumetric imaging (section 3.2.5.4). Limitations of this protocol include the difficulty in preserving cerebroid structure throughout the labelling process and the high concentration of antibodies required for whole-tissue labelling.

Despite these challenges, embedding cerebroids using a cut syringe has become a mainstay method for organoid freezing and cryosectioning in our labs. Gelatine or optimal cutting temperature compound, is used instead of agarose, to embed cryoprepped cerebroids, and the embedded samples can be snap-frozen within the syringe. The position of the cerebroid can be easily marked, and the resulting frozen cylindrical block is a convenient size for manipulation, long-term storage, and cryosectioning.

Lastly, an observation made during the course of this research project revealed that the majority of current "organoid research" primarily focuses on the application of the technology rather than its further advancement (Qu *et al.* 2024). To truly enhance the potential of organoids and to continue the creation of better models of human physiology, an interdisciplinary approach becomes imperative, possibly with a new name, to focus and clarify the way forward. We propose the term "Promethology" as a fitting designation for this work that seeks to transcend mere technology usage and with which to instead emphasise the comprehensive development and utilization of crafted living complex human tissues. The name intentionally invokes the Greek Titan Prometheus (Gr. πρόμηθευς *prōmētheús*, 'forethought'), who in Hesiod's Theogony is said to have shaped mankind out of clay and endowed them with fire, underscoring the creative mastery required and ethical responsibility inherited, when designing living human tissues (Hesiod, Evelyn-White, and Homer Carmina minora 1914).

3.4 Conclusion

In summary, we present here a streamlined and economical method for the consistent production of primary hippocampal cultures from human-derived iPSCs. Furthermore, the neural cells within these culture systems, in addition to displaying characteristics of normal, healthy neurons, also exhibit consistent and reproducible responses to physiological stimuli which were investigated further in Chapter 4. Lastly, we propose that cerebroids, and subsequent cerebroid-based systems, are viable methods to study neurodegenerative diseases such as AD in human-derived tissues.

COUPLED DYSREGULATION OF CALCIUM HANDLING AND BIOENERGETICS IN A HUMAN NEURAL PRESENILIN MODEL

4.1 Introduction

AD pathophysiology involves intricate disruptions in calcium signalling and cellular bioenergetics (as discussed in sections 1.3.1 and 1.3.3). However, translating findings from animal models to human cellular contexts remains challenging. Previous research in our lab and others has reported altered calcium signalling and impaired metabolic health in AD models (Cavendish *et al.* 2019; Kaar, Weir, and Rae 2024). In particular, the 3xTG mouse model of AD exhibits larger intracellular Ca^{2+} transients in primary cortical neurons and enhanced CICR in hippocampal slices upon caffeine challenge (Chakroborty *et al.* 2009; Smith *et al.* 2005). Spatial learning deficits in 3xTG animals are rescued by crossing with synaptopodin KO mice, consistent with synaptopodin's role in ER Ca^{2+} store release (Aloni *et al.* 2019). Synaptopodin is an actin-associated protein that assembles a specialized ER subdomain in dendritic spines, the spine apparatus, thereby facilitating Ca^{2+} release through IP_3R during synaptic activity (Korkotian and Segal 2011). Aged 3xTG cortical neurons also display spontaneous Ca^{2+} oscillations that are absent in wild-type cells, suggesting a constitutive ER Ca^{2+} leak and chronic dyshomeostasis (Li *et al.* 2023a) that is exacerbated with time. In 3xTGhippocampal neurons, mitochondrial respiration is significantly decreased and glycolysis increased, indicating a bioenergetic shift (Yao *et al.* 2009). Furthermore, in the hypothalamus, mitochondrial dysfunction appears as early as two months of age in 3xTG females, but requires six months to manifest in males; sex-based differences also emerge in the expression of mitochondrial complex II and III subunits (Adlimoghaddam, Fontaine, and Albensi 2024). Collectively, these studies strongly implicate ER Ca^{2+} dysregulation as central to AD neuropathology.

Although both APP and PSN1 mutations have been shown to disrupt Ca^{2+} handling and metabolism in cell culture experiments (Gazda, Kuznicki, and Wegierski 2017; Lopez Sanchez *et al.* 2017), early ER related Ca^{2+} disruption in hippocampal neurons of 3xTG mice appears specifically attributable to PSN1 dysfunction. KI of the $PSN1_{M146V}$ mutation impairs hippocampus-dependent contextual learning and correlates with reduced adult neurogenesis in the dentate gyrus (Wang *et al.* 2004). Moreover, reverse transcription PCR experiments have shown that APP_{Swe} and tau_{P301L} transgenes are not expressed in hippocampal cultures from 3xTG mice before day 18 in culture, indicating that the early Ca^{2+} dysregulation observed at day 13 in culture is primarily attributable

to the $PSN1_{M146V}$ mutation (Zhang *et al.* 2010).

More broadly, if such Ca^{2+} dysregulation and bioenergetic reprogramming represent core features of AD pathophysiology, similar phenotypes would be expected to emerge not only in familial models but also, at least in part, in more common sporadic forms of the disease. In this context, however, it remains unclear whether the constitutive ER Ca^{2+} leak, spontaneous oscillations, and bioenergetic shift seen in 3xTG neurons also occur in human cells carrying analogous PSN1 mutations. The $PSN1_{M146V}$ mutation substitutes methionine for valine in exon 5, within the protein's second transmembrane domain (Alzheimer's Disease Collaborative Group 1995). Likewise, the $PSN1_{M139V}$ mutation substitutes methionine for valine in the same domain but at position 139 rather than 146 (Alzheimer's Disease Collaborative Group 1995). The availability of patient-derived iPSCs harbouring $PSN1_{M139V}$ enables investigation of presenilin-mediated Ca^{2+} disruptions during early human neuronal differentiation.

4.1.1 Chapter Aims

We hypothesised that human neural cultures derived from iPSCs originating from an individual expressing a mutation in the presenilin-1 (PSEN1), a known EOFAD-causing variant, would display altered intracellular calcium signalling and modified cellular metabolism to iPSCs derived from a healthy comparator.

To investigate this hypothesis, the specific aims of this chapter were as follows:

1. To use calcium imaging to determine if cellular homeostasis was modified in NPCs, novel 2D DGNs, and 3D cerebroids derived from iPSCs containing the PSEN1 mutation.
2. To Seahorse XF96 Analyzer to assess cellular metabolism in healthy- and familial AD-derived NPCs.

Techniques used:

1. Neural progenitor cell culture (2.4).
2. Neural progenitor cell coverslip culture (2.4.6).
3. Perfusion bath calcium imaging (2.8).
4. Seahorse MitoStress Testing (2.9.1).

Flow chart of experimental designs (present in corresponding Methods).
Data analysis (2.8.3, 2.9.3).

4.2 Results

4.2.1 PSEN1 mutant NPCs show increased basal cytosolic calcium

The Calcium Hypothesis of AD posits a bidirectional relationship between intracellular Ca^{2+} dysregulation and Aβ pathology, in which disturbances in calcium homeostasis can both arise from, and contribute to, amyloidogenic processes (see section 1.3.1). In the context of sporadic AD, this may occur following external insult or oxidative stress accumulated over the lifetime of an individual. For the Calcium hypothesis to encompass and explain all current evidence for AD induction, FAD mutations would need to cause either an innate disturbance in homeostatic calcium balance within neural cells, or a susceptibility to damage and/or disruption of calcium regulating components. As such, any mutation-linked disturbances may already be observable in NPCs without the need to fully differentiate into mature neurons.

Similar to previous research in neurons from rodent models of AD (Kaar 2019), the PSN1 mutant NPC line M139V demonstrated higher levels of cytosolic Ca^{2+} fluorescence (13.64$\pm$0.9523 A.F.U., n = 65 cells from 6 coverslips, from 3 independent differentiations) than controls (7.10$\pm$0.3501, n = 79, 10, 4.)(Welch's t test comparison, mean$\pm$SEM, $p < 0.0001$, Fig. 4.1).

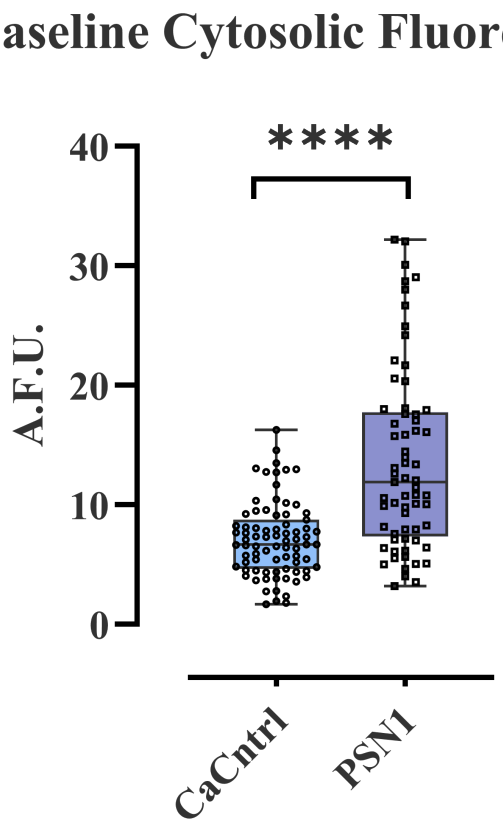

Figure 4.1: **Basal cytosolic calcium fluorescence is increased in NPCs containing a PSEN1 mutation.** Box & whisker plot (box = median +/- quartile range, whiskers = min to max values) illustrate relative fluorescence in neural progenitor cells (NPCs) derived from healthy (CaCntrl) donor and an individual with Alzheimer's disease (AD) with a $PSEN1_{M139V}$ mutation (PSN1). Each data point represents a single cell. **** indicates $p < 0.0001$. A.F.U.: arbitrary fluorescence units.

4.2.2 Voltage-gated calcium entry is increased in PSEN1 mutant NPCs

Given the elevated resting levels of Ca^{2+} in PSN1 NPCs, we examined whether alterations in Ca^{2+} influx was a contributory factor to the observed phenotype. NPCs depolarise in response to elevated extracellular KCl. Due to the high permeability of the resting neural membrane to K^{+}, increasing extracellular potassium depolarises cells and triggers Ca^{2+} entry through L-type voltage-gated calcium channels (VGCCs) (Rienecker, Poston, and Saha 2020). Multiple AD animal models containing different PSEN1 mutations exhibit increased VGCC expression and activity, potentially in response to inaccurate sensing of intracellular calcium stores (Cook *et al.* 2005).

To activate VGCCs, NPCs were exposed for 30 s to 50 mM extracellular K^{+} (Fig 4.2), and the resulting fluorescence increase was compared between control and PSN1 mutant NPCs (Mann-Whitney test; data given as Median, IQR[Q1,Q3], with U statistic and P value; control n = 73, 10, 4. PSN1 n = 71, 6, 3. Fig 4.3). PSN1 NPCs showed significantly greater total peak area (627.6, [361.1, 1021] vs. 2777, [1503, 3953] AUC, U = 325.5, $p < 0.0001$), maximal peak amplitude (31.19, [18.61, 49.10] vs. 78.80, [63.95, 102.4] A.F.U., U = 516.5, $p < 0.0001$) and relative fluorescence change from baseline (93.37, [55.87, 149.8] vs. 512.1, [146.0, 755.7], U = 1010, $p < 0.0001$), whereas the duration of Ca^{2+} transients did not differ (140.5, [103.2, 147.6] vs. 141.5, [127.6, 145.8] s, U = 2152, $p = 0.2710$).

These results are indicative of the PSN1 mutation enhancing VGCC Ca^{2+} entry in NPCs.

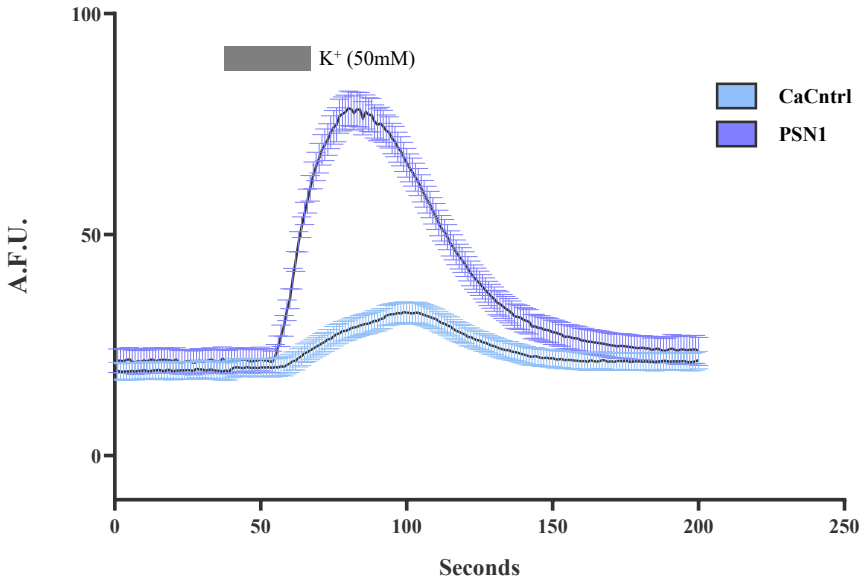

Figure 4.2: **Neural progenitor cells containing a PSN1 mutation show enhanced calcium response to 50 mM extracellular K^+.** Time course traces of calcium fluorescence signal of NPCs in response to 30 s exposure to 50 mM K^+. CaCntrl in blue, PSN1 in purple. Data are presented as mean±SEM. A.F.U.: arbitrary fluorescence units.

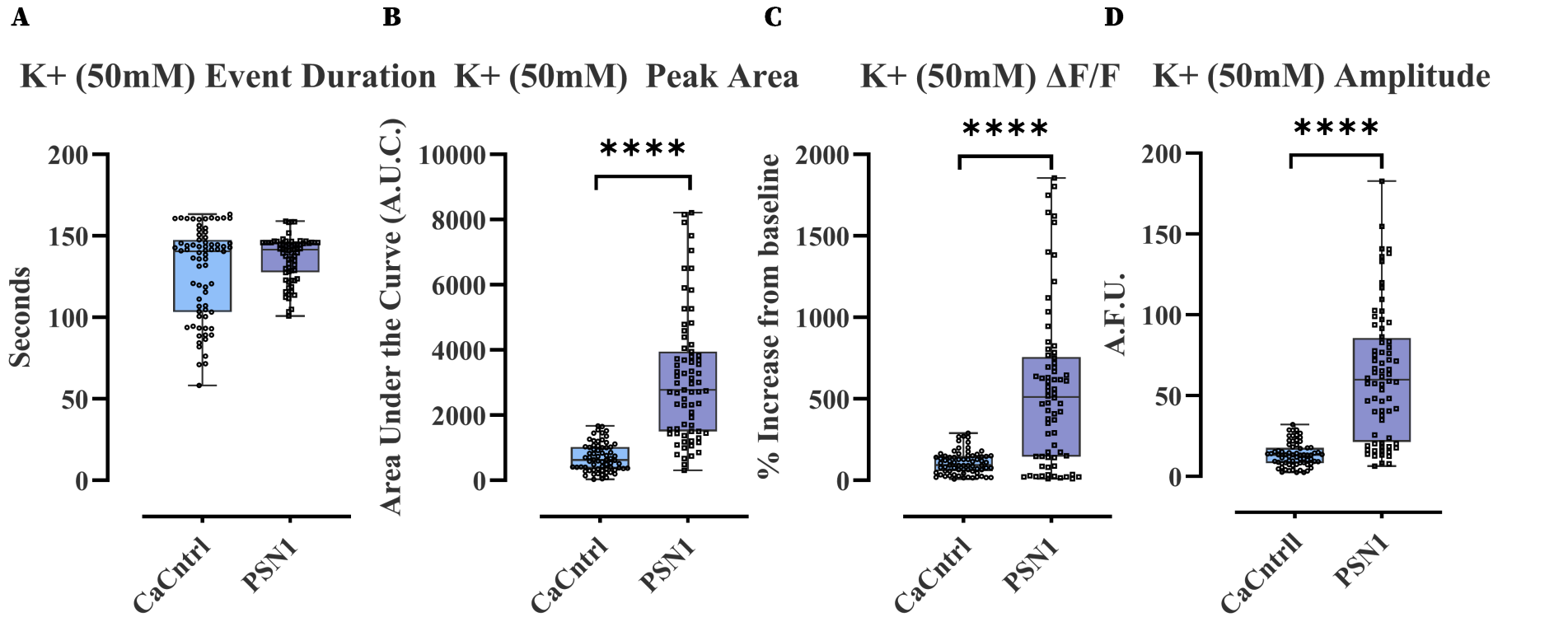

Figure 4.3: **Calcium signalling in response to 50 mM K^+ is increased in PSEN1 mutant NPCs.** Box & whisker plots (box = median +/- quartile range, whiskers = min to max values) illustrate relative fluorescence in cells from neural progenitor cells (NPCs) derived from healthy (CaCntrl) and an individual with Alzheimer's disease (AD) with a $PSEN1_{M139V}$ mutation (PSN1) in response to a thirty second exposure to an additional 50mM extracellular K^+. **A**: duration of the fluorescence peak. **B**: total area under the curve of the fluorescence peak. **C**: relative change in fluorescence peak amplitude from baseline. **D**: the absolute change in fluorescence amplitude. Each data point represents a single cell. **** indicates P <0.0001. A.F.U.: arbitrary fluorescence units.

4.2.3 Calcium store release is increased in PSEN1 mutant NPCs

Given that NPCs do not possess fully functional group 1 metabotropic glutamate receptors (mGluRs), Ca^{2+} release from the ER cannot be consistently evoked by DHPG (Suzuki *et al.* 2006). Instead, total intracellular Ca^{2+} store release was induced by the calcium ionophore, ionomycin. Although ionomycin is a relatively 'blunt' tool, it forms pores in both intracellular and plasma membranes, it was chosen for its consistent efficacy in our NPC experiments.

To quantify calcium release, NPCs were exposed to 10 μM ionomycin for 2 min. PSN1 NPCs exhibited a significantly larger relative fluorescence change (median, [IQR]: 343.1, [52.4, 554.8]; n = 64, 6, 3.) than controls (160.2, [101.4, 228.5]; n = 65, 10, 4.=; Mann–Whitney U = 1874, p = 0.0006; Fig. 4.4B). In contrast, there were no differences in peak area under the curve (1695, [1169, 2888] vs. 1554, [440.3, 2972] AUC; U = 2018, p = 0.1660) or maximal peak amplitude (25.43, [15.03, 47.41] vs. 22.56, [8.130, 43.03]; U = 1811, p = 0.1622).

These data indicate that although the $PSEN1_{M139V}$ mutation did not alter the overall magnitude of the ionomycin-evoked Ca^{2+} response, it was associated with altered calcium release kinetics. To confirm the magnitude, and direction of this change in release dynamics further analyses were conducted.

The times for fluorescence signals to reach half their maximum amplitude were significantly shorter in PSN1 NPCs (94.31±2.3567, n = 64, 6, 3.) than CaCntrl NPCs (108.87±1.9007, n = 65, 10, 4.)(Welch's t-test, mean±SEM, $p < 0.0001$, Fig. 4.5).

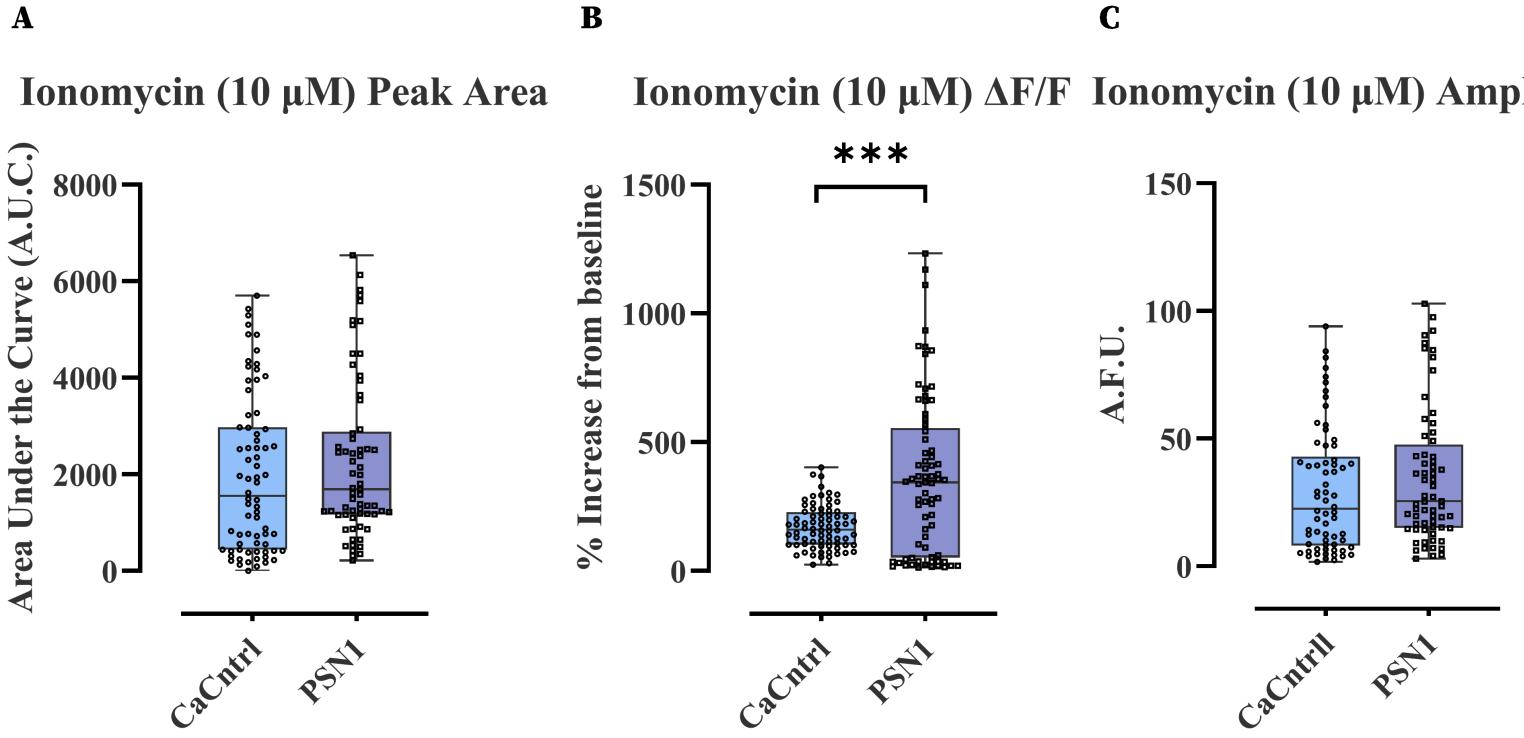

Figure 4.4: **Cellular calcium increases in response to 10 µM ionomycin is altered in PSN1 mutant NPCs.** Box & whisker plots (box = median +/- quartile range, whiskers = min to max values) show responses of NPCs derived from healthy (CaCntrl) and $PSEN1_{M139V}$ (PSN1) AD donors to 10 µM ionomycin (2 min), and measured for a defined time period following exposure **A**: total area under the curve of the fluorescence peak. **B**: relative fluorescence change from baseline. **C**: the absolute change in fluorescence amplitude. Each data point represents a single cell. *** indicates $p < 0.001$. A.F.U.: arbitrary fluorescence units.

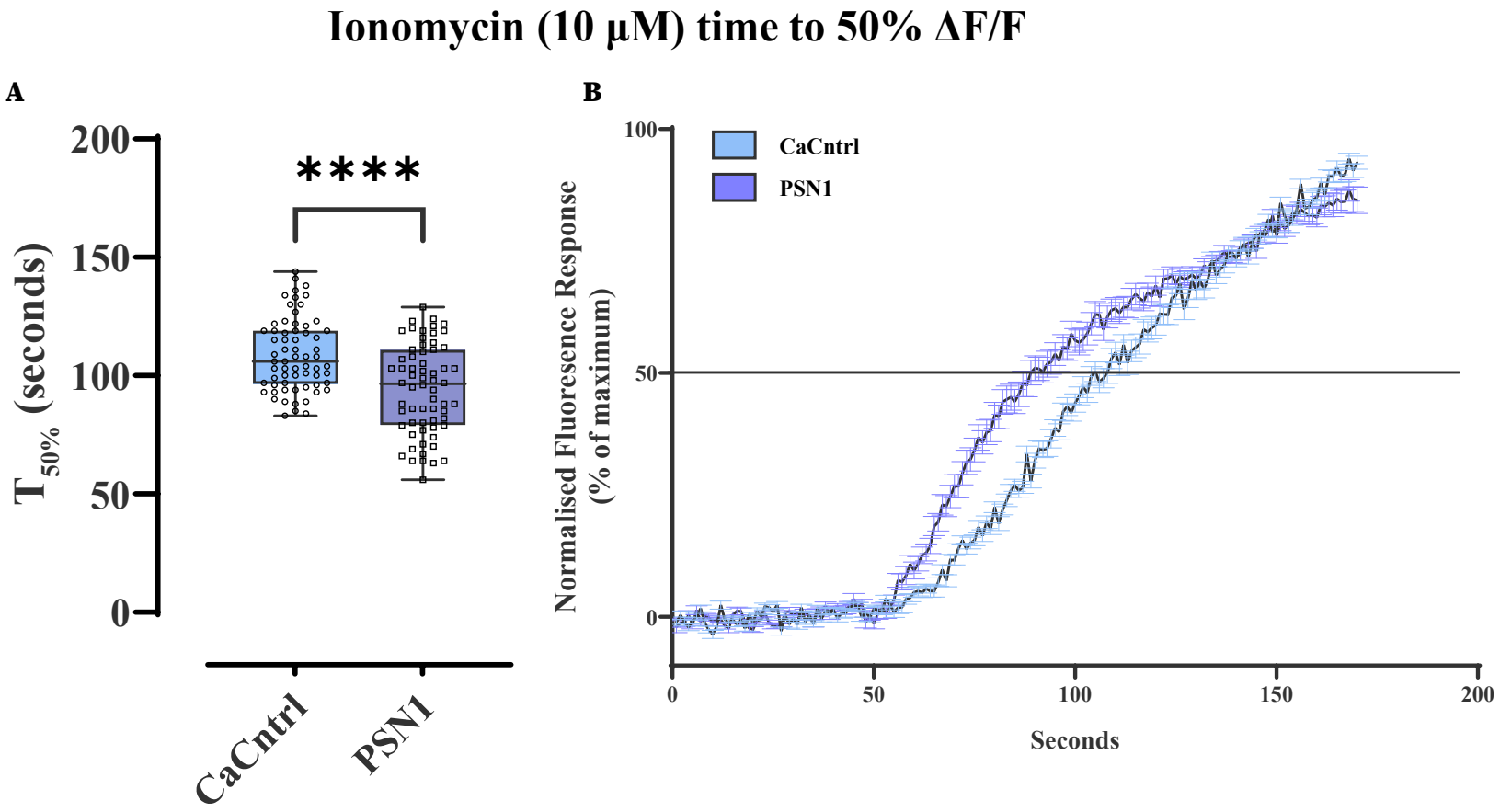

Figure 4.5: **Cellular calcium increases in response to 10 µM ionomycin is accelerated in PSN1 mutant NPCs. A**: Box & whisker plots (box = median +/- quartile range, whiskers = min to max values) show the time (seconds) for the relative fluorescence of NPCs to reach 50% of the maximal signal from baseline in response to 10 µM ionomycin. Each data point represents a single cell. **** indicates $p < 0.0001$. **B**: Time course of the normalised fluorescence response (0-100% ΔF/F) of the same cells (CaCntrl in blue, PSN1 in purple). The horizontal line marks 50% of maximal calcium fluorescence signal induced by ionomycin (10 µM). Data are presented as mean±SEM.

4.2.4 Bioenergetics are suppressed in PSEN1 mutant NPCs

The disruption of intracellular calcium homeostasis observed in PSN1-mutant NPCs raises the question of whether broader homeostatic processes, particularly cellular metabolism, may also be compromised. Mitochondria play a central role in both energy production and calcium buffering, and there exists a well-established interplay between calcium signalling and metabolic regulation in neurons (Liiv *et al.* 2024). The processes of synaptic activity and plasticity are highly energy-dependent, relying on the tight coupling of ATP generation to calcium fluxes across mitochondrial and endoplasmic reticulum membranes (Baloyannis 2020). A disturbance in this coupling, particularly if it occurs early in development, may indicate a fundamental vulnerability in the bioenergetic machinery of neurons predisposed to AD. Importantly, if these impairments are genetically encoded or developmentally programmed, they may be detectable in NPCs, the immediate precursors to mature neural cells.

To test this possibility, Seahorse XF96 Cell Mito Stress Tests were performed on NPCs derived from control and PSEN1 mutant iPSC lines (full methods in section 2.9.1). Oxygen consumption rate (OCR) and extracellular acidification rate (ECAR) were measured following sequential injections of oligomycin, carbonyl cyanide-4 (trifluoromethoxy) phenylhydrazone (FCCP), and rotenone/antimycin A. To account for independent experimental plate variance, intra-plate well correlation, and unbalanced well replications per experiment post outlier removal, a linear mixed-effects model (Measure~Cell_line + Drug_treatment + (1|Experiment)), weighted by the number of aggregated wells within a plate, was applied to the calculated bioenergetic measures (for full explanation of bioenergetic measures see 2.13).

In contrast to the elevated basal intracellular calcium concentration ($[Ca^{2+}]_i$) and potentiated responses to certain stimuli, PSN1 NPCs showed suppression of bioenergetic measures (Fig. 4.6A) and (Fig. 4.7A). Custom *post-hoc* analyses comparing PSEN1 ($n_{bio} = 5$ independent experiments and $n_{well} = 57$ aggregated wells across all experiments) and CaCntrl ($n_{bio} = 5, n_{well} = 59$) NPCs showed significantly reduced basal respiration (-0.044ΔOCR, $p < 0.0001$, Fig. 4.6B), ATP-linked respiration (-0.0386ΔOCR, $p < 0.0005$, Fig. 4.6C) maximal respiration (-0.155ΔOCR, $p < 0.0001$, Fig. 4.6D), non-mitochondrial respiration (-0.017ΔOCR, $p < 0.0001$, Fig. 4.6E), spare respiratory capacity (-0.111ΔOCR, $p < 0.0001$, data not shown), and proton leak (-0.006ΔOCR, $p < 0.0001$, Fig. 4.6F)(OCR units = (pmol $O_2 \cdot min^{-1} \cdot \mu g^{-1} \cdot mL^{-1}$ Protein)) in the PSN1 NPCs relative to control. However, no significant changes between lines was observed in coupling efficiency (-0.453ΔOCR, $p = 0.7848$, Fig. 4.6G), a measure assessing the relationship between basal respiration and ATP synthesis.

Similarly, for ECAR-derived measures (ECAR units = (mpH·min^{-1}·μg^{-1}·mL^{-1} Protein)), basal ECAR (-0.010ΔECAR, $p < 0.0010$, Fig. 4.7B), maximal ECAR (-0.020ΔECAR, $p < 0.0001$, Fig. 4.7C), and glycolytic reserve capacity (-0.010ΔECAR, $p < 0.0001$, Fig. 4.7D) were all significantly decreased in PSN1 NPCs compared to controls.

Together, these findings demonstrate that PSN1-mutant NPCs exhibit a broad suppression of both mitochondrial respiration and glycolytic flux, while the preserved coupling efficiency rules out an inherent ATP-synthesis defect. Such a global down-regulation of bioenergetic capacity may render developing neurons particularly vulnerable to metabolic stress.

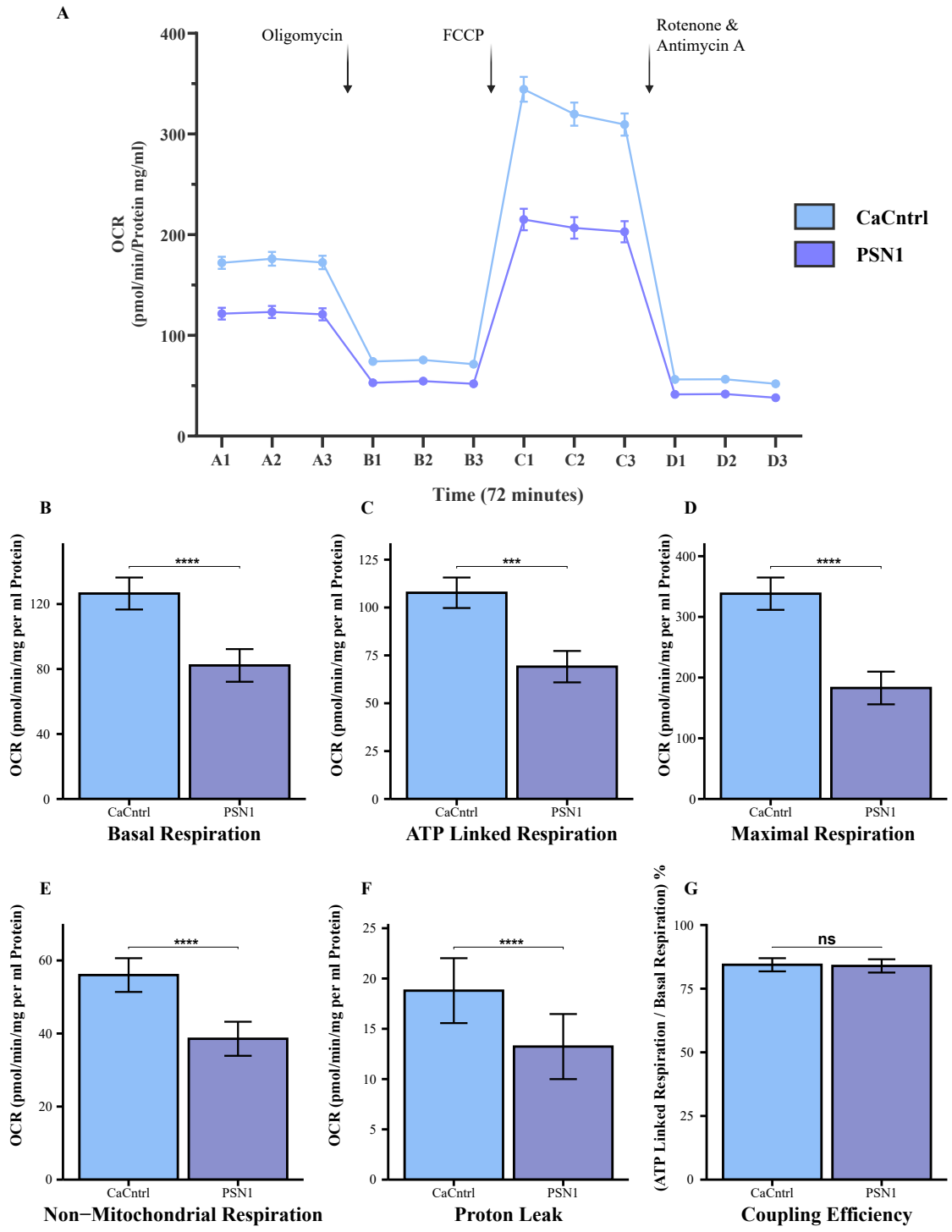

Figure 4.6: **Oxygen consumption rate (OCR) measures are suppressed in PSN1 mutant NPCs**. **A**: Traces illustrating oxygen consumption rate (OCR) over a period of 72 minutes in control (CaCntrl, in blue) and presenilin-mutant (PSN1, in purple) NPCs at 12 distinct time points. Data are presented as mean±SEM. The additions of oligomycin, FCCP, and rotenone and antimycin A between recordings are denoted with arrows. Bar charts (model-estimated marginal mean±SEM) show cell line differences in **B**: basal respiration, **C**: ATP linked respiration, **D**: maximal respiration, **E**: non-mitochondrial respiration, **F**: proton leak and **G**: coupling efficiency in 5 independent experimental plates of CaCntrl ($n_{well} = 59$ total) and PSN1 ($n_{well} = 57$ total) NPCs. *** and **** indicate $p < 0.001$ and $p < 0.0001$ respectively.

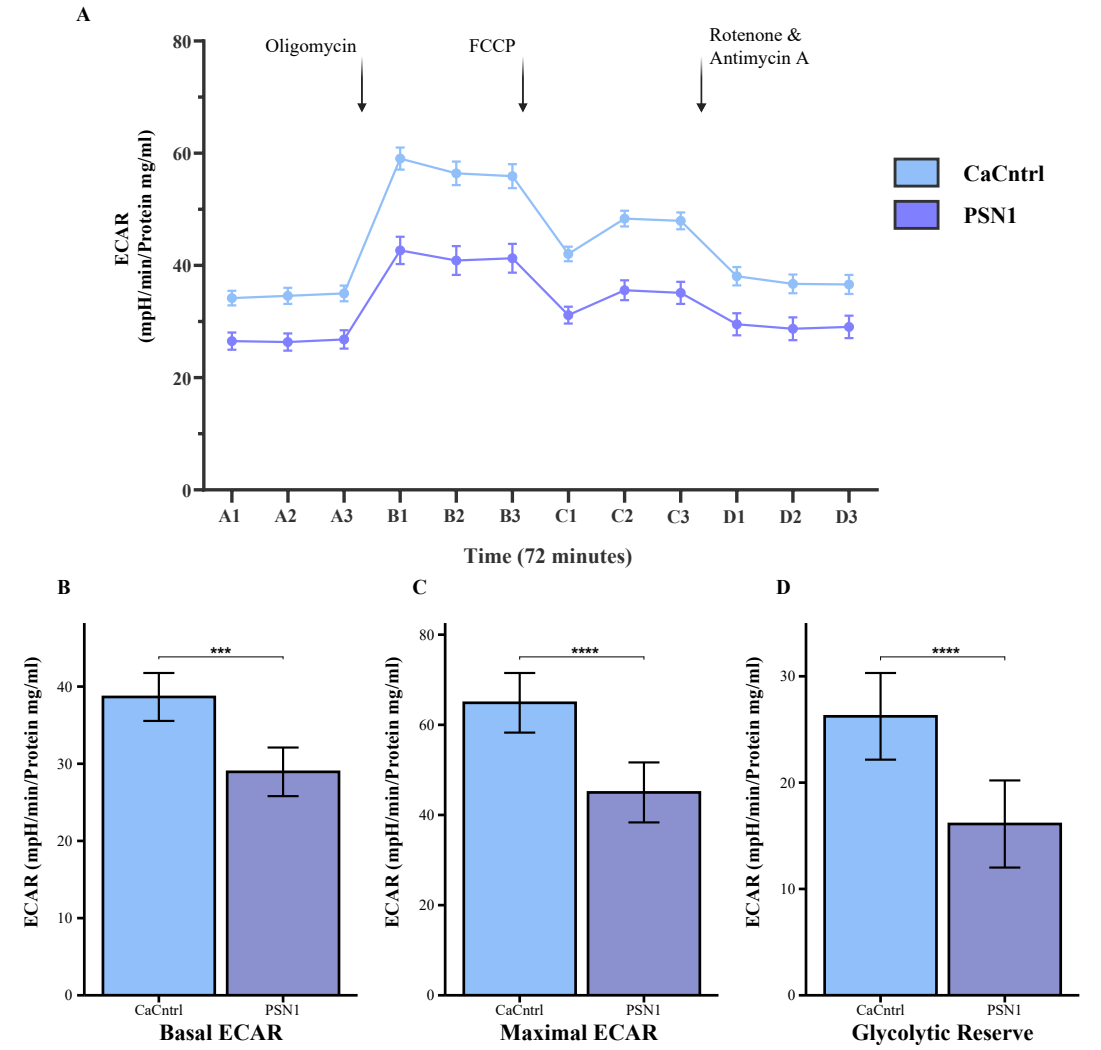

Figure 4.7: **Extracellular acidification rate (ECAR) measures are suppressed in PSN1 mutant NPCs. A**: Traces illustrating extracellular acidification rate (ECAR) over a period of 72 minutes in control (CaCntrl, in blue) and presenilin-mutant (PSN1, in purple) NPCs at 12 distinct time points. Data are presented as mean±SEM. The additions of oligomycin, FCCP, and rotenone and antimycin A between recordings are denoted with arrows. Bar charts (model-estimated marginal mean±SEM) show cell line differences in **B**: basal ECAR, **C**: maximal ECAR and **D**: glycolytic reserve in coupling efficiency in 5 independent experimental plates of CaCntrl ($n_{well} = 59$ total) and PSN1 ($n_{well} = 57$ total) NPCs. *** and **** indicate $p < 0.001$ and $p < 0.0001$ respectively.

4.2.5 Real-time OCR measurements corroborate suppressed metabolic state in PSN1 NPCs

While Seahorse Analyser assessment of OCR is considered a gold-standard in research, it is still an end-point experiment conducted outside of the cells standard culture environment. To see if the suppressed metabolic state of PSN1 NPCs observed in the previous Seahorse experiments (section 4.2.4) would be present in standard culture conditions, we used the Resipher system by Lucid Scientific to continually measure OCR over 90 hours (see 2.9.4). While OCR measurement commenced as soon as cells were returned to the incubator, the first 24 hours were excluded from analysis fue to the fact that we designated this as a stabilization period for the cells.

A linear mixed-effects model applied to the data (Measurement~Cell_line $*$ poly(Time,2) $+$ (1 $+$ poly(Time,2)|ID)) reaffirmed a significant effect of the cell line (estimate difference $=-0.16$, $p = 0.0234$) on NPCs metabolic state, with the PSN1 ($n = 11$ wells) line exhibiting lower OCR than CaCntrl ($n = 12$ wells) NPCs (Fig. 4.8). This model was chosen as it allowed for repeated measurements, and could account for inter-well variability within groups. Additionally, the temporal dynamics of cell line differences in OCR were also observable. OCR in both cell lines changed non-linearly over time ($p < 0.0000$ for both linear and quadratic time terms). Indicating that mitochondrial activity does not follow a simple unidirectional trend, but involves both an initial increase and a later plateau or decline. While OCR increased in both cell lines over time, reflecting early adaptation or cell proliferation-associated metabolic demand, PSN1-mutant cells showed a steeper initial increase ($p = 0.0018$ for the interaction between cell line and linear time). However, this was followed by an earlier and more pronounced decline in OCR in the PSN1-mutant cells ($p <0.0000$ for the interaction between cell line and quadratic time).

As in the seahorse experiments, PSN1 NPCs showed a suppressed OCR in comparison to CaCntrl healthy control cells, now accompanied by an altered metabolic-temporal profile. The sharper rise and subsequent fall in OCR in PSN1 NPCs may indicate a compensatory metabolic response that is ultimately unsustainable.

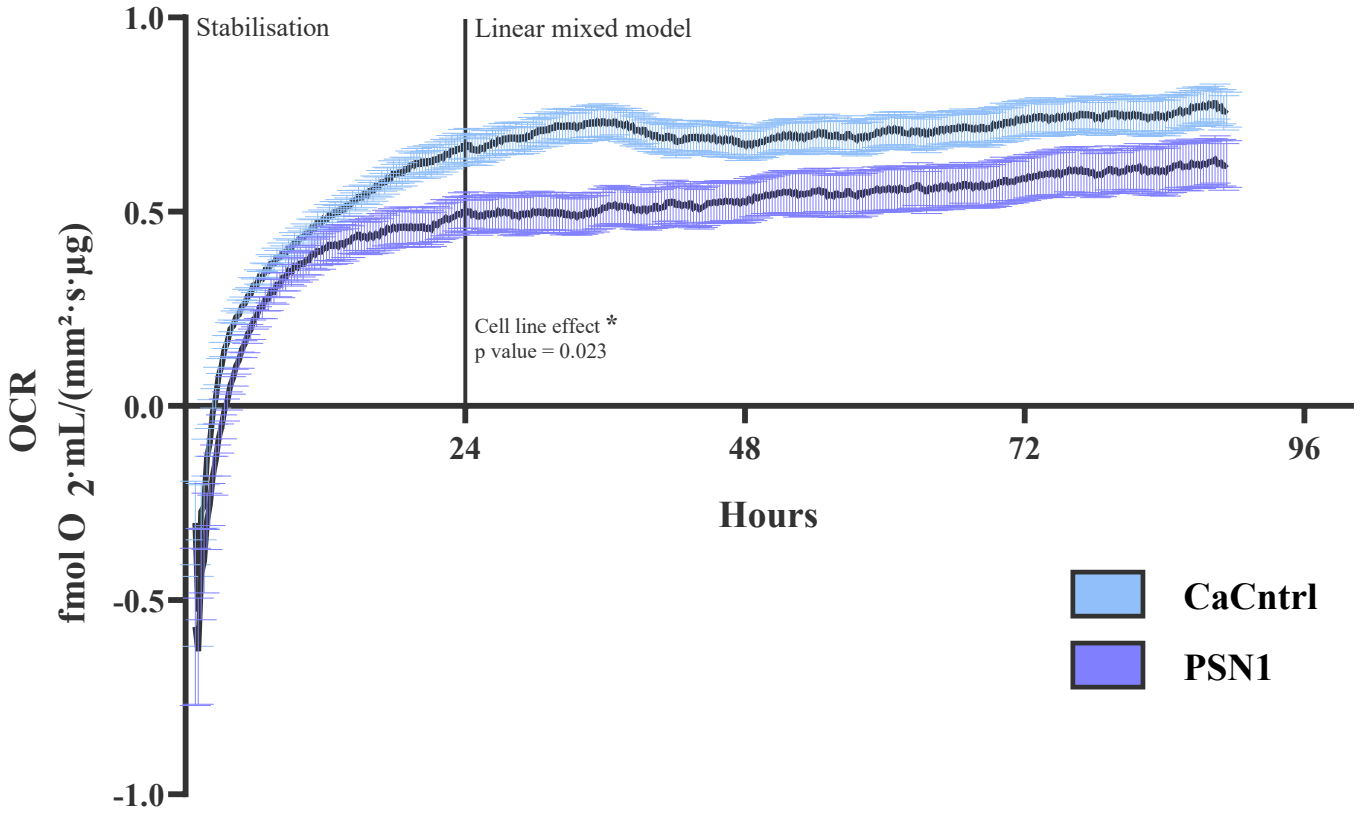

Figure 4.8: **Real-time measures of OCR in NPCs.** Traces illustrating continual measures of oxygen consumption rate (OCR) (units = $\left(\text{fmol } O_2 \cdot \text{mL} \cdot \text{mm}^{-2} \cdot \text{s}^{-1} \cdot \mu\text{g}^{-1} \text{ Protein}\right)$) over a period of 90 hours in control (CaCntrl $n_{wells} = 12$, in blue) and presenilin-mutant (PSN1 $n_{wells} = 11$, in purple) NPCs maintained in a standard cell culture incubator. Data represent normalized and grouped measurements across well replicates from a single experiment, stabilized for 24 hours prior to analyses, normalised to well protein. Random effects accounted for variation across wells. Data are presented as mean±SEM.

4.2.6 Dantrolene pretreatment differentially alters NPC respiration and glycolysis

Given the elevated levels of cytosolic calcium in PSN1 NPCs (section 4.2.1) which contrasted with the suppression of most components of mitochondrial glycolysis and the electron transport chain (section 4.2.4) in the same cells, we sought to examine a direct link between the $[Ca^{2+}]_i$ and bioenergetic phenotypes. To do this PSN1 and CaCntrl NPCs were exposed to 10 μM dantrolene for 24 hours prior to the Mito Stress Test. Dantrolene is an inhibitor of RyR-mediated Ca^{2+} release from the ER, which should lead to a decrease in cytosolic calcium (Noda *et al.* 2022).

As with the examination of cell line as a factor affecting metabolic behaviour (see section 4.2.4), OCR and ECAR were measured following sequential injections of oligomycin, FCCP, and rotenone/antimycin A (Fig. 4.9A). To again account for independent experimental plate variance, intra-plate well correlation, and unbalanced well replications per experiment and experimental condition post outlier removal, a linear mixed-effects model (Measure~Cell_line + Drug_treatment + (1|Experiment)), weighted by the number of aggregated wells within a plate, was applied to the data. Custom *post-hoc* analyses reported the following differences with Benjamini-Hochberg adjusted p values.

The significant suppression of basal respiration in PSN1-mutant cells ($n_{bio} = 10, n_{well} = 110$) compared to CaCntrl cells ($n_{bio} = 10, n_{well} = 110$) was corroborated in this analysis with more well replicates (-0.041ΔOCR, $p < 0.0001$, Fig. 4.9B, OCR units = (pmol $O_2 \cdot min^{-1} \cdot \mu g^{-1} \cdot mL^{-1}$ Protein)). Unexpectedly, dantrolene pretreatment significantly increased basal respiration in both cell lines ($+0.020\Delta$OCR, $p = 0.0139$, CaCntrl Control $n_{bio} = 5, n_{well} = 59$, CaCntrl Dantrolene ($n_{bio} = 5, n_{well} = 51$), PSN1 Control ($n_{bio} = 5, n_{well} = 57$), PSN1 Dantrolene ($n_{bio} = 5, n_{well} = 53$), but interestingly the basal respiration of PSN1 NPCs returned to a level statistically indistinguishable from healthy controls (-0.020, $p = 0.0662$).

A similar pattern of a significant reduction in a given energetic measure in PSN1 cells, a significant increase in a given measure following dantrolene pretreatment, and a sufficient rise in treated PSN1 cells to statistically equivalent levels as untreated healthy controls, was also seen for ATP-linked respiration (cell line effect -0.035ΔOCR, $p < 0.0001$; dantrolene treatment $+0.008\Delta$OCR, $p = 0.0043$; PSN1 Dantrolene$-$CaCntrl Control -0.017ΔOCR, $p = 0.1257$; Fig. 4.10A) and non-mitochondrial respiration (cell line effect -0.017ΔOCR, $p < 0.0001$; dantrolene treatment $+0.010\Delta$OCR, $p = 0.0043$; PSN1 Dantrolene$-$CaCntrl Control -0.007ΔOCR, $p = 0.1495$; Fig. 4.11A). However,

an increase in PSN1 cells to healthy control levels following drug treatment was not seen for maximal respiration (cell line effect -0.140ΔOCR, $p < 0.0001$; dantrolene treatment $+0.066\Delta$OCR, $p = 0.0014$; PSN1 Dantrolene$-$CaCntrl Control -0.073, $p = 0.0081$; Fig. 4.10B), spare respiratory capacity (cell line effect -0.099ΔOCR, $p < 0.0001$; dantrolene treatment $+0.046\Delta$OCR, $p = 0.0017$; PSN1 Dantrolene$-$CaCntrl Control -0.053, $p = 0.0070$; Fig. 4.11B). Dantrolene treatment had no effect on proton leak (cell line effect -0.006ΔOCR, $p < 0.0001$; dantrolene treatment $+0.002\Delta$OCR, $p = 0.1130$; PSN1 Dantrolene$-$CaCntrl Control -0.004, $p = 0.0910$; Fig. 4.12A) nor coupling efficiency (cell line effect $-0.004\Delta\%$, $p < 0.8289$; dantrolene treatment $+0.007\Delta\%$, $p = 0.8289$; PSN1 Dantrolene$-$CaCntrl Control $+0.004\Delta\%$, $p = 0.8289$; Fig. 4.12B) relative to control.

Within the ECARiderived measures (Fig. 4.13A, ECAR units = (mpH$\cdot$min$^{-1}\cdot\mu$g$^{-1}\cdot$ mL^{-1} Protein)), dantrolene pretreatment significantly increased basal ECAR (cell line effect -0.008ΔECAR, $p < 0.0118$; dantrolene treatment $+0.006\Delta$ECAR $p = 0.0388$; PSN1 Dantrolene$-$CaCntrl Control -0.002ΔECAR, $p = 0.5766$; Fig. 4.13B), but did not have a significant effect on maximal ECAR (cell line effect -0.016ΔECAR, $p < 0.0118$; dantrolene treatment $+0.006\Delta$ECAR, $p = 0.1083$; PSN1 Dantrolene$-$CaCntrl Control -0.010ΔECAR, $p = 0.0778$; Fig. 4.14A) nor glycolytic reserve (cell line effect -0.008ΔECAR, $p < 0.0001$; dantrolene treatment -0.001ΔECAR, $p = 0.978$; PSN1 Dantrolene$-$CaCntrl Control -0.008ΔECAR, $p = 0.0023$; Fig. 4.14B) compared to control.

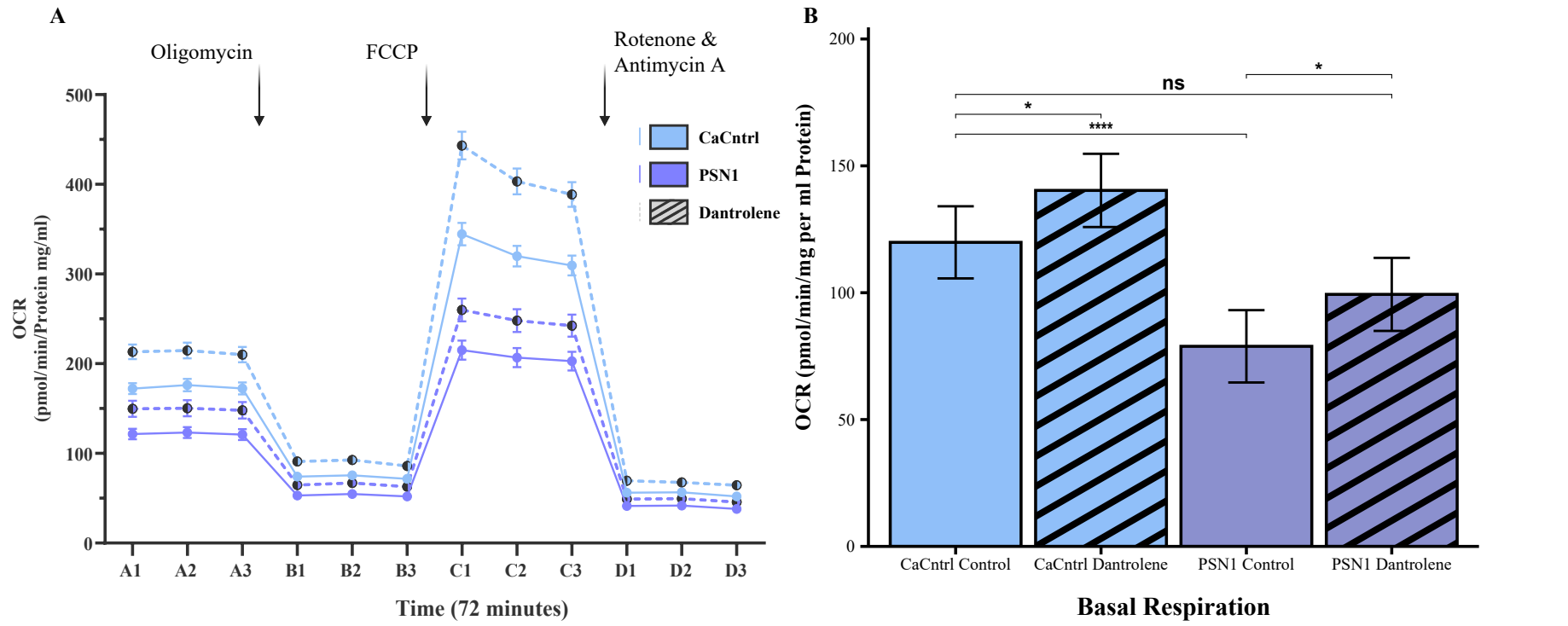

Figure 4.9: **Dantrolene pretreatment increases basal respiration in NPCs. A**: Traces illustrating oxygen consumption rate (OCR) over a period of 72 minutes in control (CaCntrl, in blue) and presenilin-mutant (PSN1, in purple) NPCs, either pre-treated for 24 hours with 10 μM dantrolene (Dantrolene, striped boxes) or not (Control, plain box) at 12 distinct time points. Data are presented as mean±SEM. The additions of oligomycin, FCCP, and rotenone and antimycin A between recordings are denoted with arrows. **B**: Bar chart (model-estimated marginal mean±SEM) show cell line and drug treatment differences in basal respiration. * and **** indicate $p < 0.05$ and $p < 0.0001$ respectively.

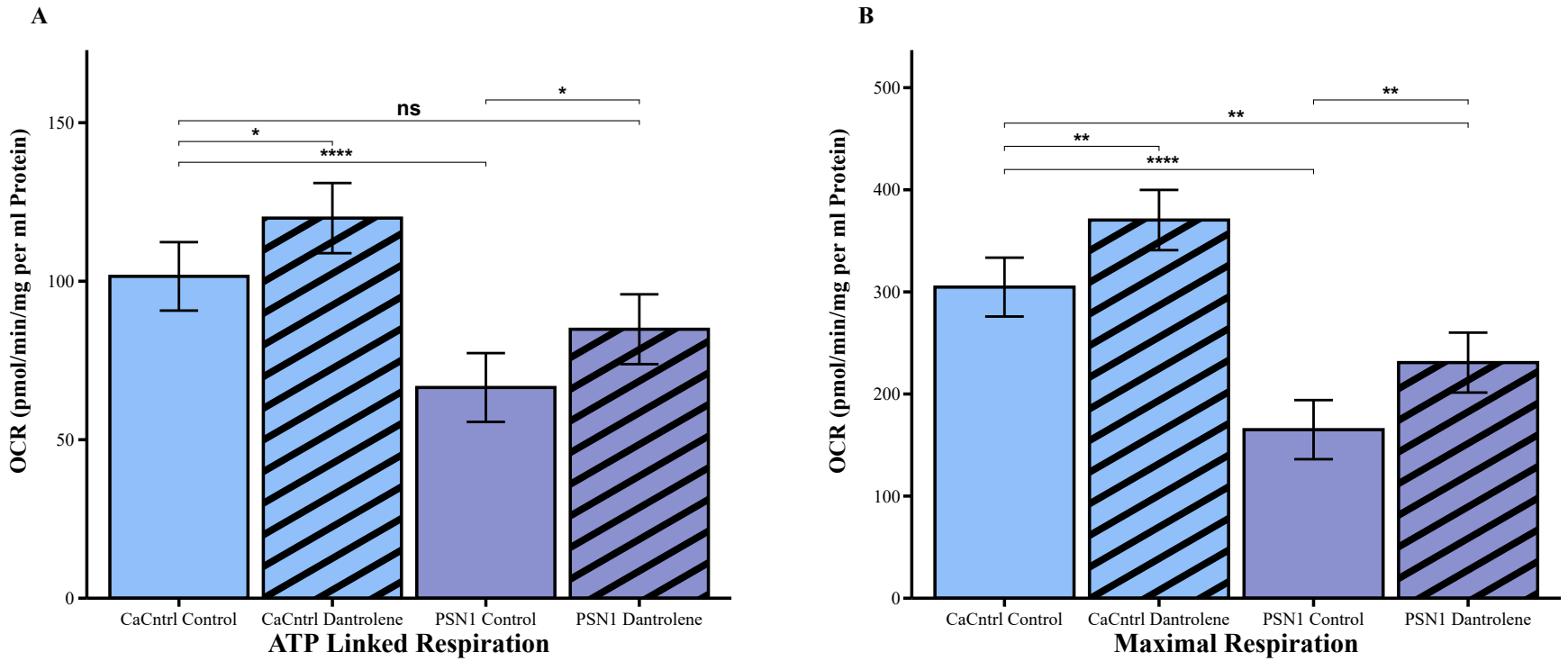

Figure 4.10: **Dantrolene pretreatment increases ATP-linked and maximal respiration in NPCs.** Bar charts (model-estimated marginal mean±SEM) show cell line and drug treatment differences in **A**: ATP-linked respiration, and **B**: maximal respiration in control (CaCntrl, in blue) and presenilin-mutant (PSN1, in purple) NPCs, either pre-treated for 24 hours with 10 µM dantrolene (Dantrolene, striped boxes) or not (Control, plain box). *, ** and **** indicate $p < 0.05$, $p < 0.01$ and $p < 0.0001$ respectively.

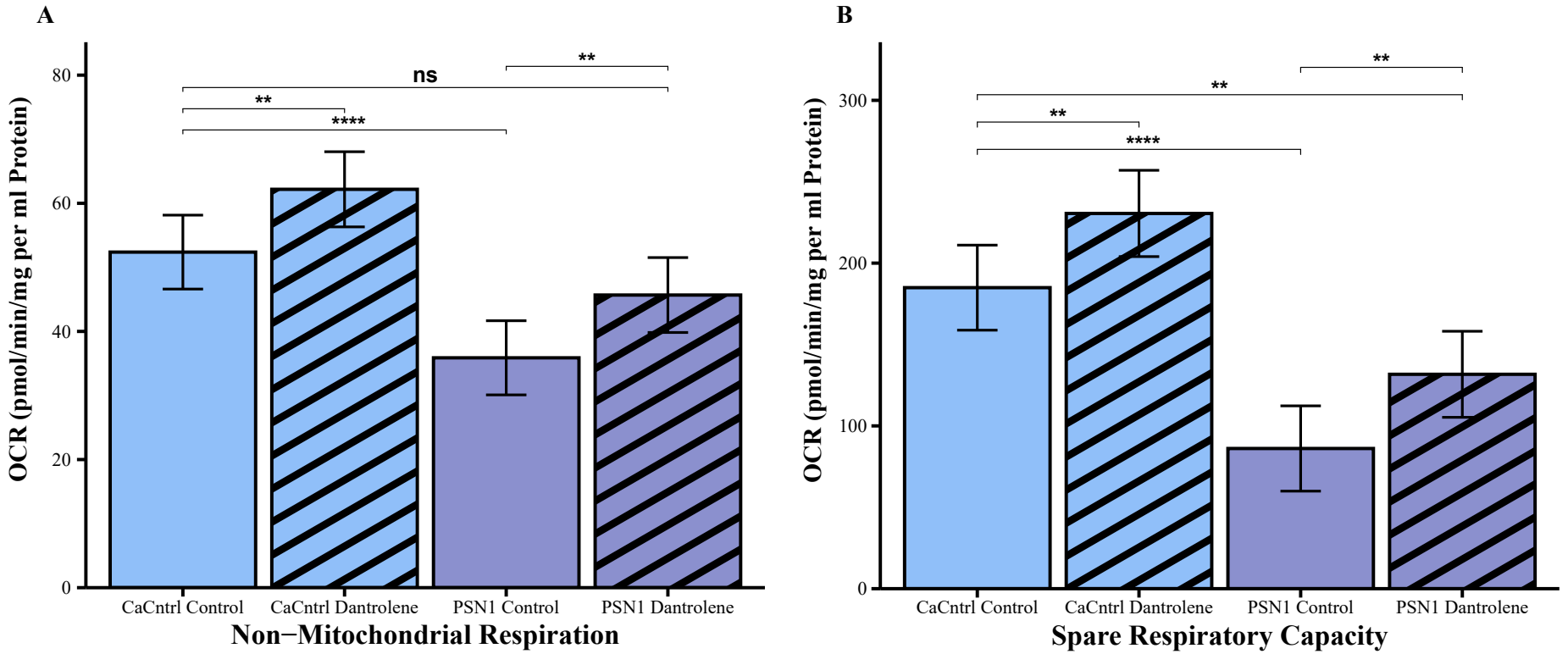

Figure 4.11: **Dantrolene pretreatment increases non-mitochondrial respiration and spare respiratory capacity in NPCs.** Bar charts (model-estimated marginal mean±SEM) show cell line and drug treatment differences in **A**: non-mitochondrial respiration, and **B**: spare respiratory capacity in control (CaCntrl, in blue) and presenilin-mutant (PSN1, in purple) NPCs, either pre-treated for 24 hours with 10 μM dantrolene (Dantrolene, striped boxes) or not (Control, plain box). ** and **** indicate $p < 0.01$ and $p < 0.0001$ respectively.

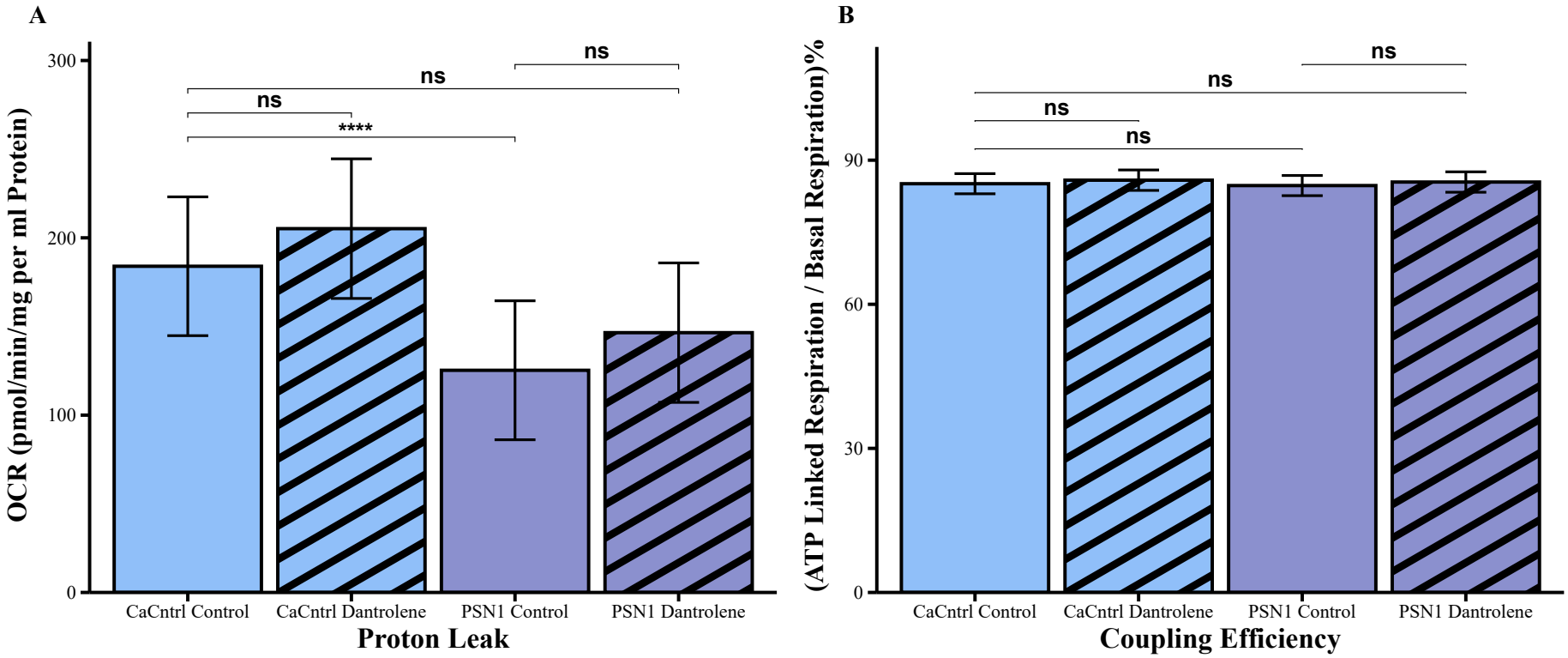

Figure 4.12: **Dantrolene pretreatment does not affect NPC proton Leak or coupling Efficiency.** Bar charts (model-estimated marginal mean±SEM) show cell line and drug treatment comparisons in **A**: proton leak, and **B**: coupling efficiency in control (CaCntrl, in blue) and presenilin-mutant (PSN1, in purple) NPCs, either pre-treated for 24 hours with 10 μM dantrolene (Dantrolene, striped boxes) or not (Control, plain box). **** indicate $p < 0.0001$.

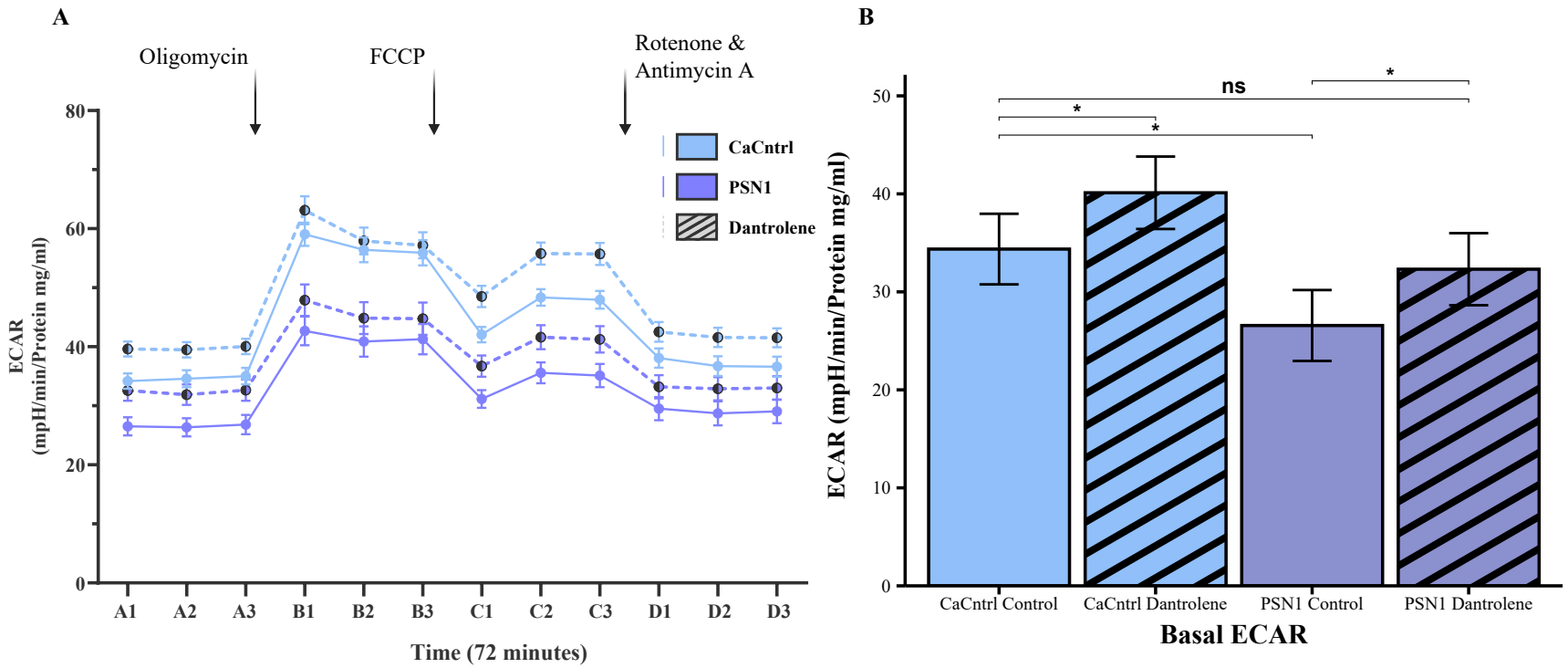

Figure 4.13: **Dantrolene pretreatment increases basal ECAR in NPCs. A**: Traces illustrating extracellular acidification rate (ECAR) over a period of 72 minutes in control (CaCntrl, in blue) and presenilin-mutant (PSN1, in purple) NPCs, either pre-treated for 24 hours with 10 μM dantrolene (Dantrolene, striped boxes) or not (Control, plain box) at 12 distinct time points. Data are presented as mean±SEM. The additions of oligomycin, FCCP, and rotenone and antimycin A between recordings are denoted with arrows. **B**: Bar chart (model-estimated marginal mean±SEM) show cell line and drug treatment differences in basal ECAR. * indicate $p < 0.05$.

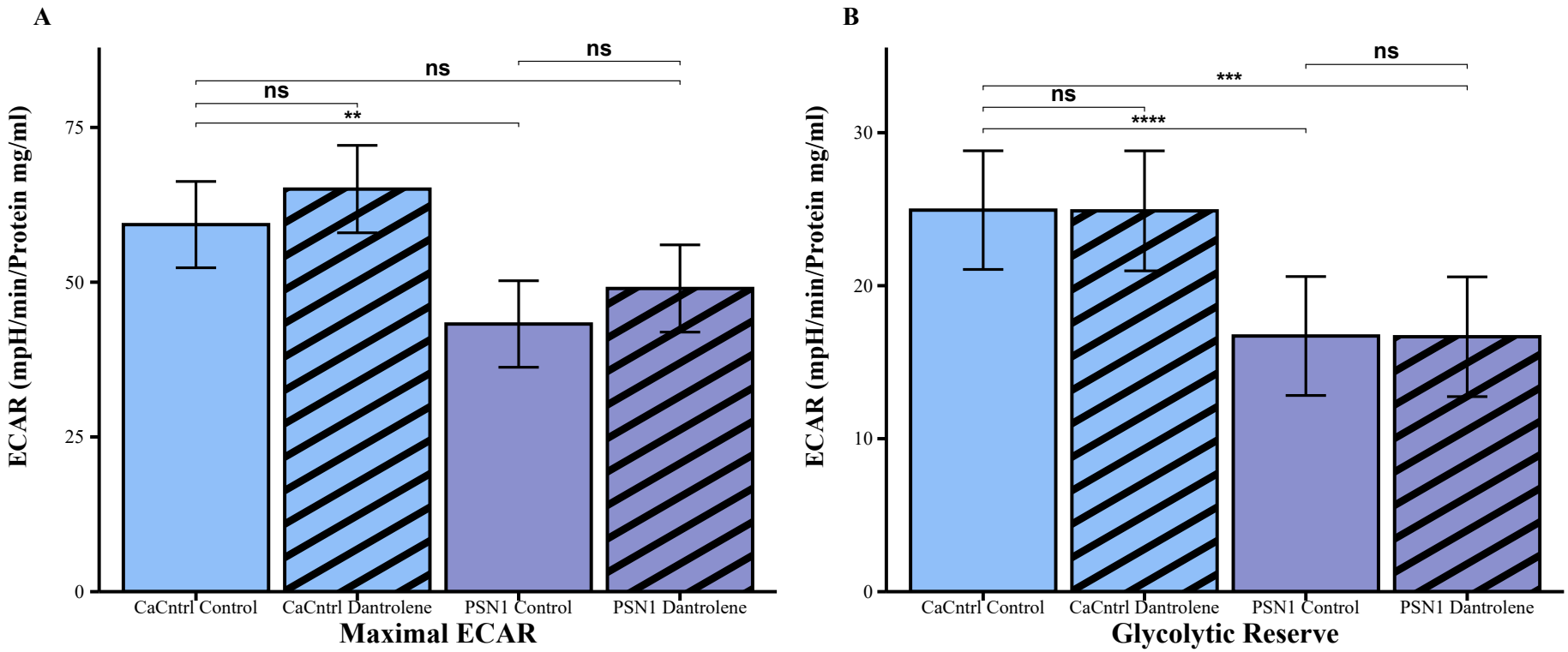

Figure 4.14: **Dantrolene pretreatment does not affect maximal ECAR or glycolytic reserve in NPCs.** Bar charts (model-estimated marginal mean±SEM) show cell line and drug treatment comparisons in **A**: maximal ECAR, and **B**: glycolytic reserve in control (CaCntrl, in blue) and presenilin-mutant (PSN1, in purple) NPCs, either pre-treated for 24 hours with 10 µM dantrolene (Dantrolene, striped boxes) or not (Control, plain box). ** and **** indicate $p < 0.01$ and $p < 0.0001$ respectively.

4.2.7 Acute NMDA treatment shows weak effect on baseline NPC metabolic readings

Contrasting with the actions of dantrolene, exposure of cells to NMDA (2 μM) induces a rapid transient increase in cytosolic calcium *via* the opening of the glutamate-gated Ca^{2+}channels, NMDA receptors. Thus, if suppressing $[Ca^{2+}]_i$ restored some of the metabolic deficits present in PSN1 NPCs, we wondered if increasing intracellular $[Ca^{2+}]_i$ would have a contrasting effect.

Differing from the previous Mito Stress Test experimental designs, OCR and ECAR were measured following sequential injections of NMDA, oligomycin, FCCP, and rotenone/antimycin A (Fig. 4.15A). Prior to the full assessment of all bioenergetic measures, the acute effects of 2 μM NMDA treatment on basal respiration, and the effects of time on basal respiration were assessed using a linear mixed-effects model (Measure~Cell_line + Effective_treatment + time + (1|ID))(CaCntrl Pre-treatment $n_{bio} = 5$, $n_{well} = 59$, CaCntrl Post-treatment $n_{bio} = 5$, $n_{well} = 50$, PSN1 Pre-treatment $n_{bio} = 5$, $n_{well} = 57$, PSN1 Post-treatment ($n_{bio} = 4$, $n_{well} = 33$; OCR units = (pmol $O_2 \cdot$ $\text{min}^{-1} \cdot \mu\text{g}^{-1} \cdot \text{mL}^{-1}$ Protein)). This was to account for any changes occurring in the time between the first basal respiration/ECAR reading prior to NMDA injection, and the reading afterwards (approximately 6 minutes). Custom *post-hoc* analyses following Benjamini-Hochberg adjustment showed a significant reduction in basal respiration following both drug treatment(NMDA−Sham -0.007ΔOCR, p = 0.0325, Fig. 4.15B, C) and a treatment-free waiting step time-matched to the drug treatment measures (Post-treatment−Pre-treatment -0.003ΔOCR, p = 0.0325, Fig. 4.15D, E).

The matched ECAR comparison (Fig. 4.16A, ECAR units = ($\text{mpH} \cdot \text{min}^{-1} \cdot \mu\text{g}^{-1} \cdot$ mL^{-1} Protein)) detected no effect of acute NMDA treatment (NMDA−Sham -0.000ΔECAR, p = 0.6430, Fig. 4.16B, C) or time (Post-treatment−Pre-treatment $+0.001$ ΔECAR, p = 0.1530, Fig. 4.16D, E) on basal ECAR.

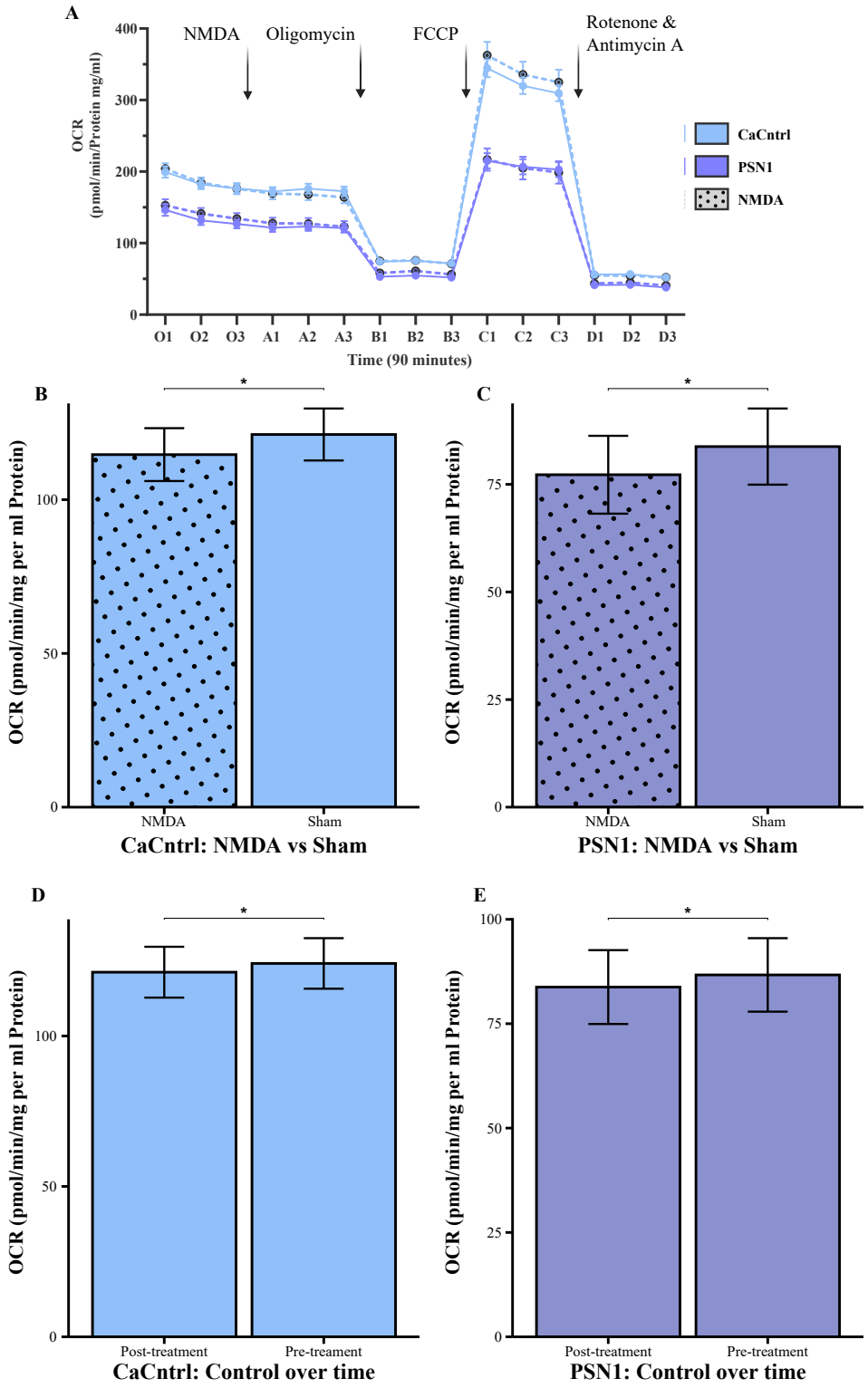

Figure 4.15: **Acute NMDA exposure and time decreases basal NPC respiration. A**: Traces illustrating oxygen consumption rate (OCR) over a period of 90 minutes in control (CaCntrl, in blue) and presenilin-mutant (PSN1, in purple) NPCs, either treated with 2 µM NMDA (NMDA, dotted boxes) or not (Control, plain box) at 15 distinct time points. Data are presented as mean±SEM. The additions of NDMA, oligomycin, FCCP, and rotenone and antimycin A between recordings are denoted with arrows. Bar charts (model-estimated marginal mean±SEM) show **B, C**: drug treatment and **D, E**: time differences in basal respiration. * indicate $p < 0.05$.

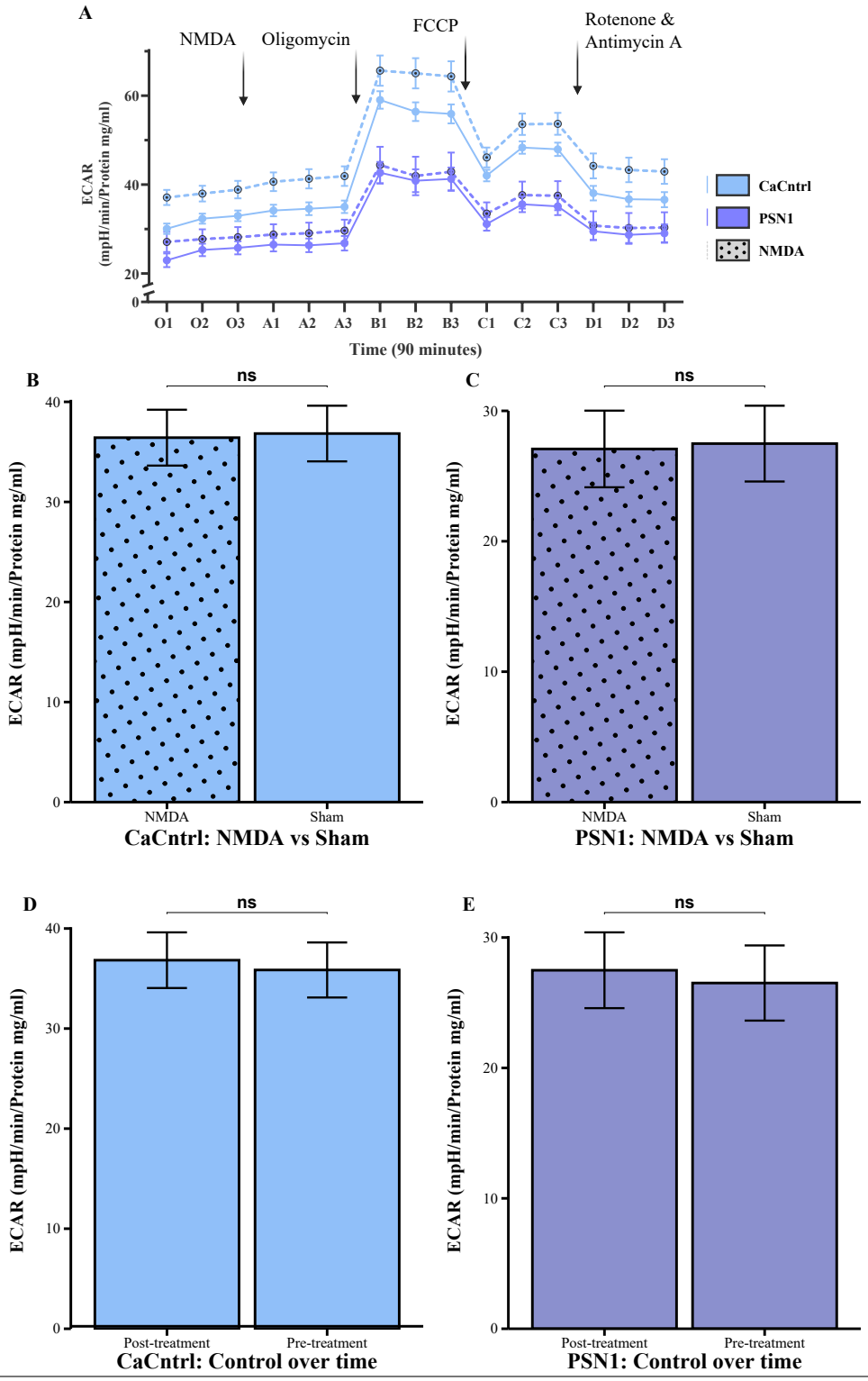

Figure 4.16: **Neither time nor acute NMDA exposure affect basal NPC ECAR. A**: Traces illustrating extracellular acidification rate (ECAR) over a period of 90 minutes in control (CaCntrl, in blue) and presenilin-mutant (PSN1, in purple) NPCs, either treated with 2 µM NMDA (NMDA, dotted boxes) or not (Control, plain box) at 15 distinct time points. Data are presented as mean±SEM. The additions of NDMA, oligomycin, FCCP, and rotenone and antimycin A between recordings are denoted with arrows. Bar charts (model-estimated marginal mean±SEM) show **B, C**: drug treatment and **D, E**: time differences in basal respiration.

4.2.8 NMDA treatment shows no effect on NPC metabolic measures

Despite detection of a mild effect of NMDA on basal respiration in paired analysis, no statistically significant differences induced by NMDA treatment were observed by unpaired analysis using a simplified linear mixed-effects model (Measure~Cell_line + Drug_treatment + (1|Experiment)) in standard basal respiration (cell line eddect -0.034ΔOCR, $p = 0.1480$; NMDA treatment -0.005ΔOCR, $p = 0.6972$; PSN1 NMDA $-$CaCntrl Control -0.040ΔOCR, p=0.1758; Fig. 4.17A), ATP-linked respiration (cell line effect -0.030ΔOCR, $p = 0.2336$; NMDA treatment -0.006ΔOCR, $p = 0.6291$; PSN1 NMDA$-$CaCntrl Control -0.035ΔOCR, $p = 0.2336$; Fig. 4.17B), maximal respiration (cell line effect -0.125ΔOCR, $p < 0.0001$; NMDA treatment $+0.100\Delta$OCR, p=0.6536; PSN1 NMDA$-$CaCntrl Control -0.115ΔOCR, p=0.0020; Fig. 4.18A), non-mitochondrial respiration (cell line effect -0.014ΔOCR, $p < 0.0001$; NMDA treatment $+0.005\Delta$OCR, $p = 0.8897$; PSN1 NMDA$-$CaCntrl Control -0.013ΔOCR, $p < 0.0093$; Fig. 4.18B), proton leak (cell line effect -0.006ΔOCR, $p = 0.0017$; NMDA treatment -0.000ΔOCR, $p = 0.8334$; PSN1 NMDA$-$CaCntrl Control -0.006ΔOCR, $p = 0.0252$; Fig. 4.19A), coupling efficiency (cell line effect $+0.007\Delta\%$, $p = 0.7623$; NMDA treatment $-0.040\Delta\%$, $p = 0.5452$; PSN1 NMDA$-$CaCntrl Control $-0.032\Delta\%$, $p = 0.7466$; Fig. 4.19B), spare respiratory capacity (cell line effect -0.089ΔOCR, $p < 0.0001$; NMDA treatment $+0.017\Delta$OCR, $p = 0.2480$; PSN1 NMDA$-$CaCntrl Control -0.071ΔOCR, $p = 0.0055$; Fig. 4.20A), basal ECAR (cell line effect -0.010ΔECAR, p=0.0579; NMDA treatment $+0.005\Delta$ECAR, $p = 0.3021$; PSN1 NMDA$-$CaCntrl Control -0.005ΔECAR, $p = 0.3021$; Fig. 4.20B), maximal ECAR (cell line effect -0.019ΔECAR, p=0.0002; NMDa treatment $+0.005\Delta$ECAR, p=0.2480; PSN1 NMDA$-$CaCntrl Control $+0.005\Delta$ECAR, p=0.1568; Fig. 4.21A), or glycolytic reserve (cell line effect -0.09ΔECAR, $p = 0.0212$; NMDA treatment $+0.001\Delta$ECAR, p=0.7695; PSN1 NMDA$-$CaCntrl Control -0.008ΔECAR, $p = 0.2053$; Fig. 4.21B) in either cell line.

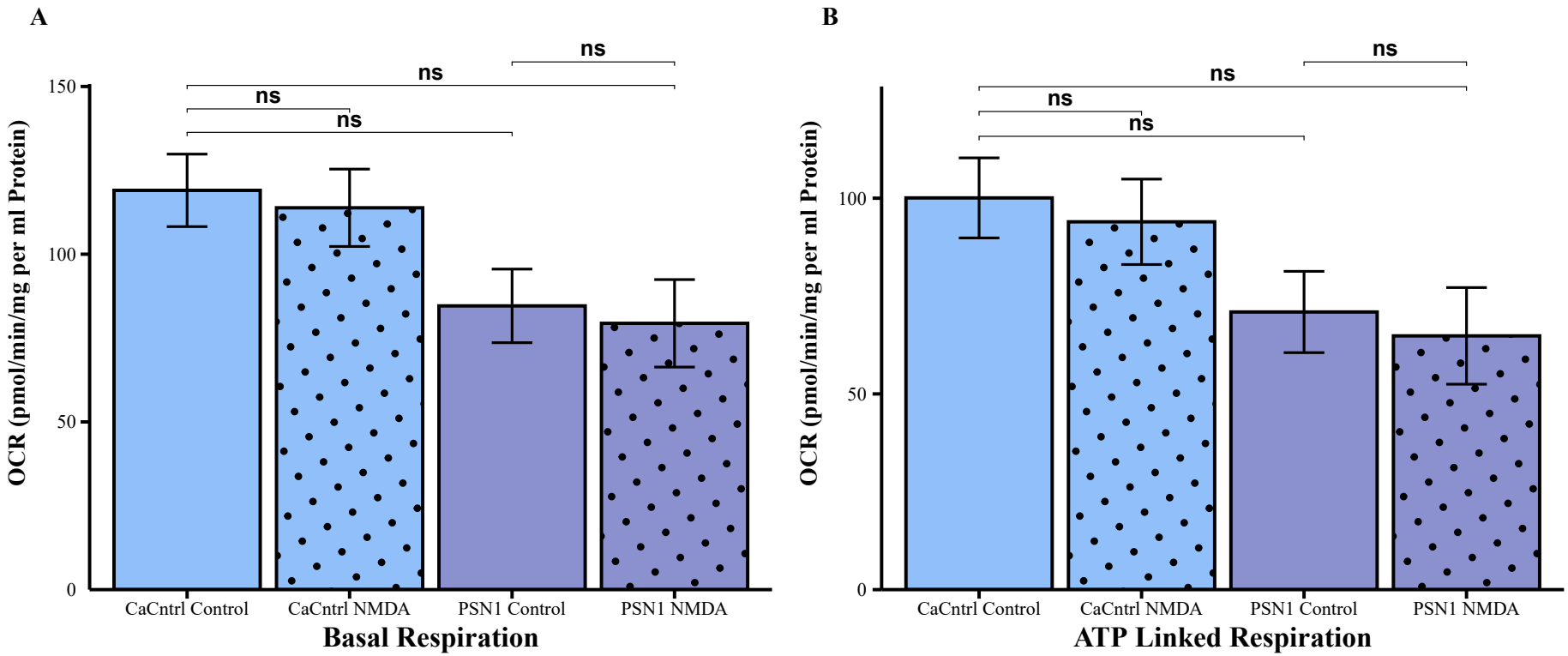

Figure 4.17: **Acute NMDA exposure has no effect on NPC Basal nor ATP-Linked Respiration in unpaired analysis.** Bar charts (model-estimated marginal mean±SEM) show cell line and drug treatment differences in **A**: basal and **B**: ATP-linked respiration in control (CaCntrl, in blue) and presenilin-mutant (PSN1, in purple) NPCs, either with 2 µM NMDA (NMDA, dotted boxes) or not (Control, plain box).

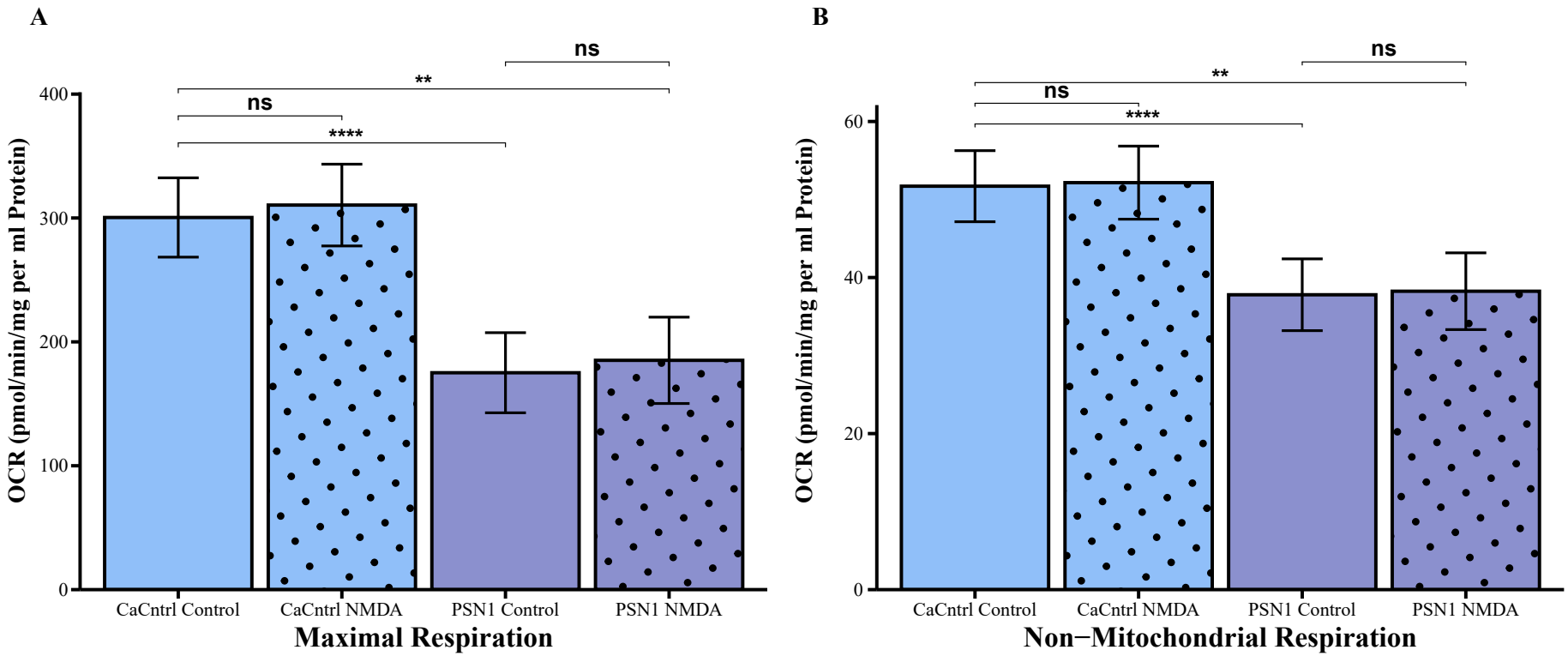

Figure 4.18: **Acute NMDA exposure has no effect on maximal or non-mitochondrial respiration in NPCs.** Bar charts (model-estimated marginal mean±SEM) show cell line and drug treatment differences in **A**: maximal and **B**: non-mitochondrial respiration in control (CaCntrl, in blue) and presenilin-mutant (PSN1, in purple) NPCs, either with 2 μM NMDA (NMDA, dotted boxes) or not (Control, plain box). ** and **** indicate $p < 0.01$ and $p < 0.0001$ respectively.

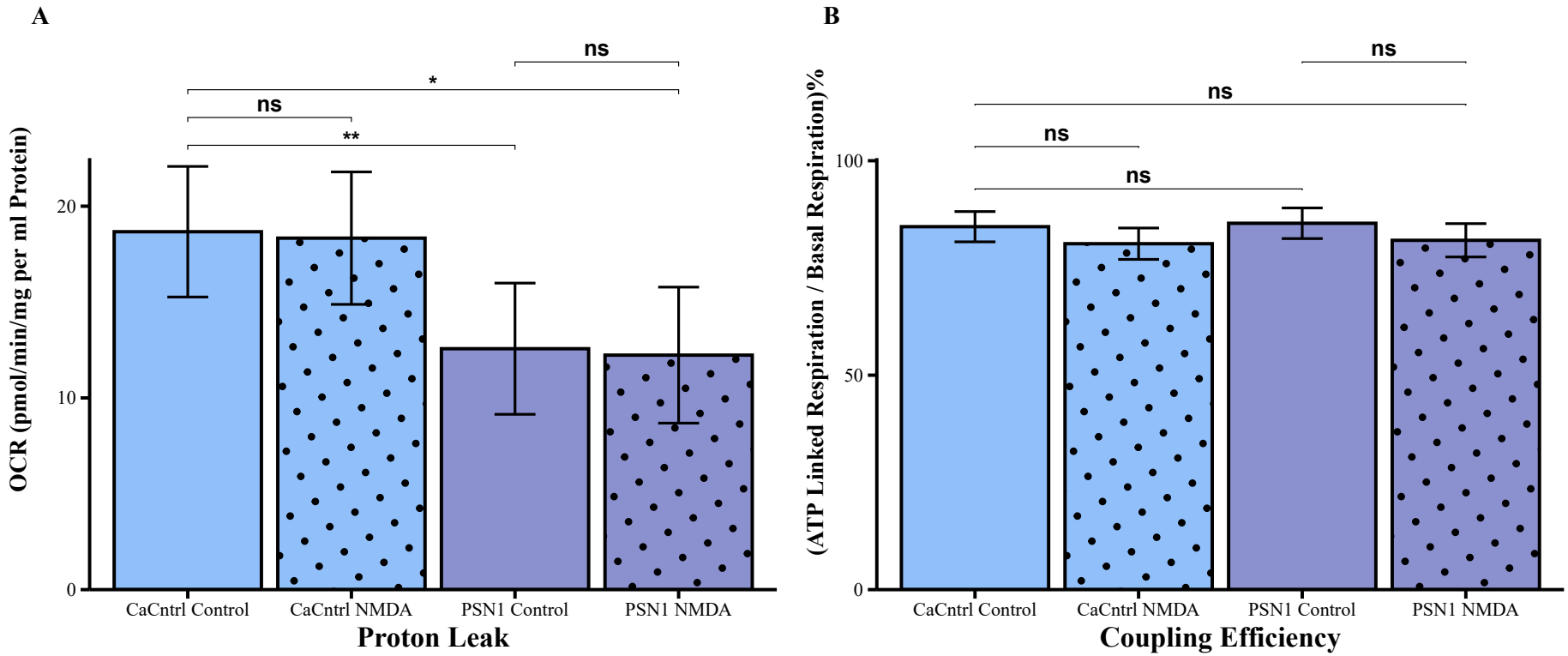

Figure 4.19: **Acute NMDA exposure has no effect on proton leak or coupling efficiency in NPCs.** Bar charts (model-estimated marginal mean±SEM) show cell line and drug treatment differences in **A**: proton leak and **B**: coupling efficiency in control (CaCntrl, in blue) and presenilin-mutant (PSN1, in purple) NPCs, either with 2 µM NMDA (NMDA, dotted boxes) or not (Control, plain box). * and ** indicate $p < 0.05$ and $p < 0.01$ respectively.

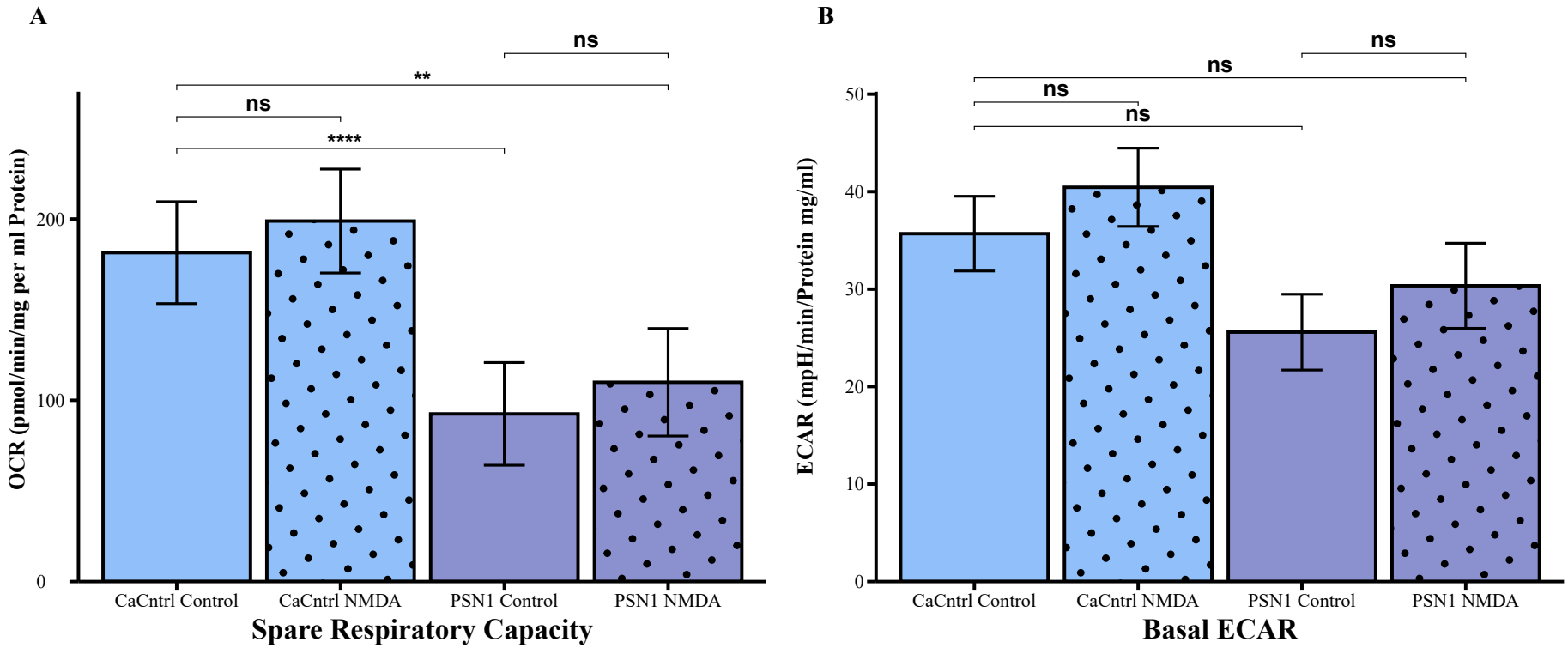

Figure 4.20: **Acute NMDA exposure has no effect on spare respiratory capacity or basal ECAR in NPCs.** Bar charts (model-estimated marginal mean±SEM) show cell line and drug treatment differences in **A**: spare respiratory capacity and **B**: basal ECAR in control (CaCntrl, in blue) and presenilin-mutant (PSN1, in purple) NPCs, either with 2 μM NMDA (NMDA, dotted boxes) or not (Control, plain box). * and *** indicate $p < 0.05$ and $p < 0.001$ respectively.

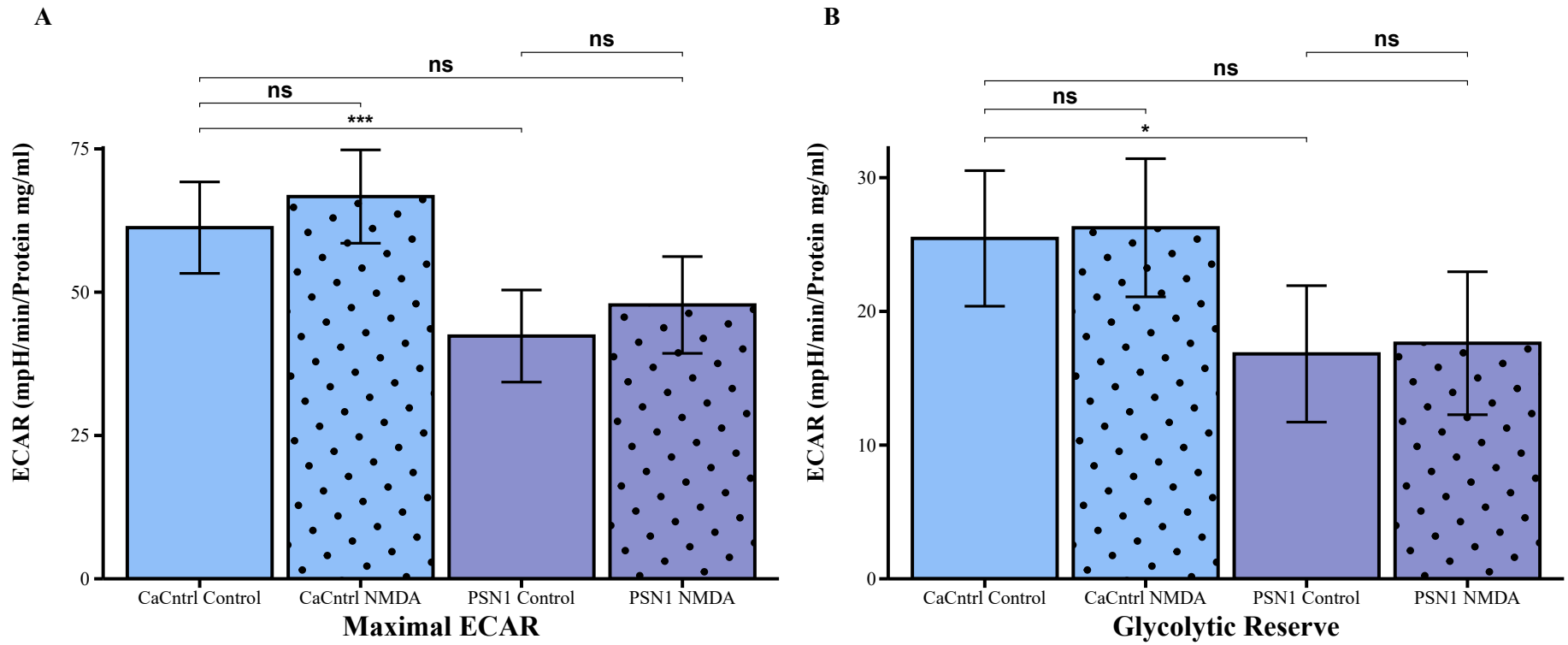

Figure 4.21: **Acute NMDA exposure has no effect on maximal ECAR or glycolytic reserve in NPCs.** Bar charts (model-estimated marginal mean±SEM) show cell line and drug treatment differences in **A**: maximal ECAR and **B**: glycolytic reserve in control (CaCntrl, in blue) and presenilin-mutant (PSN1, in purple) NPCs, either with 2 μM NMDA (NMDA, dotted boxes) or not (Control, plain box). * and *** indicate $p < 0.05$ and $p < 0.001$ respectively.

4.3 Discussion

PSEN1-mutant iPSC-derived cells exhibited a clear disturbance in calcium homeostasis accompanied by a suppressed metabolic phenotype. First, we observed that basal cytosolic calcium levels were significantly elevated in NPCs harbouring the $PSEN1_{M139V}$ mutation. This finding is consistent both with our own laboratory's previous observations, as well as with reports in the literature using the $PSEN1_{M146V}$-expressing 3xTG AD model, likewise leads to increased resting intracellular calcium (Kaar, Weir, and Rae 2024; Smith *et al.* 2005). Second, VGCC activity was augmented in PSN1 NPCs, whereas the duration of intracellular calcium transients was unchanged, indicating that there was no effect on calcium buffering and clearance. Despite this, the response amplitude (ΔF/F) to ionomycin stimulation did not differ between mutant and control lines, and there was no change in peak fluorescence, suggesting that total accessible calcium remained similar. The apparent discrepancy between higher basal intracellular calcium levels and unaltered peak amplitude and the magnitude of the evoked calcium responses(peak area under the curve) may reflect a maintained physiological upper limit to the transient paired with and increase in peak area that failed to reach statistical significance under our experimental conditions. The change in ΔF/F was explained by further investigation of the signal kinetics. There are a couple of plausible explanations for the faster calcium rise in PSN1 NPCs. Even though the effects of ionomycin are non-receptor-mediated, local microdomains of higher free ER Ca^{2+} can trigger adjacent IP_3Rs or RyRs in CICR, which, as discussed previously (section 1.2), is known to be heightened in AD models (Payne *et al.* 2013). If ER tubules are more closely apposed to the cytosol or plasma membrane, ionomycin-opened pores may empty more directly into cytosolic microdomains, speeding the rise in fluorescent signal. As noted in section 4.2.3, ionomycin is a relatively 'blunt' tool for estimating the release of intracellular calcium stores, since any measured signal invariably includes contaminating influx of extracellular Ca^{2+}. Although all experiments were performed in defined extracellular solutions (Table 2.10), we cannot quantify how much variability in our measurements arises from this external influx. Precisely assessing calcium levels within specific organellars requires the genetically-encoded calcium indicators (Olszakier *et al.* 2025), but such tools were not at the lab's disposal at the time.

In parallel with altered calcium handling, PSN1 NPCs displayed a suppressed bioenergetic profile in both Seahorse XF and Resipher assays. Basal and maximal respiration, as well as spare respiratory capacity, were all significantly reduced relative to controls. Coupling efficiency, however, remained unchanged, indicating that ATP-synthase function per se was not impaired. Notably, although we initially predicted that elevated $[Ca^{2+}]_i$ would stimulate mitochondrial dehydrogenases and thereby increase oxidative

metabolism, we in fact observed the opposite, suggesting a defect downstream of calcium uptake or an adaptive downregulation of respiratory capacity.

To probe whether reducing calcium flux might restore metabolic function, we pretreated cells with dantrolene, a RyR antagonist expected to diminish ER calcium release. Contrary to our initial assumption that dantrolene would further suppress metabolism, we found that it actually significantly increased both basal and maximal respiration in PSN1 and control lines (with the exception of proton leak, coupling efficiency, maximal ECAR, and glycolytic reserve, which were unaffected). Because proton leak was unchanged, it is unlikely that dantrolene acts *via* uncoupling at the inner mitochondrial membrane. Similarly, unchanged glycolytic parameters suggests that there was no compensatory shift toward glycolysis. Instead, these results imply that in the basal state PSN1 cells may experience mitochondrial calcium overload; by limiting ER calcium release, dantrolene may be alleviating this overload, thereby improving mitochondrial efficiency.

We also examined the effect of NMDAR activation on cellular respiration. Overall, NMDA had no significant impact on this facet of cellular function, except in paired analyses of immediate post-treatment oxygen consumption. Although subtle, this trend aligns with the hypothesis that excessive calcium influx through NMDARs could contribute to transient mitochondrial dysregulation. However, the effect was not robust, and further work, such as direct measurement of mitochondrial calcium uptake, will be required to substantiate the evidence for such a mechanism. If the effect we observed was real, similar to our results with dantrolene, it is the opposite what we initially predicted, with an NMDAR-mediated increase in $[Ca^{2+}]_i$ leading to a decrease in basal metabolism. This would align with the implication that the cells are already in a state of calcium overload prior to drug treatment.

Resipher real-time impedance measurements supported the proposal that the PSN1 cells displayed a suppressed metabolic phenotype compared to controls. The mutant line showed a steeper initial rise in oxygen consumption followed by an earlier decline compared to controls, indicating a significantly impaired ability to sustain elevated oxidative phosphorylation during the growth and expansion phase. This dynamic profile reinforces the static Seahorse data and highlights the functional consequence of presenilin-linked calcium dysregulation on bioenergetic resilience. However, to disentangle the potential contribution of PSEN1 protein dysfunction to mitotic capacity from differences in oxygen consumption between the two lines, additional experiments directly assessing proliferation would be appropriate, for example scratch wound-healing assays (Labovitz *et al.* 2026) or continuous in-incubator cell tracking using an IncuCyte

imaging system (Ahmad, Wood, and Scott 2022).

A methodological limitation that may have reduced the sensitivity of the Seahorse experiments should be noted. Specifically, we normalized Seahorse data to total protein content, the only quantification method available in our laboratory at the time. However, total protein measurements cannot account for any cell loss or death that occurs prior to, or during, the assay, with washing and pipetting steps introducing additional variability. Future studies should implement alternative normalization strategies, such as nuclear staining or cell counting, to improve accuracy (Yoo *et al.* 2024).

4.4 Conclusion

These results demonstrate that the M139V presenilin mutation perturbs calcium homeostasis in iPSC-derived neural progenitors, leading to a compromised respiratory phenotype that may be partially rescued by modulating ER calcium release. These findings validate insights derived previously from certain AD-animal models in a human context.

Preface to Chapter 5

Previous work that has been conducted seeking to understand the potential role of herpes simplex viruses in the aetiology of certain neurodegenerative diseases have used animal models or observational clinical data. As discussed in the general introduction (section 1.3.5), while these data offer significant correlative evidence for HSV's involvement in human AD induction they cannot proffer a solid causative link between the two. HSV's ability to interact and "hijack" innate neuronal trafficking systems is of particular interest in our lab. An initial planned component of this thesis work was the use of human cerebral organoids to study direct effects of HSV infection on human brain tissue. Due to unforeseen circumstances, this work could not be carried out. However, the following chapter is a systematic review that was conducted in the early stages of the project in order to compile the body of current knowledge that had found direct modulation of human neuronal trafficking components by HSV 1 or 2, and to also outline measurable variables in any future studies.

Chapter 5 was released as a preprint on medRxiv on January 09 2025:

Direct Evidence of alteration to the human neural intracellular trafficking system following exposure to HSV: A systematic Review of the Literature

Michael B. Vaughan, Dante J. Bellai & Mark G. Rae
doi: /10.1101/2025.01.09.25320268

5.1 Introduction

5.1.1 Rationale

Human herpes viruses are a collection of DNA viruses that are defined by their ability to remain dormant within host cells between periods of symptomatic infection (Cohen 2020; Davison *et al.* 2009). Herpes simplex viruses 1 and 2 (HSV-1, HSV-2) are estimated to infect 66.6% (0-49 years of age) and 13.2% (15-49 years of age) of the global population respectively (James *et al.* 2020).

Most commonly associated with the oral or genital lesions that occur during periods of active infections, both HSV subtypes can survive within sensory neurons for the lifetime of infected individuals (Fields, Knipe, and Howley 2007–). Following primary infection of the oral or genital mucosa, viral replicants undergo retrograde microtubule-associated transport along axons of the sensory ganglia innervating infected tissue (Antinone and Smith 2010; Hafezi *et al.* 2012). These neurons then either undergo productive lytic infection, establish a latent infection, or achieve some intermediate state between the two (Singh and Tscharke 2020). Lytic infection involves a well characterised process of viral replication-associated gene expression, while viral latency is a process of near total viral gene repression (Nicoll, Proença, and Efstathiou 2012; Whitley and Roizman 2001). In recent years there is growing recognition that viral reactivation, observed *via* the detection of viral shedding, occurs more commonly than mucosal symptom presentation (Ramchandani *et al.* 2016; Schiffer *et al.* 2014). Similarly, it is now appreciated that rather than the viral genome remaining "silent" within neurons during periods of latency, there are in fact repeated attempted reactivations that are quelled before active viral replication commences (Ma *et al.* 2014; Russell and Tscharke 2016). Such continuous activity begs the question; what effect does continual pathogen transcription, replication and suppression have on neurons?

While herpes simplex encephalitis is a recognised rare acute infection of the central nervous system (1 in 250000 - 500000 cases per year) that is primarily characterised by inflammation (Rohani *et al.* 2023; Whitley 2006), the pathology of chronic neurotropic infection with HSV is not well understood. The possible involvement of differing herpes viruses in the development of Alzheimer's disease (AD) is tentatively supported by recent findings, such as the presence of HSV in amyloid plaques (Wozniak, Mee, and Itzhaki 2009), the apparent neuroprotective effects of herpesviridae antivirals in reducing risk of dementia development (Lopatko Lindman *et al.* 2021; Tzeng *et al.* 2018), and associations between HSV-1 infection susceptibility and the AD risk factor allele APOE-ε4 (Bhattacharjee *et al.* 2008; Burgos *et al.* 2003; Linard *et al.* 2021). Multiple reviews and talks are available outlining the full evidence for and against this

Herpes-AD hypothesis (Itzhaki 2018, 2021; Wainberg *et al.* 2021).

Within our lab, the role of intracellular trafficking disruption in the aetiology of certain neurodegenerative conditions is of particular interest. Several well-known neurodegenerative diseases are caused by protein misfolding or genetic mutations affecting components of the vesicle trafficking system, such as microtubule integrity and endosome mobility (Lewis 2021)(Fig.5.1 A). For example, AD is characterised by the accumulation and aggregation of amyloid β (Aβ) and hyperphosphorylated tau proteins, Parkinson's disease (PD) is associated with the misfolding of alpha-synuclein, and Huntington's disease is caused by a genetic mutation leading to the expansion of CAG repeats in the HTT gene, resulting in the production of a misfolded huntingtin protein; Each misfolded protein disrupts intracellular trafficking, leading to neuronal cell death (Cookson 2009; Li and Li 2004; Selkoe and Hardy 2016). Conversely, amyotrophic lateral sclerosis, Charcot-Marie-Tooth Disease, and hereditary spastic paraplegia, are each caused by mutations in genes encoding trafficking components (TDP-43, RAB7A, and SPG4 respectively) (Blackstone, O'Kane, and Reid 2011; Burkhardt *et al.* 2013; Saveri *et al.* 2020). This is notable as the herpes viruses utilise the intracellular trafficking system for viral entry and egress (Döhner *et al.* 2002)(Fig.5.1b). This usage of intracellular components, paired with near ubiquitous population seropositivity and the lifelong nature of the infections, has led to the belief that repeated disruption of what will here be termed the human intraneuronal trafficking (HINT) system by HSV over several decades could instigate neurodegenerative processes.

5.1.2 Objectives

The primary objective of this systematic review of the literature was to investigate the known/confirmed effects of HSV on the HINT system. The secondary objective was to identify specific alterations in HINT components induced by HSV for future studies into the possible relation between viral infection and neurodegenerative diseases.

Given the human-specific nature of neurodegenerative diseases and the limitations of aetiological discovery in animal studies to date, we have focused exclusively on primary research assessing the intracellular trafficking system during and following HSV infection in human neuronal cells.

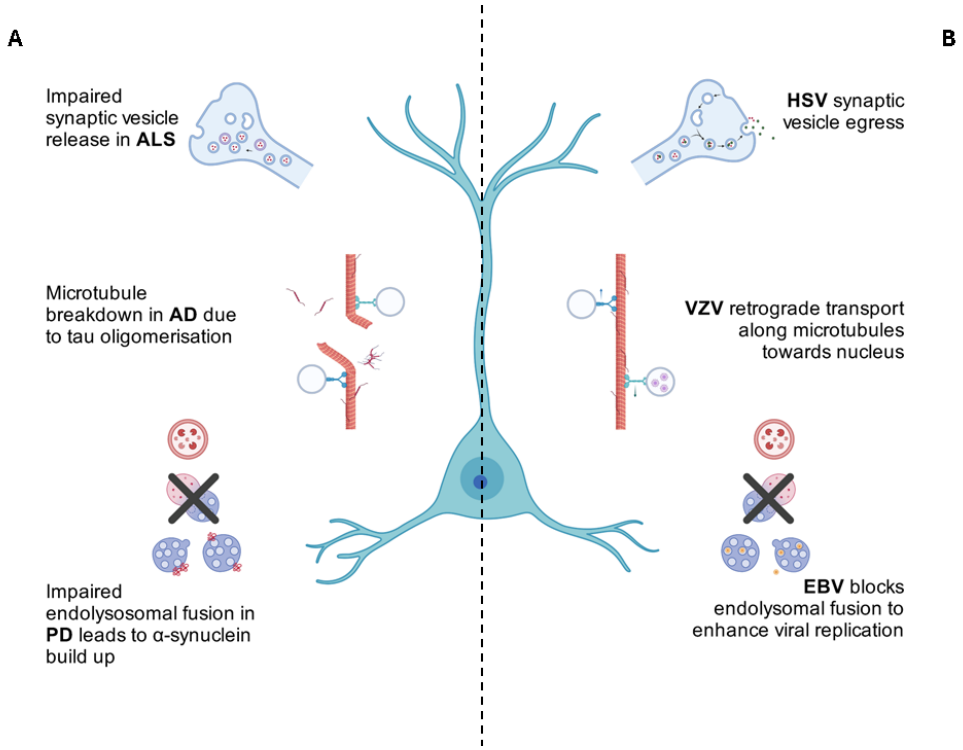

Figure 5.1: **HINT & Herpes:** *Commonly recognised intracellular trafficking elements that are disrupted by neurodegeneration (A) and herpes viruses infection (B). Neurodegenerative diseases referenced include amyotrophic lateral sclerosis (ALS), Alzheimer's disease (AD), and Parkinson's disease (PD), alongside herpes simplex virus (HSV), varicella–zoster virus (VZV), and Epstein–Barr virus (EBV).*

5.1.3 Research Question

Is there any evidence of alterations to the neural endosomal network of humans after exposure to HSV-1 and/or HSV-2 when compared to controls (unaffected cells)?

5.2 Methods

The search strategy was jointly designed by MBV and DJB and agreed upon with MGR. The search, selection of studies, and data extraction were performed independently by both MBV and DJB. Agreement on final report inclusion was achieved after review of the full-text articles that met eligibility criteria by both MBV and DJB. Final data synthesis and generation of the current manuscript was carried out by MBV and MGR in line with Preferred Reporting Items for Systematic Reviews and Meta-Analyses (PRISMA) 2020 guidelines (Page *et al.* 2021).

5.2.1 Search Strategy

The initial search strategy design for this study used the population, intervention, comparison and outcome (PICO) model(Thomas *et al.* 2019). As such, the PICO terms for this systematic review were as follows:

P: endosomal/intracellular trafficking network.
I: HSV1 and HSV2.
C: uninfected cells.
O: alteration of the intracellular/endosomal network.

The "O" term herein refers to modifications in the network's organellar systems, compared to normal, including an increase and/or decrease in the number of organelles, an increase and/or decrease in organellar signalling proteins, an increase and/or decrease in the speed at which organelles move within the cell, a change in the concentration of organelle contents, a difference in the permeability of organelle membrane or an enlargement and/or shrinking of the organelles in size. During search term testing, inclusion of C & O terms was overly limiting such that known reports relevant to the research question were missed. As such, the final searches only used P & I based terms.

The following search terms were used:

endosome*, trans-golgi network, endocyt*, transport vesicles, endoplasmic reticulum, golgi apparatus, lysosom*, transcytosis, exosom*, exocytos*, pinocytos*, rab gtp-binding proteins, rab, rab* AND herpes simplex, herpesvirus 1 human, herpesvirus 2, human, hsv.

For full search term descriptions and database listings see the supplementary information.

5.2.2 Eligibility Criteria

Search results were assessed for any mention of intracellular trafficking components and HSV-1 and/or HSV-2. Studies were excluded if they were not original primary research, were not yet peer-reviewed, unavailable in English or did not assess human neuronal cells (Table 5.1).

Table 5.1: **Search Eligibility Criteria.**

	Inclusion	**Exclusion**
Population	Primary or cultured human neuronal cells. Cell lines that can be reasonably considered neuronal due to origin or the presence of neuro-specific cellular components.	Non-neuronal human cells/tissues. Non-human cells/tissues.
Intervention	Studies specifically assessing HSV-1 and/or HSV-2 infection.	Studies assessing other herpes viruses, or non-herpetic viral infection.
Observations	Studies presenting primary data on intracellular trafficking components in response to or in the presence of HSV.	Studies presenting data on any other cellular component/system in response to HSV including intercellular trafficking/communication.
Publication type	Any report presenting original primary research data.	Review articles / experimental proposals / editorials / commentaries
Language	Studies published in English.	Studies not published in English.
Peer review	Studies published in a peer-reviewed journal.	Studies not published in a peer-reviewed journal, including preprints.

The Web of Science, Scopus and Medline databases, were searched on the 5th July 2021. This was repeated on the 28th of December 2021, the 10th of June 2023 and the 18th of January 2023 to assess any newly published reports. Using our broad search terms, 6292 records were initially identified (Fig.5.2). Following automated duplicate removal by EndNote software, and manual duplicate removal, 4185 reports were screened by title, then by abstract content. 48 articles were screened based on their full text. Additional eligible studies were located by assessing the bibliographies of reports that met final eligibility criteria during the systematic search.

To address the aims of this study, eligible reports were further screened based upon the presentation of observations/data of modification of the HINT system (described above "O search term") due to HSV1/2 herpes virus infection. Reports that focussed on viral binding sites, transport mechanisms, or the effects of cellular activity on viral particles

were excluded from our study.

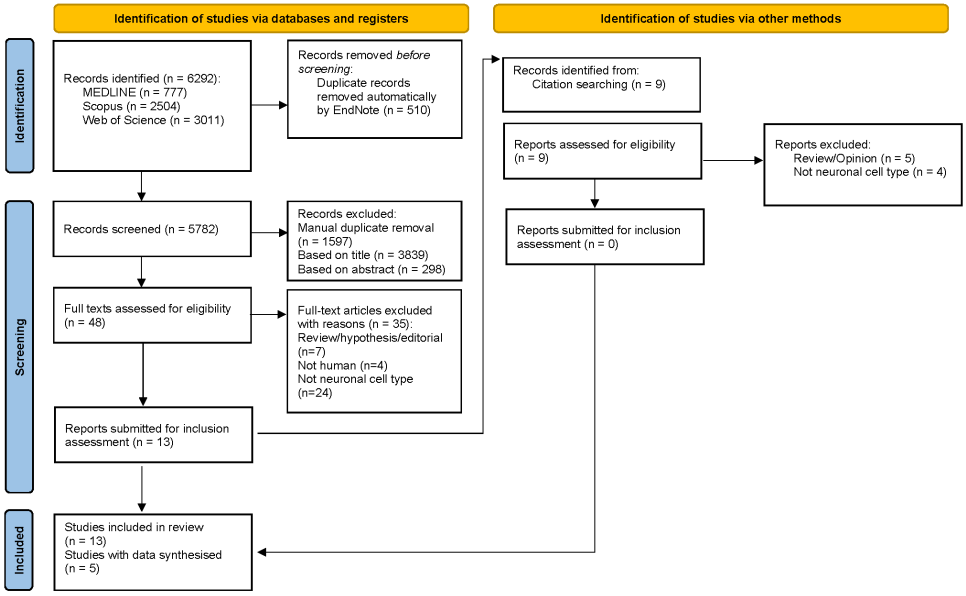

Figure 5.2: **Flow chart of screening, and criteria for inclusion and exclusion of articles**

5.3 Results and Discussion

Our database search produced 13 articles that met the eligibility criteria outlined in Table 5.3. Of these, only five presented observations/data on effects on HSV on HINT, and will be assessed separately in detail. Six of the remaining eligible reports came from contemporary work from two separate labs, both of which worked on understanding the mechanisms of HSV transport and assembly within axons (Holland *et al.* 1999),(Saksena *et al.* 2006),(Miranda-Saksena *et al.* 2009) and (Snyder, Wisner, and Johnson 2006),(Snyder, Polcicova, and Johnson 2008),(Wisner *et al.* 2011). Movaqar *et al.* (2021) described the effect of autophagic activity on viral proliferation(Movaqar *et al.* 2021), while Musarrat and colleagues (2021) only presented human cell data regarding viral binding proteins(Musarrat, Chouljenko, and Kousoulas 2021). It is notable that in all eligible reports, only HSV-1, not HSV-2 was studied. While these results are interesting in and of themselves, adding to the body of species-specific viral understanding, they do not provide actionable HINT data.

Table 5.3: **Summary of Studies Meeting Eligibility Criteria.**

Author (Year)	Title	Cell Type	Viral Strain	Key Findings
(Acuña-Hinrichsen *et al.* 2019)	Herpes Simplex Virus Type 1 Enhances Expression of the Synaptic Protein Arc for Its Own Benefit	H4 human neuroglioma, SH-SY5Y	HSV-1	•Neuronal *in vivo* and *in vitro* infection of HSV-1 significantly increased Arc protein levels dependent on active HSV-1 replication. •Silencing Arc protein decreased HSV-1 protein and viral progeny levels.
(Holland *et al.* 1999)	Anterograde transport of herpes simplex virus proteins in axons of peripheral human fetal neurons: an immunoelectron microscopy study	Foetal DRG	HSV-1 (CW1)	•Along the length of DRG axons nucleocapsid and tegument proteins frequently colocalized, but rarely associated with glycoproteins gB, gC, and gD. •No virus detected exiting from the mid-region of the axon. •Evidence of viral assembly in axon terminus following separate axonal transport of virus nucleocapsids and glycoproteins.
(Kristen *et al.* 2018)	The lysosome system is severely impaired in a cellular model of neurodegeneration induced by HSV-1 and oxidative stress	SK-N-MC human neuroblastoma cells, human wild-type APP695 (SKAPPwt), K670N/ M671L (SK-APPswe)	HSV-1 KOS 1.1	•HSV-1 infection increased expression of a set of oxidative stress-regulated genes. •HSV-1 infection and oxidative stress increased lysosomal load, reduced activity of separate lysosomal hydrolases, and impaired endocytosis-mediated degradation of epidermal growth factor receptor.
(Saksena *et al.* 2006)	Herpes simplex virus type 1 accumulation, envelopment, and exit in growth cones and varicosities in mid-distal regions of axons	Foetal DRG	HSV-1 (CW1), HSV-1 vUL37-GFP	•Enveloped and unenveloped capsids observed in axon varicosities and growth cones. •These are likely sites of HSV-1 envelopment.
(Miranda-Saksena *et al.* 2009)	Herpes Simplex Virus Utilizes the Large Secretory Vesicle Pathway for Anterograde Transport of Tegument and Envelope Proteins and for Viral Exocytosis from Growth Cones of Human Fetal Axons	Foetal DRG	HSV-1 (CW1), HSV-1 vUL37-GFP	•Viral tegument and envelope proteins transported independently of viral capsids within the axon. •Two types of transport vesicles utilised: tubulovesicular membrane structures and large dense-cored vesicles. •Both transport vesicle types derived from the Golgi network.
(Movaqar *et al.* 2021)	The propagation of HSV-1 in high autophagic activity	Be2M17 neuroblastoma cells	HSV-1 KOS	•Beclin-1 induction of autophagy pre- and post- HSV-1 infection reduced viral load over 48 hours in trialled cell lines. •3-methyladenine inhibition of autophagy increased viral load over 48 hours in trialled cell lines. •Neuroblastoma cells evoked a greater increase in autophagosome formation following Beclin-1 transfection than HeLa cells.

Author (Year)	Title	Cell Type	Viral Strain	Key Findings
(Musarrat, Chouljenko, and Kousoulas 2021)	Cellular and Viral Determinants of Herpes Simplex Virus 1 Entry and Intracellular Transport toward the Nuclei of Infected Cells	SK-N-SH neuroblastoma cell	HSV-1 McKrae-GFP	•The Akt pathway was essential for HSV-1 entry to Vero and neuroblastoma cells. •HSV-1 infection causes phosphorylation of the intermediate dynein chain 1B via an Akt/PKC-independent pathway. •Viral capsid protein VP5 interacts directly with the EB1 cofactor and the dynactins, DCTN1/p150 and DCTN4/p62.
(Salgado *et al.* 2023)	Herpes Simplex Virus Type 1 Induces AD-like Neurodegeneration Markers in Human Progenitor and Differentiated ReNcell VM Cells	ReNcell VM neural stem cell, Differentiated ReNcell	HSV-1 KOS1.1	•The ReNcell VM human neural stem cell line can be differentiated into neurons, astrocytes and oligodendrocytes. •Differentiated and undifferentiated ReNcell VM cells are susceptible to HSV-1 infection and are viable model systems for the *in vitro* study of neuro-viral infection. •HSV-1 infection induces an Alzheimer's disease-like phenotype in differentiated and undifferentiated ReNcell VM cells.
(Santana *et al.* 2012)	Herpes simplex virus type I induces the accumulation of intracellular beta-amyloid in autophagic compartments and the inhibition of the non-amyloidogenic pathway in human neuroblastoma cells	SK-N-MC human neuroblastoma cell, APP-SK-N-MC, (SK-LC3)	HSV-1 KOS1.1	•HSV-1 infection induced intracellular accumulation of amyloidβ while inhibiting amyloidβ secretion. •HSV-1 specifically induced amyloidβ accumulation within autophagic vesicles, but fusion of these vesicles with lysosomes was impaired. •Viral reproduction not required to induce amyloidβ accumulation.
(Snyder, Wisner, and Johnson 2006)	Herpes simplex virus capsids are transported in neuronal axons without an envelope containing the viral glycoproteins	SK-N-SH human neuroblastomal cells	HSV-1 F	•HSV glycoproteins and capsids occured in separate transport structures within observed axons. •Axonal transport of viral glycoproteins occured in absence of capsids.
(Snyder, Polcicova, and Johnson 2008)	Herpes Simplex Virus gE/gI and US9 Proteins Promote Transport of both Capsids and Virion Glycoproteins in Neuronal Axons	SK-N-SH human neuroblastomal cells	HSV-1 F	•Removal of gE, gI, or US9 from HSV greatly reduced transport of both viral capsids and glycoproteins (gB and gD) in axons. •Capsid transport more sensitive to loss of either gE/gI or US9 than glycoprotein transport.
(Viloria and Garcia 1976)	Human herpes simplex encephalitis (cellular events)	Autopsied neural tissue	HSV-1	•Herpes encephalitis diagnosis of patient confirmed by morphologic studies and viral isolation. •Herpetic lesions confined to central nervous system, primarily the temporal cortex, hippocampi and dentate nucleus. •Herpes virus induced disruption of nuclear membrane and dilation of perinuclear cisternae, replacing endoplasmic reticular and Golgi apparatus membranes.

Author (Year)	Title	Cell Type	Viral Strain	Key Findings
(Wisner *et al.* 2011)	Anterograde Transport of Herpes Simplex Virus Capsids in Neurons by both Separate and Married Mechanisms	SK-N-SH neuroblastoma cells	HSV-1 YK614	•Both enveloped and individual HSV particles undergo anterograde transport within axons. •Culture system selection and imaging method affect ratio of HSV capsids and enveloped particles during anterograde transport observation.

5.3.1 HINT Alteration

The five final reports presenting relevant HINT data (see Table 5.5) consisted of three papers from the group of Aldudo & Bullido which directly investigated the link between HSV and AD(Kristen *et al.* 2018; Salgado *et al.* 2023; Santana *et al.* 2012), one independent study investigating the role of HSV-1 in neurodegeneration(Acuña-Hinrichsen *et al.* 2019), and one clinical report of herpes simplex encephalitis(Viloria and Garcia 1976).

5.3.2 Lysosome

The collected works of Kristen, Santana and Salgado, coming from the Alduo & Bullido group, all report the effects of HSV-1 on lysosomal health: Specifically, lysosomal function, lysosomal fusion, and lysosomal load.

In 2012 Santana *et al.*(Santana *et al.* 2012) reported increased microtubule-associated protein 1 light chain 3 (LC3)-positive autophagic vesicles within neuroblastoma cell lines in response to HSV-1 infection, with Aβ observed to co-localize with these autophagic vesicles following infection. The effects were HSV-1 specific as they were not replicated following neuroblastoma infection with a Sindbis viral construct. Despite the assumed final merging of autophagic vesicles with lysosomes, no co-localization of Aβ nor LC3 was observed. They concluded that the reduced proteolytic cleavage of intracellular Aβ occurs due to reduced maturation of autophagic vesicles, and reduced fusion with lysosomes.

Using microarray gene expression analysis on oxidative stress regulated genes in HSV-1 infected neuroblastoma, Kristen *et al.* (2018)(Kristen *et al.* 2018) revealed five significantly enriched genes linked to lysosomal system function; Cathepsin F (CTSF), lipase A (LIPA); ATPase H^+ transporting accessory protein 1 (ATP6AP1); Niemann-Pick disease, type C1 (NPC1); and lysosomal-associated membrane protein 2 (LAMP2). Both HSV-1 infection and acute oxidative stress produced an increase in lysosomal load, defined by increased lysosomotropic probe fluorescence, reflecting acidic lysosomal compartment signal. Lysosomal load increase typically results from either increased intake of substrates or diminished degradation within the lysosome. HSV-1 infection decreased lysosomal cathespin activity, suggesting that the increased load was due to reduced functionality. Additionally, HSV-1 infection impaired receptor-mediated lysosomal degradation of epidermal growth factor receptor (EGFR). While they concluded that infection induced a great strain on the lysosomal system, they believed that the lysosomal defects reported in their cell model of infection were not directly related to altered lysosomal gene expression. The upregulation of lysosomal genes could be a

protective response to counteract impaired lysosomal function.

Finally, Salgado *et al.* (2023)(Salgado *et al.* 2023) assessed differences in HSV-1 infection in cells of differing differentiation state using their ReNcell VM cell model. Again, HSV-1 infection increased the number of LC3-positive autophagic vesicles in both differentiated and progenitor ReNcell VM cells, as well as decreasing lysosomal cathepsin activity in both cell types. Notably, in contrast to the increase in lysosomal load reported in the neuroblastoma model by Kristen *et al.*, progenitor ReNcell VM cells displayed a reduction in LysoTracker Red fluorescence following HSV-1 infection, whereas differentiated cells showed no significant alteration.

Lysosomal dysfunction is proposed to be a key aetiological factor in the pathogenesis of several neurodegenerative diseases such as AD and PD, specifically with regard to impaired clearance of disruptive proteins. The accumulation of autophagic vesicles and impaired degradation pathways observed in HSV-1-infected cells closely mirrors the lysosomal deficits seen in these conditions (Navarro-Romero, Montpeyó, and Martinez-Vicente 2020; Zhang *et al.* 2022). For example, cells harbouring AD-related mutations in presenilin 2 (PSN2) expressed increased numbers of LC3-positive autophagosomes, with reduced autophagosome-lysosome fusion (Fedeli *et al.* 2019).

Neural progenitor cell (NPC) and mature neurons respond differently to viral infections due to distinct expression profiles of antiviral genes and innate immune responses (Zhang *et al.* 2018). NPCs often exhibit higher levels of autophagic activity compared to differentiated cells in order to facilitate expansive proliferation (Paik *et al.* 2009; Renault *et al.* 2009) and the cytoskeletal remodelling that occurs during differentiation (Ha *et al.* 2019; Vázquez *et al.* 2012).

5.3.3 ER and Golgi

Although the case study of Viloria & Garcia (Viloria and Garcia 1976) is very obviously an acute infection, it did meet all of the inclusion criteria for our study. The main observation of interest from this paper that we extracted is the complete ablation and replacement of the ER and Golgi apparatus following HSV-1.

Corroborating literature exist describing ER and Golgi remodelling by HSV-1 in other cell models (Lv *et al.* 2019). For example, infected Vero cells showed temporary ER enlargement 12 hours post infection, which returned to normal after a further 4 hours (Sutter *et al.* 2012). In the same cells, prior to fragmentation, Golgi membranes signifi-

cantly enlarged at 9, 12 and 16 hours post-infection (Sutter *et al.* 2012). Infected HEp-2 cells showed ER membrane concentration around the nuclear rim (Maeda *et al.* 2017). In these same cell lines (but notably not in human 143TK-cells), the Golgi apparatus was fragmented and dispersed throughout the cytosol 8 to 12 hours post-infection (Campadelli *et al.* 1993).

It is commonly understood that the ER and Golgi are involved in HSV viron assembly within the cell, often through the provision of necessary membrane components (Albecka *et al.* 2016; Poliquin, Levine, and Shore 1985; Wild *et al.* 2018). Disruption of ER proteostasis by physiological/environmental insults leads to an accumulation of misfolded proteins, which is an ER stress response. The highly conserved unfolded protein response (UPR) can detect such ER stress, and attempt to correct it by increasing the expression of genes that regulate ER folding and degradation (Walter and Ron 2011). HSV-1, as well as many other viruses, have evolved to disable UPR during infection (Johnston and McCormick 2019). HSV-1 does so by specifically inhibiting UPR *via* the recruitment of protein phosphatase 1 to dephosphorylate eIF2α, thereby blocking protein kinase R-like ER kinase (PERK) stress signal transduction (Cheng, Feng, and He 2005; He, Gross, and Roizman 1997). Impaired UPR leads to unchecked protein synthesis and expansion of the ER membrane to compensate (Borgese, Francolini, and Snapp 2006; Schuck *et al.* 2009).

5.3.4 ARC Protein

Activity-regulated cytoskeleton-associated protein (ARC) is the only neuron-specific element to appear in these results. Rather than being an active trafficking component, ARC is a hub protein that regulates trafficking components essential for neuronal plasticity(Li *et al.* 2005). Most notably with regard to AD research, ARC binds directly to presenilin 1 (PSN1), the primary component of the γ-secretase complex (Myrum *et al.* 2015; Wu *et al.* 2011) which is responsible for cleaving full length amyloid precursor protein into Aβ fragments (Nelson *et al.* 2010).

Acuña-Hinrichsen *et al.* (2019)(Acuña-Hinrichsen *et al.* 2019) investigated whether recurrent HSV-1 viral reactivations at the neuronal level caused neuronal damage/dysfunction or specifically impacted upon synaptic plasticity. They observed that HSV-1-infected mouse brains, primary mouse neurons, H4 neuroglioma cells and neuronally-differentiated SH-SY5Y cells all showed upregulated ARC mRNA expression. Interestingly, within human cells, ARC protein levels increased during the eighth hour of infection, whereas expression in mouse cells had increased rapidly by hour two. In both species the effect

was only transitory.

Within the H4 neuroglioma cells, even though ARC plays a role in α-amino-3-hydroxy-5-methyl-4-isoxazolepropionic acid receptor (AMPAR) internalization under basal conditions, during HSV-1 infection, AMPARs are redistributed in an ARC-independent manner. Results from mouse cells demonstrated the requirement for active viral replication to induce a sustained increase in ARC levels. Further, ARC distributed in a similar pattern to the Golgi marker GM130, strongly suggesting that ARC is located at the Golgi apparatus during infections, and that ARC protein plays a crucial role in the production of HSV-1 viral progeny.

Further, with regard to HSV-1 mediated effects on ARC, Bergstöm *et al.,* (2021) observed a reduction of ARC mRNA expression in human iPSC-derived cortical neurons 48 hours post-infection (Bergström *et al.* 2021). They specifically discussed the study of Acuña-Hinrichsen *et al.,* (2019)(Acuña-Hinrichsen *et al.* 2019), but only the data related to primary mouse cortical neurons, and cited experimental design/ species differences as the possible cause for the discrepancy between their results. However, following a review of the data from both papers, we suggest that the most likely reason for their incongruent results was time point selection, as Acuña-Hinrichsen *et al.,* (2019) present peak ARC mRNA expression at eight hours post-infection followed by decline, whereas Bergstöm *et al.,* (2021) showed only decreased expression at 48 hours. Therefore, there may have been a post-HSV-1 increase in ARC mRNA expression that was missed, followed by a decline to sub-basal levels.

Table 5.5: **Direct Evidence of HSV alteration of HINT System.**

Author (Year)	Cell Type	Viral Strain	Viral Dosage	Infection Period (hours)	Post Exposure Cultivation	HINT Component	Alteration	Viral Lifecycle stage
(Acuña-Hinrichsen *et al.* 2019)	H4 neuroglioma SH-SY5Y	HSV-1 F	10 pfu/cell	1	1, 4, 8, 24 hrs	ARC Protein	Increased	Likely due to active replication
(Kristen *et al.* 2018)	SK-N-MC neuroblastoma SKAPPwt SK-APPswe	HSV-1 KOS 1.1	10 pfu/cell	1	18 hrs	Lysosomal Load Lysosomal Function	Increased Decreased	Prior to active replication
(Salgado *et al.* 2023)	ReNcell VM neural stem cell	HSV-1 KOS1.1	1, 3 pfu/cell	1	3, 5, 18 hrs	Tau Protein Lysosomal Load Lysosomal Function	Phosphorylated Decreased Decreased	Early but non confirmed
	Differentiated ReNcell VM					Tau Protein Lysosomal Load Lysosomal Function	Phosphorylated Unchanged Decreased	
(Santana *et al.* 2012)	SK-N-MC neuroblastoma APP-SK-N-MC SK-LC3	HSV-1 KOS1.1	0.1, 1 pfu/cell	1	48 hrs	Autophagosome-Lysosome Fusion	Decreased	Not defined here
(Viloria and Garcia 1976)	Autopsied neural tissue	HSV-1	$10^{2.2}$ $TCID_{50}$	Patient symptomatic for minimum 19 days		Endoplasmic Reticulum & Golgi	Abolished	Fatal infection

5.4 Conclusion

Due to the specific nature of the original hypothesis, it is perhaps not too surprising that the majority of final synthesised results (Table 5.5) focus upon investigating the role of HSV in neurodegeneration, mainly AD. What is surprising is the sheer dearth of research investigating the effects of HSV-1 infection on human neuronal tissue as it is well known that HSV activity differs between species, cell type, and modality. Even with the limited number of reports presented here, we observed species- and cell type- specific differences in response to HSV-1 infection, a finding that underscores the critical need for cell type- and species-specific research rather than extrapolating from cell line or animal study data.

This systematic review highlights the significant gaps in our understanding of the effects of HSV infection on human neuronal cells, particularly regarding the intracellular trafficking system. Despite the extensive history of research on HSV-1, there is insufficient primary evidence detailing its specific impacts on the neural endosomal network and intracellular trafficking in human neurons. However, the advent and continuous improvement of iPSC technologies provides the opportunity to bridge these knowledge gaps (Takahashi *et al.* 2016). iPSCs can be differentiated into various neural cell types, allowing for more accurate and relevant *in vitro* models of human neurobiology for use in future viral research.

None of the studies discussed herein adequately contributed to the exploration of chronic viral infection and repeated viral reactivation and their roles in neurodegeneration. ARC level increases were likely due to initial active replication, lysosomal/autophagosomal disruptions occurred in early infection or initially prior to active replication, and ER and Golgi disruption was only directly observed in a fatal case of encephalitis. If the hypothesis that long term sub-clinical non-cytotoxic reactivation of HSV can instigate neurodegenerative disease processes is to be maintained and further posited, new specifically designed experiments need to be conducted.

While current evidence points to significant effects of HSV-1 on neuronal intracellular trafficking systems, primary evidence is still lacking in detail and scope. Findings from our review advocate for increased utilization of cell- and species-specific models to establish more stable foundations for hypotheses regarding HSV involvement in neurodegeneration and brain ageing.

5.4.1 Limitations

This systematic review has several limitations that should be considered when interpreting the findings. Firstly, the limitation of investigating only studies written in English may have constrained the total number of studies assessed, and introduced a potential bias by excluding relevant research published in other languages, leading to an incomplete representation of the existing research. Secondly, the heterogeneity of studies included in this review posed challenges for the final synthesis of results and hindered a robust comparison of study quality. This possible variability in experimental rigour could have influenced the overall findings and the strength of the conclusions drawn.

The most notable limitation of this study is the narrow scope of the findings, due to the limited number of eligible studies. Although the initial research question was highly specific, generating truly comprehensive search terms proved challenging given the broad range of components that can be considered part of the HINT system. For instance, a publication that was later found to have relevant cell data (Bergström *et al.* 2021) was not discovered during the systematic search, likely because the components were reported in the context of 'neuronal plasticity' rather than 'intracellular transport'. However, one must note, while the final number of studies presented was small, a large number of studies were screened but ultimately deemed ineligible.

Lastly, no standard risk of bias assessment could be conducted due to the small number of final results, the lack of applicable metrics within those results, and the heterogenous mix of study designs.

6.1 Overview of Research Findings

In this thesis, we have investigated the utility of novel stem-cell based technologies for AD research. Historically, due to the dearth of living human tissue available for research, in addition to the ethical issues surrounding its acquisition (Carlos *et al.* 2019), AD aetiological studies had traditionally relied on the use of animal models. However, the inability of these models to fully recapitulate the entirety of AD associated pathologies, highlighted the role of species-specific differences, at least partly, in the poor translational success of preclinical findings (Banik *et al.* 2015; Drummond and Wisniewski 2017). With the advent of iPSC technology, viable human material became available to the field at large (Cerneckis, Cai, and Shi 2024). Using both 2D and 3D neural differentiation methods, we focussed on the ability of these culture systems to validate and extend animal model discoveries in human cell and tissues.

The hippocampus, is a central region involved in memory, and a major site of adult neurogenesis within the mammalian brain (Abbott and Nigussie 2020; Poo *et al.* 2016). During the early stages of AD, the hippocampus undergoes rapid loss of tissue, tauopathy, and amyloid deposition (Ball *et al.* 1985; Rao *et al.* 2022; Reitz *et al.* 2009). Prior work, in our lab and others, has shown disrupted calcium handling in hippocampal neurons of mice carrying EOFAD-associated PSEN1 mutations (Chakroborty *et al.* 2009; Goussakov, Miller, and Stutzmann 2010; Kaar 2019; Kaar, Weir, and Rae 2024). To translate these findings into a human context, we started generating human-derived neural cells and tissue from iPSCs. NPCs were produced from healthy control, and $PSEN1_{M139V}$-mutant iPSCs. These NPCs expressed expected protein markers, adopted normal morphology, and were amenable to classic calcium imaging assays.

Next, we devised a novel differentiation protocol to derive DG-specific neurons. By first expanding NPCs in a monolayer format, cryopreserving them, and then guiding their maturation, our method shortened the minimum culture period of an experiment to 28 days. In contrast, previous approaches relied on 3D neurosphere formation and uninterrupted differentiation from iPSCs to mature neurons requiring at least 60 days in culture for an experiment (Yu *et al.* 2014). DGNs produced with our protocol exhibited mature physiological behaviour and expression of the DG marker PROX1.

During my undergraduate research thesis, we characterised disrupted calcium handling in hippocampal brain slices from 3xTG mice, corroborating results seen in 2D primary hippocampal cultures (Vaughan *et al.* 2018). To again translate these findings into a

human model and possibly reduce animal use, we generated cerebroids from iPSCs. These cerebroids expressed expected neural markers, maintained viable tissue architecture, and supported slicing and bulk calcium-dye loading, yielding detectable calcium signals. However, the variable slice anatomy and immature cytoarchitecture limited assay reproducibility of low-resolution imaging and required additional *post-hoc* cell type confirmation. In more recent years, studies have been published overcoming these issues, by using iPSCs lines containing genetically-encoded calcium sensor proteins (Oliva *et al.* 2024), applying dye imaging techniques to more mature ALI-CO cultures (Tang *et al.* 2023), or by substituting calcium imaging with direct electrophysiological recordings using multi-electrode arrays (Sharf *et al.* 2022).

Having established NPC cultures as a viable experimental material, we went on to compare physiological behaviours between a patient-derived $PSEN1_{M139V}$-mutant line, and a healthy control. As had been seen previously in primary hippocampal cultures, and slices, from 3xTG mice (Kaar 2019; Vaughan *et al.* 2018), PSEN1-mutant cells had higher basal levels of cytosolic calcium compared to controls. This phenotype is often attributed to impaired presenilin-mediated passive Ca^{2+} leak from the ER, resulting in ER Ca^{2+} overload and enhanced cytosolic Ca^{2+} elevations following activation of release pathways (Bandara, Malmersjö, and Meyer 2013; Tu *et al.* 2006). The increased calcium flux in response to elevated K^{+} and ionomycin also suggest alterations in calcium handling. With a sensitisation towards primed excitatory states, and possible eventual excitotoxic cell death (Guo *et al.* 1999). Observing this alteration in human progenitor cells reinforces the knowledge that AD pathology likely starts long behaviour clinical presentation.

Moving on from the calcium hypotheses of AD we investigated the effect of the $PSEN1_{M139V}$-mutation on NPC bioenergetics. We found a global suppression of respiratory and glycolytic measures in $PSEN1_{M139V}$-mutant NPCs. The strength of this suppression is interesting as while 3xTG mouse neurons have deficits in mitochondrial structure, density and mobility (Cavendish *et al.* 2019), presenilin-deficient animal neurons and astrocytes display unaltered mitochondrial phenotypes (Contino *et al.* 2021). The presence, severity, and direction of the metabolic consequences of presenilin disruption appear to be strongly mutation-specific (Han *et al.* 2021). When we assessed the effect intracellular calcium reduction *via* dantrolene application, we were surprised to see an increase in bioenergetic measures (primarily respiratory, not glycolytic), as opposed to the predicted decrease in metabolic activity. While others have used end-point OCR measurements to assess metabolic activity, we are some of the first to present continual monitoring of NPCs within a stable incubator system. Alongside corroborating the results of the Seahorse assays, we observed a temporal-behavioural

difference between $PSEN1_{M139V}$-mutant and healthy control NPCs.

In the late-2010's interest in the role of HSV in AD re-emerged in the literature (Chen *et al.* 2018; Itzhaki *et al.* 2016; Tzeng *et al.* 2018), we sought to assess the available human specific data pertaining to HSV and the HINT system. The endolysosomal hypothesis presented a compelling mechanism for viral interaction with AD pathology, outside of acute immune events. Our systematic review found a limited collection of human-specific evidence for HSV disruption of the HINT system, but was able to highlight the cell type-, and species- specific nature of viral interactions. We found lysosomal overloading, ER and golgi breakdown, activity-regulated cytoskeleton-associated protein (ARC) mRNA expression as potential metrics of HINT disruption by HSV for future studies.

BIBLIOGRAPHY

[1] Abbott, L. C. and Nigussie, F. -"Adult Neurogenesis in the Mammalian Dentate Gyrus". *Anatomia, Histologia, Embryologia* 49.1 (Jan. 2020), pp. 3–16. ISSN: 1439-0264.

[2] Acuña-Hinrichsen, F., Muñoz, M., Hott, M., Martin, C., Mancilla, E., Salazar, P., Leyton, L., Zambrano, A., Concha, M. I., Burgos, P. V., and Otth, C. -"Herpes Simplex Virus Type 1 Enhances Expression of the Synaptic Protein Arc for Its Own Benefit". *Frontiers in Cellular Neuroscience* 12 (Jan. 2019), p. 505. ISSN: 1662-5102.

[3] ADAPT Research Group. -"Naproxen and Celecoxib Do Not Prevent AD in Early Results from a Randomized Controlled Trial". *Neurology* 68.21 (May 2007), pp. 1800–1808.

[4] Adlakha, Y. K. -"Human 3D Brain Organoids: Steering the Demolecularization of Brain and Neurological Diseases". *Cell Death Discovery* 9.1 (July 2023), p. 221. ISSN: 2058-7716.

[5] Adlimoghaddam, A., Fontaine, K. M., and Albensi, B. C. -"Age- and Sex-Associated Alterations in Hypothalamic Mitochondrial Bioenergetics and Inflammatory-Associated Signaling in the 3xTg Mouse Model of Alzheimer's Disease". *Biology of Sex Differences* 15.1 (Nov. 2024), p. 95. ISSN: 2042-6410.

[6] Ahmad, S., Wood, K. C., and Scott, J. E. -"A High Throughput Proliferation and Cytotoxicity Assay for Co-Cultured Isogenic Cell Lines". *MethodsX* 9 (Jan. 2022), p. 101927. ISSN: 2215-0161.

[7] Albanese, A., Swaney, J. M., Yun, D. H., Evans, N. B., Antonucci, J. M., Velasco, S., Sohn, C. H., Arlotta, P., Gehrke, L., and Chung, K. -"Multiscale 3D Phenotyping of Human Cerebral Organoids". *Scientific Reports* 10.1 (Dec. 2020), p. 21487. ISSN: 2045-2322.

[8] Albecka, A., Laine, R. F., Janssen, A. F., Kaminski, C. F., and Crump, C. M. -"HSV-1 Glycoproteins Are Delivered to Virus Assembly Sites Through Dynamin-Dependent Endocytosis". *Traffic* 17.1 (2016), pp. 21–39. ISSN: 1600-0854.

[9] Alexander, A. G., Marfil, V., and Li, C. -"Use of Caenorhabditis Elegans as a Model to Study Alzheimer's Disease and Other Neurodegenerative Diseases". *Frontiers in Genetics* 5 (2014), p. 279. ISSN: 1664-8021.

[10] Alisky, J. M., van de Wetering, C. I., and Davidson, B. L. -"Widespread Dispersal of Cholera Toxin Subunit b to Brain and Spinal Cord Neurons Following Systemic Delivery". *Experimental Neurology* 178.1 (Nov. 2002), pp. 139–146. ISSN: 0014-4886.

[11] Aloni, E., Oni-Biton, E., Tsoory, M., Moallem, D. H., and Segal, M. -"Synaptopodin Deficiency Ameliorates Symptoms in the 3xTg Mouse Model of Alzheimer's Disease". *Journal of Neuroscience* 39.20 (May 2019), pp. 3983–3992. ISSN: 0270-6474, 1529-2401.

[12] Alonso, A., Zaidi, T., Novak, M., Grundke-Iqbal, I., and Iqbal, K. -"Hyperphosphorylation Induces Self-Assembly of Tau into Tangles of Paired Helical Filaments/Straight Filaments". *Proceedings of the National Academy of Sciences of the United States of America* 98.12 (June 2001), pp. 6923–6928. ISSN: 0027-8424.

[13] Alzheimer, A. -"Über eigenartige Krankheitsfälle des späteren Alters". *Zeitschrift für die gesamte Neurologie und Psychiatrie* 4.1 (Dec. 1911), p. 356. ISSN: 0303-4194.

[14] Alzheimer, A. -"Über Eine Eigenartige Erkrankung Der Hirnrinde". *Psychiatrie und phychish-Gerichtliche Medizin* 64 (1907), pp. 146–148.

[15] Alzheimer's Association Calcium Hypothesis Workgroup, Arancio, O., Bezprozvanny, I., Berger, T., Bouteiller, J.-M., Carillo, M., Disterhoft, J., Foskett, K., Khachaturian, A., LaFerla, F., Landfield, P., Masliah, E., Mattson, M., Michaelis, M., Nixon, R., Snyder, H., Stutzmann, G., Thibault, O., Yang, A., Khachaturian, Z., and Scholz, K. -"Calcium Hypothesis of Alzheimer's Disease and Brain Aging: A Framework for Integrating New Evidence into a Comprehensive Theory of Pathogenesis". *Alzheimer's & Dementia: The Journal of the Alzheimer's Association* 13.2 (Feb. 2017), 178–182.e17. ISSN: 1552-5279.

[16] Alzheimer's Disease Collaborative Group. -"The Structure of the Presenilin 1 (S182) Gene and Identification of Six Novel Mutations in Early Onset AD Families". *Nature Genetics* 11.2 (Oct. 1995), pp. 219–222. ISSN: 1061-4036.

[17] -"Alzheimer's Disease Neuroimaging Initiative". ADNI.

[18] St-Amour, I., Turgeon, A., Goupil, C., Planel, E., and Hébert, S. S. -"Co-Occurrence of Mixed Proteinopathies in Late-Stage Huntington's Disease". *Acta Neuropathologica* 135.2 (Feb. 2018), pp. 249–265. ISSN: 1432-0533.

[19] Andorfer, C., Kress, Y., Espinoza, M., de Silva, R., Tucker, K. L., Barde, Y.-A., Duff, K., and Davies, P. -"Hyperphosphorylation and Aggregation of Tau in Mice Expressing Normal Human Tau Isoforms". *Journal of Neurochemistry* 86.3 (Aug. 2003), pp. 582–590. ISSN: 0022-3042.

[20] Andrews, M. G. and Kriegstein, A. R. -"Challenges of Organoid Research". *Annual Review of Neuroscience* 45 (Volume 45, 2022 July 2022), pp. 23–39. ISSN: 0147-006X, 1545-4126.

[21] Andrews, S. J., Renton, A. E., Fulton-Howard, B., Podlesny-Drabiniok, A., Marcora, E., and Goate, A. M. -"The Complex Genetic Architecture of Alzheimer's Disease: Novel Insights and Future Directions". *eBioMedicine* 90 (Apr. 2023). ISSN: 2352-3964.

[22] Annaert, W. G., Levesque, L., Craessaerts, K., Dierinck, I., Snellings, G., Westaway, D., George-Hyslop, P. S., Cordell, B., Fraser, P., and De Strooper, B. -"Presenilin 1 Controls Gamma-Secretase Processing of Amyloid Precursor Protein in Pre-Golgi Compartments of Hippocampal Neurons". *The Journal of Cell Biology* 147.2 (Oct. 1999), pp. 277–294. ISSN: 0021-9525.

[23] Antinone, S. E. and Smith, G. A. -"Retrograde Axon Transport of Herpes Simplex Virus and Pseudorabies Virus: A Live-Cell Comparative Analysis". *Journal of Virology* 84.3 (Feb. 2010), pp. 1504–1512. ISSN: 0022-538X.

[24] Antón-Bolaños, N., Faravelli, I., Faits, T., Andreadis, S., Kastli, R., Trattaro, S., Adiconis, X., Wei, A., Sampath Kumar, A., Di Bella, D. J., Tegtmeyer, M., Nehme, R., Levin, J. Z., Regev, A., and Arlotta, P. -"Brain Chimeroids Reveal Individual Susceptibility to Neurotoxic Triggers". *Nature* 631.8019 (July 2024), pp. 142–149. ISSN: 1476-4687.

[25] Araki, T., Ikegaya, Y., and Koyama, R. -"The Effects of Microglia- and Astrocyte-Derived Factors on Neurogenesis in Health and Disease". *European Journal of Neuroscience* 54.5 (2021), pp. 5880–5901. ISSN: 1460-9568.

[26] Arber, C., Villegas-Llerena, C., Toombs, J., Pocock, J. M., Ryan, N. S., Fox, N. C., Zetterberg, H., Hardy, J., and Wray, S. -"Amyloid Precursor Protein Processing in Human Neurons with an Allelic Series of the PSEN1 Intron 4 Deletion Mutation and Total Presenilin-1 Knockout". *Brain Communications* 1.1 (Jan. 2019), fcz024. ISSN: 2632-1297.

[27] Area-Gomez, E. -"Chapter Eleven - Assessing the Function of Mitochondria-Associated ER Membranes". *Methods in Enzymology*. Ed. by A. N. Murphy and D. C. Chan. Vol. 547. Mitochondrial Function. Academic Press, Jan. 2014, pp. 181–197.

[28] Area-Gomez, E., de Groof, A. J. C., Boldogh, I., Bird, T. D., Gibson, G. E., Koehler, C. M., Yu, W. H., Duff, K. E., Yaffe, M. P., Pon, L. A., and Schon, E. A. -"Presenilins Are Enriched in Endoplasmic Reticulum Membranes Associated with Mitochondria". *The American Journal of Pathology* 175.5 (Nov. 2009), pp. 1810–1816. ISSN: 1525-2191.

[29] Arendt, T., Stieler, J. T., and Holzer, M. -"Tau and Tauopathies". *Brain Research Bulletin*. Cytoskeletal Proteins in Health and Neurodegenerative Disease 126 (Sept. 2016), pp. 238–292. ISSN: 0361-9230.

[30] Arias, C., Montiel, T., Quiroz-Báez, R., and Massieu, L. -"β-Amyloid Neurotoxicity Is Exacerbated during Glycolysis Inhibition and Mitochondrial Impairment in the Rat Hippocampus *in Vivo* and in Isolated Nerve Terminals: Implications for Alzheimer's Disease". *Experimental Neurology* 176.1 (July 2002), pp. 163–174. ISSN: 0014-4886.

[31] Arias-Cavieres, A., Barrientos, G. C., Sánchez, G., Elgueta, C., Muñoz, P., and Hidalgo, C. -"Ryanodine Receptor-Mediated Calcium Release Has a Key Role in Hippocampal LTD Induction". *Frontiers in Cellular Neuroscience* 12 (Nov. 2018). ISSN: 1662-5102.

[32] Arif, M., Kazim, S. F., Grundke-Iqbal, I., Garruto, R. M., and Iqbal, K. -"Tau Pathology Involves Protein Phosphatase 2A in Parkinsonism-dementia of Guam". *Proceedings of the National Academy of Sciences* 111.3 (Jan. 2014), pp. 1144–1149.

[33] Armstrong, R. A. -"A Critical Analysis of the 'Amyloid Cascade Hypothesis'". *Folia Neuropathologica* 52.3 (2014), pp. 211–225. ISSN: 1509-572X.

[34] Arrasate, M., Mitra, S., Schweitzer, E. S., Segal, M. R., and Finkbeiner, S. -"Inclusion Body Formation Reduces Levels of Mutant Huntingtin and the Risk of Neuronal Death". *Nature* 431.7010 (Oct. 2004), pp. 805–810. ISSN: 1476-4687.

[35] Arriagada, P. V., Growdon, J. H., Hedley-Whyte, E. T., and Hyman, B. T. -"Neurofibrillary Tangles but Not Senile Plaques Parallel Duration and Severity of Alzheimer's Disease". *Neurology* 42.3 (Mar. 1992), pp. 631–631.

[36] Baas, P. W., Deitch, J. S., Black, M. M., and Banker, G. A. -"Polarity Orientation of Microtubules in Hippocampal Neurons: Uniformity in the Axon and Nonuniformity in the Dendrite". *Proceedings of the National Academy of Sciences of the United States of America* 85.21 (Nov. 1988), pp. 8335–8339. ISSN: 0027-8424.

[37] Bagyinszky, E., Giau, V. V., Shim, K., Suk, K., An, S. S. A., and Kim, S. -"Role of Inflammatory Molecules in the Alzheimer's Disease Progression and Diagnosis". *Journal of the Neurological Sciences* 376 (May 2017), pp. 242–254. ISSN: 0022-510X.

[38] Balaji, R., Bielmeier, C., Harz, H., Bates, J., Stadler, C., Hildebrand, A., and Classen, A.-K. -"Calcium Spikes, Waves and Oscillations in a Large, Patterned Epithelial Tissue". *Scientific Reports* 7.1 (Feb. 2017), p. 42786. ISSN: 2045-2322.

[39] Ball, M. J., Fisman, M., Hachinski, V., Blume, W., Fox, A., Kral, V. A., Kirshen, A. J., Fox, H., and Merskey, H. -"A New Definition of Alzheimer's Disease: A Hippocampal Dementia". *Lancet (London, England)* 1.8419 (Jan. 1985), pp. 14–16. ISSN: 0140-6736.

[40] Baloyannis, S. -"Mitochondria and Brain Disorders". BoD – Books on Demand, Mar. 2020. ISBN: 978-1-78985-531-9.

[41] Baloyannis, S. J. -"Mitochondrial Alterations in Alzheimer's Disease". *Journal of Alzheimer's Disease* 9.2 (July 2006), pp. 119–126. ISSN: 1387-2877.

[42] Bandara, S., Malmersjö, S., and Meyer, T. -"Regulators of Calcium Homeostasis Identified by Inference of Kinetic Model Parameters from Live Single Cells Perturbed by siRNA". *Science Signaling* 6.283 (July 2013), ra56. ISSN: 1937-9145.

[43] Banik, A., Brown, R. E., Bamburg, J., Lahiri, D. K., Khurana, D., Friedland, R. P., Chen, W., Ding, Y., Mudher, A., Padjen, A. L., Mukaetova-Ladinska, E., Ihara, M., Srivastava, S., Padma Srivastava, M., Masters, C. L., Kalaria, R. N., and Anand, A. -"Translation of Pre-Clinical Studies into Successful Clinical Trials for Alzheimer's Disease: What Are the Roadblocks and How Can They Be Overcome?1". *Journal of Alzheimer's Disease* 47.4 (Aug. 2015), pp. 815–843. ISSN: 1387-2877.

[44] Banker, G. A. and Cowan, W. M. -"Rat Hippocampal Neurons in Dispersed Cell Culture". *Brain Research* 126.3 (May 1977), pp. 397–425. ISSN: 0006-8993.

[45] Bassett, A. R. -"Editing the Genome of hiPSC with CRISPR/Cas9: Disease Models". *Mammalian Genome* 28.7 (2017), pp. 348–364. ISSN: 0938-8990.

[46] Behbahani, H., Pavlov, P. F., Wiehager, B., Nishimura, T., Winblad, B., and Ankarcrona, M. -"Association of Omi/HtrA2 with γ-Secretase in Mitochondria". *Neurochemistry International* 57.6 (Nov. 2010), pp. 668–675. ISSN: 0197-0186.

[47] Behl, C. -"In 2024, the Amyloid-Cascade-Hypothesis Still Remains a Working Hypothesis, No Less but Certainly No More". *Frontiers in Aging Neuroscience* 16 (Sept. 2024). ISSN: 1663-4365.

[48] Bergström, P., Trybala, E., Eriksson, C. E., Johansson, M., Satir, T. M., Widéhn, S., Fruhwürth, S., Michno, W., Nazir, F. H., Hanrieder, J., Paludan, S. R., Agholme, L., Zetterberg, H., and Bergström, T. -"Herpes Simplex Virus 1 and 2 Infections during Differentiation of Human Cortical Neurons". *Viruses* 13.10 (10 Oct. 2021), p. 2072. ISSN: 1999-4915.

[49] Berridge, M. J. -"Calcium Signalling and Cell Proliferation". *BioEssays* 17.6 (1995), pp. 491–500. ISSN: 1521-1878.

[50] Berridge, M. J. -"Calcium Hypothesis of Alzheimer's Disease". *Pflugers Archiv: European Journal of Physiology* 459.3 (Feb. 2010), pp. 441–449. ISSN: 1432-2013.

[51] Berridge, M. J., Bootman, M. D., and Lipp, P. -"Calcium - a Life and Death Signal". *Nature* 395.6703 (Oct. 1998), pp. 645–648. ISSN: 1476-4687.

[52] Berridge, M. J., Bootman, M. D., and Roderick, H. L. -"Calcium Signalling: Dynamics, Homeostasis and Remodelling". *Nature Reviews. Molecular Cell Biology* 4.7 (July 2003), pp. 517–529. ISSN: 1471-0072.

[53] Berridge, M. J., Lipp, P., and Bootman, M. D. -"The Versatility and Universality of Calcium Signalling". *Nature Reviews Molecular Cell Biology* 1.1 (Oct. 2000), pp. 11–21. ISSN: 1471-0080.

[54] Bertram, L. and Tanzi, R. E. -"The Current Status of Alzheimer's Disease Genetics: What Do We Tell the Patients?" *Pharmacological Research* 50.4 (Oct. 2004), pp. 385–396. ISSN: 1043-6618.

[55] Bezprozvanny, I. and Mattson, M. P. -"Neuronal Calcium Mishandling and the Pathogenesis of Alzheimer's Disease". *Trends in Neurosciences* 31.9 (Sept. 2008), pp. 454–463. ISSN: 0166-2236.

[56] Bhattacharjee, P. S., Neumann, D. M., Foster, T. P., Bouhanik, S., Clement, C., Vinay, D., Thompson, H. W., and Hill, J. M. -"Effect of Human Apolipoprotein E Genotype on the Pathogenesis of Experimental Ocular HSV-1". *Experimental Eye Research* 87.2 (Aug. 2008), pp. 122–130. ISSN: 0014-4835.

[57] Bigio, E. H., Lipton, A. M., Yen, S.-H., Hutton, M. L., Baker, M., Nacharaju, P., White III, C. L., Davies, P., Lin, W., and Dickson, D. W. -"Frontal Lobe Dementia With Novel Tauopathy: Sporadic Multiple System Tauopathy With Dementia". *Journal of Neuropathology & Experimental Neurology* 60.4 (Apr. 2001), pp. 328–341. ISSN: 0022-3069.

[58] Birnbaum, J. H., Wanner, D., Gietl, A. F., Saake, A., Kündig, T. M., Hock, C., Nitsch, R. M., and Tackenberg, C. -"Oxidative Stress and Altered Mitochondrial Protein Expression in the Absence of Amyloid-β and Tau Pathology in iPSC-derived Neurons from Sporadic Alzheimer's Disease Patients". *Stem Cell Research* 27 (Mar. 2018), pp. 121–130. ISSN: 1876-7753.

[59] Blackstone, C., O'Kane, C. J., and Reid, E. -"Hereditary Spastic Paraplegias: Membrane Traffic and the Motor Pathway". *Nature reviews. Neuroscience* 12.1 (Jan. 2011), pp. 31–42. ISSN: 1471-003X.

[60] Blanco-Silvente, L., Capellà, D., Garre-Olmo, J., Vilalta-Franch, J., and Castells, X. -"Predictors of Discontinuation, Efficacy, and Safety of Memantine Treatment for Alzheimer's Disease: Meta-Analysis and Meta-Regression of 18 Randomized Clinical Trials Involving 5004 Patients". *BMC Geriatrics* 18.1 (July 2018), p. 168. ISSN: 1471-2318.

[61] Bons, N., Mestre, N., Ritchie, K., Petter, A., Podlisny, M., and Selkoe, D. -"Identification of Amyloid Beta Protein in the Brain of the Small, Short-Lived Lemurian Primate Microcebus Murinus". *Neurobiology of Aging* 15.2 (1994), pp. 215–220. ISSN: 0197-4580.

[62] Bootman, M. D., Collins, T. J., Peppiatt, C. M., Prothero, L. S., MacKenzie, L., De Smet, P., Travers, M., Tovey, S. C., Seo, J. T., Berridge, M. J., Ciccolini, F., and Lipp, P. -"Calcium Signalling–an Overview". *Seminars in Cell & Developmental Biology* 12.1 (Feb. 2001), pp. 3–10. ISSN: 1084-9521.

[63] Borchers, A.-C., Janz, M., Schäfer, J.-H., Moeller, A., Kümmel, D., Paululat, A., Ungermann, C., and Langemeyer, L. -"Regulatory Sites in the Mon1–Ccz1 Complex Control Rab5 to Rab7 Transition and Endosome Maturation". *Proceedings of the National Academy of Sciences* 120.30 (July 2023), e2303750120.

[64] Borchers, A.-C., Langemeyer, L., and Ungermann, C. -"Who's in Control? Principles of Rab GTPase Activation in Endolysosomal Membrane Trafficking and Beyond". *The Journal of Cell Biology* 220.9 (Sept. 2021), e202105120. ISSN: 1540-8140.

[65] Borgese, N., Francolini, M., and Snapp, E. -"Endoplasmic Reticulum Architecture: Structures in Flux". *Current Opinion in Cell Biology* 18.4 (Aug. 2006), pp. 358–364. ISSN: 0955-0674.

[66] Bott, C. J., Johnson, C. G., Yap, C. C., Dwyer, N. D., Litwa, K. A., and Winckler, B. -"Nestin in Immature Embryonic Neurons Affects Axon Growth Cone Morphology and Semaphorin3a Sensitivity". *Molecular Biology of the Cell* 30.10 (May 2019), pp. 1214–1229. ISSN: 1059-1524.

[67] Braak, H. and Braak, E. -"Neuropathological Stageing of Alzheimer-related Changes". *Acta Neuropathologica* 82.4 (Sept. 1991), pp. 239–259. ISSN: 1432-0533.

[68] Braak, H., Alafuzoff, I., Arzberger, T., Kretzschmar, H., and Del Tredici, K. -"Staging of Alzheimer Disease-Associated Neurofibrillary Pathology Using Paraffin Sections and Immunocytochemistry". *Acta Neuropathologica* 112.4 (Oct. 2006), pp. 389–404. ISSN: 1432-0533.

[69] Braidy, N., Poljak, A., Jayasena, T., Mansour, H., Inestrosa, N. C., and Sachdev, P. S. -"Accelerating Alzheimer's Research through 'natural' Animal Models". *Current Opinion in Psychiatry* 28.2 (Mar. 2015), pp. 155–164. ISSN: 1473-6578.

[70] Braun, G. A., Dear, A. J., Sanagavarapu, K., Zetterberg, H., and Linse, S. -"Amyloid-β Peptide 37, 38 and 40 Individually and Cooperatively Inhibit Amyloid-β 42 Aggregation". *Chemical Science* 13.8 (Feb. 2022), pp. 2423–2439. ISSN: 2041-6520.

[71] Breitner, J., Haneuse, S. J., Walker, R., Dublin, S., Crane, P. K., Gray, S. L., and Larson, E. B. -"Risk of Dementia and AD with Prior Exposure to NSAIDs in an Elderly Community-Based Cohort". *Neurology* 72.22 (June 2009), pp. 1899–1905.

[72] Brewer, G. J. and Cotman, C. W. -"Survival and Growth of Hippocampal Neurons in Defined Medium at Low Density: Advantages of a Sandwich Culture Technique or Low Oxygen". *Brain Research* 494.1 (Aug. 1989), pp. 65–74. ISSN: 0006-8993.

[73] Brunner, J. W., Lammertse, H. C. A., van Berkel, A. A., Koopmans, F., Li, K. W., Smit, A. B., Toonen, R. F., Verhage, M., and van der Sluis, S. -"Power and Optimal Study Design in iPSC-based Brain Disease Modelling". *Molecular Psychiatry* 28.4 (Apr. 2023), pp. 1545–1556. ISSN: 1476-5578.

[74] Buée, L., Bussière, T., Buée-Scherrer, V., Delacourte, A., and Hof, P. R. -"Tau Protein Isoforms, Phosphorylation and Role in Neurodegenerative Disorders1". *Brain Research Reviews* 33.1 (Aug. 2000), pp. 95–130. ISSN: 0165-0173.

[75] Buggia-Prévot, V., Fernandez, C. G., Riordan, S., Vetrivel, K. S., Roseman, J., Waters, J., Bindokas, V. P., Vassar, R., and Thinakaran, G. -"Axonal BACE1 Dynamics and Targeting in Hippocampal Neurons: A Role for Rab11 GTPase". *Molecular Neurodegeneration* 9.1 (Jan. 2014), p. 1. ISSN: 1750-1326.

[76] Burgos, J. S., Ramirez, C., Sastre, I., Bullido, M. J., and Valdivieso, F. -"ApoE4 Is More Efficient than E3 in Brain Access by Herpes Simplex Virus Type 1". *NeuroReport* 14.14 (Oct. 2003), p. 1825. ISSN: 0959-4965.

[77] Burkhardt, M. F., Martinez, F. J., Wright, S., Ramos, C., Volfson, D., Mason, M., Garnes, J., Dang, V., Lievers, J., Shoukat-Mumtaz, U., Martinez, R., Gai, H., Blake, R., Vaisberg, E., Grskovic, M., Johnson, C., Irion, S., Bright, J., Cooper, B., Nguyen, L., Griswold-Prenner, I., and Javaherian, A. -"A Cellular Model for Sporadic ALS Using Patient-Derived Induced Pluripotent Stem Cells". *Molecular and Cellular Neuroscience*. RNA and Splicing Regulation in Neurodegeneration 56 (Sept. 2013), pp. 355–364. ISSN: 1044-7431.

[78] Button, K. S., Ioannidis, J. P. A., Mokrysz, C., Nosek, B. A., Flint, J., Robinson, E. S. J., and Munafò, M. R. -"Power Failure: Why Small Sample Size Undermines the Reliability of Neuroscience". *Nature Reviews Neuroscience* 14.5 (May 2013), pp. 365–376. ISSN: 1471-0048.

[79] Cai, H., Wang, Y., McCarthy, D., Wen, H., Borchelt, D. R., Price, D. L., and Wong, P. C. -"BACE1 Is the Major β-Secretase for Generation of Aβ Peptides by Neurons". *Nature Neuroscience* 4.3 (Mar. 2001), pp. 233–234. ISSN: 1546-1726.

[80] Campadelli, G., Brandimarti, R., Di Lazzaro, C., Ward, P. L., Roizman, B., and Torrisi, M. R. -"Fragmentation and Dispersal of Golgi Proteins and Redistribution of Glycoproteins and Glycolipids Processed through the Golgi Apparatus after Infection with Herpes Simplex Virus 1." *Proceedings of the National Academy of Sciences of the United States of America* 90.7 (Apr. 1993), pp. 2798–2802. ISSN: 0027-8424.

[81] Camus, S., Ko, W. K. D., Pioli, E., and Bezard, E. -"Why Bother Using Non-Human Primate Models of Cognitive Disorders in Translational Research?" *Neurobiology of Learning and Memory* 124 (Oct. 2015), pp. 123–129. ISSN: 1095-9564.

[82] Cappello, V., Marchetti, L., Parlanti, P., Landi, S., Tonazzini, I., Cecchini, M., Piazza, V., and Gemmi, M. -"Ultrastructural Characterization of the Lower Motor System in a Mouse Model of Krabbe Disease". *Scientific Reports* 6.1 (Dec. 2016), p. 1. ISSN: 2045-2322.

[83] Carlos, A. F., Poloni, T. E., Medici, V., Chikhladze, M., Guaita, A., and Ceroni, M. -"From Brain Collections to Modern Brain Banks: A Historical Perspective". *Alzheimer's & Dementia : Translational Research & Clinical Interventions* 5 (Feb. 2019), pp. 52–60. ISSN: 2352-8737.

[84] Carpita, B., Massoni, L., Battaglini, S., Palego, L., Cremone, I. M., Massimetti, G., Betti, L., Giannaccini, G., and Dell'Osso, L. -"IL-6, Homocysteine, and Autism Spectrum Phenotypes: An Investigation among Adults with Autism Spectrum Disorder and Their First-Degree Relatives". *CNS Spectrums* 28.5 (Oct. 2023), pp. 620–628. ISSN: 1092-8529, 2165-6509.

[85] Cataldo, A. M., Petanceska, S., Peterhoff, C. M., Terio, N. B., Epstein, C. J., Villar, A., Carlson, E. J., Staufenbiel, M., and Nixon, R. A. -"App Gene Dosage Modulates Endosomal Abnormalities of Alzheimer's Disease in a Segmental Trisomy 16 Mouse Model of down Syndrome". *The Journal of Neuroscience: The Official Journal of the Society for Neuroscience* 23.17 (July 2003), pp. 6788–6792. ISSN: 1529-2401.

[86] Cataldo, A. M., Petanceska, S., Terio, N. B., Peterhoff, C. M., Durham, R., Mercken, M., Mehta, P. D., Buxbaum, J., Haroutunian, V., and Nixon, R. A. -"Aβ Localization in Abnormal Endosomes: Association with Earliest Aβ Elevations in AD and Down Syndrome". *Neurobiology of Aging* 25.10 (Nov. 2004), pp. 1263–1272. ISSN: 0197-4580.

[87] Cataldo, A. M., Peterhoff, C. M., Troncoso, J. C., Gomez-Isla, T., Hyman, B. T., and Nixon, R. A. -"Endocytic Pathway Abnormalities Precede Amyloid β Deposition in Sporadic Alzheimer's Disease and Down Syndrome". *The American Journal of Pathology* 157.1 (July 2000), pp. 277–286. ISSN: 0002-9440.

[88] Cavendish, J. Z., Sarkar, S. N., Colantonio, M. A., Quintana, D. D., Ahmed, N., White, B. A., Engler-Chiurazzi, E. B., and Simpkins, J. W. -"Mitochondrial Movement and Number Deficits in Embryonic Cortical Neurons from 3xTg-AD Mice". *Journal of Alzheimer's disease : JAD* 70.1 (2019), pp. 139–151. ISSN: 1387-2877.

[89] Centeno, E. G. Z., Cimarosti, H., and Bithell, A. -"2D versus 3D Human Induced Pluripotent Stem Cell-Derived Cultures for Neurodegenerative Disease Modelling". *Molecular Neurodegeneration* 13.1 (May 2018), p. 27. ISSN: 1750-1326.

[90] Cerneckis, J., Cai, H., and Shi, Y. -"Induced Pluripotent Stem Cells (iPSCs): Molecular Mechanisms of Induction and Applications". *Signal Transduction and Targeted Therapy* 9.1 (Apr. 2024), p. 112. ISSN: 2059-3635.

[91] Chakroborty, S., Goussakov, I., Miller, M. B., and Stutzmann, G. E. -"Deviant Ryanodine Receptor-Mediated Calcium Release Resets Synaptic Homeostasis in Presymptomatic 3xTg-AD Mice". *The Journal of Neuroscience: The Official Journal of the Society for Neuroscience* 29.30 (July 2009), pp. 9458–9470. ISSN: 1529-2401.

[92] Chambers, S. M., Fasano, C. A., Papapetrou, E. P., Tomishima, M., Sadelain, M., and Studer, L. -"Highly Efficient Neural Conversion of Human ES and iPS Cells by Dual Inhibition of SMAD Signaling". *Nature Biotechnology* 27.3 (Mar. 2009), pp. 275–280. ISSN: 1546-1696.

[93] Chanda, D., Ray, S., Chakraborti, D., Sen, S., and Mitra, A. -"Interleukin-6 Levels in Patients With Diabetic Polyneuropathy". *Cureus* 14.2 (), e21952. ISSN: 2168-8184.

[94] Charreau, B., Tesson, L., Soulillou, J. P., Pourcel, C., and Anegon, I. -"Transgenesis in Rats: Technical Aspects and Models". *Transgenic Research* 5.4 (July 1996), pp. 223–234. ISSN: 0962-8819.

[95] Chatterjee, I., Li, F., Kohler, E. E., Rehman, J., Malik, A. B., and Wary, K. K. -"Induced Pluripotent Stem (iPS) Cell Culture Methods and Induction of Differentiation into Endothelial Cells". *Induced Pluripotent Stem (iPS) Cells: Methods and Protocols*. Ed. by K. Turksen and A. Nagy. New York, NY: Springer, 2016, pp. 311–327. ISBN: 978-1-4939-3055-5.

[96] Chen, B., Retzlaff, M., Roos, T., and Frydman, J. -"Cellular Strategies of Protein Quality Control". *Cold Spring Harbor Perspectives in Biology* 3.8 (Aug. 2011), a004374. ISSN: 1943-0264.

[97] Chen, G., Xu, T.-h., Yan, Y., Zhou, Y.-r., Jiang, Y., Melcher, K., and Xu, H. E. -"Amyloid Beta: Structure, Biology and Structure-Based Therapeutic Development". *Acta Pharmacologica Sinica* 38.9 (Sept. 2017), pp. 1205–1235. ISSN: 1745-7254.

[98] Chen, V. C.-H., Wu, S.-I., Huang, K.-Y., Yang, Y.-H., Kuo, T.-Y., Liang, H.-Y., Huang, K.-L., and Gossop, M. -"Herpes Zoster and Dementia: A Nationwide Population-Based Cohort Study". *The Journal of Clinical Psychiatry* 79.1 (2018), p. 16m11312. ISSN: 1555-2101.

[99] Chen, Y., Durakoglugil, M. S., Xian, X., and Herz, J. -"ApoE4 Reduces Glutamate Receptor Function and Synaptic Plasticity by Selectively Impairing ApoE Receptor Recycling". *Proceedings of the National Academy of Sciences of the United States of America* 107.26 (June 2010), pp. 12011–12016. ISSN: 1091-6490.

[100] Chen, Z.-Y. and Zhang, Y. -"Animal Models of Alzheimer's Disease: Applications, Evaluation, and Perspectives". *Zoological Research* 43.6 (Nov. 2022), pp. 1026–1040. ISSN: 2095-8137.

[101] Cheney, R. E. and Baker, J. P. -"Myosins, Divergent". *Guidebook to the Cytoskeletal and Motor Proteins*. Ed. by T. Kreis and R. Vale. Oxford University Press, July 1999. ISBN: 978-0-19-859957-9.

[102] Cheng, G., Feng, Z., and He, B. -"Herpes Simplex Virus 1 Infection Activates the Endoplasmic Reticulum Resident Kinase PERK and Mediates eIF-2alpha Dephosphorylation by the Gamma(1)34.5 Protein". *Journal of Virology* 79.3 (Feb. 2005), pp. 1379–1388. ISSN: 0022-538X.

[103] Chklovskii, D. B. -"Synaptic Connectivity and Neuronal Morphology: Two Sides of the Same Coin". *Neuron* 43.5 (Sept. 2004), pp. 609–617. ISSN: 0896-6273.

[104] Choe, M. S., Yeo, H. C., Kim, J. S., Lee, J., Lee, H. J., Kim, H.-R., Baek, K. M., Jung, N.-Y., Choi, M., and Lee, M. Y. -"Simple Modeling of Familial Alzheimer's Disease Using Human Pluripotent Stem Cell-Derived Cerebral Organoid Technology". *Stem Cell Research & Therapy* 15.1 (Apr. 2024), p. 118. ISSN: 1757-6512.

[105] Chun, H., Marriott, I., Lee, C. J., and Cho, H. -"Elucidating the Interactive Roles of Glia in Alzheimer's Disease Using Established and Newly Developed Experimental Models". *Frontiers in Neurology* 9 (Sept. 2018). ISSN: 1664-2295.

[106] Chung, C. G., Lee, H., and Lee, S. B. -"Mechanisms of Protein Toxicity in Neurodegenerative Diseases". *Cellular and Molecular Life Sciences* 75.17 (Sept. 2018), pp. 3159–3180. ISSN: 1420-9071.

[107] Clavaguera, F., Bolmont, T., Crowther, R. A., Abramowski, D., Frank, S., Probst, A., Fraser, G., Stalder, A. K., Beibel, M., Staufenbiel, M., Jucker, M., Goedert, M., and Tolnay, M. -"Transmission and Spreading of Tauopathy in Transgenic Mouse Brain". *Nature Cell Biology* 11.7 (July 2009), pp. 909–913. ISSN: 1476-4679.

[108] Coen, K., Flannagan, R. S., Baron, S., Carraro-Lacroix, L. R., Wang, D., Vermeire, W., Michiels, C., Munck, S., Baert, V., Sugita, S., Wuytack, F., Hiesinger, P. R., Grinstein, S., and Annaert, W. -"Lysosomal Calcium Homeostasis Defects, Not Proton Pump Defects, Cause Endo-Lysosomal Dysfunction in PSEN-deficient Cells". *The Journal of Cell Biology* 198.1 (July 2012), pp. 23–35. ISSN: 1540-8140.

[109] Cohen, J. -"Statistical Power Analysis for the Behavioral Sciences". 2nd ed. New York: Routledge, May 2013. ISBN: 978-0-203-77158-7.

[110] Cohen, J. I. -"Herpesvirus Latency". *The Journal of Clinical Investigation* 130.7 (July 2020), pp. 3361–3369. ISSN: 0021-9738.

[111] Conde, C. and Cáceres, A. -"Microtubule Assembly, Organization and Dynamics in Axons and Dendrites". *Nature Reviews Neuroscience* 10.5 (May 2009), pp. 319–332. ISSN: 1471-0048.

[112] Contino, S., Suelves, N., Vrancx, C., Vadukul, D. M., Payen, V. L., Stanga, S., Bertrand, L., and Kienlen-Campard, P. -"Presenilin-Deficient Neurons and Astrocytes Display Normal Mitochondrial Phenotypes". *Frontiers in Neuroscience* 14 (Jan. 2021). ISSN: 1662-453X.

[113] Cook, D. G., Li, X., Cherry, S. D., and Cantrell, A. R. -"Presenilin 1 Deficiency Alters the Activity of Voltage-Gated Ca2+ Channels in Cultured Cortical Neurons". *Journal of Neurophysiology* (Dec. 2005).

[114] Cookson, M. R. -"α-Synuclein and Neuronal Cell Death". *Molecular Neurodegeneration* 4.1 (Feb. 2009), p. 9. ISSN: 1750-1326.

[115] Cooper, G. M. -"Microtubules". *The Cell: A Molecular Approach. 2nd Edition*. Sinauer Associates, 2000.

[116] Correia, S. C., Perry, G., and Moreira, P. I. -"Mitochondrial Traffic Jams in Alzheimer's Disease - Pinpointing the Roadblocks". *Biochimica et Biophysica Acta (BBA) - Molecular Basis of Disease* 1862.10 (Oct. 2016), pp. 1909–1917. ISSN: 0925-4439.

[117] Cummings, J., Lee, G., Mortsdorf, T., Ritter, A., and Zhong, K. -"Alzheimer's Disease Drug Development Pipeline: 2017". *Alzheimer's & Dementia: Translational Research & Clinical Interventions* 3.3 (Sept. 2017), pp. 367–384. ISSN: 2352-8737.

[118] Cummings, J., Lee, G., Nahed, P., Kambar, M. E. Z. N., Zhong, K., Fonseca, J., and Taghva, K. -"Alzheimer's Disease Drug Development Pipeline: 2022". *Alzheimer's & Dementia: Translational Research & Clinical Interventions* 8.1 (2022), e12295. ISSN: 2352-8737.

[119] Cummings, J., Lee, G., Ritter, A., Sabbagh, M., and Zhong, K. -"Alzheimer's Disease Drug Development Pipeline: 2019". *Alzheimer's & Dementia: Translational Research & Clinical Interventions* 5 (Jan. 2019), pp. 272–293. ISSN: 2352-8737.

[120] Cummings, J., Lee, G., Ritter, A., Sabbagh, M., and Zhong, K. -"Alzheimer's Disease Drug Development Pipeline: 2020". *Alzheimer's & Dementia: Translational Research & Clinical Interventions* 6.1 (2020), e12050. ISSN: 2352-8737.

[121] Cummings, J., Lee, G., Ritter, A., and Zhong, K. -"Alzheimer's Disease Drug Development Pipeline: 2018". *Alzheimer's & Dementia: Translational Research & Clinical Interventions* 4 (Jan. 2018), pp. 195–214. ISSN: 2352-8737.

[122] Cummings, J., Lee, G., Zhong, K., Fonseca, J., and Taghva, K. -"Alzheimer's Disease Drug Development Pipeline: 2021". *Alzheimer's & Dementia: Translational Research & Clinical Interventions* 7.1 (2021), e12179. ISSN: 2352-8737.

[123] Cummings, J., Morstorf, T., and Lee, G. -"Alzheimer's Drug-Development Pipeline: 2016". *Alzheimer's & Dementia: Translational Research & Clinical Interventions* 2.4 (Nov. 2016), pp. 222–232. ISSN: 2352-8737.

[124] Cummings, J., Zhou, Y., Lee, G., Zhong, K., Fonseca, J., and Cheng, F. -"Alzheimer's Disease Drug Development Pipeline: 2023". *Alzheimer's & Dementia: Translational Research & Clinical Interventions* 9.2 (2023), e12385. ISSN: 2352-8737.

[125] Cummings, J., Zhou, Y., Lee, G., Zhong, K., Fonseca, J., and Cheng, F. -"Alzheimer's Disease Drug Development Pipeline: 2024". *Alzheimer's & Dementia: Translational Research & Clinical Interventions* 10.2 (2024), e12465. ISSN: 2352-8737.

[126] Cummings, J. L., Gonzalez, M. I., Pritchard, M. C., May, P. C., Toledo-Sherman, L. M., and Harris, G. A. -"The Therapeutic Landscape of Tauopathies: Challenges and Prospects". *Alzheimer's Research & Therapy* 15.1 (Oct. 2023), p. 168. ISSN: 1758-9193.

[127] Cummings, J. L., Lindle, J., Dalla, I., Zhou, Y., Zhong, K., and Cheng, F. -"Globalization of Alzheimer's Disease Clinical Trials: Current Characteristics and Future Goals". *International Psychogeriatrics* 37.6 (Dec. 2025), p. 100108. ISSN: 1041-6102.

[128] Cummings, J. L., Zhou, Y., Lee, G., Zhong, K., Fonseca, J., Leisgang-Osse, A. M., and Cheng, F. -"Alzheimer's Disease Drug Development Pipeline: 2025". *Alzheimer's & Dementia: Translational Research & Clinical Interventions* 11.2 (2025), e70098. ISSN: 2352-8737.

[129] D'Alessandro, M. C. B., Kanaan, S., Geller, M., Praticò, D., and Daher, J. P. L. -"Mitochondrial Dysfunction in Alzheimer's Disease". *Ageing Research Reviews* 107 (May 2025), p. 102713. ISSN: 1568-1637.

[130] Das, U., Scott, D. A., Ganguly, A., Koo, E. H., Tang, Y., and Roy, S. -"Activity-Induced Convergence of APP and BACE-1 in Acidic Microdomains via an Endocytosis-Dependent Pathway". *Neuron* 79.3 (Aug. 2013), pp. 447–460. ISSN: 0896-6273.

[131] Das, U., Wang, L., Ganguly, A., Saikia, J. M., Wagner, S. L., Koo, E. H., and Roy, S. -"Visualization of APP and BACE-1 Approximation in Neurons: New Insights into the Amyloidogenic Pathway". *Nature neuroscience* 19.1 (Jan. 2016), pp. 55–64. ISSN: 1097-6256.

[132] Datta, D., Leslie, S. N., Wang, M., Morozov, Y. M., Yang, S., Mentone, S., Zeiss, C., Duque, A., Rakic, P., Horvath, T. L., van Dyck, C. H., Nairn, A. C., and Arnsten, A. F. -"Age-Related Calcium Dysregulation Linked with Tau Pathology and Impaired Cognition in Non-Human Primates". *Alzheimer's & Dementia* 17.6 (2021), pp. 920–932. ISSN: 1552-5279.

[133] Davison, A. J., Eberle, R., Ehlers, B., Hayward, G. S., McGeoch, D. J., Minson, A. C., Pellett, P. E., Roizman, B., Studdert, M. J., and Thiry, E. -"The Order Herpesvirales". *Archives of Virology* 154.1 (Jan. 2009), pp. 171–177. ISSN: 1432-8798.

[134] De Castro, F. and Merchán, M. A. -"Editorial: The Major Discoveries of Cajal and His Disciples: Consolidated Milestones for the Neuroscience of the XXIst Century". *Frontiers in Neuroanatomy* 10 (Oct. 2016), p. 85. ISSN: 1662-5129.

[135] De la Torre, J. C. -"Is Alzheimer's Disease a Neurodegenerative or a Vascular Disorder? Data, Dogma, and Dialectics". *The Lancet. Neurology* 3.3 (Mar. 2004), pp. 184–190. ISSN: 1474-4422.

[136] DeBoer, S. R., Dolios, G., Wang, R., and Sisodia, S. S. -"Differential Release of β-Amyloid from Dendrite- Versus Axon-Targeted APP". *The Journal of Neuroscience* 34.37 (Sept. 2014), pp. 12313–12327. ISSN: 0270-6474.

[137] Desai, A. and Mitchison, T. J. -"Microtubule Polymerization Dynamics". *Annual Review of Cell and Developmental Biology* 13 (1997), pp. 83–117. ISSN: 1081-0706.

[138] Devi, L., Prabhu, B. M., Galati, D. F., Avadhani, N. G., and Anandatheerthavarada, H. K. -"Accumulation of Amyloid Precursor Protein in the Mitochondrial Import Channels of Human Alzheimer's Disease Brain Is Associated with Mitochondrial Dysfunction". *Journal of Neuroscience* 26.35 (Aug. 2006), pp. 9057–9068. ISSN: 0270-6474, 1529-2401.

[139] Diezma-Martín, A. M., Morales-Casado, M. I., Jiménez-Díaz, L., Navarro-López, J. D., Mondéjar-Marín, B., Parra-Serrano, J., Vadillo-Bermejo, A., Marsal-Alonso, C., and Beneyto-Martín, P. -"Association between Autoimmune Diseases and Alzheimer's Disease: Analysis Using Big Data Tools". *Revista Clínica Española (English Edition)* 224.10 (Dec. 2024), pp. 627–633. ISSN: 2254-8874.

[140] Divry, P. -"Etude histo-chimique des plaques séniles". *Journal Belge de Neurologie et de Psychiatrie* 27 (1927), pp. 643–57.

[141] Doherty, G. J. and McMahon, H. T. -"Mechanisms of Endocytosis". *Annual Review of Biochemistry* 78 (2009), pp. 857–902. ISSN: 1545-4509.

[142] Döhner, K., Wolfstein, A., Prank, U., Echeverri, C., Dujardin, D., Vallee, R., and Sodeik, B. -"Function of Dynein and Dynactin in Herpes Simplex Virus Capsid Transport". *Molecular Biology of the Cell* 13.8 (Aug. 2002), pp. 2795–2809. ISSN: 1059-1524.

[143] Doody, R. S., Thomas, R. G., Farlow, M., Iwatsubo, T., Vellas, B., Joffe, S., Kieburtz, K., Raman, R., Sun, X., Aisen, P. S., Siemers, E., Liu-Seifert, H., and Mohs, R. -"Phase 3 Trials of Solanezumab for Mild-to-Moderate Alzheimer's Disease". *New England Journal of Medicine* 370.4 (Jan. 2014), pp. 311–321. ISSN: 0028-4793.

[144] Dranka, B. P., Benavides, G. A., Diers, A. R., Giordano, S., Zelickson, B. R., Reily, C., Zou, L., Chatham, J. C., Hill, B. G., Zhang, J., Landar, A., and Darley-Usmar, V. M. -"Assessing Bioenergetic Function in Response to Oxidative Stress by Metabolic Profiling". *Free Radical Biology and Medicine* 51.9 (Nov. 2011), pp. 1621–1635. ISSN: 0891-5849.

[145] -"Drugs for Alzheimer's Disease: Best Avoided. No Therapeutic Advantage". *Prescrire International* 21.128 (June 2012), p. 150. ISSN: 1167-7422.

[146] Drummond, E. and Wisniewski, T. -"Alzheimer's Disease: Experimental Models and Reality". *Acta Neuropathologica* 133.2 (Feb. 2017), pp. 155–175. ISSN: 1432-0533.

[147] Dumanchin, C., Czech, C., Campion, D., Cuif, M. H., Poyot, T., Martin, C., Charbonnier, F., Goud, B., Pradier, L., and Frebourg, T. -"Presenilins Interact with Rab11, a Small GTPase Involved in the Regulation of Vesicular Transport". *Human Molecular Genetics* 8.7 (July 1999), pp. 1263–1269. ISSN: 0964-6906.

[148] Durmaz, A., Kumral, E., Durmaz, B., Onay, H., Aslan, G. I., Ozkinay, F., Pehlivan, S., Orman, M., and Cogulu, O. -"Genetic Factors Associated with the Predisposition to Late Onset Alzheimer's Disease". *Gene* 707 (July 2019), pp. 212–215. ISSN: 0378-1119.

[149] Edler, M. K., Sherwood, C. C., Meindl, R. S., Hopkins, W. D., Ely, J. J., Erwin, J. M., Mufson, E. J., Hof, P. R., and Raghanti, M. A. -"Aged Chimpanzees Exhibit Pathologic Hallmarks of Alzheimer's Disease". *Neurobiology of Aging* 59 (Nov. 2017), pp. 107–120. ISSN: 1558-1497.

[150] Edmondson, R., Broglie, J. J., Adcock, A. F., and Yang, L. -"Three-Dimensional Cell Culture Systems and Their Applications in Drug Discovery and Cell-Based Biosensors". *Assay and Drug Development Technologies* 12.4 (May 2014), pp. 207–218. ISSN: 1540-658X.

[151] Ehebauer, M., Hayward, P., and Arias, A. M. -"Notch, a Universal Arbiter of Cell Fate Decisions". *Science (New York, N.Y.)* 314.5804 (Dec. 2006), pp. 1414–1415. ISSN: 1095-9203.

[152] Eimer, W. A., Vijaya Kumar, D. K., Navalpur Shanmugam, N. K., Rodriguez, A. S., Mitchell, T., Washicosky, K. J., György, B., Breakefield, X. O., Tanzi, R. E., and Moir, R. D. -"Alzheimer's Disease-Associated β-Amyloid Is Rapidly Seeded by Herpesviridae to Protect against Brain Infection". *Neuron* 99.1 (July 2018), 56–63.e3. ISSN: 0896-6273.

[153] -"EudraCT No. 2009-011098-34 (Lornoxicam Alzheimer Trial)-https://www.clinicaltrialsregister.eu/". EU Clinical Trials Register.

[154] Fagni, L., Chavis, P., Ango, F., and Bockaert, J. -"Complex Interactions between mGluRs, Intracellular Ca2+ Stores and Ion Channels in Neurons". *Trends in Neurosciences* 23.2 (Feb. 2000), pp. 80–88. ISSN: 0166-2236.

[155] Faraji, P., Kühn, H., and Ahmadian, S. -"Multiple Roles of Apolipoprotein E4 in Oxidative Lipid Metabolism and Ferroptosis During the Pathogenesis of Alzheimer's Disease". *Journal of Molecular Neuroscience* 74.3 (July 2024), p. 62. ISSN: 1559-1166.

[156] Faul, F., Erdfelder, E., Buchner, A., and Lang, A.-G. -"Statistical Power Analyses Using G*Power 3.1: Tests for Correlation and Regression Analyses". *Behavior Research Methods* 41.4 (Nov. 2009), pp. 1149–1160. ISSN: 1554-3528.

[157] Fedeli, C., Filadi, R., Rossi, A., Mammucari, C., and Pizzo, P. -"PSEN2 (Presenilin 2) Mutants Linked to Familial Alzheimer Disease Impair Autophagy by Altering Ca2+ Homeostasis". *Autophagy* 15.12 (Dec. 2019), pp. 2044–2062. ISSN: 1554-8627.

[158] Feng, R., Rampon, C., Tang, Y.-P., Shrom, D., Jin, J., Kyin, M., Sopher, B., Martin, G. M., Kim, S.-H., Langdon, R. B., Sisodia, S. S., and Tsien, J. Z. -"Deficient Neurogenesis in Forebrain-Specific Presenilin-1 Knockout Mice Is Associated with Reduced Clearance of Hippocampal Memory Traces". *Neuron* 32.5 (Dec. 2001), pp. 911–926. ISSN: 0896-6273.

[159] Feringa, F. M., Elmagd, A. A., Kruijff, I. D., Heijneman, J., Koppes, S., Mohammed, Y., Giera, M., and van der Kant, R. -"AD Risk Variants in APOE Differentially Affect Lipid Metabolism in iPSC Derived Neurons, Astrocytes and Microglia". *Alzheimer's & Dementia* 19.S12 (2023), e078698. ISSN: 1552-5279.

[160] Fernandez-Funez, P., de Mena, L., and Rincon-Limas, D. E. -"Modeling the Complex Pathology of Alzheimer's Disease in Drosophila". *Experimental Neurology* 274 (Pt A Dec. 2015), pp. 58–71. ISSN: 1090-2430.

[161] Fernández-Nogales, M., Cabrera, J. R., Santos-Galindo, M., Hoozemans, J. J. M., Ferrer, I., Rozemuller, A. J. M., Hernández, F., Avila, J., and Lucas, J. J. -"Huntington's Disease Is a Four-Repeat Tauopathy with Tau Nuclear Rods". *Nature Medicine* 20.8 (Aug. 2014), pp. 881–885. ISSN: 1546-170X.

[162] Fields, B. N., Knipe, D. M., and Howley, P. M. -"Fields Virology". 5th ed. Philadelphia: Wolters Kluwer Health/Lippincott Williams & Wilkins, 2007–. ISBN: 978-0-7817-6060-7.

[163] Finch, E. A. and Augustine, G. J. -"Local Calcium Signalling by Inositol-1,4,5-Trisphosphate in Purkinje Cell Dendrites". *Nature* 396.6713 (Dec. 1998), pp. 753–756. ISSN: 1476-4687.

[164] Fiock, K. L., Smith, J. D., Crary, J. F., and Hefti, M. M. -"β-Amyloid and Tau Pathology in the Aging Feline Brain". *The Journal of Comparative Neurology* 528.1 (Jan. 2020), pp. 108–113. ISSN: 1096-9861.

[165] Fisher, D. W., Bennett, D. A., and Dong, H. -"Sexual Dimorphism in Predisposition to Alzheimer's Disease". *Neurobiology of Aging* 70 (Oct. 2018), pp. 308–324. ISSN: 0197-4580.

[166] Fortini, M. E. -"Notch and Presenilin: A Proteolytic Mechanism Emerges". *Current Opinion in Cell Biology* 13.5 (Oct. 2001), pp. 627–634. ISSN: 0955-0674.

[167] Fox, M., Knapp, L. A., Andrews, P. W., and Fincher, C. L. -"Hygiene and the World Distribution of Alzheimer's Disease: Epidemiological Evidence for a Relationship between Microbial Environment and Age-Adjusted Disease Burden". *Evolution, Medicine, and Public Health* 2013.1 (Jan. 2013), pp. 173–186. ISSN: 2050-6201.

[168] Franzini-Armstrong, C. and Protasi, F. -"Ryanodine Receptors of Striated Muscles: A Complex Channel Capable of Multiple Interactions". *Physiological Reviews* 77.3 (July 1997), pp. 699–729. ISSN: 0031-9333.

[169] Frommberger, U. H., Bauer, J., Haselbauer, P., Fräulin, A., Riemann, D., and Berger, M. -"Interleukin-6-(IL-6) Plasma Levels in Depression and Schizophrenia: Comparison between the Acute State and after Remission". *European Archives of Psychiatry and Clinical Neuroscience* 247.4 (Aug. 1997), pp. 228–233. ISSN: 1433-8491.

[170] Frost, J. L., Le, K. X., Cynis, H., Ekpo, E., Kleinschmidt, M., Palmour, R. M., Ervin, F. R., Snigdha, S., Cotman, C. W., Saido, T. C., Vassar, R. J., St George-Hyslop, P., Ikezu, T., Schilling, S., Demuth, H.-U., and Lemere, C. A. -"Pyroglutamate-3 Amyloid-β Deposition in the Brains of Humans, Non-Human Primates, Canines, and Alzheimer Disease-like Transgenic Mouse Models". *The American Journal of Pathology* 183.2 (Aug. 2013), pp. 369–381. ISSN: 1525-2191.

[171] Fu, W., Shi, D., Westaway, D., and Jhamandas, J. H. -"Bioenergetic Mechanisms in Astrocytes May Contribute to Amyloid Plaque Deposition and Toxicity *". *Journal of Biological Chemistry* 290.20 (May 2015), pp. 12504–12513. ISSN: 0021-9258, 1083-351X.

[172] Fuentealba, L. C., Obernier, K., and Alvarez-Buylla, A. -"Adult Neural Stem Cells Bridge Their Niche". *Cell Stem Cell* 10.6 (June 2012), pp. 698–708. ISSN: 1934-5909, 1875-9777.

[173] Furuichi, T., Kohda, K., Miyawaki, A., and Mikoshiba, K. -"Intracellular Channels". *Current Opinion in Neurobiology* 4.3 (June 1994), pp. 294–303. ISSN: 0959-4388.

[174] Gadadhar, A., Marr, R., and Lazarov, O. -"Presenilin-1 Regulates Neural Progenitor Cell Differentiation in the Adult Brain". *The Journal of Neuroscience* 31.7 (Feb. 2011), pp. 2615–2623. ISSN: 0270-6474.

[175] Games, D., Adams, D., Alessandrini, R., Barbour, R., Borthelette, P., Blackwell, C., Carr, T., Clemens, J., Donaldson, T., Gillespie, F., Guido, T., Hagopian, S., Johnson-Wood, K., Khan, K., Lee, M., Leibowitz, P., Lieberburg, I., Little, S., Masliah, E., McConlogue, L., Montoya-Zavala, M., Mucke, L., Paganini, L., Penniman, E., Power, M., Schenk, D., Seubert, P., Snyder, B., Soriano, F., Tan, H., Vitale, J., Wadsworth, S., Wolozin, B., and Zhao, J. -"Alzheimer-Type Neuropathology in Transgenic Mice Overexpressing V717F β-Amyloid Precursor Protein". *Nature* 373.6514 (Feb. 1995), pp. 523–527. ISSN: 1476-4687.

[176] Gao, C., Shang, J., Sun, Z., Xia, M., Gao, D., Sun, R., Li, W., Wang, F., and Zhang, J. -"Presenilin2 D439A Mutation Induces Dysfunction of Mitochondrial Fusion/Fission Dynamics and Abnormal Regulation of GTPase Activity". *Molecular Neurobiology* 61.8 (Aug. 2024), pp. 5047–5070. ISSN: 1559-1182.

[177] Garavaglia, A., Moiana, A., Camnasio, S., Bolognini, D., Papait, R., Rigamonti, D., and Cattaneo, E. -"Adaptation of NS Cells Growth and Differentiation to High-Throughput Screening-Compatible Plates". *BMC Neuroscience* 11.1 (Jan. 2010), p. 7. ISSN: 1471-2202.

[178] Garcia, G., Pinto, S., Cunha, M., Fernandes, A., Koistinaho, J., and Brites, D. -"Neuronal Dynamics and miRNA Signaling Differ between SH-SY5Y APPSwe and PSEN1 Mutant iPSC-Derived AD Models upon Modulation with miR-124 Mimic and Inhibitor". *Cells* 10.9 (Sept. 2021), p. 2424. ISSN: 2073-4409.

[179] Gardener, S. L., Rainey-Smith, S. R., Villemagne, V. L., Fripp, J., Doré, V., Bourgeat, P., Taddei, K., Fowler, C., Masters, C. L., Maruff, P., Rowe, C. C., Ames, D., Martins, R. N., and the AIBL Investigators. -"Higher Coffee Consumption Is Associated With Slower Cognitive Decline and Less Cerebral Aβ-Amyloid Accumulation Over 126 Months: Data From the Australian Imaging, Biomarkers, and Lifestyle Study". *Frontiers in Aging Neuroscience* 13 (Nov. 2021). ISSN: 1663-4365.

[180] Gasparini, L., Benussi, L., Bianchetti, A., Binetti, G., Curti, D., Govoni, S., Moraschi, S., Racchi, M., and Trabucchi, M. -"Energy Metabolism Inhibition Impairs Amyloid Precursor Protein Secretion from Alzheimer's Fibroblasts". *Neuroscience Letters* 263.2 (Mar. 1999), pp. 197–200. ISSN: 0304-3940.

[181] Gasparini, L., Racchi, M., Benussi, L., Curti, D., Binetti, G., Bianchetti, A., Trabucchi, M., and Govoni, S. -"Effect of Energy Shortage and Oxidative Stress on Amyloid Precursor Protein Metabolism in COS Cells". *Neuroscience Letters* 231.2 (Aug. 1997), pp. 113–117. ISSN: 0304-3940.

[182] Gauthier, N. C., Monzo, P., Gonzalez, T., Doye, A., Oldani, A., Gounon, P., Ricci, V., Cormont, M., and Boquet, P. -"Early Endosomes Associated with Dynamic F-actin Structures Are Required for Late Trafficking of H. Pylori VacA Toxin". *The Journal of Cell Biology* 177.2 (Apr. 2007), pp. 343–354. ISSN: 0021-9525.

[183] Gazda, K., Kuznicki, J., and Wegierski, T. -"Knockdown of Amyloid Precursor Protein Increases Calcium Levels in the Endoplasmic Reticulum". *Scientific Reports* 7.1 (Nov. 2017), p. 14512. ISSN: 2045-2322.

[184] Gendron, T. F. and Petrucelli, L. -"The Role of Tau in Neurodegeneration". *Molecular Neurodegeneration* 4.1 (Mar. 2009), p. 13. ISSN: 1750-1326.

[185] Geula, C., Nagykery, N., and Wu, C.-K. -"Amyloid-β Deposits in the Cerebral Cortex of the Aged Common Marmoset (Callithrix Jacchus): Incidence and Chemical Composition". *Acta Neuropathologica* 103.1 (Jan. 2002), pp. 48–58. ISSN: 1432-0533.

[186] Giandomenico, S. L., Mierau, S. B., Gibbons, G. M., Wenger, L. M. D., Masullo, L., Sit, T., Sutcliffe, M., Boulanger, J., Tripodi, M., Derivery, E., Paulsen, O., Lakatos, A., and Lancaster, M. A. -"Cerebral Organoids at the Air–Liquid Interface Generate Diverse Nerve Tracts with Functional Output". *Nature Neuroscience* 22.4 (Apr. 2019), pp. 669–679. ISSN: 1546-1726.

[187] Gibbs, R. A. *et al.* -"Genome Sequence of the Brown Norway Rat Yields Insights into Mammalian Evolution". *Nature* 428.6982 (Apr. 2004), pp. 493–521. ISSN: 1476-4687.

[188] Gill, D. L., Ghosh, T. K., and Mullaney, J. M. -"Calcium Signalling Mechanisms in Endoplasmic Reticulum Activated by Inositol 1,4,5-Trisphosphate and GTP". *Cell Calcium* 10.5 (July 1989), pp. 363–374. ISSN: 0143-4160.

[189] Ginsberg, S. D., Alldred, M. J., Counts, S. E., Cataldo, A. M., Neve, R. L., Jiang, Y., Wuu, J., Chao, M. V., Mufson, E. J., Nixon, R. A., and Che, S. -"Microarray Analysis of Hippocampal CA1 Neurons Implicates Early Endosomal Dysfunction during Alzheimer's Disease Progression". *Biological Psychiatry* 68.10 (Nov. 2010), pp. 885–893. ISSN: 1873-2402.

[190] Giulian, D., Li, J., Leara, B., and Keenen, C. -"Phagocytic Microglia Release Cytokines and Cytotoxins That Regulate the Survival of Astrocytes and Neurons in Culture". *Neurochemistry International* 25.3 (Sept. 1994), pp. 227–233. ISSN: 0197-0186.

[191] Glass, M. R., Waxman, E. A., Yamashita, S., Lafferty, M., Beltran, A. A., Farah, T., Patel, N. K., Singla, R., Matoba, N., Ahmed, S., Srivastava, M., Drake, E., Davis, L. T., Yeturi, M., Sun, K., Love, M. I., Hashimoto-Torii, K., French, D. L., and Stein, J. L. -"Cross-Site Reproducibility of Human Cortical Organoids Reveals Consistent Cell Type Composition and Architecture". *Stem Cell Reports* 19.9 (Aug. 2024), p. 1351.

[192] Götz, J. and Ittner, L. M. -"Animal Models of Alzheimer's Disease and Frontotemporal Dementia". *Nature Reviews. Neuroscience* 9.7 (July 2008), pp. 532–544. ISSN: 1471-0048.

[193] Goussakov, I., Miller, M. B., and Stutzmann, G. E. -"NMDA-Mediated Ca2+ Influx Drives Aberrant Ryanodine Receptor Activation in Dendrites of Young Alzheimer's Disease Mice". *The Journal of Neuroscience* 30.36 (Sept. 2010), pp. 12128–12137. ISSN: 0270-6474.

[194] Graham, V., Khudyakov, J., Ellis, P., and Pevny, L. -"SOX2 Functions to Maintain Neural Progenitor Identity". *Neuron* 39.5 (Aug. 2003), pp. 749–765. ISSN: 0896-6273.

[195] Grbovic, O. M., Mathews, P. M., Jiang, Y., Schmidt, S. D., Dinakar, R., Summers-Terio, N. B., Ceresa, B. P., Nixon, R. A., and Cataldo, A. M. -"Rab5-Stimulated up-Regulation of the Endocytic Pathway Increases Intracellular Beta-Cleaved Amyloid Precursor Protein Carboxyl-Terminal Fragment Levels and Abeta Production". *The Journal of Biological Chemistry* 278.33 (Aug. 2003), pp. 31261–31268. ISSN: 0021-9258.

[196] Gulati, G. S., Sikandar, S. S., Wesche, D. J., Manjunath, A., Bharadwaj, A., Berger, M. J., Ilagan, F., Kuo, A. H., Hsieh, R. W., Cai, S., Zabala, M., Scheeren, F. A., Lobo, N. A., Qian, D., Yu, F. B., Dirbas, F. M., Clarke, M. F., and Newman, A. M. -"Single-Cell Transcriptional Diversity Is a Hallmark of Developmental Potential". *Science (New York, N.Y.)* 367.6476 (Jan. 2020), pp. 405–411. ISSN: 1095-9203.

[197] Güner, G. and Lichtenthaler, S. F. -"The Substrate Repertoire of γ-Secretase/Presenilin". *Seminars in Cell & Developmental Biology* 105 (Sept. 2020), pp. 27–42. ISSN: 1096-3634.

[198] Gunn-Moore, D. A. -"Cognitive Dysfunction in Cats: Clinical Assessment and Management". *Topics in Companion Animal Medicine* 26.1 (Feb. 2011), pp. 17–24. ISSN: 1946-9837.

[199] Guo, Q., Fu, W., Sopher, B. L., Miller, M. W., Ware, C. B., Martin, G. M., and Mattson, M. P. -"Increased Vulnerability of Hippocampal Neurons to Excitotoxic Necrosis in Presenilin-1 Mutant Knock-in Mice". *Nature Medicine* 5.1 (1 Jan. 1999), pp. 101–106. ISSN: 1546-170X.

[200] Ha, S., Jeong, S.-H., Yi, K., Chu, J. J.-M., Kim, S., Kim, E.-K., and Yu, S.-W. -"Autophagy Mediates Astrogenesis in Adult Hippocampal Neural Stem Cells". *Experimental Neurobiology* 28.2 (Apr. 2019), pp. 229–246.

[201] Hafezi, W., Lorentzen, E. U., Eing, B. R., Müller, M., King, N. J. C., Klupp, B., Mettenleiter, T. C., and Kühn, J. E. -"Entry of Herpes Simplex Virus Type 1 (HSV-1) into the Distal Axons of Trigeminal Neurons Favors the Onset of Nonproductive, Silent Infection". *PLOS Pathogens* 8.5 (May 2012), e1002679. ISSN: 1553-7374.

[202] Haidar, M., Schmid, B., Ruiz, A., Ebneth, A., and Cabrera-Socorro, A. -"Generation of Three Isogenic, Gene-Edited iPSC Lines Carrying the APOE-Christchurch Mutation into the Three Common APOE Variants: *APOE2Ch*, *APOE3Ch* and *APOE4Ch*". *Stem Cell Research* 77 (June 2024), p. 103414. ISSN: 1873-5061.

[203] Hamerlinck, L., D'haene, E., Van Loon, N., Vaughan, M. B., Pérez Baca, M. d. R., Leimbacher, S., Colombo, L., Vantomme, L., Daal, E., Dheedene, A., Goel, H., Menten, B., Callewaert, B., and Vergult, S. -"Non-Coding Structural Variants Identify a Commonly Affected Regulatory Region Steering FOXG1 Transcription in Early Neurodevelopment". *medRxiv* (2025).

[204] Hammer, J. A. and Wagner, W. -"Functions of Class V Myosins in Neurons*". *Journal of Biological Chemistry* 288.40 (Oct. 2013), pp. 28428–28434. ISSN: 0021-9258.

[205] Hampel, H., Hardy, J., Blennow, K., Chen, C., Perry, G., Kim, S. H., Villemagne, V. L., Aisen, P., Vendruscolo, M., Iwatsubo, T., Masters, C. L., Cho, M., Lannfelt, L., Cummings, J. L., and Vergallo, A. -"The Amyloid-β Pathway in Alzheimer's Disease". *Molecular Psychiatry* 26.10 (Oct. 2021), pp. 5481–5503. ISSN: 1476-5578.

[206] Han, J., Park, H., Maharana, C., Gwon, A.-R., Park, J., Baek, S. H., Bae, H.-G., Cho, Y., Kim, H. K., Sul, J. H., Lee, J., Kim, E., Kim, J., Cho, Y., Park, S., Palomera, L. F., Arumugam, T. V., Mattson, M. P., and Jo, D.-G. -"Alzheimer's Disease-Causing Presenilin-1 Mutations Have Deleterious Effects on Mitochondrial Function". *Theranostics* 11.18 (Aug. 2021), pp. 8855–8873. ISSN: 1838-7640.

[207] Handler, M., Yang, X., and Shen, J. -"Presenilin-1 Regulates Neuronal Differentiation during Neurogenesis". *Development (Cambridge, England)* 127.12 (June 2000), pp. 2593–2606. ISSN: 0950-1991.

[208] Hanes, J., Zilka, N., Bartkova, M., Caletkova, M., Dobrota, D., and Novak, M. -"Rat Tau Proteome Consists of Six Tau Isoforms: Implication for Animal Models of Human Tauopathies". *Journal of Neurochemistry* 108.5 (Mar. 2009), pp. 1167–1176. ISSN: 1471-4159.

[209] Haney, M. S., Pálovics, R., Munson, C. N., Long, C., Johansson, P. K., Yip, O., Dong, W., Rawat, E., West, E., Schlachetzki, J. C. M., Tsai, A., Guldner, I. H., Lamichhane, B. S., Smith, A., Schaum, N., Calcuttawala, K., Shin, A., Wang, Y.-H., Wang, C., Koutsodendris, N., Serrano, G. E., Beach, T. G., Reiman, E. M., Glass, C. K., Abu-Remaileh, M., Enejder, A., Huang, Y., and Wyss-Coray, T. -"APOE4/4 Is Linked to Damaging Lipid Droplets in Alzheimer's Disease Microglia". *Nature* 628.8006 (Apr. 2024), pp. 154–161. ISSN: 1476-4687.

[210] Hanger, D. P., Anderton, B. H., and Noble, W. -"Tau Phosphorylation: The Therapeutic Challenge for Neurodegenerative Disease". *Trends in Molecular Medicine* 15.3 (Mar. 2009), pp. 112–119. ISSN: 1471-4914.

[211] Hanger, D. P., Byers, H. L., Wray, S., Leung, K.-Y., Saxton, M. J., Seereeram, A., Reynolds, C. H., Ward, M. A., and Anderton, B. H. -"Novel Phosphorylation Sites in Tau from Alzheimer Brain Support a Role for Casein Kinase 1 in Disease Pathogenesis". *The Journal of Biological Chemistry* 282.32 (Aug. 2007), pp. 23645–23654. ISSN: 0021-9258.

[212] Hannan, S. B., Dräger, N. M., Rasse, T. M., Voigt, A., and Jahn, T. R. -"Cellular and Molecular Modifier Pathways in Tauopathies: The Big Picture from Screening Invertebrate Models". *Journal of Neurochemistry* 137.1 (Apr. 2016), pp. 12–25. ISSN: 1471-4159.

[213] Hansen, D. V., Lui, J. H., Flandin, P., Yoshikawa, K., Rubenstein, J. L., Alvarez-Buylla, A., and Kriegstein, A. R. -"Non-Epithelial Stem Cells and Cortical Interneuron Production in the Human Ganglionic Eminences". *Nature Neuroscience* 16.11 (Nov. 2013), pp. 1576–1587. ISSN: 1546-1726.

[214] Hansson, C. A., Frykman, S., Farmery, M. R., Tjernberg, L. O., Nilsberth, C., Pursglove, S. E., Ito, A., Winblad, B., Cowburn, R. F., Thyberg, J., and Ankarcrona, M. -"Nicastrin, Presenilin, APH-1, and PEN-2 Form Active γ-Secretase Complexes in Mitochondria *". *Journal of Biological Chemistry* 279.49 (Dec. 2004), pp. 51654–51660. ISSN: 0021-9258, 1083-351X.

[215] Hardy, J. -"The Discovery of Alzheimer-causing Mutations in the APP Gene and the Formulation of the "Amyloid Cascade Hypothesis"". *The FEBS journal* 284.7 (Apr. 2017), pp. 1040–1044. ISSN: 1742-4658.

[216] Hardy, J. A. and Higgins, G. A. -"Alzheimer's Disease: The Amyloid Cascade Hypothesis". *Science* 256.5054 (Apr. 1992), pp. 184–185.

[217] Härtig, W., Brückner, G., Schmidt, C., Brauer, K., Bodewitz, G., Turner, J. D., and Bigl, V. -"Co-Localization of Beta-Amyloid Peptides, Apolipoprotein E and Glial Markers in Senile Plaques in the Prefrontal Cortex of Old Rhesus Monkeys". *Brain Research* 751.2 (Mar. 1997), pp. 315–322. ISSN: 0006-8993.

[218] Hasaka, T. P., Myers, K. A., and Baas, P. W. -"Role of Actin Filaments in the Axonal Transport of Microtubules". *The Journal of Neuroscience: The Official Journal of the Society for Neuroscience* 24.50 (Dec. 2004), pp. 11291–11301. ISSN: 1529-2401.

[219] Hayashi, T., Rizzuto, R., Hajnoczky, G., and Su, T.-P. -"MAM: More than Just a Housekeeper". *Trends in Cell Biology* 19.2 (Feb. 2009), pp. 81–88. ISSN: 0962-8924, 1879-3088.

[220] He, B., Gross, M., and Roizman, B. -"The γ134.5 Protein of Herpes Simplex Virus 1 Complexes with Protein Phosphatase 1α to Dephosphorylate the α Subunit of the Eukaryotic Translation Initiation Factor 2 and Preclude the Shutoff of Protein Synthesis by Double-Stranded RNA-activated Protein Kinase". *Proceedings of the National Academy of Sciences of the United States of America* 94.3 (Feb. 1997), pp. 843–848. ISSN: 0027-8424.

[221] He, P. and Shen, Y. -"Interruption of β-Catenin Signaling Reduces Neurogenesis in Alzheimer's Disease". *Journal of Neuroscience* 29.20 (May 2009), pp. 6545–6557. ISSN: 0270-6474, 1529-2401.

[222] He, Z., Dony, L., Fleck, J. S., Szałata, A., Li, K. X., Slišković, I., Lin, H.-C., Santel, M., Atamian, A., Quadrato, G., Sun, J., Pașca, S. P., Camp, J. G., Theis, F. J., and Treutlein, B. -"An Integrated Transcriptomic Cell Atlas of Human Neural Organoids". *Nature* 635.8039 (Nov. 2024), pp. 690–698. ISSN: 1476-4687.

[223] Heneka, M. T., van der Flier, W. M., Jessen, F., Hoozemanns, J., Thal, D. R., Boche, D., Brosseron, F., Teunissen, C., Zetterberg, H., Jacobs, A. H., Edison, P., Ramirez, A., Cruchaga, C., Lambert, J.-C., Laza, A. R., Sanchez-Mut, J. V., Fischer, A., Castro-Gomez, S., Stein, T. D., Kleineidam, L., Wagner, M., Neher, J. J., Cunningham, C., Singhrao, S. K., Prinz, M., Glass, C. K., Schlachetzki, J. C. M., Butovsky, O., Kleemann, K., De Jaeger, P. L., Scheiblich, H., Brown, G. C., Landreth, G., Moutinho, M., Grutzendler, J., Gomez-Nicola, D., McManus, R. M., Andreasson, K., Ising, C., Karabag, D., Baker, D. J., Liddelow, S. A., Verkhratsky, A., Tansey, M., Monsonego, A., Aigner, L., Dorothée, G., Nave, K.-A., Simons, M., Constantin, G., Rosenzweig, N., Pascual, A., Petzold, G. C., Kipnis, J., Venegas, C., Colonna, M., Walter, J., Tenner, A. J., O'Banion, M. K., Steinert, J. R., Feinstein, D. L., Sastre, M., Bhaskar, K., Hong, S., Schafer, D. P., Golde, T., Ransohoff, R. M., Morgan, D., Breitner, J., Mancuso, R., and Riechers, S.-P. -"Neuroinflammation in Alzheimer Disease". *Nature Reviews Immunology* (Dec. 2024), pp. 1–32. ISSN: 1474-1741.

[224] Henriques, A. G., Domingues, S. C. T. S., Fardilha, M., da Cruz e Silva, E. F., and da Cruz e Silva, O. A. B. -"Sodium Azide and 2-Deoxy-D-glucose-induced Cellular Stress Affects Phosphorylation-Dependent AβPP Processing". *Journal of Alzheimer's Disease* 7.3 (Jan. 2005), pp. 201–212. ISSN: 1387-2877.

[225] Hernández-Sapiéns, M. A., Reza-Zaldívar, E. E., Márquez-Aguirre, A. L., Gómez-Pinedo, U., Matias-Guiu, J., Cevallos, R. R., Mateos-Díaz, J. C., Sánchez-González, V. J., and Canales-Aguirre, A. A. -"Presenilin Mutations and Their Impact on Neuronal Differentiation in Alzheimer's Disease". *Neural Regeneration Research* 17.1 (June 2021), pp. 31–37. ISSN: 1673-5374.

[226] Hesiod, Evelyn-White, H. G. (G., and Homer Carmina minora. -"Hesiod, the Homeric Hymns, and Homerica; with an English Translation by Hugh G. Evelyn-White". London Heinemann, 1914.

[227] Hettige, N. C., Peng, H., Wu, H., Zhang, X., Yerko, V., Zhang, Y., Jefri, M., Soubannier, V., Maussion, G., Alsuwaidi, S., Ni, A., Rocha, C., Krishnan, J., McCarty, V., Antonyan, L., Schuppert, A., Turecki, G., Fon, E. A., Durcan, T. M., and Ernst, C. -"FOXG1 Dose Tunes Cell Proliferation Dynamics in Human Forebrain Progenitor Cells". *Stem Cell Reports* 17.3 (Mar. 2022), pp. 475–488. ISSN: 2213-6711.

[228] Heyser, C. J., Masliah, E., Samimi, A., Campbell, I. L., and Gold, L. H. -"Progressive Decline in Avoidance Learning Paralleled by Inflammatory Neurodegeneration in Transgenic Mice Expressing Interleukin 6 in the Brain". *Proceedings of the National Academy of Sciences of the United States of America* 94.4 (Feb. 1997), pp. 1500–1505. ISSN: 0027-8424.

[229] Hibaoui, Y., Grad, I., Letourneau, A., Sailani, M. R., Dahoun, S., Santoni, F. A., Gimelli, S., Guipponi, M., Pelte, M. F., Béna, F., Antonarakis, S. E., and Feki, A. -"Modelling and Rescuing Neurodevelopmental Defect of Down Syndrome Using Induced Pluripotent Stem Cells from Monozygotic Twins Discordant for Trisomy 21". *EMBO molecular medicine* 6.2 (Feb. 2014), pp. 259–277. ISSN: 1757-4684.

[230] Hirai, K., Aliev, G., Nunomura, A., Fujioka, H., Russell, R. L., Atwood, C. S., Johnson, A. B., Kress, Y., Vinters, H. V., Tabaton, M., Shimohama, S., Cash, A. D., Siedlak, S. L., Harris, P. L., Jones, P. K., Petersen, R. B., Perry, G., and Smith, M. A. -"Mitochondrial Abnormalities in Alzheimer's Disease". *The Journal of Neuroscience: The Official Journal of the Society for Neuroscience* 21.9 (May 2001), pp. 3017–3023. ISSN: 1529-2401.

[231] Hirokawa, N. -"Kinesin and Dynein Superfamily Proteins and the Mechanism of Organelle Transport". *Science (New York, N.Y.)* 279.5350 (Jan. 1998), pp. 519–526. ISSN: 0036-8075.

[232] Holcomb, L., Gordon, M. N., McGowan, E., Yu, X., Benkovic, S., Jantzen, P., Wright, K., Saad, I., Mueller, R., Morgan, D., Sanders, S., Zehr, C., O'Campo, K., Hardy, J., Prada, C. M., Eckman, C., Younkin, S., Hsiao, K., and Duff, K. -"Accelerated Alzheimer-type Phenotype in Transgenic Mice Carrying Both Mutant Amyloid Precursor Protein and Presenilin 1 Transgenes". *Nature Medicine* 4.1 (Jan. 1998), pp. 97–100. ISSN: 1078-8956.

[233] Holland, D. J., Miranda-Saksena, M., Boadle, R. A., Armati, P., and Cunningham, A. L. -"Anterograde Transport of Herpes Simplex Virus Proteins in Axons of Peripheral Human Fetal Neurons: An Immunoelectron Microscopy Study". *Journal of Virology* 73.10 (Oct. 1999), pp. 8503–8511. ISSN: 0022-538X.

[234] Holmes, C., Cunningham, C., Zotova, E., Woolford, J., Dean, C., Kerr, S., Culliford, D., and Perry, V. H. -"Systemic Inflammation and Disease Progression in Alzheimer Disease". *Neurology* 73.10 (Sept. 2009), pp. 768–774. ISSN: 0028-3878.

[235] Hou, P., Zielonka, M., Serneels, L., Martinez-Muriana, A., Fattorelli, N., Wolfs, L., Poovathingal, S., T'Syen, D., Balusu, S., Theys, T., Fiers, M., Mancuso, R., Howden, A. J. M., and Strooper, B. D. -"The γ-Secretase Substrate Proteome and Its Role in Cell Signaling Regulation". *Molecular Cell* 83.22 (Nov. 2023), 4106–4122.e10. ISSN: 1097-2765.

[236] Howard, J. and Hyman, A. A. -"Dynamics and Mechanics of the Microtubule plus End". *Nature* 422.6933 (Apr. 2003), pp. 753–758. ISSN: 1476-4687.

[237] Hoyer, S. -"Is Sporadic Alzheimer Disease the Brain Type of Non-Insulin Dependent Diabetes Mellitus? A Challenging Hypothesis". *Journal of Neural Transmission (Vienna, Austria: 1996)* 105.4–5 (1998), pp. 415–422. ISSN: 0300-9564.

[238] Hsiao, K., Chapman, P., Nilsen, S., Eckman, C., Harigaya, Y., Younkin, S., Yang, F., and Cole, G. -"Correlative Memory Deficits, Abeta Elevation, and Amyloid Plaques in Transgenic Mice". *Science (New York, N.Y.)* 274.5284 (Oct. 1996), pp. 99–102. ISSN: 0036-8075.

[239] Hu, Y., Hung, A. C., Cui, H., Dawkins, E., Bolós, M., Foa, L., Young, K. M., and Small, D. H. -"Role of Cystatin C in Amyloid Precursor Protein-Induced Proliferation of Neural Stem/Progenitor Cells". *The Journal of Biological Chemistry* 288.26 (June 2013), pp. 18853–18862. ISSN: 1083-351X.

[240] Huntley, J. D., Fleming, S. M., Mograbi, D. C., Bor, D., Naci, L., Owen, A. M., and Howard, R. -"Understanding Alzheimer's Disease as a Disorder of Consciousness". *Alzheimer's & Dementia : Translational Research & Clinical Interventions* 7.1 (Nov. 2021), e12203. ISSN: 2352-8737.

[241] Hurley, J. H., Boura, E., Carlson, L.-A., and Różycki, B. -"Membrane Budding". *Cell* 143.6 (Dec. 2010), pp. 875–887. ISSN: 1097-4172.

[242] Huttenlocher, P. R. and Dabholkar, A. S. -"Regional Differences in Synaptogenesis in Human Cerebral Cortex". *The Journal of Comparative Neurology* 387.2 (Oct. 1997), pp. 167–178. ISSN: 0021-9967.

[243] Huttenlocher, P. R. -"Synaptic Density in Human Frontal Cortex — Developmental Changes and Effects of Aging". *Brain Research* 163.2 (Mar. 1979), pp. 195–205. ISSN: 0006-8993.

[244] Inestrosa, N. C., Reyes, A. E., Chacón, M. A., Cerpa, W., Villalón, A., Montiel, J., Merabachvili, G., Aldunate, R., Bozinovic, F., and Aboitiz, F. -"Human-like Rodent Amyloid-Beta-Peptide Determines Alzheimer Pathology in Aged Wild-Type Octodon Degu". *Neurobiology of Aging* 26.7 (July 2005), pp. 1023–1028. ISSN: 0197-4580.

[245] Ionov, I. D. and Pushinskaya, I. I. -"Amyloid-Beta Production in Aged Guinea Pigs: Atropine-Induced Enhancement Is Reversed by Naloxone". *Neuroscience Letters* 480.1 (Aug. 2010), pp. 83–86. ISSN: 1872-7972.

[246] Isidro, F. -"Brain Aging and Alzheimer's Disease, a Perspective from Non-Human Primates". *Aging (Albany NY)* 16.20 (Oct. 2024), pp. 13145–13171. ISSN: 1945-4589.

[247] Itzhaki, R. F. -"Corroboration of a Major Role for Herpes Simplex Virus Type 1 in Alzheimer's Disease". *Frontiers in Aging Neuroscience* 10 (2018). ISSN: 1663-4365.

[248] Itzhaki, R. F. -"Overwhelming Evidence for a Major Role for Herpes Simplex Virus Type 1 (HSV1) in Alzheimer's Disease (AD); Underwhelming Evidence Against". *Vaccines* 9.6 (June 2021), p. 679. ISSN: 2076-393X.

[249] Itzhaki, R. F., Lathe, R., Balin, B. J., Ball, M. J., Bearer, E. L., Braak, H., Bullido, M. J., Carter, C., Clerici, M., Cosby, S. L., Del Tredici, K., Field, H., Fulop, T., Grassi, C., Griffin, W. S. T., Haas, J., Hudson, A. P., Kamer, A. R., Kell, D. B., Licastro, F., Letenneur, L., Lövheim, H., Mancuso, R., Miklossy, J., Otth, C., Palamara, A. T., Perry, G., Preston, C., Pretorius, E., Strandberg, T., Tabet, N., Taylor-Robinson, S. D., and Whittum-Hudson, J. A. -"Microbes and Alzheimer's Disease". *Journal of Alzheimer's disease: JAD* 51.4 (2016), pp. 979–984. ISSN: 1875-8908.

[250] Itzhaki, R. F., Lin, W.-R., Shang, D., Wilcock, G. K., Faragher, B., and Jamieson, G. A. -"Herpes Simplex Virus Type 1 in Brain and Risk of Alzheimer's Disease". *The Lancet* 349.9047 (Jan. 1997), pp. 241–244. ISSN: 0140-6736, 1474-547X.

[251] Ivanova, H., Vervliet, T., Missiaen, L., Parys, J. B., De Smedt, H., and Bultynck, G. -"Inositol 1,4,5-Trisphosphate Receptor-Isoform Diversity in Cell Death and Survival". *Biochimica Et Biophysica Acta* 1843.10 (Oct. 2014), pp. 2164–2183. ISSN: 0006-3002.

[252] Jacob, F., Pather, S. R., Huang, W.-K., Zhang, F., Wong, S. Z. H., Zhou, H., Cubitt, B., Fan, W., Chen, C. Z., Xu, M., Pradhan, M., Zhang, D. Y., Zheng, W., Bang, A. G., Song, H., Torre, J. C. de la, and Ming, G.-l. -"Human Pluripotent Stem Cell-Derived Neural Cells and Brain Organoids Reveal SARS-CoV-2 Neurotropism Predominates in Choroid Plexus Epithelium". *Cell Stem Cell* 27.6 (Dec. 2020), 937–950.e9. ISSN: 1934-5909, 1875-9777.

[253] Jacob, H. J. and Kwitek, A. E. -"Rat Genetics: Attaching Physiology and Pharmacology to the Genome". *Nature Reviews. Genetics* 3.1 (Jan. 2002), pp. 33–42. ISSN: 1471-0056.

[254] Jain, A., Gut, G., Sanchis-Calleja, F., Tschannen, R., He, Z., Luginbühl, N., Zenk, F., Chrisnandy, A., Streib, S., Harmel, C., Okamoto, R., Santel, M., Seimiya, M., Holtackers, R., Rohland, J. K., Jansen, S. M. J., Lutolf, M. P., Camp, J. G., and Treutlein, B. -"Morphodynamics of Human Early Brain Organoid Development". *Nature* (June 2025), pp. 1–10. ISSN: 1476-4687.

[255] James, C., Harfouche, M., Welton, N. J., Turner, K. M., Abu-Raddad, L. J., Gottlieb, S. L., and Looker, K. J. -"Herpes Simplex Virus: Global Infection Prevalence and Incidence Estimates, 2016". *Bulletin of the World Health Organization* 98.5 (May 2020), pp. 315–329. ISSN: 0042-9686.

[256] Janbek, J., Laursen, T. M., Frimodt-Møller, N., Magyari, M., Haas, J. G., Lathe, R., and Waldemar, G. -"Hospital-Diagnosed Infections, Autoimmune Diseases, and Subsequent Dementia Incidence". *JAMA Network Open* 6.9 (Sept. 2023), e2332635. ISSN: 2574-3805.

[257] Jansen, I. E., Savage, J. E., Watanabe, K., Bryois, J., Williams, D. M., Steinberg, S., Sealock, J., Karlsson, I. K., Hägg, S., Athanasiu, L., Voyle, N., Proitsi, P., Witoelar, A., Stringer, S., Aarsland, D., Almdahl, I. S., Andersen, F., Bergh, S., Bettella, F., Bjornsson, S., Brækhus, A., Bråthen, G., de Leeuw, C., Desikan, R. S., Djurovic, S., Dumitrescu, L., Fladby, T., Hohman, T. J., Jonsson, P. V., Kiddle, S. J., Rongve, A., Saltvedt, I., Sando, S. B., Selbæk, G., Shoai, M., Skene, N. G., Snaedal, J., Stordal, E., Ulstein, I. D., Wang, Y., White, L. R., Hardy, J., Hjerling-Leffler, J., Sullivan, P. F., van der Flier, W. M., Dobson, R., Davis, L. K., Stefansson, H., Stefansson, K., Pedersen, N. L., Ripke, S., Andreassen, O. A., and Posthuma, D. -"Genome-Wide Meta-Analysis Identifies New Loci and Functional Pathways Influencing Alzheimer's Disease Risk". *Nature Genetics* 51.3 (Mar. 2019), pp. 404–413. ISSN: 1546-1718.

[258] Jaye, S., Sandau, U. S., and Saugstad, J. A. -"Clathrin Mediated Endocytosis in Alzheimer's Disease: Cell Type Specific Involvement in Amyloid Beta Pathology". *Frontiers in Aging Neuroscience* 16 (Apr. 2024), p. 1378576. ISSN: 1663-4365.

[259] Jean, N. N., Désiré, O. E., Serge Ely, D., Larson, B., Thiérry-Audrey, T., Ivan Cyr, M. K., Yasmine, O. N., Landry Erik, M., Dominique, P., and Barthélemy, N. -"Assessment of the Risks of Zoonotic Infection at the Primatology Centre of the Interdisciplinary Medical Research Centre of Franceville in Gabon". *Journal of Medical Primatology* 53.5 (2024), e12741. ISSN: 1600-0684.

[260] Jewett, B. E. and Thapa, B. -"Physiology, NMDA Receptor". *StatPearls*. Treasure Island (FL): StatPearls Publishing, 2025.

[261] Jiang, X. and Nardelli, J. -"Cellular and Molecular Introduction to Brain Development". *Neurobiology of disease* 92 (Pt A Aug. 2016), pp. 3–17. ISSN: 0969-9961.

[262] Jiang, Z., Cote, J., Kwon, J. M., Goate, A. M., and Wu, J. Y. -"Aberrant Splicing of Tau Pre-mRNA Caused by Intronic Mutations Associated with the Inherited Dementia Frontotemporal Dementia with Parkinsonism Linked to Chromosome 17". *Molecular and Cellular Biology* 20.11 (June 2000), pp. 4036–4048. ISSN: 0270-7306.

[263] Johnson, G. V. W. and Stoothoff, W. H. -"Tau Phosphorylation in Neuronal Cell Function and Dysfunction". *Journal of Cell Science* 117 (Pt 24 Nov. 2004), pp. 5721–5729. ISSN: 0021-9533.

[264] Johnson, J. W. and Kotermanski, S. E. -"Mechanism of Action of Memantine". *Current Opinion in Pharmacology* 6.1 (Feb. 2006), pp. 61–67. ISSN: 1471-4892.

[265] Johnston, B. P. and McCormick, C. -"Herpesviruses and the Unfolded Protein Response". *Viruses* 12.1 (Dec. 2019), p. 17. ISSN: 1999-4915.

[266] Kaar, A. -"Investigating Neuronal Calcium Homeostasis in Murine Models of Alzheimer's Disease". Doctoral Thesis. University College Cork, 2019.

[267] Kaar, A., Weir, M. P., and Rae, M. G. -"Altered Neuronal Group 1 Metabotropic Glutamate Receptor- and Endoplasmic Reticulum-Mediated Ca2+ Signaling in Two Rodent Models of Alzheimer's Disease". *Neuroscience Letters* 823 (Feb. 2024), p. 137664. ISSN: 0304-3940.

[268] Kalinin, S., Willard, S. L., Shively, C. A., Kaplan, J. R., Register, T. C., Jorgensen, M. J., Polak, P. E., Rubinstein, I., and Feinstein, D. L. -"Development of Amyloid Burden in African Green Monkeys". *Neurobiology of Aging* 34.10 (Oct. 2013), pp. 2361–2369. ISSN: 1558-1497.

[269] Kamat, P. K., Kalani, A., Rai, S., Swarnkar, S., Tota, S., Nath, C., and Tyagi, N. -"Mechanism of Oxidative Stress and Synapse Dysfunction in the Pathogenesis of Alzheimer's Disease: Understanding the Therapeutics Strategies". *Molecular Neurobiology* 53.1 (Jan. 2016), pp. 648–661. ISSN: 1559-1182.

[270] Kanaan, N. M. -"Tau Here, Tau There, Tau Almost Everywhere: Clarifying the Distribution of Tau in the Adult CNS". *Cytoskeleton (Hoboken, N.J.)* 81.1 (Jan. 2024), pp. 107–115. ISSN: 1949-3584.

[271] Kanton, S. and Paşca, S. P. -"Human Assembloids". *Development* 149.20 (Nov. 2022), dev201120. ISSN: 0950-1991.

[272] Karimi Tari, P., Parsons, C. G., Collingridge, G. L., and Rammes, G. -"Memantine: Updating a Rare Success Story in pro-Cognitive Therapeutics". *Neuropharmacology* 244 (Feb. 2024), p. 109737. ISSN: 0028-3908.

[273] Karki, S. and Holzbaur, E. L. -"Cytoplasmic Dynein and Dynactin in Cell Division and Intracellular Transport". *Current Opinion in Cell Biology* 11.1 (Feb. 1999), pp. 45–53. ISSN: 0955-0674.

[274] Keck, S., Nitsch, R., Grune, T., and Ullrich, O. -"Proteasome Inhibition by Paired Helical Filament-Tau in Brains of Patients with Alzheimer's Disease". *Journal of Neurochemistry* 85.1 (Apr. 2003), pp. 115–122. ISSN: 0022-3042.

[275] Kelley, K. W. and Pașca, S. P. -"Human Brain Organogenesis: Toward a Cellular Understanding of Development and Disease". *Cell* 185.1 (Jan. 2022), pp. 42–61. ISSN: 1097-4172.

[276] Keren-Shaul, H., Spinrad, A., Weiner, A., Matcovitch-Natan, O., Dvir-Szternfeld, R., Ulland, T. K., David, E., Baruch, K., Lara-Astaiso, D., Toth, B., Itzkovitz, S., Colonna, M., Schwartz, M., and Amit, I. -"A Unique Microglia Type Associated with Restricting Development of Alzheimer's Disease". *Cell* 169.7 (June 2017), 1276–1290.e17. ISSN: 0092-8674, 1097-4172.

[277] Kim, H.-M., Noh, H. B., Lee, S.-H., Lee, K.-G., Chang, B., Cheong, E., Lee, C. J., and Hwang, D.-Y. -"Fine-Tuning of Dual-SMAD Inhibition to Differentiate Human Pluripotent Stem Cells into Neural Crest Stem Cells". *Cell Proliferation* 54.9 (2021), e13103. ISSN: 1365-2184.

[278] Kim, S., Sato, Y., Mohan, P. S., Peterhoff, C., Pensalfini, A., Rigoglioso, A., Jiang, Y., and Nixon, R. A. -"Evidence That the Rab5 Effector APPL1 Mediates APP-βCTF-induced Dysfunction of Endosomes in Down Syndrome and Alzheimer's Disease". *Molecular Psychiatry* 21.5 (May 2016), pp. 707–716. ISSN: 1476-5578.

[279] Kim, W.-Y. and Shen, J. -"Presenilins Are Required for Maintenance of Neural Stem Cells in the Developing Brain". *Molecular Neurodegeneration* 3.1 (Jan. 2008), p. 2. ISSN: 1750-1326.

[280] Kinney, J. W., Bemiller, S. M., Murtishaw, A. S., Leisgang, A. M., Salazar, A. M., and Lamb, B. T. -"Inflammation as a Central Mechanism in Alzheimer's Disease". *Alzheimer's & Dementia : Translational Research & Clinical Interventions* 4 (Sept. 2018), pp. 575–590. ISSN: 2352-8737.

[281] Kirchhausen, T., Owen, D., and Harrison, S. C. -"Molecular Structure, Function, and Dynamics of Clathrin-Mediated Membrane Traffic". *Cold Spring Harbor Perspectives in Biology* 6.5 (May 2014), a016725. ISSN: 1943-0264.

[282] Kistemaker, L., van Bodegraven, E. J., de Vries, H. E., and Hol, E. M. -"Vascularized Human Brain Organoids: Current Possibilities and Prospects". *Trends in Biotechnology* 43.6 (June 2025), pp. 1275–1285. ISSN: 0167-7799.

[283] Klinger, S. C., Højland, A., Jain, S., Kjolby, M., Madsen, P., Svendsen, A. D., Olivecrona, G., Bonifacino, J. S., and Nielsen, M. S. -"Polarized Trafficking of the Sorting Receptor SorLA in Neurons and MDCK Cells". *The FEBS journal* 283.13 (July 2016), pp. 2476–2493. ISSN: 1742-4658.

[284] Klompstra, T. M., Yoon, K.-J., and Koo, B.-K. -"Evolution of Organoid Genetics". *European Journal of Cell Biology* 104.2 (June 2025), p. 151481. ISSN: 0171-9335.

[285] Kobayashi, S., Sawano, A., Nojima, Y., Shibuya, M., and Maru, Y. -"The C-Cbl/CD2AP Complex Regulates VEGF-induced Endocytosis and Degradation of Flt-1 (VEGFR-1)". *FASEB journal: official publication of the Federation of American Societies for Experimental Biology* 18.7 (May 2004), pp. 929–931. ISSN: 1530-6860.

[286] Kolahdouzan, M. and Hamadeh, M. J. -"The Neuroprotective Effects of Caffeine in Neurodegenerative Diseases". *CNS Neuroscience & Therapeutics* 23.4 (2017), pp. 272–290. ISSN: 1755-5949.

[287] Kong, H., Jones, P. P., Koop, A., Zhang, L., Duff, H. J., and Chen, S. R. W. -"Caffeine Induces Ca2+ Release by Reducing the Threshold for Luminal Ca2+ Activation of the Ryanodine Receptor". *The Biochemical Journal* 414.3 (Sept. 2008), pp. 441–452. ISSN: 1470-8728.

[288] Koo, E. H. and Squazzo, S. L. -"Evidence That Production and Release of Amyloid Beta-Protein Involves the Endocytic Pathway". *The Journal of Biological Chemistry* 269.26 (July 1994), pp. 17386–17389. ISSN: 0021-9258.

[289] Korkotian, E. and Segal, M. -"Synaptopodin Regulates Release of Calcium from Stores in Dendritic Spines of Cultured Hippocampal Neurons". *The Journal of Physiology* 589 (Pt 24 Dec. 2011), pp. 5987–5995. ISSN: 0022-3751.

[290] Kosanke, M., Davenport, C., Szepes, M., Wiehlmann, L., Kohrn, T., Dorda, M., Gruber, J., Menge, K., Sievert, M., Melchert, A., Gruh, I., Göhring, G., and Martin, U. -"iPSC Culture Expansion Selects against Putatively Actionable Mutations in the Mitochondrial Genome". *Stem Cell Reports* 16.10 (Oct. 2021), pp. 2488–2502. ISSN: 2213-6711.

[291] Kraska, A., Dorieux, O., Picq, J.-L., Petit, F., Bourrin, E., Chenu, E., Volk, A., Perret, M., Hantraye, P., Mestre-Frances, N., Aujard, F., and Dhenain, M. -"Age-Associated Cerebral Atrophy in Mouse Lemur Primates". *Neurobiology of Aging* 32.5 (May 2011), pp. 894–906. ISSN: 1558-1497.

[292] Krencik, R. and Zhang, S.-C. -"Directed Differentiation of Functional Astroglial Subtypes from Human Pluripotent Stem Cells". *Nature Protocols* 6.11 (Nov. 2011), pp. 1710–1717. ISSN: 1750-2799.

[293] Kristen, H., Sastre, I., Muñoz-Galdeano, T., Recuero, M., Aldudo, J., and Bullido, M. J. -"The Lysosome System Is Severely Impaired in a Cellular Model of Neurodegeneration Induced by HSV-1 and Oxidative Stress". *Neurobiology of Aging* 68 (Aug. 2018), pp. 5–17. ISSN: 01974580.

[294] Kuchibhotla, K. V., Goldman, S. T., Lattarulo, C. R., Wu, H.-Y., Hyman, B. T., and Bacskai, B. J. -"Aβ Plaques Lead to Aberrant Regulation of Calcium Homeostasis In Vivo Resulting in Structural and Functional Disruption of Neuronal Networks". *Neuron* 59.2 (July 2008), pp. 214–225. ISSN: 0896-6273.

[295] Kujoth, G. C., Hiona, A., Pugh, T. D., Someya, S., Panzer, K., Wohlgemuth, S. E., Hofer, T., Seo, A. Y., Sullivan, R., Jobling, W. A., Morrow, J. D., Van Remmen, H., Sedivy, J. M., Yamasoba, T., Tanokura, M., Weindruch, R., Leeuwenburgh, C., and Prolla, T. A. -"Mitochondrial DNA Mutations, Oxidative Stress, and Apoptosis in Mammalian Aging". *Science (New York, N.Y.)* 309.5733 (July 2005), pp. 481–484. ISSN: 1095-9203.

[296] Kulminski, A. M., Shu, L., Loika, Y., Nazarian, A., Arbeev, K., Ukraintseva, S., Yashin, A., and Culminskaya, I. -"APOE Region Molecular Signatures of Alzheimer's Disease across Races/Ethnicities". *Neurobiology of Aging* 87 (Mar. 2020), 141.e1–141.e8. ISSN: 0197-4580.

[297] Kumar, A., Dogra, S., and Prakash, A. -"Protective Effect of Naringin, a Citrus Flavonoid, against Colchicine-Induced Cognitive Dysfunction and Oxidative Damage in Rats". *Journal of Medicinal Food* 13.4 (Aug. 2010), pp. 976–984. ISSN: 1557-7600.

[298] Kumar, S., Frost, J. L., Cotman, C. W., Head, E., Palmour, R., Lemere, C. A., and Walter, J. -"Deposition of Phosphorylated Amyloid-β in Brains of Aged Nonhuman Primates and Canines". *Brain Pathology* 28.3 (May 2018), pp. 427–430. ISSN: 1015-6305.

[299] Kuns, B., Rosani, A., Patel, P., and Varghese, D. -"Memantine". *StatPearls*. Treasure Island (FL): StatPearls Publishing, 2025.

[300] Kwak, Y.-D., Wang, R., Li, J. J., Zhang, Y.-W., Xu, H., and Liao, F.-F. -"Differential Regulation of BACE1 Expression by Oxidative and Nitrosative Signals". *Molecular Neurodegeneration* 6.1 (Mar. 2011), p. 17. ISSN: 1750-1326.

[301] Labovitz, J. E., Kulaga, P., DuBois, E. M., Li, K., and O'Shea, T. M. -"In Vitro Wound Simulation: A High-Throughput Device for Scratch Assays". *Methods (San Diego, Calif.)* 246 (Feb. 2026), pp. 223–235. ISSN: 1046-2023.

[302] Lambert, J.-C. *et al.* -"Meta-Analysis of 74,046 Individuals Identifies 11 New Susceptibility Loci for Alzheimer's Disease". *Nature Genetics* 45.12 (Dec. 2013), pp. 1452–1458. ISSN: 1546-1718.

[303] Lancaster, M. A. -"Pluripotent Stem Cell-Derived Organoids: A Brief History of Curiosity-Led Discoveries". *BioEssays* 46.12 (2024), p. 2400105. ISSN: 1521-1878.

[304] Lancaster, M. A. and Knoblich, J. A. -"Generation of Cerebral Organoids from Human Pluripotent Stem Cells". *Nature Protocols* 9.10 (Oct. 2014), pp. 2329–2340. ISSN: 1750-2799.

[305] Lancaster, M. A., Renner, M., Martin, C.-A., Wenzel, D., Bicknell, L. S., Hurles, M. E., Homfray, T., Penninger, J. M., Jackson, A. P., and Knoblich, J. A. -"Cerebral Organoids Model Human Brain Development and Microcephaly". *Nature* 501.7467 (7467 Sept. 2013), pp. 373–379. ISSN: 1476-4687.

[306] Langerscheidt, F., Wied, T., Al Kabbani, M. A., van Eimeren, T., Wunderlich, G., and Zempel, H. -"Genetic Forms of Tauopathies: Inherited Causes and Implications of Alzheimer's Disease-like TAU Pathology in Primary and Secondary Tauopathies". *Journal of Neurology* 271.6 (June 2024), pp. 2992–3018. ISSN: 1432-1459.

[307] Lathe, R. and Haas, J. G. -"Distribution of Cellular HSV-1 Receptor Expression in Human Brain". *Journal of NeuroVirology* 23.3 (June 2017), pp. 376–384. ISSN: 1538-2443.

[308] Latta, C. H., Brothers, H. M., and Wilcock, D. M. -"Neuroinflammation in Alzheimer's Disease; A Source of Heterogeneity and Target for Personalized Therapy". *Neuroscience* 302 (Aug. 2015), pp. 103–111. ISSN: 1873-7544.

[309] Lee, J.-H. and Sun, W. -"Neural Organoids, a Versatile Model for Neuroscience". *Molecules and Cells* 45.2 (Feb. 2022), pp. 53–64. ISSN: 1016-8478.

[310] Lesné, S., Koh, M. T., Kotilinek, L., Kayed, R., Glabe, C. G., Yang, A., Gallagher, M., and Ashe, K. H. -"RETRACTED ARTICLE: A Specific Amyloid-β Protein Assembly in the Brain Impairs Memory". *Nature* 440.7082 (Mar. 2006), pp. 352–357. ISSN: 1476-4687.

[311] Letourneau, P. C. -"Actin in Axons: Stable Scaffolds and Dynamic Filaments". *Results and Problems in Cell Differentiation* 48 (2009), pp. 65–90. ISSN: 0080-1844.

[312] Leuner, K., Schütt, T., Kurz, C., Eckert, S. H., Schiller, C., Occhipinti, A., Mai, S., Jendrach, M., Eckert, G. P., Kruse, S. E., Palmiter, R. D., Brandt, U., Dröse, S., Wittig, I., Willem, M., Haass, C., Reichert, A. S., and Müller, W. E. -"Mitochondrion-Derived Reactive Oxygen Species Lead to Enhanced Amyloid Beta Formation". *Antioxidants & Redox Signaling* 16.12 (June 2012), pp. 1421–1433. ISSN: 1523-0864.

[313] Levy-Lahad, E., Wasco, W., Poorkaj, P., Romano, D. M., Oshima, J., Pettingell, W. H., Yu, C. E., Jondro, P. D., Schmidt, S. D., and Wang, K. -"Candidate Gene for the Chromosome 1 Familial Alzheimer's Disease Locus". *Science (New York, N.Y.)* 269.5226 (Aug. 1995), pp. 973–977. ISSN: 0036-8075.

[314] Lewis, J., Dickson, D. W., Lin, W. L., Chisholm, L., Corral, A., Jones, G., Yen, S. H., Sahara, N., Skipper, L., Yager, D., Eckman, C., Hardy, J., Hutton, M., and McGowan, E. -"Enhanced Neurofibrillary Degeneration in Transgenic Mice Expressing Mutant Tau and APP". *Science (New York, N.Y.)* 293.5534 (Aug. 2001), pp. 1487–1491. ISSN: 0036-8075.

[315] Lewis, J., McGowan, E., Rockwood, J., Melrose, H., Nacharaju, P., Van Slegtenhorst, M., Gwinn-Hardy, K., Paul Murphy, M., Baker, M., Yu, X., Duff, K., Hardy, J., Corral, A., Lin, W. L., Yen, S. H., Dickson, D. W., Davies, P., and Hutton, M. -"Neurofibrillary Tangles, Amyotrophy and Progressive Motor Disturbance in Mice Expressing Mutant (P301L) Tau Protein". *Nature Genetics* 25.4 (Aug. 2000), pp. 402–405. ISSN: 1061-4036.

[316] Lewis, P. A. -"Vesicular Dysfunction and Pathways to Neurodegeneration". *Essays in Biochemistry* 65.7 (Dec. 2021), pp. 941–948. ISSN: 0071-1365.

[317] Li, H.-W., Zhang, L., and Qin, C. -"Current State of Research on Non-Human Primate Models of Alzheimer's Disease". *Animal Models and Experimental Medicine* 2.4 (2019), pp. 227–238. ISSN: 2576-2095.

[318] Li, H., Guo, Q., Inoue, T., Polito, V. A., Tabuchi, K., Hammer, R. E., Pautler, R. G., Taffet, G. E., and Zheng, H. -"Vascular and Parenchymal Amyloid Pathology in an Alzheimer Disease Knock-in Mouse Model: Interplay with Cerebral Blood Flow". *Molecular Neurodegeneration* 9 (Aug. 2014), p. 28. ISSN: 1750-1326.

[319] Li, L., Carter, J., Gao, X., Whitehead, J., and Tourtellotte, W. G. -"The Neuroplasticity-Associated Arc Gene Is a Direct Transcriptional Target of Early Growth Response (Egr) Transcription Factors". *Molecular and Cellular Biology* 25.23 (Dec. 2005), pp. 10286–10300. ISSN: null.

[320] Li, S.-H. and Li, X.-J. -"Huntingtin-Protein Interactions and the Pathogenesis of Huntington's Disease". *Trends in genetics: TIG* 20.3 (Mar. 2004), pp. 146–154. ISSN: 0168-9525.

[321] Li, S., Ji, X., Gao, M., Huang, B., Peng, S., and Wu, J. -"Endogenous Amyloid-formed Ca2+-Permeable Channels in Aged 3xTg AD Mice". *Function* 4.4 (May 2023), zqad025. ISSN: 2633-8823.

[322] Li, Y., Li, Z., Wang, C., Yang, M., He, Z., Wang, F., Zhang, Y., Li, R., Gong, Y., Wang, B., Fan, B., Wang, C., Chen, L., Li, H., Shi, P., Wang, N., Wei, Z., Wang, Y.-L., Jin, L., Du, P., Dong, J., and Jiao, J. -"Spatiotemporal Transcriptome Atlas Reveals the Regional Specification of the Developing Human Brain". *Cell* 186.26 (Dec. 2023), 5892–5909.e22. ISSN: 0092-8674, 1097-4172.

[323] Libé-Philippot, B., Iwata, R., Recupero, A. J., Wierda, K., Bernal Garcia, S., Hammond, L., van Benthem, A., Limame, R., Ditkowska, M., Beckers, S., Gaspariunaite, V., Peze-Heidsieck, E., Remans, D., Charrier, C., Theys, T., Polleux, F., and Vanderhaeghen, P. -"Synaptic Neoteny of Human Cortical Neurons Requires Species-Specific Balancing of SRGAP2-SYNGAP1 Cross-Inhibition". *Neuron* 112.21 (Nov. 2024), 3602–3617.e9. ISSN: 1097-4199.

[324] Lichtman, M. A., Kaushansky, K., Prchal, J. T., Levi, M. M., Burns, L. J., and Armitage, J. O. -"Williams Manual of Hematology, Ninth Edition". McGraw Hill Professional, Jan. 2017. ISBN: 978-1-259-64257-9.

[325] Liddelow, S. A., Guttenplan, K. A., Clarke, L. E., Bennett, F. C., Bohlen, C. J., Schirmer, L., Bennett, M. L., Münch, A. E., Chung, W.-S., Peterson, T. C., Wilton, D. K., Frouin, A., Napier, B. A., Panicker, N., Kumar, M., Buckwalter, M. S., Rowitch, D. H., Dawson, V. L., Dawson, T. M., Stevens, B., and Barres, B. A. -"Neurotoxic Reactive Astrocytes Are Induced by Activated Microglia". *Nature* 541.7638 (Jan. 2017), pp. 481–487. ISSN: 1476-4687.

[326] Liiv, M., Vaarmann, A., Safiulina, D., Choubey, V., Gupta, R., Kuum, M., Janickova, L., Hodurova, Z., Cagalinec, M., Zeb, A., Hickey, M. A., Huang, Y.-L., Gogichaishvili, N., Mandel, M., Plaas, M., Vasar, E., Loncke, J., Vervliet, T., Tsai, T.-F., Bultynck, G., Veksler, V., and Kaasik, A. -"ER Calcium Depletion as a Key Driver for Impaired ER-to-mitochondria Calcium Transfer and Mitochondrial Dysfunction in Wolfram Syndrome". *Nature Communications* 15.1 (July 2024), p. 6143. ISSN: 2041-1723.

[327] Lin, J. H. -"Species Similarities and Differences in Pharmacokinetics". *Drug Metabolism and Disposition: The Biological Fate of Chemicals* 23.10 (Oct. 1995), pp. 1008–1021. ISSN: 0090-9556.

[328] Linard, M., Baillet, M., Letenneur, L., Garrigue, I., Catheline, G., Dartigues, J.-F., Peres, K., and Helmer, C. -"Herpes Simplex Virus, Early Neuroimaging Markers and Incidence of Alzheimer's Disease". *Translational Psychiatry* 11.1 (1 July 2021), pp. 1–9. ISSN: 2158-3188.

[329] Linker, S. B., Narvaiza, I., Hsu, J. Y., Wang, M., Qiu, F., Mendes, A. P. D., Oefner, R., Kottilil, K., Sharma, A., Randolph-Moore, L., Mejia, E., Santos, R., Marchetto, M. C., and Gage, F. H. -"Human-Specific Regulation of Neural Maturation Identified by Cross-Primate Transcriptomics". *Current Biology* 32.22 (Nov. 2022), 4797–4807.e5. ISSN: 0960-9822.

[330] Liu, C., Zhong, Y., Apostolou, A., and Fang, S. -"Neural Differentiation of Human Embryonic Stem Cells as an *in Vitro* Tool for the Study of the Expression Patterns of the Neuronal Cytoskeleton during Neurogenesis". *Biochemical and Biophysical Research Communications* 439.1 (Sept. 2013), pp. 154–159. ISSN: 0006-291X.

[331] Liu, P.-P., Xie, Y., Meng, X.-Y., and Kang, J.-S. -"History and Progress of Hypotheses and Clinical Trials for Alzheimer's Disease". *Signal Transduction and Targeted Therapy* 4.1 (Aug. 2019), pp. 1–22. ISSN: 2059-3635.

[332] Liu, Y.-J., Spangenberg, E. E., Tang, B., Holmes, T. C., Green, K. N., and Xu, X. -"Microglia Elimination Increases Neural Circuit Connectivity and Activity in Adult Mouse Cortex". *Journal of Neuroscience* 41.6 (Feb. 2021), pp. 1274–1287. ISSN: 0270-6474, 1529-2401.

[333] Liu, Z., Ren, Z., Zhang, J., Chuang, C.-C., Kandaswamy, E., Zhou, T., and Zuo, L. -"Role of ROS and Nutritional Antioxidants in Human Diseases". *Frontiers in Physiology* 9 (May 2018). ISSN: 1664-042X.

[334] Long, H., Simmons, A., Mayorga, A., Burgess, B., Nguyen, T., Budda, B., Rychkova, A., Rhinn, H., Tassi, I., Ward, M., Yeh, F., Schwabe, T., Paul, R., Kenkare-Mitra, S., and Rosenthal, A. -"Preclinical and First-in-Human Evaluation of AL002, a Novel TREM2 Agonistic Antibody for Alzheimer's Disease". *Alzheimer's Research & Therapy* 16.1 (Oct. 2024), p. 235. ISSN: 1758-9193.

[335] Lopatko Lindman, K., Hemmingsson, E.-S., Weidung, B., Brännström, J., Josefsson, M., Olsson, J., Elgh, F., Nordström, P., and Lövheim, H. -"Herpesvirus Infections, Antiviral Treatment, and the Risk of Dementia—a Registry-based Cohort Study in Sweden". *Alzheimer's & Dementia : Translational Research & Clinical Interventions* 7.1 (Feb. 2021), e12119. ISSN: 2352-8737.

[336] Lopez, J. R., Lyckman, A., Oddo, S., Laferla, F. M., Querfurth, H. W., and Shtifman, A. -"Increased Intraneuronal Resting [Ca2+] in Adult Alzheimer's Disease Mice". *Journal of Neurochemistry* 105.1 (Apr. 2008), pp. 262–271. ISSN: 1471-4159.

[337] Lopez Sanchez, M. I. G., Waugh, H. S., Tsatsanis, A., Wong, B. X., Crowston, J. G., Duce, J. A., and Trounce, I. A. -"Amyloid Precursor Protein Drives Down-Regulation of Mitochondrial Oxidative Phosphorylation Independent of Amyloid Beta". *Scientific Reports* 7.1 (Aug. 2017), p. 9835. ISSN: 2045-2322.

[338] -"Lucid Lab https://lab.lucidsci.com/".

[339] Lucot, K. L., Bukhari, S. A., Webber, E. D., Bonham, T. A., Darian-Smith, C., Montine, T. J., and Green, S. L. -"Semi-Quantitative Assessment of Alzheimer's-like Pathology in Two Aged Polar Bears (Ursus Maritimus)". *Comparative Medicine* 72.4 (Aug. 2022), pp. 267–272. ISSN: 2769-819X.

[340] Lull, M. E. and Block, M. L. -"Microglial Activation and Chronic Neurodegeneration". *Neurotherapeutics* 7.4 (Oct. 2010), pp. 354–365. ISSN: 1878-7479.

[341] Luppi, P.-H., Sakai, K., Salvert, D., Fort, P., and Jouvet, M. -"Peptidergic Hypothalamic Afferents to the Cat Nucleus Raphe Pallidus as Revealed by a Double Immunostaining Technique Using Unconjugated Cholera Toxin as a Retrograde Tracer". *Brain Research* 402.2 (Feb. 1987), pp. 339–345. ISSN: 0006-8993.

[342] Lv, Y., Zhou, S., Gao, S., and Deng, H. -"Remodeling of Host Membranes during Herpesvirus Assembly and Egress". *Protein & Cell* 10.5 (May 2019), pp. 315–326. ISSN: 1674-800X.

[343] Ma, J. Z., Russell, T. A., Spelman, T., Carbone, F. R., and Tscharke, D. C. -"Lytic Gene Expression Is Frequent in HSV-1 Latent Infection and Correlates with the Engagement of a Cell-Intrinsic Transcriptional Response". *PLOS Pathogens* 10.7 (July 2014), e1004237. ISSN: 1553-7374.

[344] Ma, Q.-H., Futagawa, T., Yang, W.-L., Jiang, X.-D., Zeng, L., Takeda, Y., Xu, R.-X., Bagnard, D., Schachner, M., Furley, A. J., Karagogeos, D., Watanabe, K., Dawe, G. S., and Xiao, Z.-C. -"A TAG1-APP Signalling Pathway through Fe65 Negatively Modulates Neurogenesis". *Nature Cell Biology* 10.3 (Mar. 2008), pp. 283–294. ISSN: 1476-4679.

[345] Mack, D. L., Guan, X., Wagoner, A., Walker, S. J., and Childers, M. K. -"Disease-in-a-Dish: The Contribution of Patient-specific Induced Pluripotent Stem Cell Technology to Regenerative Rehabilitation". *American journal of physical medicine & rehabilitation* 93 (11 Suppl 3 Nov. 2014), S155–S168. ISSN: 0894-9115.

[346] Maeda, F., Arii, J., Hirohata, Y., Maruzuru, Y., Koyanagi, N., Kato, A., and Kawaguchi, Y. -"Herpes Simplex Virus 1 UL34 Protein Regulates the Global Architecture of the Endoplasmic Reticulum in Infected Cells". *Journal of Virology* 91.12 (May 2017), e00271–17. ISSN: 0022-538X.

[347] Mahoney, R., Thomas, E. O., Ramirez, P., Miller, H. E., Beckmann, A., Zuniga, G., Dobrowolski, R., and Frost, B. -"Pathogenic Tau Causes a Toxic Depletion of Nuclear Calcium". *Cell Reports* 32.2 (July 2020). ISSN: 2211-1247.

[348] Makarov, M., Kushnireva, L., Papa, M., and Korkotian, E. -"Presenilins and Mitochondria—an Intriguing Link: Mini-Review". *Frontiers in Neuroscience* 17 (July 2023). ISSN: 1662-453X.

[349] Malchiodi-Albedi, F., Paradisi, S., Matteucci, A., Frank, C., and Diociaiuti, M. -"Amyloid Oligomer Neurotoxicity, Calcium Dysregulation, and Lipid Rafts". *International Journal of Alzheimer's Disease* 2011.1 (2011), p. 906964. ISSN: 2090-0252.

[350] Manczak, M., Anekonda, T. S., Henson, E., Park, B. S., Quinn, J., and Reddy, P. H. -"Mitochondria Are a Direct Site of A Beta Accumulation in Alzheimer's Disease Neurons: Implications for Free Radical Generation and Oxidative Damage in Disease Progression". *Human Molecular Genetics* 15.9 (May 2006), pp. 1437–1449. ISSN: 0964-6906.

[351] Mandelkow, E. .-., Biernat, J., Drewes, G., Gustke, N., Trinczek, B., and Mandelkow, E. -"Tau Domains, Phosphorylation, and Interactions with Microtubules". *Neurobiology of Aging*. The Schmitt Symposium: The Cytoskeleton and Alzheimer's Disease 16.3 (May 1995), pp. 355–362. ISSN: 0197-4580.

[352] Mandelkow, E. .-., Stamer, K., Vogel, R., Thies, E., and Mandelkow, E. -"Clogging of Axons by Tau, Inhibition of Axonal Traffic and Starvation of Synapses". *Neurobiology of Aging*. Molecular and Cellular Basis of Synaptic Loss and Dysfunction in Alzheimer's Disease 24.8 (Dec. 2003), pp. 1079–1085. ISSN: 0197-4580.

[353] Marchenko, S. and Flanagan, L. -"Counting Human Neural Stem Cells". *Journal of Visualized Experiments: JoVE* 7 (2007), p. 262. ISSN: 1940-087X.

[354] Martins, I. S., Silva, H. F., Lazareva, E. N., Chernomyrdin, N. V., Zaytsev, K. I., Oliveira, L. M., and Tuchin, V. V. -"Measurement of Tissue Optical Properties in a Wide Spectral Range: A Review [Invited]". *Biomedical Optics Express* 14.1 (Jan. 2023), pp. 249–298. ISSN: 2156-7085.

[355] Mattson, M. P., Cheng, B., Davis, D., Bryant, K., Lieberburg, I., and Rydel, R. E. -"Beta-Amyloid Peptides Destabilize Calcium Homeostasis and Render Human Cortical Neurons Vulnerable to Excitotoxicity". *Journal of Neuroscience* 12.2 (Feb. 1992), pp. 376–389. ISSN: 0270-6474, 1529-2401.

[356] Maurice, T., Lockhart, B. P., and Privat, A. -"Amnesia Induced in Mice by Centrally Administered β-Amyloid Peptides Involves Cholinergic Dysfunction". *Brain Research* 706.2 (Jan. 1996), pp. 181–193. ISSN: 0006-8993.

[357] Maya, S., Prakash, T., and Goli, D. -"Evaluation of Neuroprotective Effects of Wedelolactone and Gallic Acid on Aluminium-Induced Neurodegeneration: Relevance to Sporadic Amyotrophic Lateral Sclerosis". *European Journal of Pharmacology* 835 (Sept. 2018), pp. 41–51. ISSN: 1879-0712.

[358] Mayor, S. and Pagano, R. E. -"Pathways of Clathrin-Independent Endocytosis". *Nature Reviews Molecular Cell Biology* 8.8 (Aug. 2007), pp. 603–612. ISSN: 1471-0080.

[359] McGeer, P. L., Itagaki, S., Boyes, B. E., and McGeer, E. G. -"Reactive Microglia Are Positive for HLA-DR in the Substantia Nigra of Parkinson's and Alzheimer's Disease Brains". *Neurology* 38.8 (Aug. 1988), pp. 1285–1291. ISSN: 0028-3878.

[360] McGeer, P. L., Itagaki, S., and McGeer, E. G. -"Expression of the Histocompatibility Glycoprotein HLA-DR in Neurological Disease". *Acta Neuropathologica* 76.6 (1988), pp. 550–557. ISSN: 0001-6322.

[361] McLean, J. W., Fukazawa, C., and Taylor, J. M. -"Rat Apolipoprotein E mRNA. Cloning and Sequencing of Double-Stranded cDNA". *The Journal of Biological Chemistry* 258.14 (July 1983), pp. 8993–9000. ISSN: 0021-9258.

[362] Merlini, M., Rafalski, V. A., Ma, K., Kim, K.-Y., Bushong, E. A., Rios Coronado, P. E., Yan, Z., Mendiola, A. S., Sozmen, E. G., Ryu, J. K., Haberl, M. G., Madany, M., Sampson, D. N., Petersen, M. A., Bardehle, S., Tognatta, R., Dean, T., Acevedo, R. M., Cabriga, B., Thomas, R., Coughlin, S. R., Ellisman, M. H., Palop, J. J., and Akassoglou, K. -"Microglial Gi-dependent Dynamics Regulate Brain Network Hyperexcitability". *Nature Neuroscience* 24.1 (Jan. 2021), pp. 19–23. ISSN: 1546-1726.

[363] Mertens, J., Paquola, A. C. M., Ku, M., Hatch, E., Böhnke, L., Ladjevardi, S., McGrath, S., Campbell, B., Lee, H., Herdy, J. R., Gonçalves, J. T., Toda, T., Kim, Y., Winkler, J., Yao, J., Hetzer, M. W., and Gage, F. H. -"Directly Reprogrammed Human Neurons Retain Aging-Associated Transcriptomic Signatures and Reveal Age-Related Nucleocytoplasmic Defects". *Cell Stem Cell* 17.6 (Dec. 2015), pp. 705–718. ISSN: 1875-9777.

[364] Miranda-Saksena, M., Boadle, R. A., Aggarwal, A., Tijono, B., Rixon, F. J., Diefenbach, R. J., and Cunningham, A. L. -"Herpes Simplex Virus Utilizes the Large Secretory Vesicle Pathway for Anterograde Transport of Tegument and Envelope Proteins and for Viral Exocytosis from Growth Cones of Human Fetal Axons". *Journal of Virology* 83.7 (Apr. 2009), pp. 3187–3199. ISSN: 1098-5514.

[365] Momota, Y., Konishi, M., Takahata, K., Kishimoto, T., Tezuka, T., Bun, S., Tabuchi, H., Ito, D., and Mimura, M. -"Case Report: Non-Alzheimer's Disease Tauopathy with Logopenic Variant Primary Progressive Aphasia Diagnosed Using Amyloid and Tau PET". *Frontiers in Neurology* 13 (Nov. 2022), p. 1049113. ISSN: 1664-2295.

[366] Moore, S. J., Cazares, V. A., Temme, S. J., and Murphy, G. G. -"Age-related Deficits in Neuronal Physiology and Cognitive Function Are Recapitulated in Young Mice Overexpressing the L-type Calcium Channel, CaV1.3". *Aging Cell* 22.3 (Jan. 2023), e13781. ISSN: 1474-9718.

[367] Morgen, K. and Frölich, L. -"The Metabolism Hypothesis of Alzheimer's Disease: From the Concept of Central Insulin Resistance and Associated Consequences to Insulin Therapy". *Journal of Neural Transmission (Vienna, Austria: 1996)* 122.4 (Apr. 2015), pp. 499–504. ISSN: 1435-1463.

[368] Morsch, R., Simon, W., and Coleman, P. D. -"Neurons May Live for Decades with Neurofibrillary Tangles". *Journal of Neuropathology and Experimental Neurology* 58.2 (Feb. 1999), pp. 188–197. ISSN: 0022-3069.

[369] Movaqar, A., Abdoli, A., Aryan, E., and Meshkat, Z. -"The Propagation of HSV-1 in High Autophagic Activity". *Microbial Pathogenesis* 152 (Mar. 2021), p. 104599. ISSN: 1096-1208.

[370] Mucke, L., Masliah, E., Yu, G. Q., Mallory, M., Rockenstein, E. M., Tatsuno, G., Hu, K., Kholodenko, D., Johnson-Wood, K., and McConlogue, L. -"High-Level Neuronal Expression of Abeta 1-42 in Wild-Type Human Amyloid Protein Precursor Transgenic Mice: Synaptotoxicity without Plaque Formation". *The Journal of Neuroscience: The Official Journal of the Society for Neuroscience* 20.11 (June 2000), pp. 4050–4058. ISSN: 1529-2401.

[371] Mugantseva, E. A. and Podolskii, I. Ya. -"Central Administration of Amyloid β-Peptide (25–35) and Individual Features of Cognitive Behavior in Rats". *Neuroscience and Behavioral Physiology* 40.9 (Nov. 2010), pp. 964–968. ISSN: 1573-899X.

[372] Müller, U., Winter, P., and Graeber, M. B. -"A Presenilin 1 Mutation in the First Case of Alzheimer's Disease". *The Lancet Neurology* 12.2 (Feb. 2013), pp. 129–130. ISSN: 1474-4422, 1474-4465.

[373] Munji, R. N., Choe, Y., Li, G., Siegenthaler, J. A., and Pleasure, S. J. -"Wnt Signaling Regulates Neuronal Differentiation of Cortical Intermediate Progenitors". *Journal of Neuroscience* 31.5 (Feb. 2011), pp. 1676–1687. ISSN: 0270-6474, 1529-2401.

[374] Murchison, D. and Griffith, W. H. -"Calcium Buffering Systems and Calcium Signaling in Aged Rat Basal Forebrain Neurons". *Aging Cell* 6.3 (June 2007), pp. 297–305. ISSN: 1474-9718.

[375] Murphy, D. B., Johnson, K. A., and Borisy, G. G. -"Role of Tubulin-Associated Proteins in Microtubule Nucleation and Elongation". *Journal of Molecular Biology* 117.1 (Nov. 1977), pp. 33–52. ISSN: 0022-2836.

[376] Musarrat, F., Chouljenko, V., and Kousoulas, K. G. -"Cellular and Viral Determinants of Herpes Simplex Virus 1 Entry and Intracellular Transport toward the Nuclei of Infected Cells". *Journal of Virology* 95.7 (Mar. 2021). Ed. by R. M. Longnecker, e02434–20. ISSN: 0022-538X, 1098-5514.

[377] Mustaly-Kalimi, S., Gallegos, W., Marr, R. A., Gilman-Sachs, A., Peterson, D. A., Sekler, I., and Stutzmann, G. E. -"Protein Mishandling and Impaired Lysosomal Proteolysis Generated through Calcium Dysregulation in Alzheimer's Disease". *Proceedings of the National Academy of Sciences* 119.49 (Dec. 2022), e2211999119.

[378] Myrum, C., Baumann, A., Bustad, H. J., Flydal, M. I., Mariaule, V., Alvira, S., Cuéllar, J., Haavik, J., Soulé, J., Valpuesta, J. M., Márquez, J. A., Martinez, A., and Bramham, C. R. -"Arc Is a Flexible Modular Protein Capable of Reversible Self-Oligomerization". *Biochemical Journal* 468 (Pt 1 May 2015), pp. 145–158. ISSN: 0264-6021.

[379] Nakayama, T. and Sawada, T. -"Involvement of Microtubule Integrity in Memory Impairment Caused by Colchicine". *Pharmacology, Biochemistry, and Behavior* 71.1–2 (2002), pp. 119–138. ISSN: 0091-3057.

[380] Navarro-Romero, A., Montpeyó, M., and Martinez-Vicente, M. -"The Emerging Role of the Lysosome in Parkinson's Disease". *Cells* 9.11 (Nov. 2020), p. 2399. ISSN: 2073-4409.

[381] Neavin, D. R., Steinmann, A. M., Farbehi, N., Chiu, H. S., Daniszewski, M. S., Arora, H., Bermudez, Y., Moutinho, C., Chan, C.-L., Bax, M., Tyebally, M., Gnanasambandapillai, V., Lam, C. E., Nguyen, U., Hernández, D., Lidgerwood, G. E., Graham, R. M., Hewitt, A. W., Pébay, A., Palpant, N. J., and Powell, J. E. -"A Village in a Dish Model System for Population-Scale hiPSC Studies". *Nature Communications* 14.1 (June 2023), p. 3240. ISSN: 2041-1723.

[382] Nelson, O., Supnet, C., Liu, H., and Bezprozvanny, I. -"Familial Alzheimer's Disease Mutations in Presenilins: Effects on Endoplasmic Reticulum Calcium Homeostasis and Correlation with Clinical Phenotypes". *Journal of Alzheimer's disease : JAD* 21.3 (2010), pp. 781–793. ISSN: 1387-2877.

[383] Nelson, P. T., Braak, H., and Markesbery, W. R. -"Neuropathology and Cognitive Impairment in Alzheimer Disease: A Complex but Coherent Relationship". *Journal of neuropathology and experimental neurology* 68.1 (Jan. 2009), pp. 1–14. ISSN: 0022-3069.

[384] Nicoll, M. P., Proença, J. T., and Efstathiou, S. -"The Molecular Basis of Herpes Simplex Virus Latency". *FEMS Microbiology Reviews* 36.3 (May 2012), pp. 684–705. ISSN: 0168-6445.

[385] Nieweg, K., Andreyeva, A., van Stegen, B., Tanriöver, G., and Gottmann, K. -"Alzheimer's Disease-Related Amyloid-β Induces Synaptotoxicity in Human iPS Cell-Derived Neurons". *Cell Death & Disease* 6.4 (Apr. 2015), e1709–e1709. ISSN: 2041-4889.

[386] Nixon, R. A. -"A "Protease Activation Cascade" in the Pathogenesis of Alzheimer's Disease". *Annals of the New York Academy of Sciences* 924.1 (2000), pp. 117–131. ISSN: 1749-6632.

[387] Nixon, R. A. -"Amyloid Precursor Protein and Endosomal-Lysosomal Dysfunction in Alzheimer's Disease: Inseparable Partners in a Multifactorial Disease". *FASEB journal: official publication of the Federation of American Societies for Experimental Biology* 31.7 (July 2017), pp. 2729–2743. ISSN: 1530-6860.

[388] Noble, W., Hanger, D. P., Miller, C. C. J., and Lovestone, S. -"The Importance of Tau Phosphorylation for Neurodegenerative Diseases". *Frontiers in Neurology* 4 (July 2013), p. 83. ISSN: 1664-2295.

[389] Noda, Y., Mukaida, K., Miyoshi, H., Nakamura, R., Yasuda, T., Saeki, N., Nishino, I., and Tsutsumi, Y. M. -"The Effects of Dantrolene in the Presence or Absence of Ryanodine Receptor Type 1 Variants in Individuals Predisposed to Malignant Hyperthermia". *Anaesthesia and Intensive Care* 50.4 (July 2022), pp. 312–319. ISSN: 0310-057X.

[390] Norberg, A. -"Sense of Self among Persons with Advanced Dementia". *Alzheimer's Disease*. Ed. by T. Wisniewski. Brisbane (AU): Codon Publications, 2019. ISBN: 978-0-646-80968-7.

[391] Nord, C. L., Valton, V., Wood, J., and Roiser, J. P. -"Power-up: A Reanalysis of 'Power Failure' in Neuroscience Using Mixture Modeling". *Journal of Neuroscience* 37.34 (Aug. 2017), pp. 8051–8061. ISSN: 0270-6474, 1529-2401.

[392] Norden, D. M., Trojanowski, P. J., Villanueva, E., Navarro, E., and Godbout, J. P. -"Sequential Activation of Microglia and Astrocyte Cytokine Expression Precedes Increased Iba-1 or GFAP Immunoreactivity Following Systemic Immune Challenge". *Glia* 64.2 (2016), pp. 300–316. ISSN: 1098-1136.

[393] O'Bryant, S. E., Zhang, F., Johnson, L. A., Hall, J., Edwards, M., Grammas, P., Oh, E., Lyketsos, C. G., and Rissman, R. A. -"A Precision Medicine Model for Targeted NSAID Therapy in Alzheimer's Disease". *Journal of Alzheimer's Disease* 66.1 (Oct. 2018), pp. 97–104. ISSN: 1387-2877.

[394] Oakley, H., Cole, S. L., Logan, S., Maus, E., Shao, P., Craft, J., Guillozet-Bongaarts, A., Ohno, M., Disterhoft, J., Van Eldik, L., Berry, R., and Vassar, R. -"Intraneuronal Beta-Amyloid Aggregates, Neurodegeneration, and Neuron Loss in Transgenic Mice with Five Familial Alzheimer's Disease Mutations: Potential Factors in Amyloid Plaque Formation". *The Journal of Neuroscience: The Official Journal of the Society for Neuroscience* 26.40 (Oct. 2006), pp. 10129–10140. ISSN: 1529-2401.

[395] Oddo, S., Caccamo, A., Kitazawa, M., Tseng, B. P., and LaFerla, F. M. -"Amyloid Deposition Precedes Tangle Formation in a Triple Transgenic Model of Alzheimer's Disease". *Neurobiology of Aging*. Molecular and Cellular Basis of Synaptic Loss and Dysfunction in Alzheimer's Disease 24.8 (Dec. 2003), pp. 1063–1070. ISSN: 0197-4580.

[396] Oliva, M. K., Bourke, J., Kornienko, D., Mattei, C., Mao, M., Kuanyshbek, A., Ovchinnikov, D., Bryson, A., Karle, T. J., Maljevic, S., and Petrou, S. -"Standardizing a Method for Functional Assessment of Neural Networks in Brain Organoids". *Journal of Neuroscience Methods* 409 (Sept. 2024), p. 110178. ISSN: 0165-0270.

[397] Olszakier, S., Hussein, W., Heinrich, R., Andreyanov, M., Blau, A., Otor, Y., Schiller, J., Kellner, S., and Berlin, S. -"Split Genetically Encoded Calcium Indicators for Interorganellar Junctions". *Proceedings of the National Academy of Sciences* 122.20 (May 2025), e2415268122.

[398] Ostrowitzki, S., Bittner, T., Sink, K. M., Mackey, H., Rabe, C., Honig, L. S., Cassetta, E., Woodward, M., Boada, M., van Dyck, C. H., Grimmer, T., Selkoe, D. J., Schneider, A., Blondeau, K., Hu, N., Quartino, A., Clayton, D., Dolton, M., Dang, Y., Ostaszewski, B., Sanabria-Bohórquez, S. M., Rabbia, M., Toth, B., Eichenlaub, U., Smith, J., Honigberg, L. A., and Doody, R. S. -"Evaluating the Safety and Efficacy of Crenezumab vs Placebo in Adults With Early Alzheimer Disease: Two Phase 3 Randomized Placebo-Controlled Trials". *JAMA Neurology* 79.11 (Nov. 2022), pp. 1113–1121. ISSN: 2168-6149.

[399] Page, M. J., McKenzie, J. E., Bossuyt, P. M., Boutron, I., Hoffmann, T. C., Mulrow, C. D., Shamseer, L., Tetzlaff, J. M., Akl, E. A., Brennan, S. E., Chou, R., Glanville, J., Grimshaw, J. M., Hróbjartsson, A., Lalu, M. M., Li, T., Loder, E. W., Mayo-Wilson, E., McDonald, S., McGuinness, L. A., Stewart, L. A., Thomas, J., Tricco, A. C., Welch, V. A., Whiting, P., and Moher, D. -"The PRISMA 2020 Statement: An Updated Guideline for Reporting Systematic Reviews". *PLOS Medicine* 18.3 (Mar. 2021), e1003583. ISSN: 1549-1676.

[400] Paik, J.-h., Ding, Z., Narurkar, R., Ramkissoon, S., Muller, F., Kamoun, W. S., Chae, S.-S., Zheng, H., Ying, H., Mahoney, J., Hiller, D., Jiang, S., Protopopov, A., Wong, W. H., Chin, L., Ligon, K. L., and DePinho, R. A. -"FoxOs Cooperatively Regulate Diverse Pathways Governing Neural Stem Cell Homeostasis". *Cell Stem Cell* 5.5 (Nov. 2009), pp. 540–553. ISSN: 1934-5909, 1875-9777.

[401] Palmqvist, S., Schöll, M., Strandberg, O., Mattsson, N., Stomrud, E., Zetterberg, H., Blennow, K., Landau, S., Jagust, W., and Hansson, O. -"Earliest Accumulation of β-Amyloid Occurs within the Default-Mode Network and Concurrently Affects Brain Connectivity". *Nature Communications* 8.1 (Oct. 2017), p. 1214. ISSN: 2041-1723.

[402] Paolicelli, R. C., Bolasco, G., Pagani, F., Maggi, L., Scianni, M., Panzanelli, P., Giustetto, M., Ferreira, T. A., Guiducci, E., Dumas, L., Ragozzino, D., and Gross, C. T. -"Synaptic Pruning by Microglia Is Necessary for Normal Brain Development". *Science* 333.6048 (Sept. 2011), pp. 1456–1458.

[403] Papp, B. and Plath, K. -"Reprogramming to Pluripotency: Stepwise Resetting of the Epigenetic Landscape". *Cell Research* 21.3 (Mar. 2011), pp. 486–501. ISSN: 1748-7838.

[404] Paquet, D., Bhat, R., Sydow, A., Mandelkow, E.-M., Berg, S., Hellberg, S., Fälting, J., Distel, M., Köster, R. W., Schmid, B., and Haass, C. -"A Zebrafish Model of Tauopathy Allows in Vivo Imaging of Neuronal Cell Death and Drug Evaluation". *The Journal of Clinical Investigation* 119.5 (May 2009), pp. 1382–1395. ISSN: 1558-8238.

[405] Park, Y.-G., Sohn, C. H., Chen, R., McCue, M., Yun, D. H., Drummond, G. T., Ku, T., Evans, N. B., Oak, H. C., Trieu, W., Choi, H., Jin, X., Lilascharoen, V., Wang, J., Truttmann, M. C., Qi, H. W., Ploegh, H. L., Golub, T. R., Chen, S.-C., Frosch, M. P., Kulik, H. J., Lim, B. K., and Chung, K. -"Protection of Tissue Physicochemical Properties Using Polyfunctional Crosslinkers". *Nature Biotechnology* 37.1 (Jan. 2019), pp. 73–83. ISSN: 1546-1696.

[406] Parra Bravo, C., Giani, A. M., Madero-Perez, J., Zhao, Z., Wan, Y., Samelson, A. J., Wong, M. Y., Evangelisti, A., Cordes, E., Fan, L., Ye, P., Zhu, D., Pozner, T., Mercedes, M., Patel, T., Yarahmady, A., Carling, G. K., Sterky, F. H., Lee, V. M. Y., Lee, E. B., DeTure, M., Dickson, D. W., Sharma, M., Mok, S.-A., Luo, W., Zhao, M., Kampmann, M., Gong, S., and Gan, L. -"Human iPSC 4R Tauopathy Model Uncovers Modifiers of Tau Propagation". *Cell* 187.10 (May 2024), 2446–2464.e22. ISSN: 1097-4172.

[407] Pașca, S. P., Arlotta, P., Bateup, H. S., Camp, J. G., Cappello, S., Gage, F. H., Knoblich, J. A., Kriegstein, A. R., Lancaster, M. A., Ming, G.-L., Muotri, A. R., Park, I.-H., Reiner, O., Song, H., Studer, L., Temple, S., Testa, G., Treutlein, B., and Vaccarino, F. M. -"A Nomenclature Consensus for Nervous System Organoids and Assembloids". *Nature* 609.7929 (Sept. 2022), pp. 907–910. ISSN: 1476-4687.

[408] Pașca, S. P., Arlotta, P., Bateup, H. S., Camp, J. G., Cappello, S., Gage, F. H., Knoblich, J. A., Kriegstein, A. R., Lancaster, M. A., Ming, G.-L., Novarino, G., Okano, H., Parmar, M., Park, I.-H., Reiner, O., Song, H., Studer, L., Takahashi, J., Temple, S., Testa, G., Treutlein, B., Vaccarino, F. M., Vanderhaeghen, P., and Young-Pearse, T. -"A Framework for Neural Organoids, Assembloids and Transplantation Studies". *Nature* 639.8054 (Mar. 2025), pp. 315–320. ISSN: 1476-4687.

[409] Paschal, B. M., Shpetner, H. S., and Vallee, R. B. -"MAP 1C Is a Microtubule-Activated ATPase Which Translocates Microtubules in Vitro and Has Dynein-like Properties". *The Journal of Cell Biology* 105.3 (Sept. 1987), pp. 1273–1282. ISSN: 0021-9525.

[410] Pavlov, P. F., Wiehager, B., Sakai, J., Frykman, S., Behbahani, H., Winblad, B., and Ankarcrona, M. -"Mitochondrial γ-Secretase Participates in the Metabolism of Mitochondria-Associated Amyloid Precursor Protein". *The FASEB Journal* 25.1 (2011), pp. 78–88. ISSN: 1530-6860.

[411] Payne, A. J., Gerdes, B. C., Naumchuk, Y., McCalley, A. E., Kaja, S., and Koulen, P. -"Presenilins Regulate the Cellular Activity of Ryanodine Receptors Differentially through Isotype-Specific N-terminal Cysteines". *Experimental Neurology* 250 (Dec. 2013), pp. 143–150. ISSN: 1090-2430.

[412] Peltola, M., Basnyat, P., Liimatainen, S., Rainesalo, S., Pesu, M., and Peltola, J. -"The Regulation of Plasma Interleukin-6 Levels Is Modified by Hippocampal Sclerosis and Its Lateralization in Drug-Resistant Temporal Lobe Epilepsy". *Acta Neurologica Scandinavica* 2023.1 (2023), p. 3030625. ISSN: 1600-0404.

[413] Penney, J., Ralvenius, W. T., Loon, A., Cerit, O., Dileep, V., Milo, B., Pao, P.-C., Woolf, H., and Tsai, L.-H. -"iPSC-derived Microglia Carrying the TREM2 R47H/+ Mutation Are Proinflammatory and Promote Synapse Loss". *Glia* 72.2 (Feb. 2024), pp. 452–469. ISSN: 1098-1136.

[414] Perdigão, C., Barata, M. A., Araújo, M. N., Mirfakhar, F. S., Castanheira, J., and Guimas Almeida, C. -"Intracellular Trafficking Mechanisms of Synaptic Dysfunction in Alzheimer's Disease". *Frontiers in Cellular Neuroscience* 14 (Apr. 2020), p. 72. ISSN: 1662-5102.

[415] Perez, S. E., Raghanti, M. A., Hof, P. R., Kramer, L., Ikonomovic, M. D., Lacor, P. N., Erwin, J. M., Sherwood, C. C., and Mufson, E. J. -"Alzheimer's Disease Pathology in the Neocortex and Hippocampus of the Western Lowland Gorilla (Gorilla Gorilla Gorilla)". *The Journal of Comparative Neurology* 521.18 (Dec. 2013), pp. 4318–4338. ISSN: 1096-9861.

[416] Perez, S. E., Sherwood, C. C., Cranfield, M. R., Erwin, J. M., Mudakikwa, A., Hof, P. R., and Mufson, E. J. -"Early Alzheimer's Disease-Type Pathology in the Frontal Cortex of Wild Mountain Gorillas (Gorilla Beringei Beringei)". *Neurobiology of aging* 39 (Mar. 2016), pp. 195–201. ISSN: 0197-4580.

[417] Petanjek, Z., Judaš, M., Šimić, G., Rašin, M. R., Uylings, H. B. M., Rakic, P., and Kostović, I. -"Extraordinary Neoteny of Synaptic Spines in the Human Prefrontal Cortex". *Proceedings of the National Academy of Sciences* 108.32 (Aug. 2011), pp. 13281–13286.

[418] Pfister, K. K., Wagner, M. C., Stenoien, D. L., Brady, S. T., and Bloom, G. S. -"Monoclonal Antibodies to Kinesin Heavy and Light Chains Stain Vesicle-like Structures, but Not Microtubules, in Cultured Cells." *Journal of Cell Biology* 108.4 (Apr. 1989), pp. 1453–1463. ISSN: 0021-9525.

[419] Phillips, E. C., Croft, C. L., Kurbatskaya, K., O'Neill, M. J., Hutton, M. L., Hanger, D. P., Garwood, C. J., and Noble, W. -"Astrocytes and Neuroinflammation in Alzheimer's Disease". *Biochemical Society Transactions* 42.5 (Sept. 2014), pp. 1321–1325. ISSN: 0300-5127.

[420] Piacentini, R., Civitelli, L., Ripoli, C., Marcocci, M. E., De Chiara, G., Garaci, E., Azzena, G. B., Palamara, A. T., and Grassi, C. -"HSV-1 Promotes Ca2+ -Mediated APP Phosphorylation and Aβ Accumulation in Rat Cortical Neurons". *Neurobiology of Aging* 32.12 (Dec. 2011), 2323.e13–26. ISSN: 1558-1497.

[421] Piacentini, R., Li Puma, D. D., Ripoli, C., Elena Marcocci, M., De Chiara, G., Garaci, E., Teresa Palamara, A., and Grassi, C. -"Herpes Simplex Virus Type-1 Infection Induces Synaptic Dysfunction in Cultured Cortical Neurons via GSK-3 Activation and Intraneuronal Amyloid-β Protein Accumulation". *Scientific Reports* 5.1 (Oct. 2015), p. 15444. ISSN: 2045-2322.

[422] Piller, C. -"Blots on a Field?" *Science (New York, N.Y.)* 377.6604 (July 2022), pp. 358–363. ISSN: 1095-9203.

[423] Plitzko, B. and Loesgen, S. -"Measurement of Oxygen Consumption Rate (OCR) and Extracellular Acidification Rate (ECAR) in Culture Cells for Assessment of the Energy Metabolism". *Bio-protocol* 8.10 (May 2018), e2850. ISSN: 2331-8325.

[424] Poliquin, L., Levine, G., and Shore, G. C. -"Involvement of Golgi Apparatus and a Restructured Nuclear Envelope during Biogenesis and Transport of Herpes Simplex Virus Glycoproteins." *Journal of Histochemistry & Cytochemistry* 33.9 (Sept. 1985), pp. 875–883. ISSN: 0022-1554.

[425] Polis, B. and Samson, A. O. -"Addressing the Discrepancies Between Animal Models and Human Alzheimer's Disease Pathology: Implications for Translational Research". *Journal of Alzheimer's Disease* 98.4 (Apr. 2024), pp. 1199–1218. ISSN: 1387-2877.

[426] Pomeshchik, Y., Klementieva, O., Gil, J., Martinsson, I., Hansen, M. G., de Vries, T., Sancho-Balsells, A., Russ, K., Savchenko, E., Collin, A., Vaz, A. R., Bagnoli, S., Nacmias, B., Rampon, C., Sorbi, S., Brites, D., Marko-Varga, G., Kokaia, Z., Rezeli, M., Gouras, G. K., and Roybon, L. -"Human iPSC-Derived Hippocampal Spheroids: An Innovative Tool for Stratifying Alzheimer Disease Patient-Specific Cellular Phenotypes and Developing Therapies". *Stem Cell Reports* 15.1 (July 2020), pp. 256–273. ISSN: 2213-6711.

[427] Poncelet, L., Ando, K., Vergara, C., Mansour, S., Suain, V., Yilmaz, Z., Reygel, A., Gilissen, E., Brion, J.-P., and Leroy, K. -"A 4R Tauopathy Develops without Amyloid Deposits in Aged Cat Brains". *Neurobiology of Aging* 81 (Sept. 2019), pp. 200–212. ISSN: 0197-4580.

[428] Poo, M.-M., Pignatelli, M., Ryan, T. J., Tonegawa, S., Bonhoeffer, T., Martin, K. C., Rudenko, A., Tsai, L.-H., Tsien, R. W., Fishell, G., Mullins, C., Gonçalves, J. T., Shtrahman, M., Johnston, S. T., Gage, F. H., Dan, Y., Long, J., Buzsáki, G., and Stevens, C. -"What Is Memory? The Present State of the Engram". *BMC biology* 14 (May 2016), p. 40. ISSN: 1741-7007.

[429] Popp, B., Krumbiegel, M., Grosch, J., Sommer, A., Uebe, S., Kohl, Z., Plötz, S., Farrell, M., Trautmann, U., Kraus, C., Ekici, A. B., Asadollahi, R., Regensburger, M., Günther, K., Rauch, A., Edenhofer, F., Winkler, J., Winner, B., and Reis, A. -"Need for High-Resolution Genetic Analysis in iPSC: Results and Lessons from the ForIPS Consortium". *Scientific Reports* 8.1 (Nov. 2018), p. 17201. ISSN: 2045-2322.

[430] Qi, C., Verheijen, B. M., Kokubo, Y., Shi, Y., Tetter, S., Murzin, A. G., Nakahara, A., Morimoto, S., Vermulst, M., Sasaki, R., Aronica, E., Hirokawa, Y., Oyanagi, K., Kakita, A., Ryskeldi-Falcon, B., Yoshida, M., Hasegawa, M., Scheres, S. H. W., and Goedert, M. -"Tau Filaments from Amyotrophic Lateral Sclerosis/Parkinsonism-Dementia Complex Adopt the CTE Fold". *Proceedings of the National Academy of Sciences of the United States of America* 120.51 (Dec. 2023), e2306767120. ISSN: 1091-6490.

[431] Qu, B., Mu, Q., Bi, H., Chen, Y., Wang, Q., Ma, X., and Lu, L. -"Interpretation of the Past, Present, and Future of Organoid Technology: An Updated Bibliometric Analysis from 2009 to 2024". *Frontiers in Cell and Developmental Biology* 12 (2024), p. 1433111. ISSN: 2296-634X.

[432] Quintana, D. D., Garcia, J. A., Anantula, Y., Rellick, S. L., Engler-Chiurazzi, E. B., Sarkar, S. N., Brown, C. M., and Simpkins, J. W. -"Amyloid-β Causes Mitochondrial Dysfunction via a Ca2+-Driven Upregulation of Oxidative Phosphorylation and Superoxide Production in Cerebrovascular Endothelial Cells". *Journal of Alzheimer's disease: JAD* 75.1 (2020), pp. 119–138. ISSN: 1875-8908.

[433] Radde, R., Bolmont, T., Kaeser, S. A., Coomaraswamy, J., Lindau, D., Stoltze, L., Calhoun, M. E., Jäggi, F., Wolburg, H., Gengler, S., Haass, C., Ghetti, B., Czech, C., Hölscher, C., Mathews, P. M., and Jucker, M. -"Abeta42-Driven Cerebral Amyloidosis in Transgenic Mice Reveals Early and Robust Pathology". *EMBO reports* 7.9 (Sept. 2006), pp. 940–946. ISSN: 1469-221X.

[434] Rajan, K. B., Weuve, J., Barnes, L. L., McAninch, E. A., Wilson, R. S., and Evans, D. A. -"Population Estimate of People with Clinical Alzheimer's Disease and Mild Cognitive Impairment in the United States (2020–2060)". *Alzheimer's & Dementia* 17.12 (2021), pp. 1966–1975. ISSN: 1552-5279.

[435] Rajavashisth, T. B., Kaptein, J. S., Reue, K. L., and Lusis, A. J. -"Evolution of Apolipoprotein E: Mouse Sequence and Evidence for an 11-Nucleotide Ancestral Unit." *Proceedings of the National Academy of Sciences* 82.23 (Dec. 1985), pp. 8085–8089.

[436] Rajendran, L., Honsho, M., Zahn, T. R., Keller, P., Geiger, K. D., Verkade, P., and Simons, K. -"Alzheimer's Disease Beta-Amyloid Peptides Are Released in Association with Exosomes". *Proceedings of the National Academy of Sciences of the United States of America* 103.30 (July 2006), pp. 11172–11177. ISSN: 0027-8424.

[437] Rakic, P. -"Guidance of Neurons Migrating to the Fetal Monkey Neocortex". *Brain Research* 33.2 (Oct. 1971), pp. 471–476. ISSN: 0006-8993.

[438] Ramchandani, M., Kong, M., Tronstein, E., Selke, S., Mikhaylova, A., Magaret, A., Huang, M.-L., Johnston, C., Corey, L., and Wald, A. -"Herpes Simplex Virus Type 1 Shedding in Tears, and Nasal and Oral Mucosa of Healthy Adults". *Sexually transmitted diseases* 43.12 (Dec. 2016), pp. 756–760. ISSN: 0148-5717.

[439] Ramey, G. D., Tang, A., Phongpreecha, T., Yang, M. M., Woldemariam, S. R., Oskotsky, T. T., Montine, T. J., Allen, I., Miller, Z. A., Aghaeepour, N., Capra, J. A., and Sirota, M. -"Exposure to Autoimmune Disorders Increases Alzheimer's Disease Risk in a Multi-Site Electronic Health Record Analysis". May 2024. (Prepublished).

[440] Ramnauth, A. D., Tippani, M., Divecha, H. R., Papariello, A. R., Miller, R. A., Nelson, E. D., Thompson, J. R., Pattie, E. A., Kleinman, J. E., Maynard, K. R., Collado-Torres, L., Hyde, T. M., Martinowich, K., Hicks, S. C., and Page, S. C. -"Spatiotemporal Analysis of Gene Expression in the Human Dentate Gyrus Reveals Age-Associated Changes in Cellular Maturation and Neuroinflammation". *Cell Reports* 44.2 (Feb. 2025), p. 115300. ISSN: 2211-1247.

[441] Ramón y Cajal, S. -"Textura del sistema nervioso del hombre y de los vertebrados : estudios sobre el plan estructural y composición histológica de los centros nerviosos adicionados de consideraciones fisiológicas fundadas en los nuevos descubrimientos. Volumen III". Madrid : Nicolás Moya, 1904.

[442] Rao, Y. L., Ganaraja, B., Murlimanju, B. V., Joy, T., Krishnamurthy, A., and Agrawal, A. -"Hippocampus and Its Involvement in Alzheimer's Disease: A Review". *3 Biotech* 12.2 (Feb. 2022), p. 55. ISSN: 2190-5738.

[443] Rapp, A., Gmeiner, B., and Hüttinger, M. -"Implication of apoE Isoforms in Cholesterol Metabolism by Primary Rat Hippocampal Neurons and Astrocytes". *Biochimie* 88.5 (May 2006), pp. 473–483. ISSN: 0300-9084.

[444] Readhead, B., Haure-Mirande, J.-V., Funk, C. C., Richards, M. A., Shannon, P., Haroutunian, V., Sano, M., Liang, W. S., Beckmann, N. D., Price, N. D., Reiman, E. M., Schadt, E. E., Ehrlich, M. E., Gandy, S., and Dudley, J. T. -"Multiscale Analysis of Independent Alzheimer's Cohorts Finds Disruption of Molecular, Genetic, and Clinical Networks by Human Herpesvirus". *Neuron* 99.1 (July 2018), 64–82.e7. ISSN: 0896-6273.

[445] Reddy, P. H. -"Abnormal Tau, Mitochondrial Dysfunction, Impaired Axonal Transport of Mitochondria, and Synaptic Deprivation in Alzheimer's Disease". *Brain Research* 1415 (Sept. 2011), pp. 136–148. ISSN: 0006-8993.

[446] Reisberg, B., Doody, R., Stöffler, A., Schmitt, F., Ferris, S., Möbius, H. J., and Memantine Study Group. -"Memantine in Moderate-to-Severe Alzheimer's Disease". *The New England Journal of Medicine* 348.14 (Apr. 2003), pp. 1333–1341. ISSN: 1533-4406.

[447] Reitz, C., Honig, L., Vonsattel, J. P., Tang, M.-X., and Mayeux, R. -"Memory Performance Is Related to Amyloid and Tau Pathology in the Hippocampus". *Journal of neurology, neurosurgery, and psychiatry* 80.7 (July 2009), pp. 715–721. ISSN: 0022-3050.

[448] Renault, V. M., Rafalski, V. A., Morgan, A. A., Salih, D. A. M., Brett, J. O., Webb, A. E., Villeda, S. A., Thekkat, P. U., Guillerey, C., Denko, N. C., Palmer, T. D., Butte, A. J., and Brunet, A. -"FoxO3 Regulates Neural Stem Cell Homeostasis". *Cell Stem Cell* 5.5 (Nov. 2009), pp. 527–539. ISSN: 1934-5909, 1875-9777.

[449] Rienecker, K. D. A., Poston, R. G., and Saha, R. N. -"Merits and Limitations of Studying Neuronal Depolarization-Dependent Processes Using Elevated External Potassium". *ASN NEURO* 12 (Nov. 2020), p. 1759091420974807. ISSN: 1759-0914.

[450] Rivera, T., Zhao, Y., Ni, Y., and Wang, J. -"Human-Induced Pluripotent Stem Cell Culture Methods Under cGMP Conditions". *Current Protocols in Stem Cell Biology* 54.1 (2020), e117. ISSN: 1938-8969.

[451] Rivers-Auty, J., Mather, A. E., Peters, R., Lawrence, C. B., Brough, D., and Alzheimer's Disease Neuroimaging Initiative. -"Anti-Inflammatories in Alzheimer's Disease—Potential Therapy or Spurious Correlate?" *Brain Communications* 2.2 (July 2020), fcaa109. ISSN: 2632-1297.

[452] Rizzu, P., Swieten, J. C. V., Joosse, M., Hasegawa, M., Stevens, M., Tibben, A., Niermeijer, M. F., Hillebrand, M., Ravid, R., Oostra, B. A., Goedert, M., Duijn, C. M. van, and Heutink, P. -"High Prevalence of Mutations in the Microtubule-Associated Protein Tau in a Population Study of Frontotemporal Dementia in the Netherlands". *The American Journal of Human Genetics* 64.2 (Feb. 1999), pp. 414–421. ISSN: 0002-9297, 1537-6605.

[453] Rodríguez-Martín, T., Cuchillo-Ibáñez, I., Noble, W., Nyenya, F., Anderton, B. H., and Hanger, D. P. -"Tau Phosphorylation Affects Its Axonal Transport and Degradation". *Neurobiology of Aging* 34.9 (Sept. 2013), pp. 2146–2157. ISSN: 0197-4580.

[454] Rogaev, E. I., Sherrington, R., Rogaeva, E. A., Levesque, G., Ikeda, M., Liang, Y., Chi, H., Lin, C., Holman, K., and Tsuda, T. -"Familial Alzheimer's Disease in Kindreds with Missense Mutations in a Gene on Chromosome 1 Related to the Alzheimer's Disease Type 3 Gene". *Nature* 376.6543 (Aug. 1995), pp. 775–778. ISSN: 0028-0836.

[455] Rogaeva, E., Kawarai, T., and George-Hyslop, P. S. -"Genetic Complexity of Alzheimer's Disease: Successes and Challenges". *Journal of Alzheimer's Disease* 9.s3 (July 2006), pp. 381–387. ISSN: 1387-2877.

[456] Rohani, H., Arjmand, R., Mozhgani, S.-H., Shafiee, A., Amini, M. J., and Forghani-Ramandi, M.-M. -"The Worldwide Prevalence of Herpes Simplex Virus Encephalitis and Meningitis: A Systematic Review and Meta-Analysis". *Turkish Archives of Pediatrics* 58.6 (Nov. 2023), pp. 580–587. ISSN: 2757-6256.

[457] Rosebrock, D., Arora, S., Mutukula, N., Volkman, R., Gralinska, E., Balaskas, A., Aragonés Hernández, A., Buschow, R., Brändl, B., Müller, F.-J., Arndt, P. F., Vingron, M., and Elkabetz, Y. -"Enhanced Cortical Neural Stem Cell Identity through Short SMAD and WNT Inhibition in Human Cerebral Organoids Facilitates Emergence of Outer Radial Glial Cells". *Nature Cell Biology* 24.6 (June 2022), pp. 981–995. ISSN: 1476-4679.

[458] Rosen, R. F., Tomidokoro, Y., Farberg, A. S., Dooyema, J., Ciliax, B., Preuss, T. M., Neubert, T. A., Ghiso, J. A., LeVine, H., and Walker, L. C. -"Comparative Pathobiology of β-Amyloid and the Unique Susceptibility of Humans to Alzheimer's Disease". *Neurobiology of Aging* 44 (Aug. 2016), pp. 185–196. ISSN: 1558-1497.

[459] Rosen, R. F., Walker, L. C., and Levine, H. -"PIB Binding in Aged Primate Brain: Enrichment of High-Affinity Sites in Humans with Alzheimer's Disease". *Neurobiology of Aging* 32.2 (Feb. 2011), pp. 223–234. ISSN: 1558-1497.

[460] Ross, J. M., Stewart, J. B., Hagström, E., Brené, S., Mourier, A., Coppotelli, G., Freyer, C., Lagouge, M., Hoffer, B. J., Olson, L., and Larsson, N.-G. -"Germline Mitochondrial DNA Mutations Aggravate Ageing and Can Impair Brain Development". *Nature* 501.7467 (Sept. 2013), pp. 412–415. ISSN: 1476-4687.

[461] Roy, S., Zhang, B., Lee, V. M.-Y., and Trojanowski, J. Q. -"Axonal Transport Defects: A Common Theme in Neurodegenerative Diseases". *Acta Neuropathologica* 109.1 (Jan. 2005), pp. 5–13. ISSN: 0001-6322.

[462] Rupp, C., Beyreuther, K., Maurer, K., and Kins, S. -"A Presenilin 1 Mutation in the First Case of Alzheimer's Disease: Revisited". *Alzheimer's & Dementia* 10.6 (2014), pp. 869–872. ISSN: 1552-5279.

[463] Russell, T. A. and Tscharke, D. C. -"Lytic Promoters Express Protein during Herpes Simplex Virus Latency". *PLOS Pathogens* 12.6 (June 2016), e1005729. ISSN: 1553-7374.

[464] Ryan, K. C., Ashkavand, Z., Sarasija, S., Laboy, J. T., Samarakoon, R., and Norman, K. R. -"Increased Mitochondrial Calcium Uptake and Concomitant Mitochondrial Activity by Presenilin Loss Promotes mTORC1 Signaling to Drive Neurodegeneration". *Aging Cell* 20.10 (2021), e13472. ISSN: 1474-9726.

[465] Sahlender, D. A., Kozik, P., Miller, S. E., Peden, A. A., and Robinson, M. S. -"Uncoupling the Functions of CALM in VAMP Sorting and Clathrin-Coated Pit Formation". *PLOS ONE* 8.5 (May 2013), e64514. ISSN: 1932-6203.

[466] Saito, T., Matsuba, Y., Mihira, N., Takano, J., Nilsson, P., Itohara, S., Iwata, N., and Saido, T. C. -"Single App Knock-in Mouse Models of Alzheimer's Disease". *Nature Neuroscience* 17.5 (May 2014), pp. 661–663. ISSN: 1546-1726.

[467] Sakaguchi, H., Kadoshima, T., Soen, M., Narii, N., Ishida, Y., Ohgushi, M., Takahashi, J., Eiraku, M., and Sasai, Y. -"Generation of Functional Hippocampal Neurons from Self-Organizing Human Embryonic Stem Cell-Derived Dorsomedial Telencephalic Tissue". *Nature Communications* 6.1 (Nov. 2015), p. 8896. ISSN: 2041-1723.

[468] Saksena, M. M., Wakisaka, H., Tijono, B., Boadle, R. A., Rixon, F., Takahashi, H., and Cunningham, A. L. -"Herpes Simplex Virus Type 1 Accumulation, Envelopment, and Exit in Growth Cones and Varicosities in Mid-Distal Regions of Axons". *Journal of Virology* 80.7 (Apr. 2006), pp. 3592–3606. ISSN: 0022-538X.

[469] Salazar, C., Valdivia, G., Ardiles, Á. O., Ewer, J., and Palacios, A. G. -"Genetic Variants Associated with Neurodegenerative Alzheimer Disease in Natural Models". *Biological Research* 49 (Feb. 2016), p. 14. ISSN: 0717-6287.

[470] Salgado, B., Sastre, I., Bullido, M. J., and Aldudo, J. -"Herpes Simplex Virus Type 1 Induces AD-like Neurodegeneration Markers in Human Progenitor and Differentiated ReNcell VM Cells". *Microorganisms* 11.5 (May 2023), p. 1205. ISSN: 2076-2607.

[471] Salloway, S., Sperling, R., Fox, N. C., Blennow, K., Klunk, W., Raskind, M., Sabbagh, M., Honig, L. S., Porsteinsson, A. P., Ferris, S., Reichert, M., Ketter, N., Nejadnik, B., Guenzler, V., Miloslavsky, M., Wang, D., Lu, Y., Lull, J., Tudor, I. C., Liu, E., Grundman, M., Yuen, E., Black, R., and Brashear, H. R. -"Two Phase 3 Trials of Bapineuzumab in Mild-to-Moderate Alzheimer's Disease". *New England Journal of Medicine* 370.4 (Jan. 2014), pp. 322–333. ISSN: 0028-4793.

[472] Sama, D. M. and Norris, C. M. -"Calcium Dysregulation and Neuroinflammation: Discrete and Integrated Mechanisms for Age-Related Synaptic Dysfunction". *Ageing Research Reviews* 12.4 (Sept. 2013), pp. 982–995. ISSN: 1872-9649.

[473] Sancho, R., Cremona, C. A., and Behrens, A. -"Stem Cell and Progenitor Fate in the Mammalian Intestine: Notch and Lateral Inhibition in Homeostasis and Disease". *EMBO reports* 16.5 (May 2015), pp. 571–581. ISSN: 1469-221X.

[474] Sandoval, S. O., Cappuccio, G., Kruth, K., Osenberg, S., Khalil, S. M., Méndez-Albelo, N. M., Padmanabhan, K., Wang, D., Niciu, M. J., Bhattacharyya, A., Stein, J. L., Sousa, A. M. M., Waxman, E. A., Buttermore, E. D., Whye, D., Sirois, C. L., Anderson, S., Anita, Bhattacharyya, Buttermore, E., Chang, Q., French, D., Hashimoto-Torii, K., Kornblum, H., Kroll, K., Lachman, H. M., Maletic-Savatic, M., Niciu, M., Novitch, B., Padmanabhan, K., Proschel, C., Sahin, M., Sousa, A., Stein, J., Wang, D., Waxman, E., Whye, D., Williams, A., Zhao, X., Williams, A., Maletic-Savatic, M., and Zhao, X. -"Rigor and Reproducibility in Human Brain Organoid Research: Where We Are and Where We Need to Go". *Stem Cell Reports* 19.6 (June 2024), pp. 796–816. ISSN: 2213-6711.

[475] Sannerud, R., Esselens, C., Ejsmont, P., Mattera, R., Rochin, L., Tharkeshwar, A. K., De Baets, G., De Wever, V., Habets, R., Baert, V., Vermeire, W., Michiels, C., Groot, A. J., Wouters, R., Dillen, K., Vints, K., Baatsen, P., Munck, S., Derua, R., Waelkens, E., Basi, G. S., Mercken, M., Vooijs, M., Bollen, M., Schymkowitz, J., Rousseau, F., Bonifacino, J. S., Van Niel, G., De Strooper, B., and Annaert, W. -"Restricted Location of PSEN2/γ-Secretase Determines Substrate Specificity and Generates an Intracellular Aβ Pool". *Cell* 166.1 (June 2016), pp. 193–208. ISSN: 1097-4172.

[476] Santacruz, K., Lewis, J., Spires, T., Paulson, J., Kotilinek, L., Ingelsson, M., Guimaraes, A., DeTure, M., Ramsden, M., McGowan, E., Forster, C., Yue, M., Orne, J., Janus, C., Mariash, A., Kuskowski, M., Hyman, B., Hutton, M., and Ashe, K. H. -"Tau Suppression in a Neurodegenerative Mouse Model Improves Memory Function". *Science (New York, N.Y.)* 309.5733 (July 2005), pp. 476–481. ISSN: 1095-9203.

[477] Santana, S., Recuero, M., Bullido, M. J., Valdivieso, F., and Aldudo, J. -"Herpes Simplex Virus Type I Induces the Accumulation of Intracellular β-Amyloid in Autophagic Compartments and the Inhibition of the Non-Amyloidogenic Pathway in Human Neuroblastoma Cells". *Neurobiology of Aging* 33.2 (Feb. 2012), 430.e19–430.e33. ISSN: 01974580.

[478] Sardo, V. L., Ferguson, W., Erikson, G. A., Topol, E. J., Baldwin, K. K., and Torkamani, A. -"The Effect of Aging on Human Induced Pluripotent Stem Cells". *Nature biotechnology* 35.1 (Jan. 2017), pp. 69–74. ISSN: 1087-0156.

[479] Sato, T., Vries, R. G., Snippert, H. J., van de Wetering, M., Barker, N., Stange, D. E., van Es, J. H., Abo, A., Kujala, P., Peters, P. J., and Clevers, H. -"Single Lgr5 Stem Cells Build Crypt-Villus Structures in Vitro without a Mesenchymal Niche". *Nature* 459.7244 (May 2009), pp. 262–265. ISSN: 1476-4687.

[480] Saura, C. A. -"Presenilin/Gamma-Secretase and Inflammation". *Frontiers in Aging Neuroscience* 2 (2010), p. 16. ISSN: 1663-4365.

[481] Saveri, P., De Luca, M., Nisi, V., Pisciotta, C., Romano, R., Piscosquito, G., Reilly, M. M., Polke, J. M., Cavallaro, T., Fabrizi, G. M., Fossa, P., Cichero, E., Lombardi, R., Lauria, G., Magri, S., Taroni, F., Pareyson, D., and Bucci, C. -"Charcot-Marie-Tooth Type 2B: A New Phenotype Associated with a Novel RAB7A Mutation and Inhibited EGFR Degradation". *Cells* 9.4 (Apr. 2020), p. 1028. ISSN: 2073-4409.

[482] Saw, G., Krishna, K., Gupta, N., Soong, T. W., Mallilankaraman, K., Sajikumar, S., and Dheen, S. T. -"Epigenetic Regulation of Microglial Phosphatidylinositol 3-Kinase Pathway Involved in Long-Term Potentiation and Synaptic Plasticity in Rats". *Glia* 68.3 (2020), pp. 656–669. ISSN: 1098-1136.

[483] Scearce-Levie, K., Sanchez, P. E., and Lewcock, J. W. -"Leveraging Preclinical Models for the Development of Alzheimer Disease Therapeutics". *Nature Reviews Drug Discovery* 19.7 (July 2020), pp. 447–462. ISSN: 1474-1784.

[484] Schaefer, T., Mittal, N., Wang, H., Ataman, M., Candido, S., Lötscher, J., Velychko, S., Tintignac, L., Bock, T., Börsch, A., Baßler, J., Rao, T. N., Zmajkovic, J., Roffeis, S., Löliger, J., Jacob, F., Dumlin, A., Schürch, C., Schmidt, A., Skoda, R. C., Wymann, M. P., Hess, C., Schöler, H. R., Zaehres, H., Hurt, E., Zavolan, M., and Lengerke, C. -"Nuclear and Cytosolic Fractions of SOX2 Synergize as Transcriptional and Translational Co-Regulators of Cell Fate". *Cell Reports* 43.10 (Oct. 2024), p. 114807. ISSN: 2211-1247.

[485] Scheff, S. W., Price, D. A., Schmitt, F. A., and Mufson, E. J. -"Hippocampal Synaptic Loss in Early Alzheimer's Disease and Mild Cognitive Impairment". *Neurobiology of Aging* 27.10 (Oct. 2006), pp. 1372–1384. ISSN: 0197-4580.

[486] Scheffer, S., Hermkens, D. M., van der Weerd, L., de Vries, H. E., and Daemen, M. J. -"Vascular Hypothesis of Alzheimer Disease". *Arteriosclerosis, Thrombosis, and Vascular Biology* 41.4 (Apr. 2021), pp. 1265–1283.

[487] Scheper, W., Zwart, R., van der Sluijs, P., Annaert, W., Gool, W. A., and Baas, F. -"Alzheimer's Presenilin 1 Is a Putative Membrane Receptor for Rab GDP Dissociation Inhibitor". *Human Molecular Genetics* 9.2 (Jan. 2000), pp. 303–310. ISSN: 0964-6906.

[488] Scheper, W., Zwart, R., and Baas, F. -"Rab6 Membrane Association Is Dependent of Presenilin 1 and Cellular Phosphorylation Events". *Brain Research. Molecular Brain Research* 122.1 (Mar. 2004), pp. 17–23. ISSN: 0169-328X.

[489] Schiffer, J. T., Mayer, B. T., Fong, Y., Swan, D. A., and Wald, A. -"Herpes Simplex Virus-2 Transmission Probability Estimates Based on Quantity of Viral Shedding". *Journal of The Royal Society Interface* 11.95 (June 2014), p. 20140160.

[490] Schmidt, F., Boltze, J., Jäger, C., Hofmann, S., Willems, N., Seeger, J., Härtig, W., and Stolzing, A. -"Detection and Quantification of β-Amyloid, Pyroglutamyl Aβ, and Tau in Aged Canines". *Journal of Neuropathology and Experimental Neurology* 74.9 (Sept. 2015), pp. 912–923. ISSN: 1554-6578.

[491] Schuck, S., Prinz, W. A., Thorn, K. S., Voss, C., and Walter, P. -"Membrane Expansion Alleviates Endoplasmic Reticulum Stress Independently of the Unfolded Protein Response". *Journal of Cell Biology* 187.4 (Nov. 2009), pp. 525–536. ISSN: 0021-9525.

[492] Schultz, C., Hubbard, G. B., Rüb, U., Braak, E., and Braak, H. -"Age-Related Progression of Tau Pathology in Brains of Baboons". *Neurobiology of Aging* 21.6 (Nov. 2000), pp. 905–912. ISSN: 0197-4580.

[493] Schütt, T., Helboe, L., Pedersen, L. Ø., Waldemar, G., Berendt, M., and Pedersen, J. T. -"Dogs with Cognitive Dysfunction as a Spontaneous Model for Early Alzheimer's Disease: A Translational Study of Neuropathological and Inflammatory Markers". *Journal of Alzheimer's disease: JAD* 52.2 (Mar. 2016), pp. 433–449. ISSN: 1875-8908.

[494] Seaks, C. E. and Wilcock, D. M. -"Infectious Hypothesis of Alzheimer Disease". *PLoS Pathogens* 16.11 (Nov. 2020), e1008596. ISSN: 1553-7366.

[495] Selkoe, D. J. and Hardy, J. -"The Amyloid Hypothesis of Alzheimer's Disease at 25 Years". *EMBO Molecular Medicine* 8.6 (June 2016), pp. 595–608. ISSN: 1757-4676.

[496] Sexton, C., Snyder, H., Beher, D., Boxer, A. L., Brannelly, P., Brion, J.-P., Buée, L., Cacace, A. M., Chételat, G., Citron, M., DeVos, S. L., Diaz, K., Feldman, H. H., Frost, B., Goate, A. M., Gold, M., Hyman, B., Johnson, K., Karch, C. M., Kerwin, D. R., Koroshetz, W. J., Litvan, I., Morris, H. R., Mummery, C. J., Mutamba, J., Patterson, M. C., Quiroz, Y. T., Rabinovici, G. D., Rommel, A., Shulman, M. B., Toledo-Sherman, L. M., Weninger, S., Wildsmith, K. R., Worley, S. L., and Carrillo, M. C. -"Current Directions in Tau Research: Highlights from Tau 2020". *Alzheimer's & Dementia* 18.5 (2022), pp. 988–1007. ISSN: 1552-5279.

[497] Shabani, K., Pigeon, J., Benaissa Touil Zariouh, M., Liu, T., Saffarian, A., Komatsu, J., Liu, E., Danda, N., Becmeur-Lefebvre, M., Limame, R., Bohl, D., Parras, C., and Hassan, B. A. -"The Temporal Balance between Self-Renewal and Differentiation of Human Neural Stem Cells Requires the Amyloid Precursor Protein". *Science Advances* 9.24 (June 2023), eadd5002.

[498] Shah, D. D., Raghani, N. R., Chorawala, M. R., Singh, S., and Prajapati, B. G. -"Harnessing Three-Dimensional (3D) Cell Culture Models for Pulmonary Infections: State of the Art and Future Directions". *Naunyn-Schmiedeberg's Archives of Pharmacology* 396.11 (Nov. 2023), pp. 2861–2880. ISSN: 1432-1912.

[499] Sharf, T., van der Molen, T., Glasauer, S. M. K., Guzman, E., Buccino, A. P., Luna, G., Cheng, Z., Audouard, M., Ranasinghe, K. G., Kudo, K., Nagarajan, S. S., Tovar, K. R., Petzold, L. R., Hierlemann, A., Hansma, P. K., and Kosik, K. S. -"Functional Neuronal Circuitry and Oscillatory Dynamics in Human Brain Organoids". *Nature Communications* 13.1 (July 2022), p. 4403. ISSN: 2041-1723.

[500] Sharp, A. H., McPherson, P. S., Dawson, T. M., Aoki, C., Campbell, K. P., and Snyder, S. H. -"Differential Immunohistochemical Localization of Inositol 1,4,5-Trisphosphate- and Ryanodine-Sensitive Ca2+ Release Channels in Rat Brain". *The Journal of Neuroscience: The Official Journal of the Society for Neuroscience* 13.7 (July 1993), pp. 3051–3063. ISSN: 0270-6474.

[501] Sherrington, R., Rogaev, E. I., Liang, Y., Rogaeva, E. A., Levesque, G., Ikeda, M., Chi, H., Lin, C., Li, G., Holman, K., Tsuda, T., Mar, L., Foncin, J.-F., Bruni, A. C., Montesi, M. P., Sorbi, S., Rainero, I., Pinessi, L., Nee, L., Chumakov, I., Pollen, D., Brookes, A., Sanseau, P., Polinsky, R. J., Wasco, W., Da Silva, H. a. R., Haines, J. L., Pericak-Vance, M. A., Tanzi, R. E., Roses, A. D., Fraser, P. E., Rommens, J. M., and St George-Hyslop, P. H. -"Cloning of a Gene Bearing Missense Mutations in Early-Onset Familial Alzheimer's Disease". *Nature* 375.6534 (June 1995), pp. 754–760. ISSN: 1476-4687.

[502] Shi, Y., Kirwan, P., Smith, J., Robinson, H. P. C., and Livesey, F. J. -"Human Cerebral Cortex Development from Pluripotent Stem Cells to Functional Excitatory Synapses". *Nature Neuroscience* 15.3 (Mar. 2012), pp. 477–486. ISSN: 1546-1726.

[503] Sierra, A., Encinas, J. M., Deudero, J. J. P., Chancey, J. H., Enikolopov, G., Overstreet-Wadiche, L. S., Tsirka, S. E., and Maletic-Savatic, M. -"Microglia Shape Adult Hippocampal Neurogenesis through Apoptosis-Coupled Phagocytosis". *Cell Stem Cell* 7.4 (Oct. 2010), pp. 483–495. ISSN: 1934-5909, 1875-9777.

[504] Singh, N. and Tscharke, D. C. -"Herpes Simplex Virus Latency Is Noisier the Closer We Look". *Journal of Virology* 94.4 (Jan. 2020), 10.1128/jvi.01701–19.

[505] Small, D. H., Gasperini, R., Vincent, A. J., Hung, A. C., and Foa, L. -"The Role of Abeta-induced Calcium Dysregulation in the Pathogenesis of Alzheimer's Disease". *Journal of Alzheimer's disease: JAD* 16.2 (2009), pp. 225–233. ISSN: 1387-2877.

[506] Smith, I. F., Hitt, B., Green, K. N., Oddo, S., and LaFerla, F. M. -"Enhanced Caffeine-Induced Ca2+ Release in the 3xTg-AD Mouse Model of Alzheimer's Disease". *Journal of Neurochemistry* 94.6 (2005), pp. 1711–1718. ISSN: 1471-4159.

[507] Smolek, T., Madari, A., Farbakova, J., Kandrac, O., Jadhav, S., Cente, M., Brezovakova, V., Novak, M., and Zilka, N. -"Tau Hyperphosphorylation in Synaptosomes and Neuroinflammation Are Associated with Canine Cognitive Impairment". *The Journal of Comparative Neurology* 524.4 (Mar. 2016), pp. 874–895. ISSN: 1096-9861.

[508] Snyder, A., Polcicova, K., and Johnson, D. C. -"Herpes Simplex Virus gE/gI and US9 Proteins Promote Transport of Both Capsids and Virion Glycoproteins in Neuronal Axons". *Journal of Virology* 82.21 (Nov. 2008), pp. 10613–10624. ISSN: 1098-5514.

[509] Snyder, A., Wisner, T. W., and Johnson, D. C. -"Herpes Simplex Virus Capsids Are Transported in Neuronal Axons without an Envelope Containing the Viral Glycoproteins". *Journal of Virology* 80.22 (Nov. 2006), pp. 11165–11177. ISSN: 0022-538X.

[510] Snyder, E. M., Nong, Y., Almeida, C. G., Paul, S., Moran, T., Choi, E. Y., Nairn, A. C., Salter, M. W., Lombroso, P. J., Gouras, G. K., and Greengard, P. -"Regulation of NMDA Receptor Trafficking by Amyloid-β". *Nature Neuroscience* 8.8 (Aug. 2005), pp. 1051–1058. ISSN: 1546-1726.

[511] Steele, J. C. -"Parkinsonism-Dementia Complex of Guam". *Movement Disorders: Official Journal of the Movement Disorder Society* 20 Suppl 12 (Aug. 2005), S99–S107. ISSN: 0885-3185.

[512] Steffen, J., Krohn, M., Paarmann, K., Schwitlick, C., Brüning, T., Marreiros, R., Müller-Schiffmann, A., Korth, C., Braun, K., and Pahnke, J. -"Revisiting Rodent Models: Octodon Degus as Alzheimer's Disease Model?" *Acta Neuropathologica Communications* 4.1 (Aug. 2016), p. 91. ISSN: 2051-5960.

[513] Stephens, R. E. and Edds, K. T. -"Microtubules: Structure, Chemistry, and Function". *Physiological Reviews* 56.4 (Oct. 1976), pp. 709–777. ISSN: 0031-9333.

[514] Stergiopoulos, A., Elkouris, M., and Politis, P. K. -"Prospero-Related Homeobox 1 (Prox1) at the Crossroads of Diverse Pathways during Adult Neural Fate Specification". *Frontiers in Cellular Neuroscience* 8 (Jan. 2015), p. 454. ISSN: 1662-5102.

[515] Sturchler-Pierrat, C., Abramowski, D., Duke, M., Wiederhold, K. H., Mistl, C., Rothacher, S., Ledermann, B., Bürki, K., Frey, P., Paganetti, P. A., Waridel, C., Calhoun, M. E., Jucker, M., Probst, A., Staufenbiel, M., and Sommer, B. -"Two Amyloid Precursor Protein Transgenic Mouse Models with Alzheimer Disease-like Pathology". *Proceedings of the National Academy of Sciences of the United States of America* 94.24 (Nov. 1997), pp. 13287–13292. ISSN: 0027-8424.

[516] Sturchler-Pierrat, C. and Staufenbiel, M. -"Pathogenic Mechanisms of Alzheimer's Disease Analyzed in the APP23 Transgenic Mouse Model". *Annals of the New York Academy of Sciences* 920 (2000), pp. 134–139. ISSN: 0077-8923.

[517] Sun, L., Zhou, R., Yang, G., and Shi, Y. -"Analysis of 138 Pathogenic Mutations in Presenilin-1 on the in Vitro Production of Aβ42 and Aβ40 Peptides by γ-Secretase". *Proceedings of the National Academy of Sciences of the United States of America* 114.4 (Jan. 2017), E476–E485. ISSN: 1091-6490.

[518] Sun, Y., Liu, Z., Zhang, Z., Kang, Y., Wang, X., Zhang, Y., Liu, Y., and Zhao, P. -"Human Induced Pluripotent Stem Cell Models for Alzheimer's Disease Research: A Bibliometric Analysis". *Frontiers in Human Neuroscience* 19 (Mar. 2025), p. 1548701. ISSN: 1662-5161.

[519] Sutter, E., de Oliveira, A. P., Tobler, K., Schraner, E. M., Sonda, S., Kaech, A., Lucas, M. S., Ackermann, M., and Wild, P. -"Herpes Simplex Virus 1 Induces *de Novo* Phospholipid Synthesis". *Virology* 429.2 (Aug. 2012), pp. 124–135. ISSN: 0042-6822.

[520] Suzuki, M., Nelson, A. D., Eickstaedt, J. B., Wallace, K., Wright, L. S., and Svendsen, C. N. -"Glutamate Enhances Proliferation and Neurogenesis in Human Neural Progenitor Cell Cultures Derived from the Fetal Cortex". *The European Journal of Neuroscience* 24.3 (Aug. 2006), pp. 645–653. ISSN: 0953-816X.

[521] Swerdlow, R. H. and Khan, S. M. -"A "Mitochondrial Cascade Hypothesis" for Sporadic Alzheimer's Disease". *Medical Hypotheses* 63.1 (2004), pp. 8–20. ISSN: 0306-9877.

[522] Takahashi, K., Tanabe, K., Ohnuki, M., Narita, M., Ichisaka, T., Tomoda, K., and Yamanaka, S. -"Induction of Pluripotent Stem Cells from Adult Human Fibroblasts by Defined Factors". *Cell* 131.5 (Nov. 2007), pp. 861–872. ISSN: 0092-8674.

[523] Takahashi, K. and Yamanaka, S. -"Induction of Pluripotent Stem Cells from Mouse Embryonic and Adult Fibroblast Cultures by Defined Factors". *Cell* 126.4 (Aug. 2006), pp. 663–676. ISSN: 0092-8674.

[524] Takahashi, K. and Yamanaka, S. -"A Decade of Transcription Factor-Mediated Reprogramming to Pluripotency". *Nature Reviews Molecular Cell Biology* 17.3 (Mar. 2016), pp. 183–193. ISSN: 1471-0080.

[525] Takaichi, Y., Chambers, J. K., Takahashi, K., Soeda, Y., Koike, R., Katsumata, E., Kita, C., Matsuda, F., Haritani, M., Takashima, A., Nakayama, H., and Uchida, K. -"Amyloid β and Tau Pathology in Brains of Aged Pinniped Species (Sea Lion, Seal, and Walrus)". *Acta Neuropathologica Communications* 9 (Jan. 2021), p. 10. ISSN: 2051-5960.

[526] Tang, B. L. -"Neuronal Protein Trafficking Associated with Alzheimer Disease". *Cell Adhesion & Migration* 3.1 (2009), pp. 118–128. ISSN: 1933-6918.

[527] Tang, J., Zheng, H., Feng, Y., Zeng, J., and Ma, S. -"Attachment Culture of Cortical Organoids at the Microwell Air-Liquid Interface". *STAR Protocols* 4.3 (Sept. 2023), p. 102502. ISSN: 2666-1667.

[528] Tang, Y., Yu, P., and Cheng, L. -"Current Progress in the Derivation and Therapeutic Application of Neural Stem Cells". *Cell Death & Disease* 8.10 (Oct. 2017), e3108–e3108. ISSN: 2041-4889.

[529] Tanzi, R. E. -"A Genetic Dichotomy Model for the Inheritance of Alzheimer's Disease and Common Age-Related Disorders". *The Journal of Clinical Investigation* 104.9 (Nov. 1999), pp. 1175–1179. ISSN: 0021-9738.

[530] Taylor, J. P., Tanaka, F., Robitschek, J., Sandoval, C. M., Taye, A., Markovic-Plese, S., and Fischbeck, K. H. -"Aggresomes Protect Cells by Enhancing the Degradation of Toxic Polyglutamine-Containing Protein". *Human Molecular Genetics* 12.7 (Apr. 2003), pp. 749–757. ISSN: 0964-6906.

[531] Teich, A. F., Patel, M., and Arancio, O. -"A Reliable Way to Detect Endogenous Murine β-Amyloid". *PloS One* 8.2 (2013), e55647. ISSN: 1932-6203.

[532] Telias, M. -"Neural Differentiation Protocols: How to Choose the Correct Approach". *Neural Regeneration Research* 18.6 (June 2023), p. 1273. ISSN: 1673-5374.

[533] Teng, E., Manser, P. T., Pickthorn, K., Brunstein, F., Blendstrup, M., Sanabria Bohorquez, S., Wildsmith, K. R., Toth, B., Dolton, M., Ramakrishnan, V., Bobbala, A., Sikkes, S. A. M., Ward, M., Fuji, R. N., Kerchner, G. A., and Tauriel Investigators. -"Safety and Efficacy of Semorinemab in Individuals With Prodromal to Mild Alzheimer Disease: A Randomized Clinical Trial". *JAMA neurology* 79.8 (Aug. 2022), pp. 758–767. ISSN: 2168-6157.

[534] Tesson, L., Cozzi, J., Ménoret, S., Rémy, S., Usal, C., Fraichard, A., and Anegon, I. -"Transgenic Modifications of the Rat Genome". *Transgenic Research* 14.5 (Oct. 2005), pp. 531–546. ISSN: 0962-8819.

[535] Thakur, S., Dhapola, R., Sarma, P., Medhi, B., and Reddy, D. H. -"Neuroinflammation in Alzheimer's Disease: Current Progress in Molecular Signaling and Therapeutics". *Inflammation* 46.1 (Feb. 2023), pp. 1–17. ISSN: 1573-2576.

[536] Thomas, J., Kneale, D., McKenzie, J. E., Brennan, S. E., and Bhaumik, S. -"Determining the Scope of the Review and the Questions It Will Address". *Cochrane Handbook for Systematic Reviews of Interventions*. John Wiley & Sons, Ltd, 2019, pp. 13–31. ISBN: 978-1-119-53660-4.

[537] Thomson, J. A., Itskovitz-Eldor, J., Shapiro, S. S., Waknitz, M. A., Swiergiel, J. J., Marshall, V. S., and Jones, J. M. -"Embryonic Stem Cell Lines Derived from Human Blastocysts". *Science (New York, N.Y.)* 282.5391 (Nov. 1998), pp. 1145–1147. ISSN: 0036-8075.

[538] Tiscornia, G., Vivas, E. L., and Belmonte, J. C. I. -"Diseases in a Dish: Modeling Human Genetic Disorders Using Induced Pluripotent Cells". *Nature Medicine* 17.12 (Dec. 2011), pp. 1570–1576. ISSN: 1546-170X.

[539] Tomiyama, T., Matsuyama, S., Iso, H., Umeda, T., Takuma, H., Ohnishi, K., Ishibashi, K., Teraoka, R., Sakama, N., Yamashita, T., Nishitsuji, K., Ito, K., Shimada, H., Lambert, M. P., Klein, W. L., and Mori, H. -"A Mouse Model of Amyloid Beta Oligomers: Their Contribution to Synaptic Alteration, Abnormal Tau Phosphorylation, Glial Activation, and Neuronal Loss in Vivo". *The Journal of Neuroscience: The Official Journal of the Society for Neuroscience* 30.14 (Apr. 2010), pp. 4845–4856. ISSN: 1529-2401.

[540] Trifunovic, A., Wredenberg, A., Falkenberg, M., Spelbrink, J. N., Rovio, A. T., Bruder, C. E., Bohlooly-Y, M., Gidlöf, S., Oldfors, A., Wibom, R., Törnell, J., Jacobs, H. T., and Larsson, N.-G. -"Premature Ageing in Mice Expressing Defective Mitochondrial DNA Polymerase". *Nature* 429.6990 (May 2004), pp. 417–423. ISSN: 1476-4687.

[541] Trinczek, B., J, B., K, B., Em, M., and E, M. -"Domains of Tau Protein, Differential Phosphorylation, and Dynamic Instability of Microtubules". *Molecular biology of the cell* 6.12 (Dec. 1995). ISSN: 1059-1524.

[542] Trylinski, M., Mazouni, K., and Schweisguth, F. -"Intra-Lineage Fate Decisions Involve Activation of Notch Receptors Basal to the Midbody in Drosophila Sensory Organ Precursor Cells". *Current biology: CB* 27.15 (Aug. 2017), 2239–2247.e3. ISSN: 1879-0445.

[543] Tsai, M.-C., Cheng, W.-L., Sheu, J.-J., Huang, C.-C., Shia, B.-C., Kao, L.-T., and Lin, H.-C. -"Increased Risk of Dementia Following Herpes Zoster Ophthalmicus". *PLoS ONE* 12.11 (Nov. 2017). ISSN: 1932-6203.

[544] Tu, H., Nelson, O., Bezprozvanny, A., Wang, Z., Lee, S.-F., Hao, Y.-H., Serneels, L., De Strooper, B., Yu, G., and Bezprozvanny, I. -"Presenilins Form ER Ca2+ Leak Channels, a Function Disrupted by Familial Alzheimer's Disease-Linked Mutations". *Cell* 126.5 (Sept. 2006), pp. 981–993. ISSN: 0092-8674.

[545] Tyumentsev, M. A., Stefanova, N. A., Kiseleva, E. V., and Kolosova, N. G. -"Mitochondria with Morphology Characteristic for Alzheimer's Disease Patients Are Found in the Brain of OXYS Rats". *Biochemistry (Moscow)* 83.9 (Sept. 2018), pp. 1083–1088. ISSN: 1608-3040.

[546] Tzeng, N.-S., Chung, C.-H., Lin, F.-H., Chiang, C.-P., Yeh, C.-B., Huang, S.-Y., Lu, R.-B., Chang, H.-A., Kao, Y.-C., Yeh, H.-W., Chiang, W.-S., Chou, Y.-C., Tsao, C.-H., Wu, Y.-F., and Chien, W.-C. -"Anti-Herpetic Medications and Reduced Risk of Dementia in Patients with Herpes Simplex Virus Infections-a Nationwide, Population-Based Cohort Study in Taiwan". *Neurotherapeutics: The Journal of the American Society for Experimental NeuroTherapeutics* 15.2 (Apr. 2018), pp. 417–429. ISSN: 1878-7479.

[547] Ueno, M., Fujita, Y., Tanaka, T., Nakamura, Y., Kikuta, J., Ishii, M., and Yamashita, T. -"Layer V Cortical Neurons Require Microglial Support for Survival during Postnatal Development". *Nature Neuroscience* 16.5 (May 2013), pp. 543–551. ISSN: 1546-1726.

[548] Urrestizala-Arenaza, N., Cerchio, S., Cavaliere, F., and Magliaro, C. -"Limitations of Human Brain Organoids to Study Neurodegenerative Diseases: A Manual to Survive". *Frontiers in Cellular Neuroscience* 18 (July 2024). ISSN: 1662-5102.

[549] Urwin, H., Ghazi-Noori, S., Collinge, J., and Isaacs, A. -"The Role of CHMP2B in Frontotemporal Dementia". *Biochemical Society Transactions* 37 (Pt 1 Feb. 2009), pp. 208–212. ISSN: 1470-8752.

[550] Uryash, A., Flores, V., Adams, J. A., Allen, P. D., and Lopez, J. R. -"Memory and Learning Deficits Are Associated With Ca2+ Dyshomeostasis in Normal Aging". *Frontiers in Aging Neuroscience* 12 (July 2020). ISSN: 1663-4365.

[551] Uttara, B., Singh, A. V., Zamboni, P., and Mahajan, R. T. -"Oxidative Stress and Neurodegenerative Diseases: A Review of Upstream and Downstream Antioxidant Therapeutic Options". *Current Neuropharmacology* 7.1 (Mar. 2009), pp. 65–74. ISSN: 1570-159X.

[552] Vacher, M. C., Durrant, C. S., Rose, J., Hall, A. J., Spires-Jones, T. L., Gunn-Moore, F., and Dagleish, M. P. -"Alzheimer's Disease-like Neuropathology in Three Species of Oceanic Dolphin". *The European Journal of Neuroscience* 57.7 (Apr. 2023), pp. 1161–1179. ISSN: 1460-9568.

[553] Vaillant-Beuchot, L., Mary, A., Pardossi-Piquard, R., Bourgeois, A., Lauritzen, I., Eysert, F., Kinoshita, P. F., Cazareth, J., Badot, C., Fragaki, K., Bussiere, R., Martin, C., Mary, R., Bauer, C., Pagnotta, S., Paquis-Flucklinger, V., Buée-Scherrer, V., Buée, L., Lacas-Gervais, S., Checler, F., and Chami, M. -"Accumulation of Amyloid Precursor Protein C-terminal Fragments Triggers Mitochondrial Structure, Function, and Mitophagy Defects in Alzheimer's Disease Models and Human Brains". *Acta Neuropathologica* 141.1 (Jan. 2021), pp. 39–65. ISSN: 1432-0533.

[554] Van der Kant, R. -"Lipidomic Analysis of Isogenic ApoE-variant iPSC-derived Glia Uncovers Coupling between Inflammatory Signaling and Lipid Metabolism." *Alzheimer's & Dementia* 18.S4 (2022), e060215. ISSN: 1552-5279.

[555] Vandenberghe, R., Rinne, J. O., Boada, M., Katayama, S., Scheltens, P., Vellas, B., Tuchman, M., Gass, A., Fiebach, J. B., Hill, D., Lobello, K., Li, D., McRae, T., Lucas, P., Evans, I., Booth, K., Luscan, G., Wyman, B. T., Hua, L., Yang, L., Brashear, H. R., Black, R. S., and for the Bapineuzumab 3000 and 3001 Clinical Study Investigators. -"Bapineuzumab for Mild to Moderate Alzheimer's Disease in Two Global, Randomized, Phase 3 Trials". *Alzheimer's Research & Therapy* 8.1 (May 2016), p. 18. ISSN: 1758-9193.

[556] Vaughan, M. B., Kaar, A., Mauleon, G., Eddington T., D., and Rae, M. G. -"Calcium Homeostasis Is Significantly Disrupted in Dentate Gyrus Neurons of Acute, Ex Vivo Brain Slices of a Mouse Model of Alzheimer's Disease." *The Physiological Society*. Europhysiology 2018. Vol. 41. London, UK: Proceedings of the Physiological Society, 2018.

[557] Vázquez, P., Arroba, A. I., Cecconi, F., de la Rosa, E. J., Boya, P., and De Pablo, F. -"Atg5 and Ambra1 Differentially Modulate Neurogenesis in Neural Stem Cells". *Autophagy* 8.2 (Feb. 2012), pp. 187–199. ISSN: 1554-8627.

[558] Veeraraghavalu, K., Choi, S. H., Zhang, X., and Sisodia, S. S. -"Presenilin 1 Mutants Impair the Self-Renewal and Differentiation of Adult Murine Subventricular Zone-Neuronal Progenitors via Cell-Autonomous Mechanisms Involving Notch Signaling". *The Journal of Neuroscience* 30.20 (May 2010), pp. 6903–6915. ISSN: 0270-6474.

[559] Viloria, J. and Garcia, J. -"Human Herpes Simplex Encephalitis (Cellular Events)". *Beiträge zur Pathologie* 157.1 (Jan. 1976), pp. 14–22. ISSN: 00058165.

[560] Vőfély, G., Berecz, T., Szabó, E., Szebényi, K., Hathy, E., Orbán, T. I., Sarkadi, B., Homolya, L., Marchetto, M. C., Réthelyi, J. M., and Apáti, Á. -"Characterization of Calcium Signals in Human Induced Pluripotent Stem Cell-Derived Dentate Gyrus Neuronal Progenitors and Mature Neurons, Stably Expressing an Advanced Calcium Indicator Protein". *Molecular and Cellular Neuroscience* 88 (Apr. 2018), pp. 222–230. ISSN: 1044-7431.

[561] Volpato, V. and Webber, C. -"Addressing Variability in iPSC-derived Models of Human Disease: Guidelines to Promote Reproducibility". *Disease Models & Mechanisms* 13.1 (Jan. 2020), p. dmm042317. ISSN: 1754-8403.

[562] Vuono, R., Winder-Rhodes, S., de Silva, R., Cisbani, G., Drouin-Ouellet, J., REGISTRY Investigators of the European Huntington's Disease Network, Spillantini, M. G., Cicchetti, F., and Barker, R. A. -"The Role of Tau in the Pathological Process and Clinical Expression of Huntington's Disease". *Brain* 138.7 (July 2015), pp. 1907–1918. ISSN: 0006-8950.

[563] Wainberg, M., Luquez, T., Koelle, D. M., Readhead, B., Johnston, C., Darvas, M., and Funk, C. C. -"The Viral Hypothesis: How Herpesviruses May Contribute to Alzheimer's Disease". *Molecular Psychiatry* 26.10 (10 Oct. 2021), pp. 5476–5480. ISSN: 1476-5578.

[564] Wakui, T., Matsumoto, T., Matsubara, K., Kawasaki, T., Yamaguchi, H., and Akutsu, H. -"Method for Evaluation of Human Induced Pluripotent Stem Cell Quality Using Image Analysis Based on the Biological Morphology of Cells". *Journal of Medical Imaging* 4.4 (Nov. 2017), p. 044003. ISSN: 2329-4302, 2329-4310.

[565] Walker, L. C., Masters, C., Beyreuther, K., and Price, D. L. -"Amyloid in the Brains of Aged Squirrel Monkeys". *Acta Neuropathologica* 80.4 (1990), pp. 381–387. ISSN: 0001-6322.

[566] Walls, K. C., Coskun, P., Gallegos-Perez, J. L., Zadourian, N., Freude, K., Rasool, S., Blurton-Jones, M., Green, K. N., and LaFerla, F. M. -"Swedish Alzheimer Mutation Induces Mitochondrial Dysfunction Mediated by HSP60 Mislocalization of Amyloid Precursor Protein (APP) and Beta-Amyloid *". *Journal of Biological Chemistry* 287.36 (Aug. 2012), pp. 30317–30327. ISSN: 0021-9258, 1083-351X.

[567] Walter, P. and Ron, D. -"The Unfolded Protein Response: From Stress Pathway to Homeostatic Regulation". *Science (New York, N.Y.)* 334.6059 (Nov. 2011), pp. 1081–1086. ISSN: 1095-9203.

[568] Wang, B., Ma, T., Yang, L., He, S., Li, J., and Sun, X. -"Association between Coffee and Tea Consumption and the Risk of Dementia in Individuals with Hypertension: A Prospective Cohort Study". *Scientific Reports* 14.1 (Sept. 2024), p. 21063. ISSN: 2045-2322.

[569] Wang, D., Chan, C.-C., Cherry, S., and Hiesinger, P. R. -"Membrane Trafficking in Neuronal Maintenance and Degeneration". *Cellular and Molecular Life Sciences* 70.16 (Aug. 2013), pp. 2919–2934. ISSN: 1420-9071.

[570] Wang, R., Dineley, K. T., Sweatt, J. D., and Zheng, H. -"Presenilin 1 Familial Alzheimer's Disease Mutation Leads to Defective Associative Learning and Impaired Adult Neurogenesis". *Neuroscience* 126.2 (Jan. 2004), pp. 305–312. ISSN: 0306-4522, 1873-7544.

[571] Wang, X., Su, B., Lee, H.-g., Li, X., Perry, G., Smith, M. A., and Zhu, X. -"Impaired Balance of Mitochondrial Fission and Fusion in Alzheimer's Disease". *The Journal of Neuroscience* 29.28 (July 2009), pp. 9090–9103. ISSN: 0270-6474.

[572] Wang, X., Su, B., Siedlak, S. L., Moreira, P. I., Fujioka, H., Wang, Y., Casadesus, G., and Zhu, X. -"Amyloid-Beta Overproduction Causes Abnormal Mitochondrial Dynamics via Differential Modulation of Mitochondrial Fission/Fusion Proteins". *Proceedings of the National Academy of Sciences of the United States of America* 105.49 (Dec. 2008), pp. 19318–19323. ISSN: 1091-6490.

[573] Wang, Y., Wu, L.-H., Hou, F., Wang, Z.-J., Wu, M.-N., Hölscher, C., and Cai, H.-Y. -"Mitochondrial Calcium Uniporter Knockdown in Hippocampal Neurons Alleviates Anxious and Depressive Behavior in the 3XTG Alzheimer's Disease Mouse Model". *Brain Research* 1840 (Oct. 2024), p. 149060. ISSN: 0006-8993.

[574] Wang, Y.-J., Chen, G.-H., Hu, X.-Y., Lu, Y.-P., Zhou, J.-N., and Liu, R.-Y. -"The Expression of Calcium/Calmodulin-Dependent Protein Kinase II-α in the Hippocampus of Patients with Alzheimer's Disease and Its Links with AD-related Pathology". *Brain Research* 1031.1 (Jan. 2005), pp. 101–108. ISSN: 0006-8993.

[575] Wang, Z., Wang, B., Yang, L., Guo, Q., Aithmitti, N., Songyang, Z., and Zheng, H. -"Presynaptic and Postsynaptic Interaction of the Amyloid Precursor Protein Promotes Peripheral and Central Synaptogenesis". *The Journal of Neuroscience* 29.35 (Sept. 2009), pp. 10788–10801. ISSN: 0270-6474.

[576] Warwick, R. A. and Hanani, M. -"Involvement of Aberrant Calcium Signalling in Herpetic Neuralgia". *Experimental Neurology* 277 (Mar. 2016), pp. 10–18. ISSN: 0014-4886.

[577] Wataya, T., Nunomura, A., Smith, M. A., Siedlak, S. L., Harris, P. L. R., Shimohama, S., Szweda, L. I., Kaminski, M. A., Avila, J., Price, D. L., Cleveland, D. W., Sayre, L. M., and Perry, G. -"High Molecular Weight Neurofilament Proteins Are Physiological Substrates of Adduction by the Lipid Peroxidation Product Hydroxynonenal". *The Journal of Biological Chemistry* 277.7 (Feb. 2002), pp. 4644–4648. ISSN: 0021-9258.

[578] Wei, H., Chadman, K. K., McCloskey, D. P., Sheikh, A. M., Malik, M., Brown, W. T., and Li, X. -"Brain IL-6 Elevation Causes Neuronal Circuitry Imbalances and Mediates Autism-like Behaviors". *Biochimica Et Biophysica Acta* 1822.6 (June 2012), pp. 831–842. ISSN: 0006-3002.

[579] Wei, W., Nguyen, L. N., Kessels, H. W., Hagiwara, H., Sisodia, S., and Malinow, R. -"Amyloid Beta from Axons and Dendrites Reduces Local Spine Number and Plasticity". *Nature Neuroscience* 13.2 (Feb. 2010), pp. 190–196. ISSN: 1546-1726.

[580] Wei, Z., Sakamuru, S., Zhang, L., Zhao, J., Huang, R., Kleinstreuer, N. C., Chen, Y., Shu, Y., Knudsen, T. B., and Xia, M. -"Identification and Profiling of Environmental Chemicals That Inhibit the TGFβ/SMAD Signaling Pathway". *Chemical Research in Toxicology* 32.12 (Dec. 2019), pp. 2433–2444. ISSN: 0893-228X.

[581] West, M. J., Coleman, P. D., Flood, D. G., and Troncoso, J. C. -"Differences in the Pattern of Hippocampal Neuronal Loss in Normal Ageing and Alzheimer's Disease". *The Lancet*. Originally Published as Volume 2, Issue 8925 344.8925 (Sept. 1994), pp. 769–772. ISSN: 0140-6736.

[582] Whishaw, I. Q., Metz, G. A., Kolb, B., and Pellis, S. M. -"Accelerated Nervous System Development Contributes to Behavioral Efficiency in the Laboratory Mouse: A Behavioral Review and Theoretical Proposal". *Developmental Psychobiology* 39.3 (Nov. 2001), pp. 151–170. ISSN: 0012-1630.

[583] Whitley, R. J. -"Herpes Simplex Encephalitis: Adolescents and Adults". *Antiviral Research*. Special Issue To Honour Professor Erik De Clercq 71.2 (Sept. 2006), pp. 141–148. ISSN: 0166-3542.

[584] Whitley, R. J. and Roizman, B. -"Herpes Simplex Virus Infections". *The Lancet* 357.9267 (May 2001), pp. 1513–1518. ISSN: 0140-6736, 1474-547X.

[585] Wigge, P., Köhler, K., Vallis, Y., Doyle, C. A., Owen, D., Hunt, S. P., and McMahon, H. T. -"Amphiphysin Heterodimers: Potential Role in Clathrin-Mediated Endocytosis". *Molecular Biology of the Cell* 8.10 (Oct. 1997), pp. 2003–2015. ISSN: 1059-1524.

[586] Wild, P., Kaech, A., Schraner, E. M., Walser, L., and Ackermann, M. -"Endoplasmic Reticulum-to-Golgi Transitions upon Herpes Virus Infection". *F1000Research* 6 (Feb. 2018), p. 1804. ISSN: 2046-1402.

[587] Wildsmith, K. R., Holley, M., Savage, J. C., Skerrett, R., and Landreth, G. E. -"Evidence for Impaired Amyloid β Clearance in Alzheimer's Disease". *Alzheimer's Research & Therapy* 5.4 (July 2013), p. 33. ISSN: 1758-9193.

[588] Wilson, P. G. and Stice, S. S. -"Development and Differentiation of Neural Rosettes Derived from Human Embryonic Stem Cells". *Stem Cell Reviews* 2.1 (2006), pp. 67–77. ISSN: 1550-8943.

[589] Wisner, T. W., Sugimoto, K., Howard, P. W., Kawaguchi, Y., and Johnson, D. C. -"Anterograde Transport of Herpes Simplex Virus Capsids in Neurons by Both Separate and Married Mechanisms". *Journal of Virology* 85.12 (June 2011), pp. 5919–5928. ISSN: 1098-5514.

[590] Wolfe, M. S. and Yankner, B. A. -"Sorting Out Presenilins in Alzheimer's Disease". *Cell* 166.1 (June 2016), pp. 13–15. ISSN: 1097-4172.

[591] Wozniak, M., Mee, A., and Itzhaki, R. -"Herpes Simplex Virus Type 1 DNA Is Located within Alzheimer's Disease Amyloid Plaques". *The Journal of Pathology* 217.1 (2009), pp. 131–138. ISSN: 1096-9896.

[592] Wu, J., Petralia, R. S., Kurushima, H., Patel, H., Jung, M.-y., Volk, L., Chowdhury, S., Shepherd, J. D., Dehoff, M., Li, Y., Kuhl, D., Huganir, R. L., Price, D. L., Scannevin, R., Troncoso, J. C., Wong, P. C., and Worley, P. F. -"Arc/Arg3.1 Regulates an Endosomal Pathway Essential for Activity-Dependent β-Amyloid Generation". *Cell* 147.3 (Oct. 2011), pp. 615–628. ISSN: 0092-8674.

[593] Wu, Y., Cheng, J., Qi, J., Hang, C., Dong, R., Low, B. C., Yu, H., and Jiang, X. -"Three-Dimensional Liquid Metal-Based Neuro-Interfaces for Human Hippocampal Organoids". *Nature Communications* 15.1 (May 2024), p. 4047. ISSN: 2041-1723.

[594] Xia, D., Watanabe, H., Wu, B., Lee, S. H., Li, Y., Tsvetkov, E., Bolshakov, V. Y., Shen, J., and Kelleher, R. J. -"Presenilin-1 Knockin Mice Reveal Loss-of-Function Mechanism for Familial Alzheimer's Disease". *Neuron* 85.5 (Mar. 2015), pp. 967–981. ISSN: 1097-4199.

[595] Xu, W., Weissmiller, A. M., White, J. A., Fang, F., Wang, X., Wu, Y., Pearn, M. L., Zhao, X., Sawa, M., Chen, S., Gunawardena, S., Ding, J., Mobley, W. C., and Wu, C. -"Amyloid Precursor Protein-Mediated Endocytic Pathway Disruption Induces Axonal Dysfunction and Neurodegeneration". *The Journal of Clinical Investigation* 126.5 (May 2016), pp. 1815–1833. ISSN: 1558-8238.

[596] Yamamoto, H., Hiragami, Y., Murayama, M., Ishizuka, K., Kawahara, M., and Takashima, A. -"Phosphorylation of Tau at Serine 416 by Ca2+/Calmodulin-Dependent Protein Kinase II in Neuronal Soma in Brain". *Journal of Neurochemistry* 94.5 (2005), pp. 1438–1447. ISSN: 1471-4159.

[597] Yamashita, T., Ninomiya, M., Acosta, P. H., García-Verdugo, J. M., Sunabori, T., Sakaguchi, M., Adachi, K., Kojima, T., Hirota, Y., Kawase, T., Araki, N., Abe, K., Okano, H., and Sawamoto, K. -"Subventricular Zone-Derived Neuroblasts Migrate and Differentiate into Mature Neurons in the Post-Stroke Adult Striatum". *Journal of Neuroscience* 26.24 (June 2006), pp. 6627–6636. ISSN: 0270-6474, 1529-2401.

[598] Yao, J., Irwin, R. W., Zhao, L., Nilsen, J., Hamilton, R. T., and Brinton, R. D. -"Mitochondrial Bioenergetic Deficit Precedes Alzheimer's Pathology in Female Mouse Model of Alzheimer's Disease". *Proceedings of the National Academy of Sciences* 106.34 (Aug. 2009), pp. 14670–14675.

[599] Yap, C. C. and Winckler, B. -"Harnessing the Power of the Endosome to Regulate Neural Development". *Neuron* 74.3 (May 2012), pp. 440–451. ISSN: 1097-4199.

[600] Yépez, V. A., Kremer, L. S., Iuso, A., Gusic, M., Kopajtich, R., Koňaříková, E., Nadel, A., Wachutka, L., Prokisch, H., and Gagneur, J. -"OCR-Stats: Robust Estimation and Statistical Testing of Mitochondrial Respiration Activities Using Seahorse XF Analyzer". *PLoS ONE* 13.7 (July 2018), e0199938. ISSN: 1932-6203.

[601] Yoo, I., Ahn, I., Lee, J., and Lee, N. -"Extracellular Flux Assay (Seahorse Assay): Diverse Applications in Metabolic Research across Biological Disciplines". *Molecules and Cells* 47.8 (Aug. 2024), p. 100095. ISSN: 1016-8478.

[602] Yoshimura, R., Kishi, T., and Iwata, N. -"Plasma Levels of IL-6 in Patients with Untreated Major Depressive Disorder: Comparison with Catecholamine Metabolites". *Neuropsychiatric Disease and Treatment* 15 (Sept. 2019), pp. 2655–2661. ISSN: 1176-6328.

[603] Yu, D. X., Di Giorgio, F. P., Yao, J., Marchetto, M. C., Brennand, K., Wright, R., Mei, A., Mchenry, L., Lisuk, D., Grasmick, J. M., Silberman, P., Silberman, G., Jappelli, R., and Gage, F. H. -"Modeling Hippocampal Neurogenesis Using Human Pluripotent Stem Cells". *Stem Cell Reports* 2.3 (Feb. 2014), pp. 295–310. ISSN: 2213-6711.

[604] Yu, J., Vodyanik, M. A., Smuga-Otto, K., Antosiewicz-Bourget, J., Frane, J. L., Tian, S., Nie, J., Jonsdottir, G. A., Ruotti, V., Stewart, R., Slukvin, I. I., and Thomson, J. A. -"Induced Pluripotent Stem Cell Lines Derived from Human Somatic Cells". *Science (New York, N.Y.)* 318.5858 (Dec. 2007), pp. 1917–1920. ISSN: 1095-9203.

[605] Yun, D. H., Park, Y.-G., Cho, J. H., Kamentsky, L., Evans, N. B., Albanese, A., Xie, K., Swaney, J., Sohn, C. H., Tian, Y., Zhang, Q., Drummond, G., Guan, W., DiNapoli, N., Choi, H., Jung, H.-Y., Ruelas, L., Feng, G., and Chung, K. -"Ultrafast Immunostaining of Organ-Scale Tissues for Scalable Proteomic Phenotyping". June 2019. (Prepublished).

[606] Zadik-Weiss, L., Ritter, S., Hermush, V., Asher, N., Avital, A., and Or, R. -"Feline Cognitive Dysfunction as a Model for Alzheimer's Disease in the Research of CBD as a Potential Treatment—a Narrative Review". *Journal of Cannabis Research* 2.1 (Dec. 2020), p. 43. ISSN: 2522-5782.

[607] Zandi, P. P. and Breitner, J. C. S. -"Do NSAIDs Prevent Alzheimer's Disease? And, If so, Why? The Epidemiological Evidence". *Neurobiology of Aging*. Neuroinflammation in Alzheimer's Disease 22.6 (Nov. 2001), pp. 811–817. ISSN: 0197-4580.

[608] Zeng, J., Hu, X.-F., Sun, D.-S., Hong, X.-Y., Ma, J.-Z., and Feng, Q. -"Alzheimer-like Behavior and Synaptic Dysfunction in 3 × Tg-AD Mice Are Reversed with Calcineurin Inhibition". *Experimental Brain Research* 242.6 (June 2024), pp. 1507–1515. ISSN: 1432-1106.

[609] Zhang, B., He, Y., Xu, Y., Mo, F., Mi, T., Shen, Q. S., Li, C., Li, Y., Liu, J., Wu, Y., Chen, G., Zhu, W., Qin, C., Hu, B., and Zhou, G. -"Differential Antiviral Immunity to Japanese Encephalitis Virus in Developing Cortical Organoids". *Cell Death & Disease* 9.7 (June 2018), pp. 1–10. ISSN: 2041-4889.

[610] Zhang, H., Sun, S., Herreman, A., Strooper, B. D., and Bezprozvanny, I. -"Role of Presenilins in Neuronal Calcium Homeostasis". *Journal of Neuroscience* 30.25 (June 2010), pp. 8566–8580. ISSN: 0270-6474, 1529-2401.

[611] Zhang, L., Trushin, S., Christensen, T. A., Bachmeier, B. V., Gateno, B., Schroeder, A., Yao, J., Itoh, K., Sesaki, H., Poon, W. W., Gylys, K. H., Patterson, E. R., Parisi, J. E., Diaz Brinton, R., Salisbury, J. L., and Trushina, E. -"Altered Brain Energetics Induces Mitochondrial Fission Arrest in Alzheimer's Disease". *Scientific Reports* 6.1 (Jan. 2016), p. 18725. ISSN: 2045-2322.

[612] Zhang, S.-C., Wernig, M., Duncan, I., Brüstle, O., and Thomson, J. -"In Vitro Differentiation of Transplantable Neural Precursors from Human Embryonic Stem Cells". *Nature Biotechnology* 19.12 (2001), pp. 1129–1133.

[613] Zhang, W., Xu, C., Sun, J., Shen, H.-M., Wang, J., and Yang, C. -"Impairment of the Autophagy–Lysosomal Pathway in Alzheimer's Diseases: Pathogenic Mechanisms and Therapeutic Potential". *Acta Pharmaceutica Sinica B* 12.3 (Mar. 2022), pp. 1019–1040. ISSN: 2211-3835.

[614] Zhang, X., Li, Y., Xu, H., and Zhang, Y.-w. -"The γ-Secretase Complex: From Structure to Function". *Frontiers in Cellular Neuroscience* 8 (Dec. 2014), p. 427. ISSN: 1662-5102.

[615] Zhao, Z., Zhang, J., Wu, Y., Xie, M., Tao, S., Lv, Q., and Wang, Q. -"Plasma IL-6 Levels and Their Association with Brain Health and Dementia Risk: A Population-Based Cohort Study". *Brain, Behavior, and Immunity* 120 (Aug. 2024), pp. 430–438. ISSN: 0889-1591.

[616] Zheng, K., Xiang, Y., Wang, Q., Jin, F., Chen, M., Ma, K., Ren, Z., and Wang, Y. -"Calcium-Signal Facilitates Herpes Simplex Virus Type 1 Nuclear Transport through Slingshot 1 and Calpain-1 Activation". *Virus Research* 188 (Aug. 2014), pp. 32–37. ISSN: 0168-1702.

[617] Zhong, M. Z., Peng, T., Duarte, M. L., Wang, M., and Cai, D. -"Updates on Mouse Models of Alzheimer's Disease". *Molecular Neurodegeneration* 19.1 (Mar. 2024), p. 23. ISSN: 1750-1326.

[618] Zhou, B., Lin, W., Long, Y., Yang, Y., Zhang, H., Wu, K., and Chu, Q. -"Notch Signaling Pathway: Architecture, Disease, and Therapeutics". *Signal Transduction and Targeted Therapy* 7.1 (Mar. 2022), pp. 1–33. ISSN: 2059-3635.

[619] Zolochevska, O. and Taglialatela, G. -"Non-Demented Individuals with Alzheimer's Disease Neuropathology: Resistance to Cognitive Decline May Reveal New Treatment Strategies". *Current pharmaceutical design* 22.26 (2016), pp. 4063–4068. ISSN: 1381-6128.

Appendices

Publications and Abstracts

Original Articles

- Stephenson KA, Xiao Q, **Vaughan MB**, Peters P, Denley C, O'Meara S, Sheehan C, Rae MG, O'Malley D (2025). 'Neuronal hyperexcitability in dystrophin-deficient mdx hippocampal neurons: the importance of interleukin-6 and GABAergic regulation' *Scientific Reports* 15,1;1-21

- Siew K, Nestler, Nelson C, D'Ambrosio V, Zhong C, Li Z, Grillo A, Wan ER, Patel V, Overbey E, Kim J, Yun S, **Vaughan MB**, Cheshire C, Cubitt L, Broni-Tabi J, Al-Jaber MY, Boyko V, Meydan C, Barker P, Arif S, Afsari F, Allen N, Al-Maadheed M, Altinok S, Bah n, Border S, Brown AL, Burling K, Cheng-Campbell M, Colón LM, Degoricija L, Figg N, Finch R, Foox J, Faridi P, French A, Gebre S, Gordon P, Houerbi N, Kahrood HV, Kiffer FC, Klosinska AS, Kubik A, Lee H, Li Y, Lucarelli N, Marullo AL, Matei I, McCann CM, Mimar S, Naglah A, Nicod J, O'Shaughnessy KM, De Oliveira LC, Oswalt L, Patras LI, Polo SHL, Rodríguez-Lopez M, Roufosse C, Sadeghi-Alavijeh O, Sanchez-Hodge R, Paul AS, Schittenhelm RB, Schweickart A, Scott RT, Lim Kam Sian TCC, da Silveira WA, Slawinski H, Snell D, Sosa J, Saravia-Butler AM, Tabetah M, Tanuwidjaya E, Walker-Samuel S, Yang X, Yasmin, Zhang H, Godovac-Zimmermann J, Sarder P, Sanders LM, Costes SV, Campbell RAA, Karouia F, Mohamed-Alis V, Rodriques S, Lynham S, Steele JR, Baranzini S, Fazelinia H, Dai Z, Uruno A, Shiba D, Yamamoto M, Almeida EAC, Blaber E, Schisler JC, Eisch AJ, Muratani M, Zwart SR, Smith SM, Galazka JM, Mason CE, Beheshti A, Walsh SB (2024). 'Cosmic kidney disease: an integrated pan-omic, physiological and morphological study into spaceflight-induced renal dysfunction'. *Nature Communications* 15,1:4923

- Siew K, Patel V, Zimmermann J, **Vaughan MB**, Cheshire C, Kubik A, Finch R, Li Z, Altinok S, De Silvera W, Rodriques S, Blaber E, Schisler J, Galazka J, Muratani M, Beheshti A, Walsh SB (2023) 'Scientific Business Abstracts: 42 The Effect of Microgravity and Galactic Cosmic Radiation on Renal Structure and Function'. *QJM: An International Journal of Medicine* hcad072

- Diercks BP, Jensen HH, Chalmers SB, Coode E, **Vaughan MB**, Tadayon R, Sáez PJ, Davis FM, Brohus M (2021). 'The first junior European Calcium Society meeting: calcium research across scales, Kingdoms and countries'. *Biochimica et Biophysica Acta (BBA)-Molecular Cell Research* 1868,6:118999

Preprint - Original Articles Under Review

- Hamerlinck L, D'haene E, Van Loon N, **Vaughan MB**, Del Rocio PBM, Leimbacher S, Colombo L, Vantomme L, Daal E, Dheedene A, Goel H, Menten B, Callewaert B, Vergult S (2025). 'Non-coding structural variants identify a commonly affected regulatory region steering FOXG1 transcription in early neurodevelopment'. *medRxiv*

- **Vaughan MB**, Bellai DJ, Rae MG (2025). 'Direct evidence of alteration to the human neural intracellular trafficking system following exposure to HSV: A systematic review'. *medRxiv*

Oral Communications

- Van Loon N, **Vaughan MB**, Okkelman I, Vergult S ,Dmitriev RI (2023). 'Fluorescence Lifetime Imaging Microscopy (FLIM)-assisted analysis of developing human neural organoids'. 18th Conference on Methods and Applications in Fluorescence (MAF 2024), September 2024, Valencia, Spain.

- **Vaughan MB**, Foley C, O'Malley D, Rae MG (2022). 'Altered calcium homeostasis in induced pluripotent stem cell-derived human neural progenitor cells containing familial presenilin1-linked Alzheimer's disease mutation, M139V'. Europhysiology, *Acta Physiologica* 236, Supplement 725:129, September 2022, Copenhagen, Denmark.

Poster Communications

- **Vaughan MB**, Colombo L, Daal E, Beyens A, Vanbelleghem E, Derudder R, Leimbacher S, D'haene E, Callewaert B, Vergult S (2025). 'Tissue-Specific 3D Genome and Splicing Signatures of Clinically Accessible Tissues Inform Sample Selection for Assessing the impact of Genomic Aberrations in Neurodevelopmental Disorders' Neurogenomics 2025, May 2025, Milan, Italy.

- Colombo L, **Vaughan MB**, Van Loon N, Leimbacher S, Daal E, D'haene E, Vergult S (2024). 'Comparison of 3D genome structure between neuronal and clinically accessible tissues'. M.M. Delacroix Foundation 2024 Autism Research Workshop, November 2024, Brussels, Belgium.

- Van Loon N, Genbrugge L, Van Wetter E, Godefroy FM, **Vaughan MB**, Hamerlinck L, Colombo L, Leimbacher S, Vantomme L, Daal E, Dmitriev RI, Vergult S (2024). 'Assessing the effect of aberrant FOXG1 expression in neural organoids'.

EMBO Workshop-'*Unlocking human brain complexity using 3D culture and single-cell omics*', October 2024, Capri, Italy.

- Hamerlinck L, D'haene E, **Vaughan MB**, Del Rocio PBM, Van Loon N, Vantomme L, Menten B, Callewaert B, De Baere E, Vergult S (2024). 'Structural variants disrupt a critical regulatory region downstream of FOXG1'. Belgian Society for Human Genetics (BeSHG) Annual Symposium 2024 : Single Cells : *to care or not to care*, April 2024, Leuven, Belgium.

- Van Loon N, **Vaughan MB**, Dmitriev RI, Vergult S (2023). 'A comprehensive comparison of different seeding densities and the use of microscaffolds to establish a reproducible protocol for unguided neural organoid differentiation'. EMBO Workshop-'*Gene regulatory mechanisms in neural fate decisions*', September 2023, Alicante, Spain.

- Stephenson KA, **Vaughan MB**, Denley C, Rae MG, O'Malley D (2022). 'Interleukin-6, a pro-inflammatory cytokine that may contribute to hippocampal dysfunction in dystrophin-deficient mdx mice'. Europhysiology, *Acta Physiologica* 236, Supplement 725:483, September 2022, Copenhagen, Denmark.

- **Vaughan MB**, Rae MG, Dmitriev RI (2019). 'Development of a human cerebroid model of Alzheimer's disease'. BNA Festival of Neuroscience, *Brain and Neuroscience Advances* 3, April 2019, Dublin, Ireland.

- **Vaughan MB,** Kaar A, Mauleon G, Eddington DT, Rae MG (2018). 'Calcium homeostasis is significantly disrupted in dentate gyrus neurons of acute, ex vivo brain slices of a mouse model of Alzheimer's disease'. New Horizons in Medical Research, December 2018, Cork, Ireland.

- **Vaughan MB**, Kaar A, Mauleon G, Eddington DT, Rae MG (2018). 'Calcium homeostasis is significantly disrupted in dentate gyrus neurons of acute, ex vivo brain slices of a mouse model of Alzheimer's disease'. Europhysiology, *Proceedings of The Physiological Society* 41, C086, September 2018, London, UK.

Invited Membership Article

- **Vaughan MB.** 'Thinking a little differently- A member reflects on life as a neurodivergent physiologist'. *Physiology News* – Issue 123, September 2022. doi.org/10.36866/pn.123.44.